FUEL INJECTION PARAMETERS STUDY FOR LOW EXHAUST EMISSIONS OF A COMMON-RAIL DIESEL ENGINE FUELED WITH DIFFERENT BIODIESELS' BLENDS

HOW HEOY GEOK

FACULTY OF ENGINEERING
UNIVERSITY OF MALAYA
KUALA LUMPUR

2018

FUEL INJECTION PARAMETERS STUDY FOR LOW EXHAUST EMISSIONS OF A COMMON-RAIL DIESEL ENGINE FUELED WITH DIFFERENT BIODIESELS' BLENDS

HOW HEOY GEOK

THESIS SUBMITTED IN FULFILMENT OF THE REQUIREMENTS FOR THE DEGREE OF DOCTOR OF PHILOSOPHY

FACULTY OF ENGINEERING
UNIVERSITY OF MALAYA
KUALA LUMPUR

2018

UNIVERSITI MALAYA

ORIGINAL LITERARY WORK DECLARATION

Name of Candidate: HOW HEOY GEOK

Matric No: KHA110005

Name of Degree: DOCTOR OF PHILOSOPHY

Title of Thesis: FUEL INJECTION PARAMETERS STUDY FOR LOW EXHAUST EMISSIONS OF A COMMON-RAIL DIESEL ENGINE FUELED WITH DIFFERENT BIODIESELS' BLENDS

Field of Study: ENERGY

I do solemnly and sincerely declare that:

(1) I am the sole author/writer of this Work;
(2) This Work is original;
(3) Any use of any work in which copyright exists was done by way of fair dealing and for permitted purposes and any excerpt or extract from, or reference to or reproduction of any copyright work has been disclosed expressly and sufficiently and the title of the Work and its authorship have been acknowledged in this Work;
(4) I do not have any actual knowledge nor do I ought reasonably to know that the making of this work constitutes an infringement of any copyright work;
(5) I hereby assign all and every rights in the copyright to this Work to the University of Malaya ("UM"), who henceforth shall be owner of the copyright in this Work and that any reproduction or use in any form or by any means whatsoever is prohibited without the written consent of UM having been first had and obtained;
(6) I am fully aware that if in the course of making this Work I have infringed any copyright whether intentionally or otherwise, I may be subject to legal action or any other action as may be determined by UM.

Candidate's Signature Date:

Subscribed and solemnly declared before,

Witness's Signature Date:

Name:

Designation:

FUEL INJECTION PARAMETERS STUDY FOR LOW EXHAUST EMISSIONS OF A COMMON-RAIL DIESEL ENGINE FUELED WITH DIFFERENT BIODIESELS' BLENDS

ABSTRACT

Nowadays, the use of diesel engines is increasing rapidly due to their superior fuel economy, higher efficiency and excellent reliability. The energy crisis of fossil fuel depletion, rising price of diesel and environmental degradation have triggered a search for clean, sustainable and alternative fuels for internal combustion engines. Biodiesel is one of the most promising alternative fuels because it is a biodegradable, non-toxic and renewable fuel. This research aims to produce biodiesel from different feedstock such as coconut, *calophyllum inophyllum* and *moringa oleifera* oil and tested in a medium-duty four-cylinder diesel engine. In addition, the in-house produced coconut biodiesel was also used in the study of the effects of biodiesel blends, fuel injection timing, split injection schemes, injection dwell angle and mass ratio on the engine performance, emissions and combustion characteristics. At the first stage, a detailed investigation and characterization of key physicochemical properties were carried out. This was followed by the investigation of the effects of the usage of all these biodiesel blends on engine performance, emissions, exhaust particulate matter and combustion under different engine operating conditions. At second stage, parametric studies relating with start of injection timing variation and multiple injection schemes using COB20 and COB50 blends were performed and benchmarked with petroleum diesel fuel as baseline. At the final stage, the impact of two-stage injection dwell angle and mass ratio on engine performance, emissions and combustion characteristics using coconut biodiesel blends were investigated. The results showed that all biodiesel fuels and its blends have physicochemical properties relatively close to those of petroleum diesel. The

experimental results also suggested that there are some penalties in engine brake power, brake specific fuel consumption (BSFC), and nitrogen oxide (NOx) blends with the presence of biodiesel fuel in the blend. The second stage experimental results revealed that a remarkably lower NOx level below 100 ppm can be obtained by retard SOI timing for both of the COB20 and COB50 fuel operations and with triple injection scheme. Multiple split injections is a practical strategies to simultaneously decrease NOx and smoke emissions when the SOI timing is fine-tuned and is an ideal alternative to operate with biodiesel fuel. For the last stage experiment, the results showed that exhaust emissions, engine performance and combustion characteristics are substantially affected by types of fuel and SOI timing but slightly influenced by two-stage injection dwell angle. Also, a considerably lower level of NOx below 90 ppm is achievable via late SOI timing for fuel operations conducted using COB20 or COB50 biodiesel blends with injection mass ratio of 25:75. Overall, the results indicated that biodiesel from coconut, *calophyllum inophyllum* and *moringa oleifera* oil can be used satisfactorily in the modern high-pressure common-rail diesel engine without modification. Besides, the results revealed that multiple and two-stage fuel injection with different mass ratio and dwell angle are practical strategies to simultaneously decrease NOx and smoke emissions when the SOI timing is fine-tuned and is an ideal alternative to operate with biodiesel fuel.

Keywords: NOx, injection timing, split injection, biodiesel, particulate matter

KAJIAN PARAMETER PANCITAN BAHAN API UNTUK EMISI EKZOS RENDAH DARI ENJIN DIESEL REL SEPUNYA DENGAN CAMPURAN BIODIESEL YANG BERBEZA

ABSTRAK

Pada masa kini, penggunaan enjin diesel meningkat secara mendadak disebabkan kebaikannya dari segi penjimatan bahan api yang unggul, kecekapan yang lebih tinggi dan kebolehpercayaan yang sangat baik. Krisis kesusutan tenaga bahan api fosil, kenaikan harga diesel dan kemerosotan alam sekitar telah mencetuskan penemuan bahan api yang bersih, mampan dan alternatif untuk enjin pembakaran dalaman. Biodiesel merupakan bahan api alternatif yang paling menjanjikan kerana ia adalah bahan api yang mesra alam, tidak beracun dan boleh diperbaharui. Kajian ini bertujuan untuk menghasilkan biodiesel daripada bahan mentah yang berlainan seperti minyak kelapa, *calophyllum inophyllum* dan *moringa oleifera* dan kajian dilakukan dengan enjin diesel empat-silinder berkuasa sederhana. Di samping itu, biodiesel kelapa yang dihasilkan juga digunakan dalam kajian terhadap kesan campuran biodiesel, masa pancitan bahan api, pancitan berbilang pisah, sudut inap pancitan dan nisbah jisim pada prestasi enjin, pelepasan ekzos dan ciri-ciri pembakaran. Pada peringkat pertama, penyiasatan dan pencirian sifat-sifat fizikal dan kimia yang terperinci terhadap biodiesel-biodiesel dan diesel telah dijalankan. Ini diikuti dengan penganalisis terhadap kesan penggunaan kesemua campuran biodiesel pada prestasi enjin, pelepasan, jirim zarahan ekzos dan pembakaran di bawah keadaan operasi enjin yang berbeza. Pada peringkat kedua, kajian berparameter yang berkaitan dengan perubahan pemasaan pancitan dan pelbagai skim pancitan dengan menggunakan campuran biodiesel kelapa COB20 dan COB50 telah dilakukan dan dibandingkan dengan diesel konvensional. Pada peringkat akhir, kesan perubahan sudut inap dan nisbah jisim dalam pancitan berperingkat-dua terhadap prestasi enjin, pelepasan ekzos dan ciri-ciri

pembakaran dengan menggunakan campuran biodiesel kelapa telah dikaji. Keputusan eksperimen menunjukkan bahawa kesemua bahan api biodiesel dan campurannya mempunyai sifat fizikokimia yang hampir dengan diesel petroleum. Keputusan eksperimen juga mencadangkan terdapat beberapa penalti dalam kuasa brek enjin, brek penggunaan bahan api tertentu (BSFC), dan oksida nitrogen (NOx) yang disebabkan dengan kehadiran bahan api biodiesel dalam campuran. Keputusan eksperimen peringkat kedua menunjukkan bahawa tahap pelepasan NOx yang rendah di bawah 100 ppm boleh dicapai dengan melengahkan masa pancitan SOI untuk kedua-dua operasi dengan bahan api COB20 dan COB50 dan dengan skim pancitan tigaan. Pancitan berbilang pisah adalah strategi praktikal untuk mengurangkan NOx dan pelepasan asap secara serentak dengan masa pancitan SOI diperhalusi dan merupakan alternatif yang unggul untuk beroperasi dengan bahan api biodiesel. Untuk pengujian tahap terakhir, keputusan eksperimen menunjukkan bahawa pelepasan ekzos, prestasi enjin dan ciri-ciri pembakaran terjejas dengan ketara oleh jenis bahan api dan pemasaan pancitan SOI tetapi sedikit dipengaruhi oleh perubahan sudut inap pancitan berperingkat-dua. Selain itu, tahap pelepasan NOx yang lebih rendah di bawah paras 90 ppm dapat dicapai melalui pemasaan pancitan SOI yang lewat untuk operasi bahan api biodiesel COB20 atau COB50 dengan nisbah jisim pancitan 25:75. Secara keseluruhannya, hasil kajian menunjukkan bahawa biodiesel daripada kelapa, *calophyllum inophyllum* dan *moringa oleifera* boleh digunakan dengan memuaskan dalam enjin diesel rel sepunya bertekanan tinggi tanpa pengubahsuaian. Selain itu, hasil eksperimen ini juga menunjukkan bahawa pancitan berbilang pisah dan berperingkat-dua dengan nisbah jisim yang berbeza dan sudut inap adalah strategi praktikal untuk mengurangkan pelepasan NOx dan asap apabila masa pancitan SOI diperhalusi dan merupakan alternatif yang unggul untuk beroperasi dengan bahan api biodiesel.

Kata kunci: NOx, masa pancitan, pancitan berbilang pisah, biodiesel, jirim zarahan

ACKNOWLEDGEMENTS

I would like to special thanks to my supervisors Professor Ir. Dr. Masjuki Hj. Hassan and Associate Prof. Dr. Md. Abul Kalam for their helpful guidance, encouragement and assistance. Without their help, progress could never have been made on this thesis. I also express my sincere gratitude to the Ministry of Higher Education (MOHE) for HIR Grant for the financial support through project no. UM.C/HIR/MOHE/ENG/07. I also would like to convey appreciation to all faculty members and staff of the Department of Mechanical Engineering, University of Malaya for giving opportunity to prepare and conduct this research. I also would like to thank to all my research group and friends for their valuable support, ideas and discussion. Additional thanks to Mr. Sulaiman Ariffin and Mr. Kamarul Bahrin Bin Musa for their technical help and assistance.

A special thanks to my family members, beloved husband, Teoh Yew Heng and lovely son, Teoh Chun Yuan. Words cannot express how grateful I am to them for all of the encouragement, support and sacrifices that they have made on my behalf.

TABLE OF CONTENTS

LIST OF FIGURES

LIST OF TABLES

LIST OF NOTATIONS AND ABBREVIATIONS

°CA	Degree crank angle
λ	Relative air-fuel ratio
ASTM	American Society for Testing and Materials
ATDC	After top dead center
B2	2% biodiesel + 98% petroleum diesel by volume
B2.5	2.5% biodiesel + 97.5% petroleum diesel by volume
B5	5% biodiesel + 95% petroleum diesel by volume
B10	10% biodiesel + 90% petroleum diesel by volume
B20	20% biodiesel + 80% petroleum diesel by volume
B30	30% biodiesel + 70% petroleum diesel by volume
B40	40% biodiesel + 60% petroleum diesel by volume
B50	50% biodiesel + 50% petroleum diesel by volume
B60	60% biodiesel + 40% petroleum diesel by volume
B80	80% biodiesel + 20% petroleum diesel by volume
B100	100% biodiesel
BMEP	Brake mean effective pressure
BSCO	Brake specific carbon monoxide
BSEC	Brake specific energy consumption
BSFC	Brake specific fuel consumption
BSNOx	Brake specific nitrogen oxide
BTDC	Before top dead center
BTE	Brake thermal efficiency
CA10	Mass fraction burned of 10%
CA50	Mass fraction burned of 50%
CA90	Mass fraction burned of 90%
CFPP	Cold filter plugging point
CI	Compression ignition
CIB	*Calophyllum inophyllum* biodiesel
CIB10	10% *calophyllum inophyllum* biodiesel + 90% petroleum diesel by volume
CIB20	20% *calophyllum inophyllum* biodiesel + 80% petroleum diesel by volume
CIB30	30% *calophyllum inophyllum* biodiesel + 70% petroleum diesel by volume
CIB50	50% *calophyllum inophyllum* biodiesel + 50% petroleum diesel by volume
CO	Carbon monoxide
CO_2	Carbon dioxide
COB	Coconut biodiesel
COB10	10% coconut biodiesel + 90% petroleum diesel by volume
COB20	20% coconut biodiesel + 80% petroleum diesel by volume
COB30	30% coconut biodiesel + 70% petroleum diesel by volume
COB50	50% coconut biodiesel + 50% petroleum diesel by volume
COME	Canola oil methyl ester
DI	Direct injection
ECM	Electronic control module

ECU	Electronic control unit
EN	European standards
FAME	Fatty acid methyl ester
FFA	Free fatty acid
GHG	Greenhouse gas
HC	Unburned hydrocarbon
HRR	Heat release rate
ID	Ignition delay
IMEP	Indicated mean effective pressure
KOH	Potassium hydroxide
MOB	*Moringa oleifera* biodiesel
MOB10	10% *moringa oleifera* biodiesel + 90% petroleum diesel by volume
MOB20	20% *moringa oleifera* biodiesel + 80% petroleum diesel by volume
MOB30	30% *moringa oleifera* biodiesel + 70% petroleum diesel by volume
MOB50	50% *moringa oleifera* biodiesel + 50% petroleum diesel by volume
Mtoe	Million tons of oil equivalent
NaOH	Sodium hydroxide
NO	Nitric Oxide
NOx	Nitrogen Oxide
PAHs	Polycyclic aromatic hydrocarbons
PM	Particulate matter
rpm	Revolution per Minute
RSM	Response surface methodology
SOC	Start of combustion
SOI	Start of injection
TDC	Top Dead Center
UHC	Unburned hydrocarbons
ULSD	Ultra low sulfur diesel
WPOME	Waste palm oil methyl ester

CHAPTER 1: INTRODUCTION

1.1 Background

The worldwide energy consumption rate is currently growing rapidly than the population growth rate, and is becoming a critical global issue. It has been reported that over the last 35 years, global primary fuel consumption has doubled (Wu & Chen, 2017). Most of the growth is in consumption of renewable sources such as wind, geothermal, solar, biomass, waste and etc has reached approximately 419.6 Mtoe in 2016, which is around 100 times higher than that in 1975 as shown in Table 1.1 (British Petroleum (BP), 2017). The worldwide energy consumption is heavily dependent upon fossil fuels which account for 85.5% whereby with crude petroleum oil consisting of 33.3%, natural gas 24.1% and coal 28.1% in 2016. The demand for the fossil fuel continues to increase steadily and most terrifyingly, it is predicted that the reserves of liquid crude oil will only able to serve just over half of usual demand by 2023 (Owen et al., 2010). The projected global energy demand of fuels by 2040 is presented in Figure 1.1 (Colton, 2014). Overall, the average growth of global energy demand is predicted about 1.0% per annum from 2010-2040.

Table 1.1: World primary energy consumption (British Petroleum (BP), 2017)

Source	1975		2016	
	Mtoe	Share (%)	Mtoe	Share (%)
Petroleum	2692.2	47.0	4418.2	33.3
Natural Gas	1064.0	18.6	3204.1	24.1
Coal	1562.1	27.3	3732.0	28.1
Nuclear Energy	82.4	1.4	592.1	4.5
Hydro electric	324.3	5.7	910.3	6.9
Renewables	4.2	0.1	419.6	3.2
Total	5729.2	100.0	13276.3	100.0

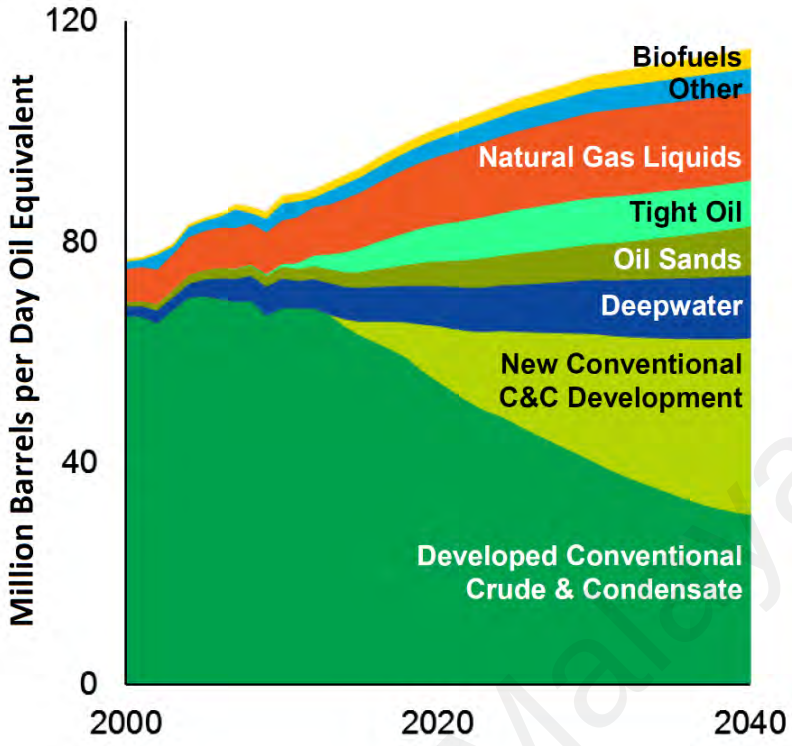

Figure 1.1: Projected world energy demand (Colton, 2014)

Moreover, petroleum fuel is one of the major contributors to environmental pollution and has adverse effects on human health. According to World Health Organization estimates, urban air pollution causes approximately 360,000 premature deaths in Asia each year (Stone et al., 2010). The main harmful pollutant from fossil fuel is carbon dioxide (CO_2), carbon monoxide (CO), nitrogen oxide (NOx), unburned hydrocarbon (HC), particulate matter (PM) and volatile organic compounds. CO_2 is an important global greenhouse gas (GHG) contributor and the trend has increased rapidly. Figure 1.2 presents the CO_2 emissions starting from 1980 and projected up to 2050. It is reported that global energy-related CO_2 emissions reached around 30.6 gigatonnes in 2010. However, if without more ambitious policies to reduce the GHG emission, it is predicted that GHG emissions will increase by another 50% by 2050, primarily driven by a projected 70% growth in CO_2 emissions from energy use (OECD, 2011). The primary cause of sea level rise is due to global warming and it is predicted that if the average

global temperature increases by more than 2 °C, hundreds of millions of people could lose their lives and up to one million species could become extinct (Ahmad 2011).

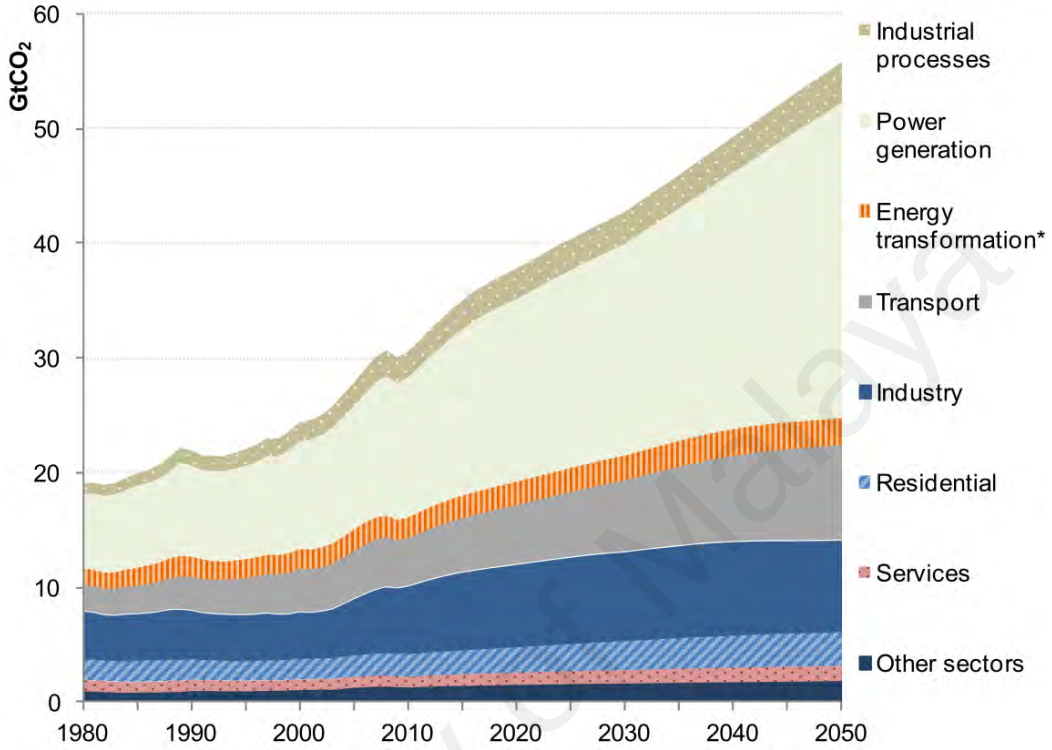

*Energy transformation includes emissions from oil refineries, coal and gas liquefaction

Figure 1.2: Global CO_2 emissions by source, from 1980-2050 (OECD, 2011)

Declining reserves of fossil fuels, as well as recognition that environmental pollution results from burning petroleum diesel fuels, have generated substantial interest in searching alternative renewable energy resources that can reduce dependence on petroleum and are friendly to the environment. In the transportation sector, one of the most promising solutions is the marginal replacement of diesel by biodiesel (Jayed et al., 2011). Biodiesel offers a very promising alternative because it can be used in diesel engine with little or no modification (Graboski & McCormick, 1998; Ramadhas et al., 2004). The use of biodiesels also creates positive impacts on the environment compared with fossil diesel. Many studies have reported substantial reductions in HC, CO and PM emissions from engines operating with biodiesel blends (He et al., 2010; Kannan et al.,

2011; Macor et al., 2011). In additions, biodiesel helps to mitigate global warming and a biodiesel life cycle study pointed out that replacing diesel by biodiesel could decrease net CO_2 emissions by 78.45% (Coronado et al., 2009).

1.2 Energy status in Malaysia

Malaysia is a developing country in Southeast Asia and it has a total landmass of 330,290 square kilometers and population of 32 million in 2017. Malaysia's energy supply mainly depend on crude oil, natural gas and coal as shown in Figure 1.3. Malaysia's total primary energy demand almost doubles from 89 Mtoe in 2013 to 160 Mtoe in 2040. The demand grows at an average annual rate of 2.2% per year. Fossil fuels remain dominant which 95% of total primary energy demand, leading by natural gas (42%), crude oil (36%) and coal (17%) in 2013 (International Energy Agency (IEA), 2017). As Malaysia has faced challenges in sustaining production of fossil fuel, Malaysia government has try to diversify its energy mix and looking for more reliable energy source for domestic demand. The potential renewable energy in Malaysia is hydropower, bioenergy, solar PV and wind. However, hydropower is the only renewable energy technology that is commercially viable on a large scale in Malaysia. Other renewable source such as biodiesel, solar PV and biomass is getting more demanding recently.

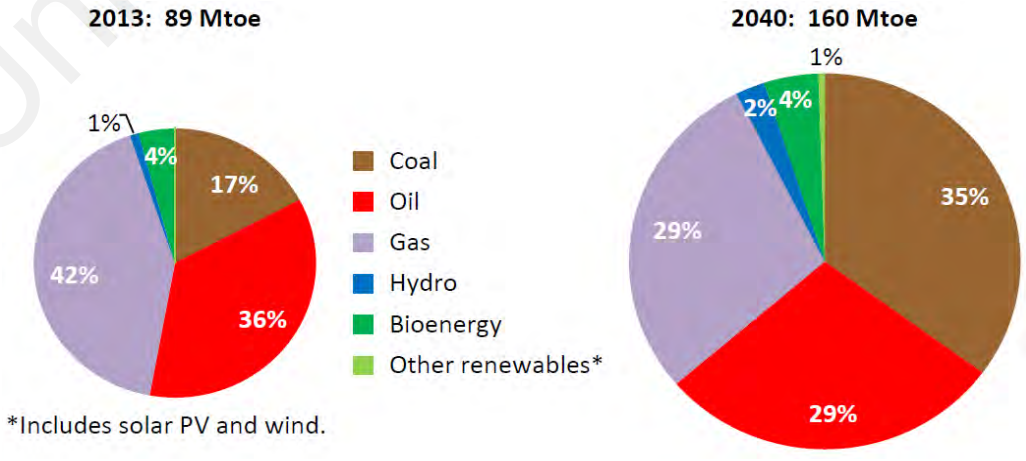

Figure 1.3: Fuel shares in primary energy demand in Malaysia (International Energy Agency (IEA), 2017)

1.3 Problem statement and motivation

Biofuels from bio-based products can be considered as an alternative substitute for fossil fuels used in transport sector because it is a renewable, non-toxic, sulphur-free, biodegradable and oxygenated fuel. However, edible oil as biodiesel feedstock has raised concerns such as food issue and environmental problems with serious destruction of vital soil resources and deforestation (Koh & Mohd. Ghazi, 2011). Therefore, the exploration of non-edible crops and the utilization of by products in the biodiesel production may significantly reduce the cost of biodiesel especially in developing countries which can hardly afford the high cost of edible oils. Thus, *calophyllum inophyllum* and *moringa oleifera* are non-edible second generation feedstock which are able to substitute diesel due to the availability, sustainability and competitive feedstock price.

Besides, the main drawbacks of vegetable oils are their high viscosity and low volatility properties which lead to an increase in smoke emissions, poor atomization, incomplete combustion and deposit formations on the injector or cylinder walls (Prasad et al., 2000; Sahoo & Das, 2009). Therefore, transesterification process is the most popular and preferred to convert vegetable oil to form biodiesel for reducing the viscosity of the oil and improving other fuel properties for better combustion efficiency (Leung et al., 2010; Suryawanshi, 2006a). In additions, the insufficient in-cylinder air motion, poor atomization and low volatility of biodiesel will lead to lower thermal efficiency, poorer combustion and higher emissions of biodiesel-fuelled diesel engines.

Moreover, the utilization of biodiesel in diesel engines has usually produced higher NOx and brake specific fuel consumption (Al-Dawody & Bhatti, 2013; Palash et al., 2013b; Rahman et al., 2013). Using alternative fuels and optimization of fuel injection parameters in diesel engine can be reliable methods to solving this problem. In fact, split

injection strategy is a promising concept for NOx emission reduction not only for petroleum diesel, but also for biodiesels. However, the major challenge for this strategies is usually caused of higher smoke emission that result from low combustion temperature. Utilizing an oxygenated fuels such as biodiesel can be a good alternative to this complication, and yet these fuels are derived from renewable sources. In addition, a number of advanced diesel fuel injection engine research is currently being carried out worldwide, but not in Malaysia. This study would establish a good starting point for this kind of engine research in Malaysia, specifically dealing with the newest and promising approach of split injection and two-stage injection in mitigation of pollutant from a CI engine. Therefore, this research study focuses on the utilization of biofuels as alternative energy sources for engines operating in advanced multiple events combustion mode.

1.4 Aims and objectives

The primary objectives of the present study are as follows:

1. To produce and characterize physicochemical properties of biodiesel from crude coconut and compare with other non-edible source of *calophyllum inophyllum* and *moringa oleifera* oil.
2. To study and investigate the performance, exhaust gaseous emissions, particulate matter, and combustion characteristics of coconut, *calophyllum inophyllum* and *moringa oleifera* biodiesel blends in common-rail diesel engine.
3. To study and optimize the split injection parameters on engine performance, emissions and combustion characteristics using coconut biodiesel blends.
4. To investigate the impact of two-stage injection dwell angle and mass ratio on engine performance, emissions and combustion characteristics using coconut biodiesel blends.

1.5 Research novelty and contribution

The original contribution of the present study includes the development of various keys experimental setup, engine performance, emissions and combustion characteristics of biodiesels fuel in common-rail injection engine. Furthermore, this study also offers better understanding of the performance of edible (coconut) and non-edible (*calophyllum inophyllum* and *moringa oleifera*) biodiesel blended fuels in an engine equipped with high-pressure common-rail diesel engine without modification. Besides, the in-house produced coconut biodiesel fuel is used in an engine equipped with various promising NOx reduction strategies such as injection timing retardation, split injection strategies and two-stage injection with dwell angle and mass ratio variation. This will contribute to introducing of biodiesel fuel in advanced fuel injection engine. The summary for contributions of the present research is as follow:

1. Proposed alternative non-edible biodiesel (*calophyllum inophyllum* and *moringa oleifera*) feedstock as biodiesel-diesel blend fuel in an engine equipped with high-pressure common-rail multi-cylinder diesel engine without modification and compared with those from edible (coconut) biodiesel and baseline diesel. The important engine-out responses were studied and analyzed, especially on the aspect of exhaust particulate matter (PM).
2. Explored the impact of multiple injection, injection dwell angle and mass ratio on diesel and biodiesel engine performance, emissions and combustion characteristics.
3. Proposed of diesel engine operating in advanced injection mode and fueled with oxygenated fuel of biodiesel.
4. Established a good starting point for advanced fuel injection strategies in biodiesel engine research in Malaysia, especially dealing with the newest and promising

approach of split injection and two-stage injection in mitigation of pollutant from a diesel engine.

From the outcome of this study, a number of research papers have been published in the high impact internal journal and conference proceedings. The publication list is presented in Appendix A.

1.6 Scope of study

Scopes of this research work are as follow:

i. Produce biodiesel from edible coconut oil and non-edible feedstock of *calophyllum inophyllum* and *moringa oleifera* oil. The physicochemical properties of crude oil and the produced biodiesel have been measured and compared with ASTM D6751 and EN14214 standard. Moreover, the fatty acid composition of methyl ester has been also determined.

ii. Engine testing for common-rail direct injection (DI) diesel engine using various biodiesel blends and baseline diesel fuels. The engine-out responses were analyzed in term of engine performance, exhaust emissions, PM and combustion characteristics.

iii. Perform split injection and independent control of the injection parameters such as injection timing, injection duration, dwell angle, injection fuel mass ratio and number of injection per cycle in common-rail diesel engine.

iv. Analyze the effect of injection parameters variation on the engine performance, emissions and combustion characteristics for COB20 and COB50 blends and compare with baseline diesel.

1.7 Organization of dissertation

The dissertation is made up of five chapters. The organization of the chapters are organized as follows:

Chapter 1 presents the overview of the research topic. The chapter contains background of the current study, problem statement, objectives, scope of study and thesis outline.

Chapter 2 provides literature review for the objective based study. The chapter starts with the overview of related studies regarding renewable energy and biodiesel fuel, followed by describing feedstock of biodiesel, biodiesel production technologies, factor affecting transesterification process and biodiesel standard and specifications. A comprehensive review is done to examine the effect of biodiesel blends and injection parameters on engine performance, exhaust emissions and combustion characteristics in CI engine.

Chapter 3 describes the methodology of this study. In this section, a brief illustration of the used equipment for fuel properties characterization has been elaborated. Experimental apparatus setup includes engine setup, test bed configuration and instrumentation for acquiring exhaust emission, PM and combustion data have been also presented.

Chapter 4 is dedicated to show all the results of this study and the results have been discussed with reference to the previous studies.

Chapter 5 provides a summary of key findings in the light of the research and recommendations for future work.

CHAPTER 2: LITERATURE REVIEWS

2.1 Introduction

This chapter reviews major publications and reports that will provide insight and understanding about the topic and related issues. This chapter begin with an overview of biodiesel as an alternative energy source, then discuss the biodiesel feedstock and technologies of biodiesel production. Then a large number of selective literatures are reviewer in order to critically compare the effect of biodiesel blends and injection parameters on engine performance, exhaust emissions and combustion characteristics in a diesel engine.

2.2 Biodiesel as an emerging energy source

Today, diesel-powered engines are used worldwide for transportation, power generation, construction, agriculture, manufacturing and industry. The use of diesel engines is increasing rapidly owing to their superior fuel economy, higher efficiency, excellent reliability and lower CO_2 emissions. The energy crisis in fossil fuel reserves, the rising price of diesel, environmental degradation and global warming highlight the need to develop clean, sustainable and alternative fuels. Even a small amount of substitution in total fuel consumption by using alternative fuels will have a significant impact on the environment and the economy. Liquid bioenergy production from vegetable oils has gained great significance among various alternative fuels because it is a renewable, non-toxic, sulphur-free, biodegradable and oxygenated fuel (Canakci, 2007a; Chauhan et al., 2012; Karavalakis et al., 2011b).

Biodiesel is a monoalkyl ester derived from a variety of vegetable oils, animal fats or waste edible oil. Nowadays, biodiesel has gained international acceptance and has been adopted worldwide as a substitute for petroleum diesel (Chang & Su, 2010). For

examples, biodiesel fuel B2 (in a volume fraction of 2% biodiesel blends and 98% diesel) is available in the USA and Brazil. In France, biodiesel is used in a volume fraction of 5% in diesel blends. Furthermore, a variety of biodiesel blends ratio is mandated in Asia, such as Malaysia (B5), Thailand (B5), Indonesia (B2.5), Philippines (B2), Taiwan (B2) and South Korea (B2). For example, as one of the main palm oil producer, Malaysian government has introduced and implemented B5 mandate which is 5% of palm oil methyl ester in diesel fuel in selected fuel station and regions of the country since mid 2011. It is predicted that a higher fraction volume of biodiesel will be introduced and implemented widely in the near future (Fernanda Pimentel et al., 2006; Higgins, 2012; Ozawa et al., 2011; Zhou & Thomson, 2009). Biodiesel feedstock vary in origin depending on the availability of local feedstock, regional climate, geographic locations and soil conditions (Atabani et al., 2012). Soybean is major feedstock for biodiesel production in the USA, while sunflower and rapeseed are the main raw materials for producing biodiesel in Europe. In Asia, palm oil, coconut and Jatropha are the main feedstock for biodiesel sources.

2.3 Advantages and disadvantages of biodiesel

There are some advantages of using biodiesel as substitute of diesel because it is renewable, nontoxic, non-flammable, portable, biodegradable, environment friendly and free from sulphur content, which makes it an ideal fuel for heavily polluted cities (Bozbas, 2008; Demirbas, 2007). The major advantage of using biodiesel is it can be used in a diesel engine without require engine modification up to B20. However, higher blends biodiesel may need some minor engine modification (Jain & Sharma, 2010). Compared to diesel fuel, biodiesel has 10-11% more oxygen which ensures higher combustion efficiency in CI engine. Biodiesel contains higher cetane number than diesel which reduces the ID (Atadashi et al., 2012; Balat & Balat, 2010). Also, biodiesel contains higher flash point compared to diesel, which makes it safe for handling, transportation,

distribution, utilization and storage (Demirbas, 2009; Shahid & Jamal, 2008). Biodiesel has better lubricity properties which improves lubrication in fuel pumps and injector units thus decreases wear and tear of engine and improves engine efficiency (Bozbas, 2008).

However, there are several drawbacks of using biodiesel as an alternative source of energy in internal combustion engine. Biodiesel exhibits 12% lower energy contents, which results in increase in fuel consumption compared to diesel fuel (Mofijur et al., 2015). Biodiesel are predominantly produced from edible oil, which conflicts with food supply availability and increase food prices. Besides, density of biodiesel is usually higher than diesel fuel, hence blending with fossil diesel fuel is needed especially in sub-freezing conditions (Murugesan et al., 2009b; Sharma et al., 2012). Oxidation stability of biodiesel is lower than that of diesel. Therefore, it can be oxidized into fatty acids in the presence of air and causes corrosion of fuel tank, pipe and injector (Fazal et al., 2011; Murugesan et al., 2009a). Furthermore, biodiesel usually emits higher NOx compared to diesel fuel. As more than 95% of biodiesel is made from edible oil, large scale production of biodiesel from edible oils for automotive fuel may cause global imbalance in the food supply and demand market problem.

2.4 Biodiesel feedstock

A considerable amount of research has been conducted on alternative feedstock for biodiesel production all over the world. In order for the biodiesel to remain competitive compare to petroleum-derived diesel, choosing an appropriate feedstock is vital issue to ensure a low production cost and large production scale (Silitonga et al., 2013). In general, biodiesel feedstock can be categorized into four main categories: (i) edible vegetable oil, (ii) non-edible vegetable oil, (iii) waste or recycled oil and (iv) animal fats. Feedstock from edible oil such as palm oil, rapeseed, soybeans, sunflower are considered to be first generation biodiesel feedstock because they were the first crops to be used to produce

biodiesel (Ahmad et al., 2011). Energy crops from non-edible oils and waste cooking oil are regarded as second generation biodiesel feedstock. Microalgae are classified as third generation biodiesel feedstock and have emerged as one of the most promising alternative sources of lipid of use in biodiesel production due to their high oil yield and rapid biomass production (Ahmad, et al., 2011; Atabani, et al., 2012; Balat, 2011; Chisti, 2007). The main biodiesel feedstock is shown in Table 2.1 (Atabani, et al., 2012).

Table 2.1: Main feedstock of biodiesel (Atabani, et al., 2012)

Category	**Feedstock**
Edible oils	Soybeans (*glycine max*), rapeseed (*brassica napus L*), rice bran oil (*oryzasativum*), barley, sesame (*sesamum indicum L.*), groundnut, sorghum, wheat, corn, coconut, canola, peanut, palm and palm kernel (*elaeis guineensis*), sunflower (*helianthus annuus*)
Non-edible oils	*Jatropha curcas,* mahua (*madhuca indica*), pongamia/karanja/honge (*pongamia pinnata*), camelina (*camelina Sativa*), cotton seed (*gossypium hirsutum*), neem (*azadirachtaindica*), jojoba (*simmondsia chinensis*), passion seed (*passiflora edulis*), moringa (*moringa oleifera*), coffee ground (*coffea arabica*), nagchampa (*calophyllum inophyllum*), *croton megalocarpus*, *pachira glabra*, *aleurites moluccana*, *terminalia belerica*
Animal fats	Pork lard, beef tallow, poultry fat, fish oil, chicken fat
Other sources	Bacteria, algae (*cyanobacteria*), microalgae (*chlorellavulgaris*), tarpenes, poplar, switchgrass, miscanthus, latexes, fungi

2.5 Technologies of biodiesel production

There are number of well-established methods for the production of biodiesel fuel from various vegetable oil feedstock. The use of straight vegetable oil in diesel engine is restricted by the high viscosity of vegetable oil (Demirbas, 2010; Misra & Murthy, 2010). High viscosity of the vegetable oil will cause poor fuel atomization, injector cocking, deposits in combustion chamber and injector tip, injector pump failure, clogged filters and etc (Agarwal et al., 2010; Sidibé et al., 2010). There is a need of refinement to turn those vegetable oils into quality biodiesel fuel. This can be accomplished in four primary

methods; dilution, pyrolysis, micro-emulsion and transesterification (Jain & Sharma, 2010; Lin et al., 2011a). A comparison of main biodiesel production technologies is shown in Table 2.2. The flow chart shown in Figure 2.1 describes the ways of producing biodiesel from non-edible oil source.

Table 2.2: Comparison of main biodiesel production technologies (Lin, et al., 2011a; Verma & Sharma, 2016)

Technologies	**Advantage**	**Disadvantage**
Dilution (direct blending)	1. Simple process 2. Liquid nature-portability 3. Readily available 4. Renewability	1. High viscosity 2. Bad volatility 3. Bad stability 4. Reactivity of unsaturated hydrocarbon chains
Micro-emulsion	1. Lower fuel viscosity 2. Better spray patterns during combustion	1. Lower energy content 2. Lower cetane number
Pyrolysis	1. Simple process 2. No-polluting	1. High temperature is required 2. Equipment is expensive 3. Low purity
Transesterification	1. Fuel properties is closer to diesel 2. High conversion efficiency 3. Low cost 4. Suitable for industrialized production 5. Renewability	1. Low free fatty acid (FFA) and water content are required (for base catalyst) 2. Pollutants will be produced because products must be neutralized and washed 3. Accompanied by side reactions 4. Difficult reaction products separation
Supercritical methanol	1. No catalyst 2. Short reaction time 3. High conversion 4. Good adaptability	1. High temperature and pressure are required 2. Equipment cost is high 3. High energy consumption

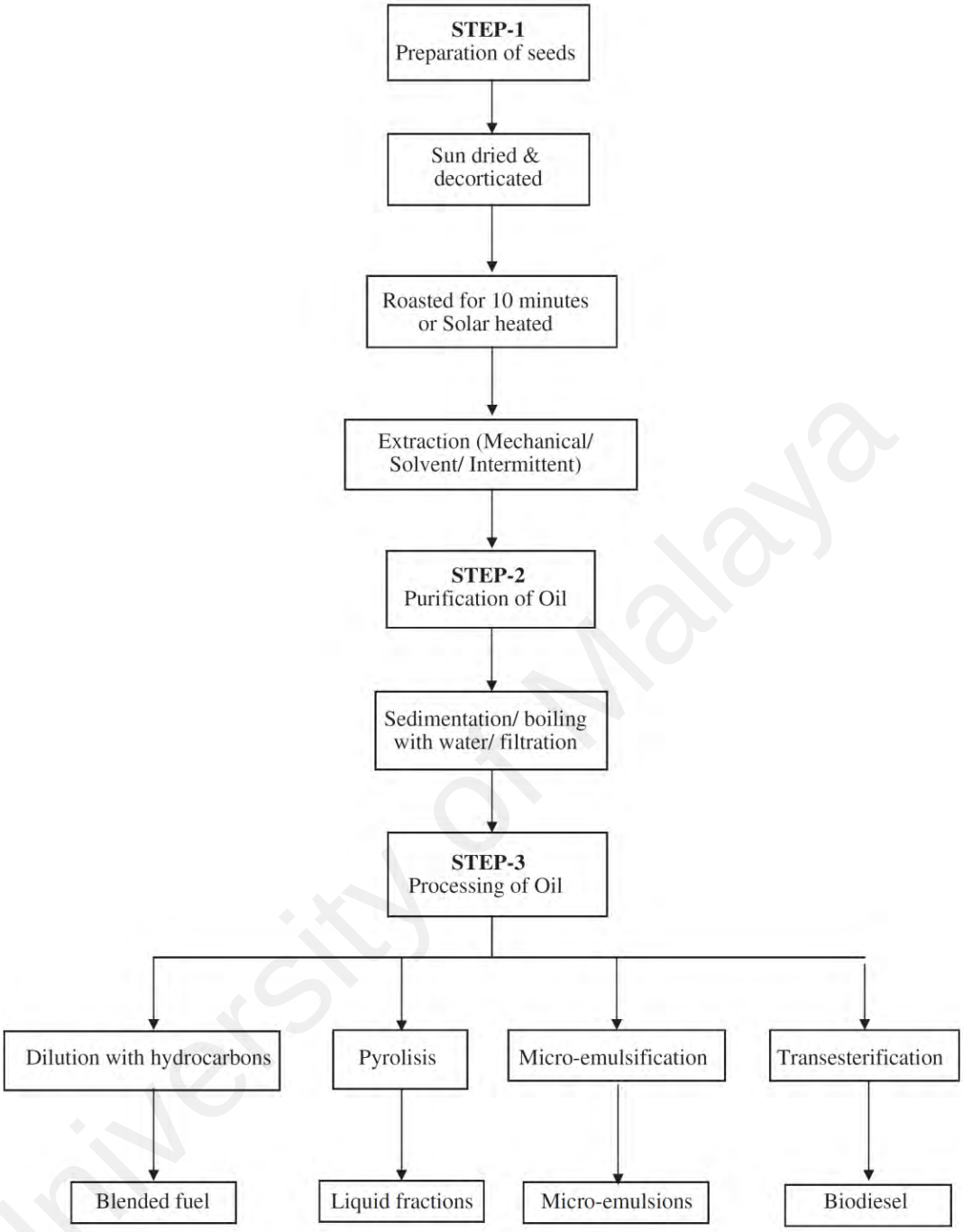

Figure 2.1: Process flowchart of non-edible crops seed to biodiesel (Atabani et al., 2013c)

2.5.1 Pyrolysis (Thermal cracking)

Pyrolysis is the process of thermal conversion of one substance into another by means of heat or with the aid of catalyst. It involves heating in the absence of air or oxygen and cleavage of chemical bonds to yield small molecules. The pyrolyzed material can be vegetable oils, animal fats, natural fatty acids and methyl esters of fatty acids. The liquid

fractions of the thermally decomposed vegetable oil are likely to approach diesel fuels. Pyrolysis of the vegetable oil can produce a product with low viscosity, equivalent calorific values, and contain acceptable amounts of sulphur, water and sediment and copper corrosion values. However, the cetane number of the pyrolyzate is lower and unacceptable amounts of ash contents, carbon residues, flash point and pour points can be produced in this process. Engine testing on pyrolysed oil has been limited to short-term tests (Jain & Sharma, 2010; Ma & Hanna, 1999a; Mahanta & Shrivastava, 2004; Srivastava & Prasad, 2000). This process is simple, pollution free, waste less and effective (Singh & Singh, 2010).

2.5.2 Micro-emulsification

The formation of micro-emulsions (co-solvency) is one of the potential solutions for solving the problem of vegetable oil viscosity. Micro-emulsion is defined as transparent, thermodynamically stable colloidal dispersion of optically isotropic fluid microstructures with dimensions generally in the 1±150 nm range. Micro-emulsions are clear, stable isotropic fluids with three components: an oil phase, an aqueous phase and a surfactant. The aqueous phase may contain salts or other ingredients, and the oil may consist of a complex mixture of different hydrocarbons and olefins. This ternary phase can improve spray characteristics by explosive vaporization of the low boiling constituents in the micelles. Micro-emulsion can be made of vegetable oils with an ester and dispersant (co-solvent), or of vegetable oils, an alcohol and a surfactant and a cetane improver, with or without diesel fuels. All micro-emulsions with butanol, hexanol and octanol can meet the maximum viscosity limitation for diesel engines (Jain & Sharma, 2010; Koh & Mohd. Ghazi, 2011; Singh & Singh, 2010).

2.5.3 Dilution

The possibility of direct use of vegetable oils as fuel has been recognized since the beginning of the diesel engine. In 1893, Rudolf Diesel, the inventor of the diesel engine successfully demonstrated an diesel engine wholly on peanut oil at the Paris Exposition. However, the straight use of vegetable oils to replace conventional fuels meets operational problems due to its high viscosity. Therefore, vegetable oils can be diluted and blended with diesel fuel in order to reduce the viscosity and density of vegetable oil. This method does not require any chemical process (Balat & Balat, 2010). Engines that utilize vegetable oil-diesel blends tend to perform better in longevity tests than straight vegetable oil fuelled engines (Basinger et al., 2010). It was reported that blending of 20-25% vegetable oil to diesel has been considered to give good results for diesel engine (Agarwal, 2007; Balat & Balat, 2008; No, 2011; Singh & Singh, 2010).

2.5.4 Esterification and transesterification (alcoholysis)

Transesterification is the most common method of converting oil into biodiesel and it has been widely used to reduce the viscosity of triglycerides due to its high conversion efficiency and low cost (Lin, et al., 2011a). Transesterification is also called alcoholysis, is the chemical reaction between triglycerides and alcohol in the presence of catalyst to produce mono-esters that are termed as biodiesel. Transesterification process consists of three consecutive reversible reactions, they are conversion of triglycerides to diglycerides, followed by the conversion of diglycerides to monoglycerides. The glycerides are then converted into glycerol and yielding one ester molecule in each step (Ramadhas et al., 2005). The overall transesterification reaction can be represented in Figure 2.2.

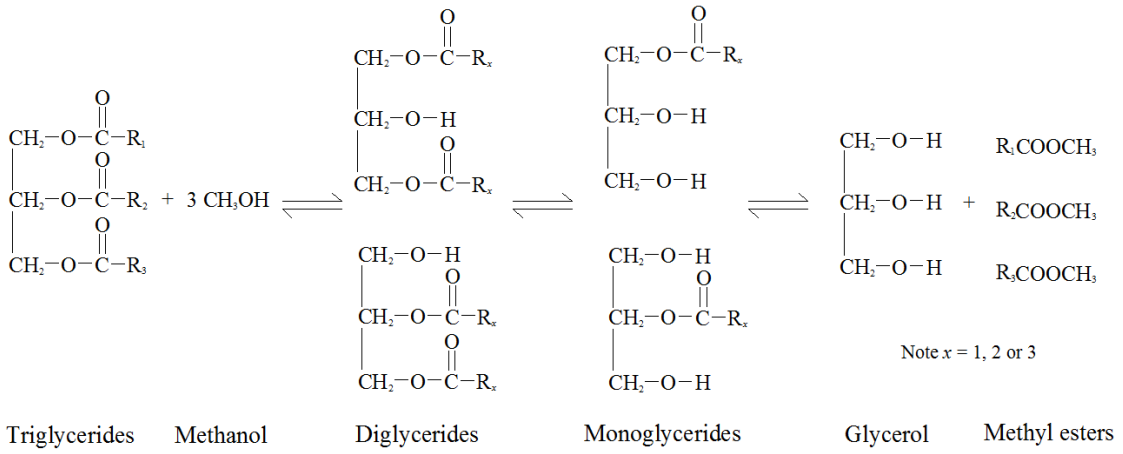

Figure 2.2: Transesterification reaction

The transesterification reaction proceeds with catalyst or without any catalyst by using primary or secondary monohydric aliphatic alcohols having 1–8 carbon atoms. The alcohols employed in the transesterification are generally short chain alcohols such as methanol, ethanol, propanol, butanol and amyl alcohol. However, methanol is preferred and generally used commercially among the other alcohols because of its low cost and its physical and chemical advantages as polar and short chain alcohol (Demirbas, 2005). In addition, methanol can also react with triglycerides quickly and easily dissolve the alkali catalyst. However, due to its low boiling point, there is a large explosion risk associated with methanol vapors which are colorless and odorless. Therefore, it should be handled carefully during biodiesel production (Leung, et al., 2010).

Generally, there are two common ways for transesterification reaction, such as, catalytic and non-catalytic transesterification. Catalytic transesterification method includes: base-catalysis, acid catalysis and enzyme catalysis. On the other hand, non-catalytic transesterification process includes: supercritical alcohol and BIOX-co solvent.

2.5.4.1 Catalytic transesterification

(a) Acid catalyzed transesterification

The acid catalyzed process is the reaction of a triglyceride (fat/oil) with an alcohol in the presence of acid catalyst preferably sulphonic and sulphuric acids to form esters (biodiesel) and glycerol. These catalysts is used to reduce FFA contents and increase high yields in alkyl esters, but the reactions are slow, requiring, typically, temperatures above 100°C.The acid-catalyzed transesterification should be carried out in the absence of water, in order to avoid the competitive formation of carboxylic acids which reduce the yields of alkyl esters (Demirbas, 2005; Mahanta & Shrivastava, 2004).

(b) Alkaline catalyzed transesterification

The alkaline catalyzed transesterification process is the reaction of a triglyceride (fat/oil) with an alcohol in the presence of alkaline catalyst such as alkaline metal alkoxides and hydroxides as well as sodium or potassium carbonates to form esters (biodiesel) and glycerol. The alkaline catalyzed transesterification of vegetable oils proceeds faster than the acid catalyzed reaction. Due to this reason, together with the fact that the alkaline catalysts are less corrosive than acidic compounds, industrial processes usually favor alkaline catalysts, such as alkaline metal alkoxides and hydroxides as well as sodium or potassium hydroxides, carbonates or alkoxides. However, the alkaline catalyzed transesterification is quite sensitive to the presence of water and FFA and required more methanol. The presence of water and high amount of free acid in the feedstock cause saponification of oil and therefore, incomplete reaction during alkaline transesterification process with subsequent formation of emulsion and difficulty in separation of glycerol (Lin, et al., 2011a; Mahanta & Shrivastava, 2004).

(c) Lipase catalyzed transesterification

The lipase catalyzed transesterification process is the reaction of a triglyceride (fat/oil) with an alcohol in the presence of lipase enzyme as a catalyst to form esters (biodiesel) and glycerol. The transesterification is typically catalyzed by lipases such as Candida antaritica, Candida rugasa, Pseudomonas cepacia, immobilized llipas (Lipozyme RMIM), Pseudomonas spp. or Rhizomucar miehei. In lipase catalyzed process no complex operations are needed not only for the recovery of glycerol but also in the elimination of catalyst and soap. This is an environmentally more attractive option to the conventional process. However, the reaction yields as well as the reaction times are still unfavorable compared to the alkaline catalyzed reaction systems (Balat & Balat, 2010; Lin, et al., 2011a; Mahanta & Shrivastava, 2004).

2.5.4.2 Non-catalytic transesterification

(a) Super critical transesterification

The simple chemical transesterification processes discussed above are confronted with two problems, i.e. the processes are relatively time consuming and needs separation of the acid or alkaline catalyst and saponified impurities from the biodiesel. These problems are not faced in the supercritical method of transesterification. In this method, vegetable oil or fats are treated in subcritical water for hydrolysis reaction to reduce fatty acids. After hydrolysis, the reaction mixture is separated into oil phase and water phase by decantation. The oil phase (upper portion) is mainly fatty acids, while the water phase (lower portion) contains glycerol in water. The separated oil phase is then mixed with methanol and treated at supercritical condition (at 340°C and 43 MPa) to produce methyl esters through esterification. After removing unreacted methanol and water produced in reaction, fatty acid methyl ester (FAME) can be obtained as biodiesel. The non-catalytic supercritical methanol process is advantageous in terms of shorter reaction time and lesser purification steps but requires high temperature and pressure. Further, since no catalyst is

used, the purification on biodiesel is much easier, trouble free and environment friendly (Balat & Balat, 2010; Mahanta & Shrivastava, 2004).

(b) BIOX-co solvent

Co-solvent options are designed to overcome slow reaction time caused by the extremely low solubility of the alcohol in the triglyceride phase. One approach that is nearing commercialization is the BIOX process. This process uses either tetrahydrofuran or methyl tert-butyl ether as a co-solvent to generate a one-phase system. The result is a fast reaction and no catalyst residues in either the ester or the glycerol phase. The tetrahydrofuran co-solvent is chosen, in part, because it has a boiling point very close to that of methanol. This system requires a rather low operating temperature, 303 K (Balat & Balat, 2010).

2.6 Factors affecting the transesterification reaction

Transesterification reaction is quite sensitive to various parameters. The reaction is either incomplete or the yield is reduced to a significant extent if the parameters are not optimised. The most imperative factors affecting the transesterification reaction are mentioned below:

1. FFA content
2. Moisture and water content
3. Alcohol and molar ratio employed
4. Types and amount of catalysts
5. Reaction temperature
6. Rate and mode of stirring
7. Purification of the final product

2.6.1 FFA content

The FFA is key parameters for determining the viability of the vegetable oil transesterification process. FFA is the saturated or unsaturated monocarboxylic acids that occur naturally in fats, oils or greases. Higher FFA content can lead to higher acid value and lower conversion efficiency. The FFA level in the oil should be below a desired limit (less than 3%) for alkaline transesterification process to take place. It was found that excess and insufficient of catalyst may cause soap formation instead of esters (Murugesan, et al., 2009a; Sharma & Singh, 2009).

2.6.2 Moisture and water content

The feedstock of oil being used for biodiesel production should be free from water content. Water content as low as 0.1% has been reported to decrease the ester conversion from vegetable oil (Canakci, 2007b). Srivastava and Verma reported the removal of moisture content of vegetable oil by heating it in oven for 1 hour at 110 °C (Srivastava & Verma, 2008).

2.6.3 Alcohol and molar ratio employed

Molar ratio of alcohol to vegetable oil is also an important parameter that affecting the yield of ester. The stoichiometry of the transesterification reaction required 3 mol of alcohol per mol of triglyceride to yield three mol of fatty ester and 1 mol of glycerol. Since transesterification is an equilibrium reaction, excess of alcohol is required to drive the reaction to the right completely. A molar ratio of 6:1 is normally used in industrial process because the yield of ester is higher than 98% by weight (Murugesan, et al., 2009a). The transesterification of cynara oil with ethanol was studied at molar ratios between 3:1 and 15:1 by Encinar et al. (Encinar et al., 2002). It was found that the best results are for molar ratios between 9:1 and 12:1. However, the use of a large excess of

alcohol can cause operating problems relevant to downstream process and difficulty in product recovery.

2.6.4 Types and amount of catalysts

Catalyst used for the transesterification of triglycerides is classified as alkali, acid, enzyme or heterogeneous catalysts. Among these alkali catalysts such as NaOH, NaOMe, KOH and KOMe are more effective. If the oil has high free acid and water content, acid catalyst is suitable, such as H2SO4, H3PO4, HCl or organic sulfonic acids. Alkali metal alkoxides are found to be more effective transesterification catalyst compared to the acid catalyst. Alkaline catalysts are preferred in industrial processes because it is less corrosive to industrial equipment. The concentration in the range of 0.5-1.0% (w/w) has found to yield 94-99% conversion of vegetable oils into ester (Murugesan, et al., 2009a).

2.6.5 Reaction temperature

The commonly employed temperature range for transesterification process is between 45 and 65 °C. Higher temperature will cause saponification and hence it must be avoided (Sharma et al., 2008). It was reported that the reaction temperature of 350 °C is considered as optimum condition while using supercritical methanol (Kusdiana & Saka, 2001).

2.6.6 Rate and mode of stirring

Stirring also plays an important role for biodiesel production. Mixing of reactants at 400 rpm with magnetic stirrer was performed by Veljković et al. (Veljković et al., 2006) to get the optimum yield. It was reported that the yield of biodiesel increased from 85% to 89.5% when magnetic stirrer was replaced with mechanical stirrer at same speed (1100rpm) (Sharma & Singh, 2008).

2.6.7 Purification of the final product

Impurities present in the oil also affect conversion level of biodiesel production. It was reported that higher conversion rate of esters can be obtained with 94 to 97% when using refined oils, compared to 67 to 84% conversion rate with crude vegetable oils (Srivastava & Prasad, 2000)

2.7 Biodiesel standard and specifications

The quality of biodiesel can be influenced by some factors such as the quality of feedstock, fatty acid composition of parent vegetable oil and animal fat, production process and the other materials used in this process, postproduction parameters and handling and storage conditions. Given the fact that most current diesel engines are designed to be powered by diesel fuel, the physicochemical properties of biodiesel should be similar to those of diesel oil. The quality standard for producing, storing and marketing of biodiesel are being technological advanced and employed worldwide in order to ensure consistency in biodiesel quality and meet the consumer expectations. Currently, the EU and the US standards are mostly followed by most of the biofuel producing countries. These standards are shown in Table 2.3.

Table 2.3: ASTM and EN specifications for biodiesel (B100)

Properties	ASTM D6751		EN 14214	
	Limit	**Method**	**Limit**	**Method**
Density	870-890 kg/m^3	ASTM D4052-91	860-900 kg/m^3	EN ISO 3675, EN ISO 12185
Flash point	130 °C minimum	ASTM D93	>101 °C minimum	EN ISO 3679
Viscosity @ 40°C	1.9-6.0 mm^2/s	ASTM D445	3.5-5.0 mm^2/s	EN ISO 3140
Cloud point	Report customer	ASTM D2500	Based on national specification	EN ISO 23015
Copper strip corrosion	Class maximum	ASTM D130	Class 1 rating	EN ISO 2160
Cetane number	47 (minimum)	ASTM D613	51 (minimum)	EN ISO 5165
Water content and sediment	0.050 (%v) maximum	ASTM D2709	500 mg/kgmaximum	EN ISO 12937
Acid number	0.50 mg KOH/g maximum	ASTM D664	0.50 mg KOH/g maximum	EN 14104
Free glycerin	0.02% (m/m) maximum	ASTM D6584	0.02% (m/m) maximum	EN 1405/14016
Total glycerol	0.24% (m/m) maximum	ASTM D6584	0.25% (m/m) maximum	EN 14105
Methanol content	0.20% (m/m) maximum	EN 14110	0.20% (m/m) maximum	EN 14110
Distillation temperature	360 °C	ASTM D1160	-	-
Oxidation stability	3 h minimum	EN ISO 14112	6 h (minimum)	EN ISO 14112
Carbon residue	0.05 maximum wt.%	ASTM D4530	0.30% (m/m) (maximum)	EN ISO 10370
Iodine number	-	-	120 g iod/100 g (maximum)	EN 14111
Heating value	Not specified	Not specified	Not specified	Not specified

2.8 Emissions regulation for diesel engine

Exhaust emissions from diesel engine have improved significantly over the last half-century due to the engine technology evolution, emission managements, and fuel quality improvement (Ouenou-Gamo et al., 1998). Diesel engines generates a variety of organic and inorganic compounds which exists in both gaseous and particulate phase with higher amounts of aromatics and sulfur. The particles have higher numbers of suspected mutagens and carcinogens chemicals adsorbed onto their surfaces. The gaseous phase also contains many toxic chemicals and irritants. These have serious adverse effects on human health and environmental impact (Ackerman et al., 2000; USEPA, 2002). The constitution of diesel exhaust differs considerably depending on type of engine, running conditions, fuel type, engine lube oil, and the present of exhaust after treatment. Typically, exhaust contains largely with PM, NOx, CO, unburned hydrocarbon (HC) and soot/ smoke. The worldwide emissions standards for passenger cars and light duty vehicles are shown in Figure 2.3 (Delphi, 2017). The European Union's criteria emissions regulations and limits for diesel engines are commonly known as Euro 1 to Euro 6. European emission standards define the acceptable limits for exhaust emissions of new vehicles sold in EU and EEA member states. The emission standards are defined in a series of European Union directives staging the progressive introduction of increasingly stringent standards as shown in Table 2.4. The most recent legislation, Euro 6d, is became effective in 01st September 2017. It also introduces emissions limits for new testing requirements under low temperature test condition (i.e. -7°C) and more strict on-board diagnostic (OBD) requirements. Recently, the Singapore government has just introduced regulations based on Euro 6 emission standard for motor vehicle beginning in 01st September 2017 (Paultan.org, 2017). Besides, Malaysia has begun adopting European emissions regulations for light-duty vehicles since 1997 and is targeting to implement Euro 5 by 2025 (Bernama, 2016; UNEP, 2013).

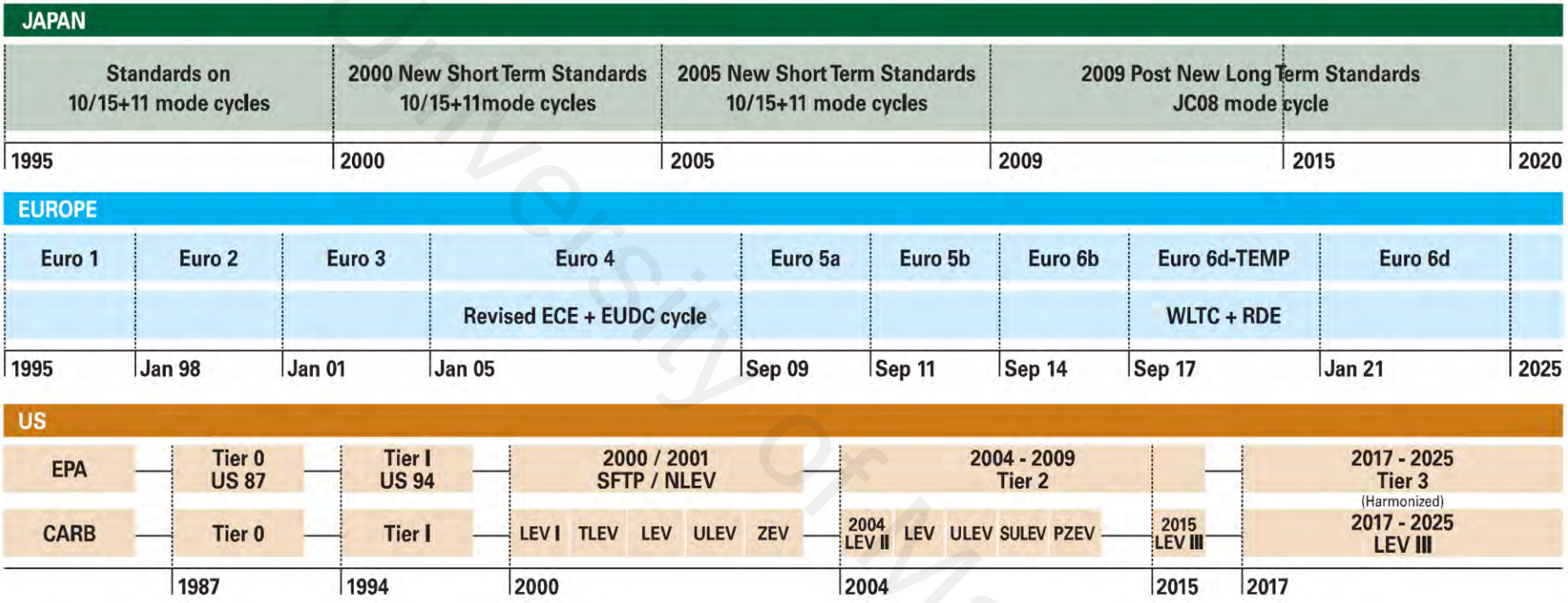

Figure 2.3: Toxic emissions standards passenger vehicle standards (Delphi, 2017)

Table 2.4: Euro exhaust emissions standards for steady-state heavy-duty diesel engines testing (DieselNet, 2017)

			CO	HC	NO_x	PM
Stage	**Date**	**Test**		**g/kWh**		
Euro I	1992, ≤ 85 kW	ECE R-49	4.5	1.1	8	0.612
	1992, > 85 kW		4.5	1.1	8	0.36
Euro II	1996.1		4	1.1	7	0.25
	1998.1		4	1.1	7	0.15
Euro III	1999.10 EEV only	ESC & ELR	1.5	0.25	2	0.02
	2000.1		2.1	0.66	5	0.10[a]
Euro IV	2005.1		1.5	0.46	3.5	0.02
Euro V	2008.1		1.5	0.46	2	0.02
Euro VI	2013.01	WHSC	1.5	0.13	0.4	0.01

[a] - PM = 0.13 g/kWh for engines < 0.75 dm^3 swept volume per cylinder and a rated power speed > 3000 rpm

2.9 Engine-out responses to biodiesel fuel

2.9.1 Impact of biodiesel on engine performance characteristics

Engine performance with biodiesel or its blends depends largely on the combustion, air turbulence, air–fuel mixture quality, injector pressure, engine operation conditions, fuel quality and origin, and other factors that make engine test results vary from one engine to another (Murillo et al., 2007). A number of studies have been conducted by evaluating engine performance parameters such as engine brake power/ torque, brake thermal efficiency, brake-specific fuel consumption or brake-specific energy consumption in biodiesel-fuelled engine.

Numerous investigations have been carried out by researchers around the world to evaluate the engine performance of different biodiesel blends. In general, calorific value of biodiesel is lower compared to diesel fuel. As a result use of biodiesel and its blends results in decreased engine performance and increased brake specific fuel consumption (BSFC). Sharon et al. (Sharon et al., 2012) compared the performance of diesel and palm oil methyl ester blends (B25, B50, B75 and B100) in a DI, naturally aspirated, single

cylinder engine. The results showed that the brake thermal efficiency (BTE) of diesel (30.90%) is higher than that of B25, B50, B75 and B100 biodiesel blends (30.56%, 29.22%, 28.65%, 29.58% and 28.65%) at full load condition. BSFC of B25, B50, and B75 was observed to be higher by 2.59%, 8.93% and 9.25% than diesel fuel respectively. Saravanan et al. (Saravanan et al., 2010) investigated engine performance of Mahua oil (Madhuca Indica) ester with diesel blend in a single cylinder, four stroke CI engine. The experiment results showed that the power loss was around 13% combined with 20% increase in fuel consumption with Mahua oil methyl ester at full load due to low heating value and high viscosity of biodiesel.

Buyukkaya (Buyukkaya, 2010) studied the effect of rapeseed oil biodiesel blends (B5, B20, B70 and B100) in a six cylinders, four-stroke, turbocharged DI diesel engine. The results indicated that there were no noticeable differences of the engine power output between diesel and B5 fuels. However, the measured brake power was lower for other biodiesel blends and all the rapeseed oil biodiesel blends showed negative effect on BSFC of the engine. It was found that B20 produced the best brake thermal efficiency of engine. The test results indicated that the only low concentration blends in terms of performance efficiency and environmentally friendly emissions (particularly for B20 and lower blends) could be recognized as the potential candidates to be certificated for full scale usage in unmodified diesel engines. Chauhan et al. (Chauhan, et al., 2012) tested Jatropha biodiesel (B5, B10, B20, B30 and B100) in a single cylinder, air cooled, DI Kirloskar DAF 10 diesel engine. The results revealed that increasing concentration of biodiesel in blends resulted in lower engine power and higher BSFC.

Contrast, several researchers reported that increment of brake torque and power when using biodiesel. Usta (Usta, 2005) conducted experiment in a four cylinder, four stroke turbocharged indirect injection diesel engine with different tobacco seed oil methyl ester

blends (10%, 17.5% and 25% by volume). The tobacco seed oil methyl ester blends resulted in slightly higher torque and power than the diesel fuel at full load due to its slightly higher density and viscosity as well as oxygen content in the fuel blends which generated more complete combustion. Altiparmak et al. (Altıparmak et al., 2007) tested the blends of tall oil methyl ester–diesel fuel in a DI diesel engine at full load condition. They observed that torque and engine power increased by 6.1% and 5.9%, respectively with tall oil methyl ester blends at high engine speeds. Similarly, Pal et al. (Pal et al., 2010) observed an increase in brake power, brake thermal efficiency and reduced BSFC with 30% biodiesel blend of Thumba oil biodiesel blend in a four cylinder, DI water cooled diesel engine. As shown in Table 2.5 provides an overview of impact of biodiesel on engine performance characteristics from the literature review.

Table 2.5: Findings on biodiesel and blends on engine performance characteristics

Biodiesel type	Engine type	Engine operating condition	Results	Ref.
Diesel and palm oil methyl ester blends (B25, B50, B75 and B100)	DI, naturally aspirated, single cylinder engine	At constant engine speed by varying loads (between 20% and 100%)	Brake thermal efficiency of diesel (30.90%) is higher than that of B25, B50, B75 and B100 biodiesel blends (30.56%, 29.22%, 28.65%, 29.58% and 28.65%) at full load condition. BSFC of B25, B50, and B75 was higher by 2.59%, 8.93% and 9.25% than diesel fuel respectively.	(Sharon, et al., 2012)
Mahua oil biodiesel	Single cylinder, four stroke CI engine	At different load conditions (0, 25, 50, 75 & 100%)	Power loss was around 13% combined with 20% increase in fuel consumption with Mahua oil methyl ester at full load.	(Saravanan, et al., 2010)
Rapeseed oil biodiesel blends (B5, B20, B70 and B100)	Six cylinders, four-stroke, turbocharged, DI diesel engine	Different engine speed with full load conditions	No noticeable differences of the engine power output between diesel and B5 fuels. Brake power was lower for other biodiesel blends and all the biodiesel blends showed negative effect on BSFC. B20 produced the best brake thermal efficiency of engine.	(Buyukkaya, 2010)
Jatropha (B5, B10, B20, B30 and B100) biodiesel	Single cylinder, air cooled, DI diesel engine	At different load conditions (5, 10, 20 & 30%)	Increasing concentration of biodiesel in blends resulted in lower engine power and higher BSFC.	(Chauhan, et al., 2012)
Tobacco seed oil methyl ester blends (10%, 17.5% and 25% by volume)	Four cylinder, four stroke, turbocharged, indirect injection diesel engine	Different engine speed with full load conditions	Tobacco seed oil methyl ester blends resulted in slightly higher torque and power at full load	(Usta, 2005)
Tall oil methyl ester–fuel (50%, 60%, 70% and 100% by volume)	Single cylinder, direct injection diesel engine	At different engine speeds full load condition	Torque and engine power increased by 6.1% and 5.9%, respectively with tall oil methyl ester blends at high engine speeds.	(Altıparmak, et al., 2007)
Thumba oil biodiesel blend (B10, B20 and B30)	Four cylinder, DI, water cooled diesel engine	At different engine speeds full load condition	Increase in brake power, brake thermal efficiency and reduced BSFC with 30% biodiesel blend of Thumba oil biodiesel blend	(Pal, et al., 2010)

2.9.2 Impact of biodiesel on exhaust emission characteristics

2.9.2.1 Regulated emissions

Biodiesel is a promising alternative to conventional diesel fuel and the demand of biodiesel for automotive application has been growing rapidly. Numerous studies have been conducted regarding emissions of regulated pollutants such as CO, CO_2, HC, NOx, and PM using biodiesel. Biodiesel contains 10% more oxygen compared to diesel which allows more carbon molecules to burn, and results in complete fuel combustion and thereby reduces exhaust emissions. Many studies have reported substantial reductions in HC, CO, and PM emissions from engines operating with biodiesel blends (He, et al., 2010; Kannan, et al., 2011; Macor, et al., 2011). However, there is no consistent trend in NOx emissions when biodiesel is used; in generally, however, a slight increase in NOx is observed with the use of biodiesel. This increase is referred to as the "biodiesel NOx effect" (Caresana, 2011; Szybist et al., 2007). The mechanism underlying this effect is still remains to be discovered. The NOx increase may not be exclusively driven by changing in a single fuel property, but rather may result from a number of coupled mechanisms whose effects tend to reinforce or cancel one another under different conditions, depending on specific combustion and fuel characteristics (Mueller et al., 2009).

Wu et al. (Wu et al., 2009) studied the emission characteristics of regulated pollutants using five methyl ester biodiesels (cottonseed, soybean, rapeseed, palm oil and waste cooking oil methyl ester) in a DI, six-cylinder diesel engine by changing the BMEP (brake mean effective pressure). Results showed that all biodiesel produced less HC and CO, but higher NOx emissions than diesel fuel. Large reduction in total PM (53% to 69%) and dry soot (79% to 83%) were found using biodiesel fuels. Similar findings were observed by Nabi et al. (Nabi et al., 2009) as cotton seed oil biodiesel mixtures showed less CO, PM, smoke emissions than those of neat diesel fuel due to the presence of oxygen and

low aromatics content in the biodiesel mixtures. However, increased in the NOx emission was experienced with biodiesel blends. Özener et al. tested soybean biodiesel in a single cylinder DI engine from 1200-3000 rpm (Özener et al., 2014). In that study, it was found that soybean biodiesel produced higher CO_2, and NOx, but lower CO and HC emissions. Raheman and Ghadge (Raheman & Ghadge, 2007) tested pure mahua methyl ester (B100) and its blends with varying proportion of high speed diesel from 20% to 80% by volume (B20, B40, B60 and B80) in a Ricardo E6 engine. The study showed that reduction in smoke level and CO emissions, whereas NOx increased with increase in percentage of mahua biodiesel in the blends. The level of emissions increased with increase in engine load for all fuels tested. The authors concluded that up to 20% of mahua biodiesel can be promoted as alternative fuel for diesel without significantly affecting the engine performance and emissions.

With regard to the selection of the biodiesel fuel, some studies revealed that unsaturated biodiesel fuel is not desired due to higher NOx emissions. Ng et al. studied the impact of blend ratios and biodiesel fuels with a wide spectrum of degree of saturation in the fatty acid composition on exhaust emissions with three types of biodiesel methyl ester, derived from coconut oil, palm oil and soybean oil (Ng et al., 2011). Nitric oxide (NO) concentration increased by 8.4% for neat soybean biodiesel, whereas a 5.4% reduction was observed for coconut and palm biodiesel. This is because high unsaturated soybean biodiesel contains the highest number of double bonds in its fatty acid composition, promoting NO formation via a prompt and thermal pathway. Puhan et al. (Puhan et al., 2010) carried out an experiment of three types of biodiesel with different molecular weights and numbers of double bonds (linseed, Jatropha and coconut oil biodiesel) in a single cylinder DI engine. The results indicated that unsaturated biodiesel fuels produced higher HC, CO, NOx, smoke emissions and exhaust gas temperature. It was also found that linseed biodiesel with high unsaturated fatty acid was not

recommended for diesel engine due to its high NOx emission and low thermal efficiency. As shown in Table 2.6 provides an overview of impact of biodiesel on engine performance characteristics from the literature review.

Table 2.6: Findings on biodiesel and blends on regulated emissions characteristics

Biodiesel type	Engine type	Engine operating condition	Results	Ref.
Cottonseed, soybean, rapeseed, palm oil and waste cooking oil methyl ester	Six-cylinder, DI, turbo-charging, intercooling diesel engine	At different BMEP conditions	All biodiesel produced less HC and CO, but higher NOx emissions than diesel. Large reduction in total PM (53% to 69%) and dry soot (79% to 83%) with using biodiesel fuels.	(Wu, et al., 2009)
Cotton seed oil biodiesel (B10, B20 and B30)	Single cylinder, 4-sroke, DI diesel engine	Different engine load conditions at 850 rpm	Biodiesel blends produced less CO, PM, smoke emissions, but higher NOx emissions than neat diesel fuel.	(Nabi, et al., 2009)
Soybean biodiesel (B10, B20, B50 and B100)	Single cylinder, 4 stroke, air-cooled DI engine	Different engine speed at full load conditions	Soybean biodiesel produced higher CO_2 and NOx, but lower CO and HC emissions.	(Özener, et al., 2014)
Mahua methyl ester (B20, B40, B60, B80 and B100)	Single cylinder, four stroke, water cooled Ricardo E6 engine	Different engine load conditions	Reduction in smoke level and CO emissions, whereas NOx increased with increase in percentage of mahua biodiesel blends.	(Raheman & Ghadge, 2007)
Coconut oil, palm oil and soybean oil biodiesel	Single-cylinder, four-stroke, light-duty DI diesel engine	Steady-state modified emissions test cycle	Low to moderate degree of unsaturation biodiesel reduced emission UHC (unburned hydrocarbons), NO and smoke opacity levels by 41.7%, 5.4% and 61.3%, respectively. While, highly unsaturated soybean biodiesel, produced higher CO, UHC, NO and smoke opacity levels that diesel.	(Ng, et al., 2011)
Linseed, Jatropha and coconut oil biodiesel	Single cylinder, four stroke, DI engine	At different engine brake power conditions	Linseed biodiesel with high unsaturated fatty acid produced higher HC, CO, NOx, smoke emissions and exhaust gas temperature.	(Puhan, et al., 2010)

2.9.2.2 Unregulated emissions

Although regulated emissions of biofuel have been extensively investigated, unregulated emissions, such as polycyclic aromatic hydrocarbons (PAHs) are lacking in comprehensive research. Recently, exhaust measurements of PAHs in vehicles has received widespread attention mainly due to the carcinogenic and mutagenic properties

of some PAHs compounds (Ravindra et al., 2008). PAHs are atmospheric pollutants that consist of fused aromatic rings. Particulate PAHs mainly originate from the combustion of fossil fuels (process of pyrosynthesis and pyrolysis), fuel pyrolysing, engine deposits, unburned fuel and lubricating oil. The formation of PAHs from automobiles depends upon: engine type, fuel type, fuel composition and quality, driving mode and engine operating conditions (Borrás et al., 2009; Ravindra, et al., 2008). Biofuel is expected to emit less aromatic hydrocarbon emissions compared with fossil fuels, because there is virtually no aromatic content in vegetable oil. Many researchers have observed a reduction of PAHs pollutants with biofuel in their studies, as shown in Table 2.7. However, adding an excess of palm-biodiesel blends can lead to incomplete combustion in the engine, resulting in a reduction of energy efficiency (Lin et al., 2006). Similar findings were observed by Tsai et al. who found a reduction of energy efficiency with B50 soy-biodiesel compared with diesel, B10 and B20 soy-biodiesel in a diesel generator (Tsai et al., 2010). Additionally, the B50 soy-biodiesel emitted more PAHs emissions due to incomplete combustion and poor nebulisation efficiency of the nozzle by over-adding biodiesel into the diesel.

Table 2.7: Findings on biodiesel and blends on PAHs emissions

Biofuel type	Engine type	Engine operating condition	Results	Ref.
B100 waste cooking oil biodiesel (sunflower + rapeseed oil); 100% fresh rapeseed oil	Six-cylinder DI, turbocharged diesel engine	At different loads of upstream and downstream catalyst	Both biofuels resulted in reduction in most of particulate PAHs, except FL and pyrene at low load upstream catalyst. Fluoranthene compound was suspected to be caused by pyrosynthesis.	(Lea-Langton et al., 2008)
B100 Brassica carinata oil biodiesel; Diesel-Bi (commercial biodiesel)	Turbocharged DI diesel engine with intercooler and exhaust gas recycling (EGR)	At 3000rpm with different load level	Total PAHs and carcinogenic PAHs contents were presented in lower concentrations in both biodiesel fuels.	(Cardone et al., 2003)
B5, B10, B20 and B30 waste cooking oil biodiesel	Six-cylinder heavy duty diesel engine	US-HDD transient-cycle	The mean reductions of total PAHs emission factor were 7.53%, 23.7%, 31.9% and 37.5% for B5, B10, B20 and B30, respectively.	(Lin et al., 2011b)
B2, B5 and B20 castor oil biodiesel	Six-cylinder heavy duty diesel engine	At 1500 rpm under steady-state condition	PAHs emissions were reduced by 2.7%, 6.3% and 17.2% with B2, B5 and B20 castor oil, respectively.	(Corrêa & Arbilla, 2006)
B20 waste cooking oil biodiesel	Four-cylinder, indirect fuel injection, turbocharged diesel engine	US EPA transient-cycle test	The total PAHs emissions were reduced by 25% using B20. The particulate-phase of PAHs was 23.3% and 10.6% for cold and warm driving conditions.	(Yang et al., 2007)
B20 and B100 soybean oil biodiesel	DI turbocharged EURO II diesel engine	ISO 8178 type C1 test cycle	The reduction of PAHs was 19.4% and 13.1% with B20 and B100, respectively. The BaP_{eq} of PAHs emissions were decreased by 15% when using B100.	(He, et al., 2010)

2.9.2.3 Exhaust PM

Various health effects of air-borne PM on human health are serious issues that govern the heart diseases, toxicity, respiratory and carcinogenic problems (Agarwal et al., 2011; Chuepeng et al., 2011; Lin et al., 2008; Puzun et al., 2011). The usage of fossil fuels in diesel engines are widely used in heavy-duty buses, cranes and constructions machines which contribute to the emissions of smoke, gaseous pollutants and carbonaceous particulates which are the diesel PMs, sulfur oxides, and polycyclic aromatic hydrocarbons (Agarwal, et al., 2011; Lin, et al., 2008). Diesel PMs that being emit from

the diesel engines consist of an elemental carbon core with several organic compounds, sulfates, nitrogen oxides, metals and irritants (Agarwal, et al., 2011). Different engine type, engine speed and load, composition of fuel and lubricating oil, start of injection, fuel injection pressure, boost pressure and emission control technology governs the particle size distribution (Agarwal, et al., 2011; Buono et al., 2012; Lapuerta et al., 2008b; Lin, et al., 2008; Puzun, et al., 2011; Ye & Boehman, 2012b). Diesel particulates are very complex ingredient which contains variety of carcinogenic and characterized in terms of specific metals, elemental carbon, and organic compounds (Agarwal, et al., 2011; Puzun, et al., 2011). PM size that is too small may be harmful to the human health (Lapuerta et al., 2008c). The increasing demand on tightening the emissions standards, both size of the PMs and quality will be restricted by the emissions regulations in the future as it is harmful to the environment and human population (Puzun, et al., 2011; Tan et al., 2012; Zhu et al., 2011). Reduction of PMs in the atmosphere has been a concern of domestic and foreign researchers. Having a reduction of PMs in the atmosphere is a main focus of the industry, nevertheless the industry must take into account of the reducing the size of the PMs of the exhaust engine which could affect the health of human being as it is very dangerous to the human respiratory system.

The major contributors to the inflections of environment are motorized vehicles (Gumus, 2010). Particles released from motorized vehicles fuelled with diesel and gasoline are very much chemically complex, containing a great mixture of both inorganic and organic compounds. NO_x and PM emissions from motor vehicles fuelled with gasoline or diesel affect serious adverse human health effects, as well as premature death, impaired lung function and cardiovascular diseases (Bergvall & Westerholm, 2009; Gumus, 2010). It also effects ecological systems, earth's climate and visibility. Sources contributing to the observed levels have been in progress for several number of years, only in recent year a measurement of $PM_{2.5}$ been implemented. Meanwhile, frequent

intensive studies and regional monitoring efforts designed to characterize the levels and sources of $PM_{2.5}$ (Gertler, 2005). A research was conducted at seven urban sites in the US where it was concluded that the primary mobile source emissions were an important contributor for all the locations (Gertler, 2005). It was also noted that the major contributor to $PM_{2.5}$ was ammonium nitrate which is expected from oxidation of NO_x emissions from motor vehicles.

The significant reduction of PM size was expected when the biodiesel blend increases because of it is free of aromatic and unsaturated components (Salamanca et al., 2012a; Salamanca et al., 2012b). The weight and size of PMs are dependent of the combustion diesel engine operation conditions (Chuepeng, et al., 2011). The variation of PM's size have been studied by the effect of speed variation whereby a various engine operating speeds were chosen. The engine was operated at a particular operating speed for a period of time, hence it will achieve a stabilization so a repeatability of experiments are ensured (Agarwal, et al., 2011). With these operating speeds that have been chosen, it was being operated at constant load using different PMs formation with different biodiesel blends (Agarwal, et al., 2011). Biodiesel gave a higher number of smaller PMs in engine exhaust compared to the petroleum diesel. Petroleum diesel also gave a higher number in size of the PMs compared to the biodiesel blend (Agarwal, et al., 2011; Chuepeng, et al., 2011). B20 was found better at some operating conditions and delivered better performance compared to B0 (Agarwal, et al., 2011). As for B30 aerosol, it was found that PMs were small in size compared to petroleum diesel PMs (Chuepeng, et al., 2011). PMs that have diameter around 20 nm show the highest deposition efficiency in the alveolar region of the lungs. Very fine particles can penetrate into epithelium and also into the blood stream (Agarwal, et al., 2011). The exposure of the diesel engine exhaust PMs may cause acute and non-chronic cancer respiratory effects and lung cancer in humans. PMs should have a typical morphology which is the spherical shape with the primary arranged in a chain

like structure whereby it can led to measure the PMs' size from the micrographs (Salamanca, et al., 2012a).

2.9.3 Effect of biodiesel on combustion characteristics

The combustion characteristics of the biodiesels can be compared by the means of cylinder gas pressure, heat release rate (HRR) and ID. One of the most important parameters in the combustion phenomenon is the ID. The ID is defined as the time interval between the start of injection (SOI) timing and start of combustion (SOC) timing. The ID is influenced by the fuel's ignition quality (defined as cetane number), compression ratio, engine speed, cylinder gas pressure, intake-air temperature, and quality of fuel atomization (Ozsezen & Canakci, 2011).

Several research studies on combustion characteristics in biodiesel fuelled engine were investigated by researchers around the world. Haik et al. (Haik et al., 2011) studied the combustion characteristics of algae oil biodiesel in an indirect injection diesel engine at different engine speeds, engine loads, injection timings and compression ratios. They reported that algae oil biodiesel exhibited slightly higher heat release, more combustion noise (maximum pressure rise rate) and lower torque compared to diesel fuel. On the other hand, it was found that the engine output can be increased by retarding the injection timing and that the combustion noise can be reduced by decreasing the engine compression ratio. Gogoi & Baruah (Gogoi & Baruah, 2011) studied the combustion characteristics in a single cylinder, four-stroke, naturally aspirated, DI diesel engine fuelled with Koroch seed oil methyl ester (B10 – B40) blends with diesel. The combustion analysis revealed that Koroch seed oil biodiesel blends exhibited similar combustion trend with diesel. The maximum heat-release rate also occurred earlier for the biodiesel blends at all the loads due to shorter ID. As compared to diesel, the cumulative heat release was higher for the blends B10, B20 and B30 over the entire range and it was

significantly less for the B40 at all the loads. However, the blends showed an early SOC with shorter ID period. The study revealed the suitability of Koroch seed oil biodiesel blends up to B30 as fuel for a diesel engine mainly used in generating sets and the agricultural applications without any significant drop in engine performance. Combustion characteristics of a water-cooled, in-line 6 cylinders DI diesel engine has been investigated experimentally with canola oil methyl ester (COME) and waste palm oil methyl ester (WPOME) by Ozsezen & Canakci (Ozsezen & Canakci, 2011) at constant engine speeds under full load condition. The results showed that the ID of WPOME and COME are shorter than that of the diesel fuel at the all engine speeds due to higher cetane number of biodiesel. The average ID for WPOME, COME and diesel were 6.85°, 8.05° and 8.15° CA, respectively. The average SOC timing with the use of the WPOME and COME advanced 1.2° CA and 0.4° CA, respectively, compared with diesel.

The effect of engine load on combustion characteristics with different non-edible biodiesel fuel from Jatropha, Karanja and Polanga oil was investigated by Sahoo and Das (Sahoo & Das, 2009) in a single cylinder diesel engine. Results showed that the ID of biodiesel blends was found to be shorter than that of diesel. The analysis revealed that neat Polanga biodiesel that resulted in maximum peak cylinder pressure was the optimum fuel blend as far as the peak cylinder pressure was concerned. The ID was consistently shorter for neat Jatropha biodiesel, varying between 5.9 and 4.2 degree crank angle (°CA) lower than diesel with the difference increasing with the load. An experimental study on effect of engine load, injection timing, injection pressure, compression ratio and fuel blends was conducted by Gumus (Gumus, 2010) in a Lombardini 6 LD 400 DI, single cylinder, four-stroke, naturally aspirated, air-cooled engine using hazelnut kernel oil methyl ester. The study revealed that increased biodiesel concentration, retarded injection timing, increased injection pressure and compression ratio resulted shorter ID. The minimum ID was obtained with B100 biodiesel at 20 Nm and injection timing of 15

degree crank angle (°CA) before top dead center (BTDC) condition. In terms of cylinder gas pressure, lower biodiesel concentration, increasing of injection timing, injection pressure and compression ratio increased the peak of cylinder gas pressure of biodiesel and its blend with diesel fuel. The combustion duration increased with addition of biodiesel content in the blend and engine load conditions. Increasing the biodiesel mass fraction of blends resulted in a decrease in the cumulative heat release and increasing of injection timing, compression ratio and injection pressure compensated the decreased in cumulative heat release.

2.10 Effect of injection parameters on performance, emissions and combustion characteristics

The importance of optimal injection parameters such as injection timing and injection pressure for alternative fuels has been studied and reported by numerous researchers. Suryawanshi and Deshpande (Suryawanshi & Deshpande, 2005) investigated the influence of retarded injection timing of Pongamia oil methyl ester fuel in a single cylinder DI diesel engine. The experiment results showed that the reduction in NOx, unburned hydrocarbon and smoke emissions were observed with 4 °CA retarded injection timing as compared with diesel at standard injection timing. The maximum cylinder gas pressure, ID, HRR were decreased when the injection timing was retarded. In addition, Sequera et al. (Sequera et al., 2011) examined the effect of fuel injection timing in a single cylinder, naturally aspirated, air-cooled four-stroke diesel engine. The results revealed that advanced injection timing by 8 °CA increased cylinder peak pressure around 20%, while retarded injection timing by 11 °CA reduced peak pressure about 10%. In terms of exhaust emissions, whereas retarded injection timing reduced CO and NOx emissions. Ganapathy et al. (Ganapathy et al., 2011) study of effect of injection timing with diesel and Jatropha biodiesel fuel using full factorial design with 27 runs. The results indicated that advance in injection timing from factory settings caused reduction in BSFC, CO, HC

and smoke levels and increase in BTE, peak cylinder pressure, maximum HRR and NO emission with Jatropha biodiesel operation. The best injection timing for Jatropha biodiesel operation with minimum BSFC, CO, HC and smoke and with maximum BTE, peak pressure, HRR was found to be 340 °CA. Nevertheless, minimum NO emission yielded an optimum injection timing of 350 °CA.

Sayin et al. (Sayin et al., 2012) conducted experiment with different injection pressures in a single cylinder, four stroke, DI diesel engine using canola biodiesel and its blends. The results showed that the increased injection pressure boosted maximum cylinder gas pressure due to increase in premixed combustible mixture and gave the better results for BSFC, BSEC (brake specific energy consumption) and BTE compared to the original and decreased injection pressures. In another study, it was found that the increased injection pressure caused to decrease in BSFC of high percentage biodiesel–diesel blends, smoke opacity, the emissions of CO, unburned hydrocarbon and increased the emissions of CO_2, O_2 and NOx (Gumus et al., 2012). Hwang et al. (Hwang et al., 2014) investigated the effects of the injection pressure and injection timing on the combustion and emission characteristics in a single-cylinder common-rail DI diesel engine fueled with waste cooking oil biodiesel and diesel fuel. The results showed that the indicated specific fuel consumption with respect to the injection timings of the biodiesel was higher than that of the diesel fuel under all conditions. The peak cylinder pressure and the peak HRR of the biodiesel were slightly lower, while the ID was slightly longer under all operating conditions. In terms of emissions, the biodiesel produced lower of smoke, CO, HC emissions especially with high fuel injection pressure. However, the NOx emissions of the biodiesel were relatively higher than those of the diesel under all experimental conditions. Ye & Boehman (Ye & Boehman, 2012a) investigated the impact of engine injection strategy on NOx and PM emissions with soybean biodiesel and ultra low sulfur diesel (ULSD) fuel in a common-rail turbocharged DI diesel engine. It was

found that an increase of fuel injection pressure significantly decreased PM emissions but caused higher NOx emissions for all load conditions. The NOx-PM emission trade-off of SOI timing at 9 ºCA BTDC showed that decrease of fuel injection pressure was an effective way to counter the biodiesel NOx effect while maintaining a similar or even lower level of PM emissions than ULSD. The heat release analysis shows that retarding the SOI after top dead center (ATDC) increased the fraction of premixed combustion for all load conditions. At the same SOI, higher fuel injection pressure leaded to faster and higher apparent HRR, and a slightly earlier SOC due to the better mixing of fuel and air.

2.10.1 Influence of injection timing and split injection strategies on performance, emissions, and combustion characteristics

The widespread use of diesel engine has caused air pollution problems. This is due to their higher exhaust discharges of NO_x, PM and smoke in comparison with that of a gasoline engine (El Diwani et al., 2009). The air pollutants jeopardize human health in different ways, necessitating the needs to curb this problem (Attfield et al., 2012; Li et al., 2003; Zhang et al., 2009). To minimize this impact, research effort are being focused on injection strategies such as variable injection timing, split injection, variable injection pressure, variable nozzle configuration, and others (Mohan et al., 2013; Park et al., 2016). Injection timing optimization can be performed in order to produce a suitable ignition delay as well as to reduce the amount of exhaust emission in diesel engine. For instance, advancing the injection timing reduces the amount of CO, HC and smoke while increases the amount of NO_x emitted (Mohan, et al., 2013). More time is available for oxidation when injection is advanced, thus reducing the amount of CO, HC and smoke, but with higher amount of NO_x emitted. In order to reduce amount of NO_x emitted, the injection can be carried out later to lessen the air temperature even though at the expense of increasing the amount of CO, HC and smoke emitted due to incomplete combustion.

Another strategy can be implemented to diesel engines to attain lower emission limit is by split injection. It can be carried out to reduce engine noise and amount of NO_x emitted. Furthermore, accurately performed split injection schemes can be favorable in reducing combustion noise, waste emissions and diesel consumption and therefore, they are effective tools (Busch et al., 2015). Besides, particulate emissions can be reduced substantially without a great increase in NO_x emissions (Herfatmanesh et al., 2013; Montgomery & Reitz, 1996). This is because high HRR can be prevented at the beginning of combustion, hence decrease the flame temperature and permit better fuel and air mixing to enhance in-cylinder charge homogeneity. Besides, energy demands of the world are increasing nowadays. Depletion of fossil diesel fuel can be slowed by adopting renewable source of energy such as biodiesel. Biodiesel can be made from vegetable oil, animal fat or waste materials such as spent coffee grounds (Liu et al., 2017b). Also, it is nontoxic, renewable and biodegradable compared to conventional diesel (Ma & Hanna, 1999b). Generally, CO, smoke and PM concentration emitted when biodiesel is used are lower compared to conventional diesel (Liu et al., 2017a; Mohamed Shameer et al., 2017). However, NO_x emission of biodiesel can be higher or lower for different types of biodiesel and operating condition (Mohamed Shameer, et al., 2017; Zhang & Boehman, 2007). Biodiesel has cetane number which is higher than ordinary petroleum diesel, which implies that it has a better ignition properties and higher combustion efficiency (Atabani et al., 2013a; Mittelbach, 1996; Mohamed Shameer, et al., 2017). Biodiesel evaporates, atomizes and breaks up slower because it has a higher kinematic viscosity and surface tension. Hence, it is important to apply a suitable injection strategies to overcome this problem.

The utilization of biodiesel in diesel engines has usually produced higher NOx and brake specific fuel consumption (Al-Dawody & Bhatti, 2013; Palash, et al., 2013b; Rahman, et al., 2013). Using alternative fuels and optimization of fuel injection

parameters in diesel engine can be reliable methods to solving this problem. According to Shivakumar et al. (Shivakumar et al., 2011) in the research of effects of biodiesel and injection timing on single-cylinder diesel engine performance, NOx emission of waste cooking oil blended fuel is relatively higher than that of baseline diesel. It is found that the NOx emission will be lower at retarded injection timing for baseline diesel and biodiesel. The smoke emission of biodiesel is less than baseline diesel and the advanced injection timing will reduce the smoke reduction of both kinds of diesel. Qi et al. (Qi et al., 2011) showed that NOx emission always decreases with the retarding injection timing when using biodiesel produced from soybean as energy source in six-cylinder diesel engine. Sayin and Gumus (Sayin & Gumus, 2011) and Ganapathy et al. (Ganapathy, et al., 2011) also obtained the same results as Shivakumar et al. (Shivakumar, et al., 2011) when Jatropha biodiesel are used correspondingly in their researches by using single-cylinder diesel engine. Recently, modern engines are trending toward multiple fuel injection events as a means to decrease emissions and improve engine performance (Cha et al., 2015; Han et al., 2016). In the investigation of effects of split injection on the emissions of biodiesel, Fang and Lee (Fang & Lee, 2009) found that NOx emission of biodiesel can be 34% lower than baseline diesel under certain injection scheme at specific condition in single-cylinder diesel engine. The injection strategies used in their study included double injection of a small first injection with an early pre-TDC timing and followed by a main injection at or after TDC. Jeon and Park (Jeon & Park, 2015) discovered that retardation of pilot injection timing will cause increasing amount of NOx emission when soybean biodiesel is used in single-cylinder diesel engine. Yehliu et al. (Yehliu et al., 2010) showed that under single injection scheme in four-cylinder diesel engine, the amount of emission of NOx is higher for biodiesel compared to baseline diesel. However, when split (pilot and main with non-equal fuel quantity) injection scheme is carried out, the NOx emission is the lowest for biodiesel. The drawback is that

there will be an increase in PM emitted when biodiesel and baseline diesel are used when split injection scheme is carried out. Park et al. (Park et al., 2011) studied about the relationship of injection timing and split injection (with up to two injections per combustion cycle) with the performance of biodiesel by using a single cylinder diesel engine. They found that NOx emission increases with advanced injection timing. Multiple injection scheme cause less soot to be emitted compared to single injection scheme except at highly advanced injection timing. The retardation of pilot injection timing reduces the amount of soot emitted. Besides, multiple injection strategy has been proposed as an effective way to reduce unburned emissions and noise (Kim & Bae, 2017; Park et al., 2015).

2.10.2 Effect of two-stage injection dwell angle on engine combustion and performance characteristics

In order to improve the performance and emission characteristics of diesel engine when biodiesel is used to replace conventional diesel, a more advanced injection strategies have to be carried out. Split injection has been proposed as one of the methods to reduce the air pollutants emitted by diesel engine. In split injection, the injection of fuel is divided into two or more portions, where each portion is injected consecutively but non-continuously. One of the purposes is to ensure that before main combustion can occur, a highly premixed fuel can be formed. This advantage of split injection has been studied by a few researchers before (Park, et al., 2011; Roh et al., 2015; Suh, 2011). In addition, post injection applied during split injection serves to reduce the amount of smoke, PM and unburned hydrocarbon (Park et al., 2004). The parameters in split injection can be changed and improved to produce a better effect on the performance and emissions characteristics of diesel engine. These parameters include injection timing, dwell angle between injections, mass injected, mass ratio of injections, number of injections, injection pressure and others. In this study, effect of different start of injection

timing and dwell angle between injections in two-stage injection scheme on the performance and emission characteristics will be investigated and discussed.

Start of injection timing is one of the factors which greatly affect diesel engine performance and emission characteristics. Shivakumar et al. (Shivakumar, et al., 2011) found that NO_x emitted when waste cooking oil is used as biodiesel is reduced when SOI is retarded while advanced SOI causes reduction in amount of smoke emitted. The same results are obtained by Sayin and Gumus (Sayin & Gumus, 2011) using $C_{18.08}H_{34.86}O_2$ biodiesel and Ganapathy et al. (Ganapathy, et al., 2011) using Jatropha oil. According to Jeon and Park (Jeon & Park, 2015), when pilot injection is applied, the retardation of SOI of pilot injection causes higher emission of NO_x compared to single injection scheme. Adam et al. (Adams et al., 2013) used gasoline and soy methyl ester biodiesel in investigating engine performance and emission characteristics. They found that with retarded injection timing, gas temperature and HRR will increase, leading to rise in NO_x emission amount.

Besides SOI, dwell angle is also an important factor. According to Cung et al. (Cung et al., 2015), when the dwell angle is reduced, the penetration rate will be increased. However, a dwell angle which is too short will cause the soot to increase. With a longer dwell angle, the peak heat release rate (PHRR) and total heat released are increased. Rohani and Bae (Rohani & Bae, 2017) found that longer dwell angle of about 30°CA will produce a more premixed charge. In split injection with five times of injection, K. Mathivanan et al. (Mathivanan et al., 2016) discovered that smoke level is the lowest when the dwell time between the fourth injection and the last injection is the longest. Liu and Song (Liu & Song, 2016) found that cylindrical pressure decreases with increasing dwell time under constant fuel quantity in double injection scheme. When the post injection is retarded and the dwell time is increased, NO_x emission can be reduced. A

shorter dwell time causes limitation in oxidation of CO and hydrocarbon (HC) due to insufficient mixing time. Using Karanja biodiesel as fuel, Dhar and Agarwal (Dhar & Agarwal, 2015) found that NO_x emission decreases with retarding start of main injection timing for every start of pilot timing. However, at fixed start of main injection, NO_x emission is almost constant with the change in start of pilot injection.

2.10.3 Impact of two-stage injection fuel quantity on engine-out responses

Ensuing the worsening of air pollution issue, stringent law has been implemented to control the pollutant emission amount from vehicles. Due to the high level exhaust emission, especially NO_x, biodiesel may not be appropriate to be used in conventional diesel engine. In order to bring down the waste emission, various injection methods can be operated with. Thus, the influences of start of injection (SOI) timing and mass ratio of injection are investigated and highlighted. According to Nik Rosli et al. (Nik Rosli et al., 2013), the smoke emission level rises with injection performed at a later timing. At early crank angle, retarding SOI will cause decrement in NOx emission level. However, NOx emission quantity increases with retarding SOI at late timing. Ge et al. (Ge et al., 2015) observed that NOx emission increases slightly while PM reduces substantially with advancing SOI timing when canola oil biodiesel blend is used. In Jeon et al. (Jeon et al., 2016) research, it is found that retarded second SOI timing will result in low peak pressure and first combustion heat release rate. They also observed that retarded pilot SOI timing will produce a higher temperature. On the other hand, Khandal et al. (Khandal et al., 2017) reported that advanced pilot injection will give rise to reduction in NOx emission quantity due to the shorter ignition delay. However, the increase in brake mean effective pressure (BMEP) will lead to elevation of smoke amount. Park et al. (Park, et al., 2011) also observed that NOx emission increases with advancing SOI timing of pilot injection.

In the conventional single injection diesel combustion, the early direct fuel injection is problematic due to the difficulties in fuel vaporization and fuel spray over-penetration. To tackle this issue, the strategy of two-stage diesel fuel injection had been applied by Kook and Bae (Kook & Bae, 2004). In this approach, the fuel was divided and supplied in two injections. The first injection is typically carried out in the compression stroke and followed by the second injection near TDC in the expansion stroke. The mass ratio between pulses in two-stage injections strategy also significantly affects the performance and emission characteristics of diesel engine. Cylinder pressure and mean temperature increase when mass of pilot injection is increased, according to the research of Wei et al. (Wei et al., 2017). Increase in mass of pilot injection also causes an increase in mass of fuel burnt. Torregrosa et al. (Torregrosa et al., 2013) found that when pilot injection mass is increased and pilot injection timing is advanced, NO_x emission will rise. Mathivanan et al. (Mathivanan, et al., 2016) discovered that peak heat release rate (PHRR) will decrease and retardation of combustion phase will occur if the first injection pulse duration is increased. When the last injection quantity decreases, more fuel will be injected in earlier injections and this produces a more homogeneous mixture and increases PHRR. According to Juneja et al. (Juneja et al., 2004), when fuel is injected close to top dead center (TDC), a longer injection duration will cause incomplete combustion to happen due to the insufficient mixing time. By carrying out split injection scheme with four pilot injections and one main injection, Su et al. (Su et al., 2003) discovered that NO_x emission decreases from 400 ppm to 300 ppm while HC emission remains almost constant when small amount of pilot injections is used. When large amount of pilot injections is applied, HC emission increases obviously. Smoke emission is found to be decreasing with increasing pilot injection quantity.

2.11 Summary

Based on the information collected through the literature search and discussions, a review was conducted of the available knowledge and research related to the effects of different types of biodiesel blends on engine-out responses as well as the influence of state-of-the-art of fuel injection technologies on engine performance. However, information about the influence of biodiesel blends in the engine equipped with split injection, in particularly dealing with two or more fuel injections of equal quantities per combustion cycle was very limited. In fact, most of the studies have been performed on single-cylinder research engine, which is not practical representative of the production engine adopted in commercial vehicles. Besides, for the comparative studies of engine performance with both of the edible and non-edible biodiesel sources, most of the early publications also lack of the information on exhaust PM analysis. This information is crucial due to the fact that PMs of the exhaust engine could affect the health of human being as it is very dangerous to the human respiratory system and cannot be overlooked. Thus a research gap remains in these fields which are addressed in this research study.

CHAPTER 3: METHODOLOGY

3.1 Introduction

This chapter describes the research methodology and the experimental setup for achieving the objectives of the current research work. Total of 13 fuels including baseline diesel fuel have been tested in this research work. Fuel properties of all the fuels have been measured according the ASTM standards. Experimental work has been carried out to investigate engine performance, exhaust emission and combustion characteristics of a four-cylinder common-rail CI engine. Figure 3.1 gives a summary of the implemented flow chart of this study.

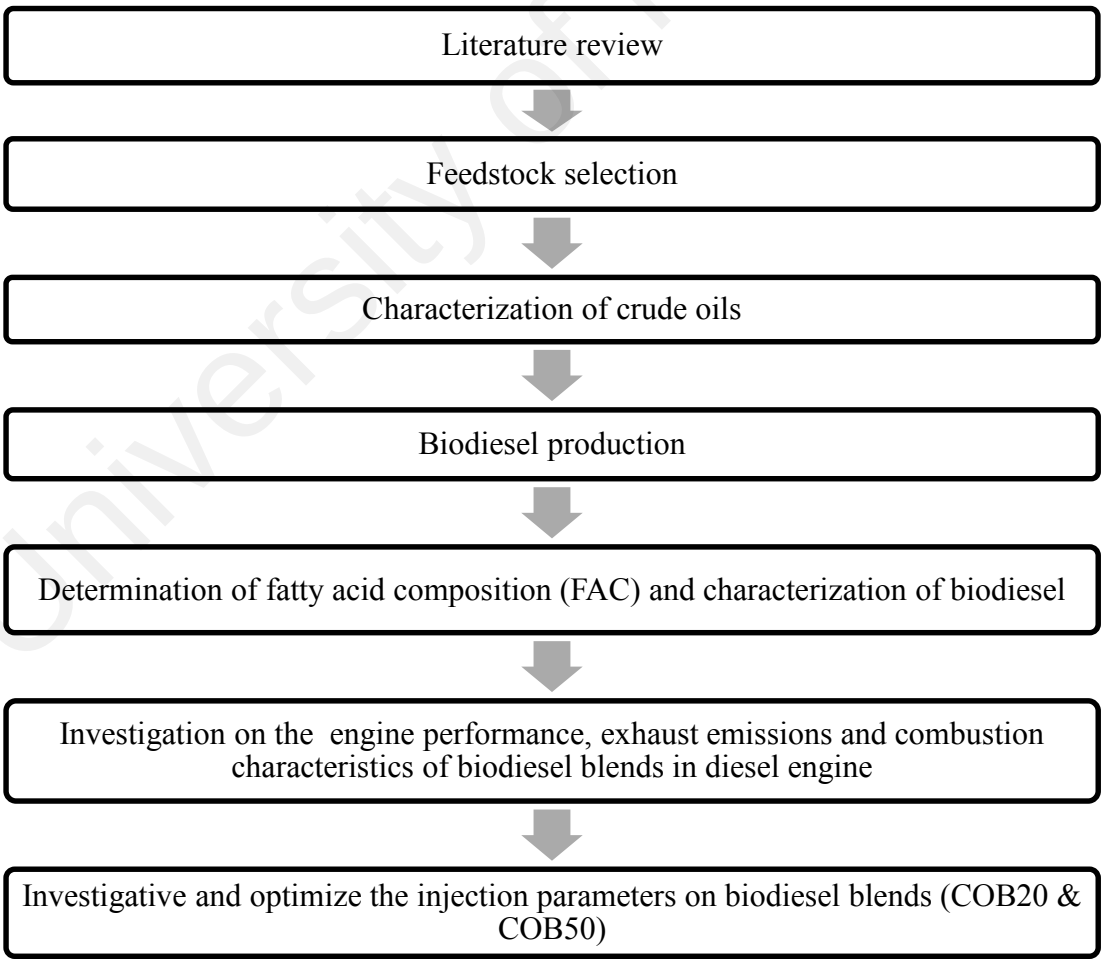

Figure 3.1: Flow chart of research methodology

3.2 Selection of feedstock

Biodiesel feedstocks vary in origin depending on the availability of local feedstock, regional climate, geographic locations and soil conditions (Atabani, et al., 2012). Soybean is major feedstock for biodiesel production in the USA, while sunflower and rapeseed are the main raw materials for producing biodiesel in Europe. In Asia, palm oil, coconut and Jatropha are the main feedstocks for biodiesel sources (How et al., 2014). Another major consideration in the selection of biodiesel feedstock is on the aspect of socio-economic benefits. The production of coconut oil crops for biodiesel usage could be beneficial for local population jobs and industries creation. Simultaneously, coconut farmers are given access to a completely new and potentially booming market once the price of coconut oil begins to follow that of fossil diesel fuel in increasingly competitive biodiesel markets. Therefore, by considering the above mentioned advantages, it is acceptable to select coconut oil as biodiesel feedstock in the present research study. Apart from choosing the coconut oil as edible biodiesel feedstock, other non-edible oils of *calophyllum inophyllum* and *moringa oleifera* are also selected for current research work due to their increasing popular all over the world (Atabani et al., 2013b).

Coconut (*Cocos nucifera Linn*) or coconut palm is one of the most important nut crops and is a member of the family *Arecaceae*. Coconut is native to the tropical eastern regions. The cultivation of coconut requires sandy, saline soils with abundant sunlight and regular rainfall throughout the year. A coconut palm tree can yield up to 75 fruits per year. Coconut palm is known for its versatility, as evidenced by the numerous domestic, commercial, and industrial uses of its different parts. *Calophyllum inophyllum*, commonly known as Penaga Laut or Bintangor in Malaysia, is a non-edible oilseed ornamental evergreen tree belongs to *Clusiaceae* family. In Greek word, the scientific name of "*Calophyllum*" means "*beautiful leaf*". It grows in areas with 1000-5000 mm rain per year at altitudes from 0-200 m. It essentially falls to a group of coastal species that grows

on sandy beaches and, to a lesser extent, along river margins further inland. The average oil yield is 11.7 kg-oil/tree or 4680 kg-oil/ha (Ong et al., 2011; Sahoo et al., 2007). *Moringa oleifera* is a member of the *Moringaceae* family, grows throughout most of the tropics, it is drought-tolerant and can survive in harsh, poor and infertile land. *Moringa oleifera* plant starts bearing pods 6–8 months after planting and reaches an average of 3 times of seed per hectare per year. The seed contains on average 40% oil by weight (Kibazohi & Sangwan, 2011). The oil is containing high in oleic acid which is around 70% of the total fatty acid profile (Rashid et al., 2008). Figure 3.2 shows the coconut, *calophyllum inophyllum* and *moringa oleifera* fruits and seeds.

Coconut

Calophyllum Inophyllum

Moringa oleifera

Figure 3.2: Coconut, *calophyllum inophyllum* and *moringa oleifera* fruits and seeds

3.3 Biodiesel production

Biodiesel production and analysis of most of the key fuel properties were done at the Department of Mechanical Engineering, University of Malaya. Generally, there are numerous ways to convert biodiesel fuel from vegetable oil such as pyrolysis, dilution, microemulsion, and transesterification. However, the most popular and economic one is still by transesterification process. This reaction has been extensively used to reduce the viscosity of crude vegetable oil and conversion of the triglycerides into ester and glycerol. A catalyst is typically employed to enhance the reaction rate and yield. In the present study, the acid value of crude *calophyllum inophyllum* and coconut oil is measured to be 37.80 and 6.0 mg KOH/g, respectively. Due to the high content of FFA of the crude *calophyllum inophyllum* and coconut oil, two step acid-base catalyst processes is employed to convert these crude oil to biodiesel. However, one step transesterification process is selected to direct convert the crude *moringa oleifera* oil to biodiesel due to its low acid values (1.6 mg KOH/g). Production of biodiesel for the crude oil has been conducted as follow:

a) Pre-treatment process (acid catalyzed esterification)
b) Alkali catalyzed transesterification process
c) Post-treatment process

3.3.1 Pre-treatment process (acid catalyzed esterification)

The *calophyllum inophyllum* biodiesel from crude oil is produced by using two-step processes of acid catalyzed esterification process and follow by base catalyzed transesterification process. Two-step processes were employed in the present study due to the high content of FFA and viscosity of the crude *calophyllum inophyllum* oil. During the acid catalyzed esterification process, sulfuric acid (H_2SO_4) is used to covert and reduces the FFA content to less than 2% by weight in the oil. After that, the crude

calophyllum inophyllum oil is transferred into a preheated reactor at a temperature of 60°C. Meanwhile, methanol (60% vol.) and H_2SO_4 catalyst (1% vol.) is prepared and premixed prior added into the reactor. The mixture is then stirred at constant stirrer speed of 800 rpm using an overhead electric motor stirrer for 2 hours. The reactor temperature is kept constant at 60°C throughout the stirring process. Subsequently, the sample oil is transferred into a separation funnel for 4 hours to separate the water and excess methanol (lower layer) from the esterified oil (upper layer). The esterified oil is washed with distilled water at 40°C. Then, the esterified oil is distilled under vacuum distillation at 60°C for 30 minutes using a rotary evaporator to further remove residual methanol and water.

3.3.2 Alkali catalyzed transesterification process

Upon the completion of esterification process, the FFA content is measured and it is observed that the value is lower than 2%. Then, the volume and density of esterified oil is carefully measured with measuring cylinder and density meter, respectively. The oil is then transferred and processed in a jacket reactor at 60°C using heating circulator water bath. Then 1% by weight of alkali catalyst (potassium hydroxide, KOH) and methanol (40% vol.) are thoroughly mixed until all the catalyst has been fully dissolved. After that, the prepared mixtures of methanol and catalyst were added into the preheated esterified oil. The final mixture is then stirred at constant stirrer speed of 800rpm using an overhead electric motor stirrer for 2 hours. The reactor temperature is kept constant at 60°C throughout the stirring process.

3.3.3 Post-treatment process

Upon the completion of phase separation of FAME and glycerol, the FAME is washed carefully with distilled water at 40°C in order to remove any impurities. The mixture is allowed to settle under normal room condition for 2 to 3 hours in a separating funnel. The

lower layer consists of impurities were drawn off. Lastly, the product is evaporated with rotary evaporator at 60°C for 30 minutes to remove residual methanol and water.

3.4 Determination of fatty acid composition

In this test 0.25g of each fuel samples is diluted with 5ml n-heptane. The solution is then entered into GC-FID. Table 3.1 shows the operating condition used to perform this analysis and the method is based on AOAC 996.06 official methods. The results of the fatty acid composition of all biodiesels will be presented and discussed in chapter 4.

Table 3.1: The GC-FID operating condition

Property	Specification
Injection volume	1 μL
Split ratio	50:1
Inlet temperature	250 ºC
Column	Agilent HP-88(60m x 0.25 mm ID,0.2μm)
Carrier gas	Hydrogen at 1 ml/min
Oven ramp conditions:	
- Initial temperature	120ºC (hold 1 min)
- 1st ramp	10ºC / min to 175ºC (hold 10 min)
- 2nd ramp	5ºC /min to 210ºC (hold 5 min)
- 3rd ramp	5ºC/min to 230ºC (hold 5 min)
Type of detector and temperature	FID & 260°C

3.5 Fuel properties measuring procedure and equipment

Viscosity, calorific value, density, oxidation stability, flash point, pour point, cloud point- these are the properties that determines the quality of the produced biodiesel. The important physical and chemical properties of the produced biodiesels were tested according to ASTM D6751 standard.

3.5.1 Dynamic viscosity, kinematic viscosity and density measurement

Density is defined as the ratio of mass to volume of fuel. In this research work, the density of all biodiesel samples were measured using SVM 3000 Stabinger viscometer according to ASTM D7042 test method. This equipment also measures dynamic viscosity

(mPa.s) using Stabinger principle. Using results of density and dynamic viscosity measuring cells, this equipment calculates kinematic viscosity (mm^2/s) at that temperature automatically. Both cells are filled in one cycle and the measurements are carried out simultaneously.

3.5.2 Flash point measurement

The minimum temperature at which fuel gives off enough vapor to produce an inflammable mixture above is known as flash point. To obtain the flash point value of the fuel according to the ASTM D93 method, a Normalab-fully automatic Pensky Martens flash point tester (NPM 440) is used. The flash point is determined by heating the fuel in a small enclosed chamber until the vapors ignite when a small flame is passed over the surface of the fuel. The cup is filled with 70 ml sample in it and closed using the lid. Then expected flash point temperature is set and the measurement procedure started. The sample is then stirred continuously and temperature raised automatically. 20 ^oC prior to expected flash point, the equipment starts to produce electrical flame and continues to do so at 1 ^oC interval. When the flame produced a non-sustained ignition which is detected by the equipment, the detection is stopped automatically and the result is shown.

3.5.3 Calorific value measurement

The heating value of all the fuel samples used in this research work is determined using IKA C 2000 calorimeter. IKA C 2000 calorimeter system can be used to determine the gross calorific value of solid and liquid materials in accordance to DIN 51900, BS 1016 T5, ISO 1928, ASTM 5468 and ASTM 4809. The combustion calorimeter measures the heat that rises from burning of fuel sample. The sample is weighed into a digestion vessel and filled with oxygen. The burning process is started by means of an ignition spark. The experiment ends when the sample is fully burned. By measuring the temperature increase, the heating value of the sample can be calculated.

3.5.4 Oxidation stability

Biodiesel which is produced from vegetable oils is considered more vulnerable to oxidation when subjected to high temperature and contact to the oxygen of the air, because of bearing the double bond molecules in the FFA. The biodiesel and its blends stability is measured by induction period. Oxidation stability of samples is evaluated with commercial appliance Metrohm-873 Biodiesel Rancimat as shown in Figure 3.3 applying accelerated oxidation test (Rancimat test) specified in EN 14112. The end of the induction period is determined by the formation of volatile acids measured by a sudden increase of conductivity during a forced oxidation of ester sample at 110°C with airflow of 10 L/h passing through the sample.

Figure 3.3: Metrohm-873 Biodiesel Rancimat

3.5.5 Cloud point and pour point

The Pour point describes a procedure for testing the fluidity of a fuel at a specified temperature. The Cloud point is defined as the temperature of a liquid specimen when the smallest observable cluster of wax crystals first appears upon cooling under prescribed conditions. An automatic NTL 450 (Norma lab, France) cloud and pour point tester is used to measure the cloud point and pour point of the samples according to the ASTM D2500 and ASTM D93 respectively.

3.5.6 Cold filter plugging point

This test method covers the determination of the cold filter plugging point (CFPP) of fuels using automated equipment. The results express an estimation of the lowest temperature which a fuel will freely flow within a fuel system. An automatic NTL 450 (Norma lab, France) cold filter plugging point tester is used to measure CFPP of the samples according to the ASTM D6371 standards.

3.5.7 Acid value measurement

In chemistry, acid value (or "neutralization number") is the mass of KOH in milligrams that is required to neutralize one gram of chemical substances. The acid number is a measure of the amount of carboxylic acid groups in a fatty acid, or in a mixture of compounds. To measure acid value of all samples according to ASTM D664 test method. A MettlerToleda G-20 Rondolino automated titration system is used. The titrant used here is 0.5M sodium hydroxide (NaOH). To test the acid value of samples the following configurations were used:

a. Acid value < 5 mg KOH/g: Amount of sample 10 g with 80 ml ethanol (95%)
b. Acid value > 5 mg KOH/g: Amount of sample 5 g with 80 ml ethanol (95%)

3.6 Engine operating conditions

Generally, the test program in this study comprises of four series of tests to assess for the following effects:

i. Effect of different biodiesels and its blends on the common-rail diesel engine under wide open throttle operating conditions;
ii. Effect of injection timing and split injection strategies on performance, emissions, and combustion characteristics of diesel engine fueled with biodiesel blended fuels;

iii. Effect of two-stage injection dwell angle and injection timing variation with baseline diesel and biodiesel blend fuels;

iv. Effect of two-stage injection fuel quantity and injection timing variation on engine-out responses with baseline diesel and biodiesel blend fuels.

In the first test series, the experiments were conducted under full load (Wide Open Throttle- WOT) conditions. The engine speed is varied from 1500 to 4000 rpm with increments of 500 rpm and with stock injection approach. These six level of engine speeds were selected as the most representative of a wide variety of engine operating ranges. Initially, diesel fuel is used as the baseline fuel for the basis of comparison. Following this, mixtures of diesel and methyl ester (coconut, *calophyllum inophyllum, moringa*) with 10, 20, 30, and 50% volumetric proportions were tested. Consequently, a total of 13 runs experimental conditions, including baseline diesel were tested in this test series. When the engine is fuelled with neat methyl ester and its blended fuels, the engine ran satisfactorily throughout the entire test, which is performed at room temperature, and had no starting difficulties.

In the second test series, the engine speed is held constant at 2000 rpm and with 60 Nm of torque. The influences of biodiesel blended fuels on engine out-responses, such as combustion, tail-pipe emissions and performance characteristics under different split injection approach (single, double and triple) and injection timing (-12° ATDC to 2° ATDC) conditions were studied. Split injection approach can be implemented by dividing the single injection event into two or three consecutive equal injection events for each engine combustion cycle with certain dwell timing of 1.3 ms between consecutive injections. The advantages of this injection strategy is that it reduces combustion flame temperature and enables ample fuel and air mixing so that charge homogeneity can be improved. Figure 3.4 delineates the timing schemes for single, double and triple injection

strategies studied in this test series. Obviously, the investigated approaches vary in the splitting schematization of main injection. Firstly, single injection is carried out in the fuel injection event. During second approach, the fuel injection process is performed by two similar injection pulses, while in the third fuel injection event three equal amount injection pulses were introduced. It has to be emphasized that the strategy of splitting the single injection pulse into two and three identical pulses is that the sum of entire engine power is fixed for every profile and SOI timing. In each test scheme, a commercial diesel fuel is used as baseline fuel for comparison purposes.

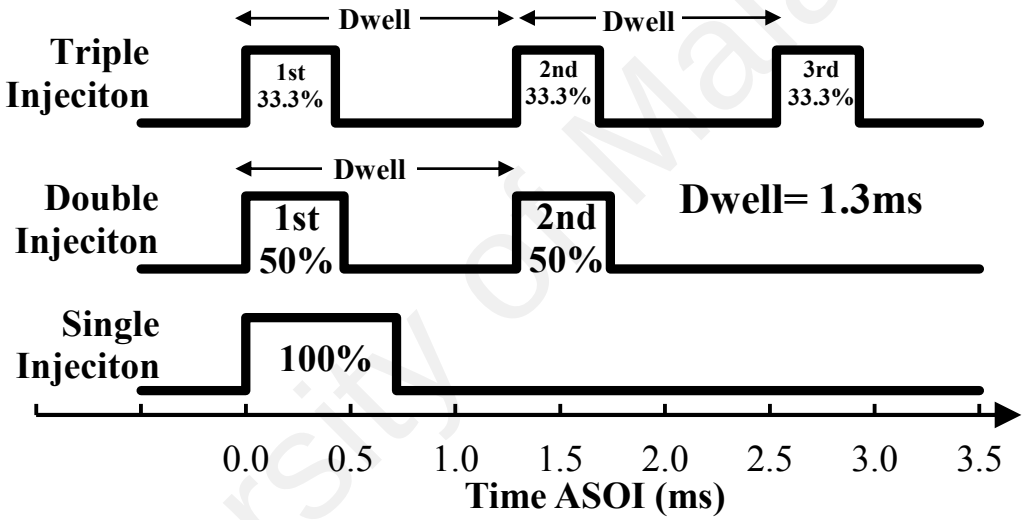

Figure 3.4: Timing chart for second test series with various split injection strategies

In the third test series, the engine operating conditions are fixed as shown in Table 3.2 throughout this test series. Load which is lower than the maximum value is applied by dynamometer to the engine as vehicles normally work under part load condition. It can be seen that two-stage injection strategy is carried out for all test cases under this test series. The mass ratio of first injection to second injection is 50:50 as depicted in Figure 3.5, where the quantity of fuel injected during first injection is same as that of second injection. Two-stage injection strategy is investigated due to its advantage in improving the exhaust emissions. By dividing fuel to be introduced into cylinder via two injections, the maximum temperature achieved can be reduced owing to the longer combustion

period and better fuel air mixture can be formed. First injection combustion can create a suitable environment with higher temperature for the combustion of second injection to occur effectively. Late injection combustion serves to promote complete reaction between fuel and air.

According to Table 3.3, test cases examined in this test series are designed by manipulating types of fuel, SOI timings and dwell angles. Different fuel types contain different biodiesel composition and this will greatly affect the exhaust emission. On the other hand, change in SOI timings cause the start of combustion to happen at different position with corresponding condition and the ignition delay to be lengthened or shortened. Dwell angles affect the combustion characteristics and engine performance in about the same way as SOI timing where the position of start of combustion is change. Hence, the study of simultaneous effects of these three parameters has to be done to optimize the engine performance. A test case consists of combination of three levels, where each level originates from corresponding variable parameter. All possible combinations will be investigated in this experiment. First, combination of baseline diesel and dwell angle of 12°CA is fixed in studying the effect of variation in SOI timings. Then, dwell angle is changed and the steps are repeated. When all dwell angles and SOI timings have been tested using baseline diesel, the entire procedures are carried out using COB20 and COB50.

Table 3.2: Engine operating condition for third test series

Fixed parameter	Value
Engine angular velocity	2000rpm
Torque	60Nm
Fuel injection strategy	Two-stage
Mass ratio (first: second)	50:50

Table 3.3: Test cases for third test series

Variable parameter	Level
Types of fuel	Diesel, COB20, and COB50
First injection SOI timings (°ATDC)	-12, -10, -8, -6, -4, -2, 0, 2
Dwell angles (°CA)	12, 15, 18

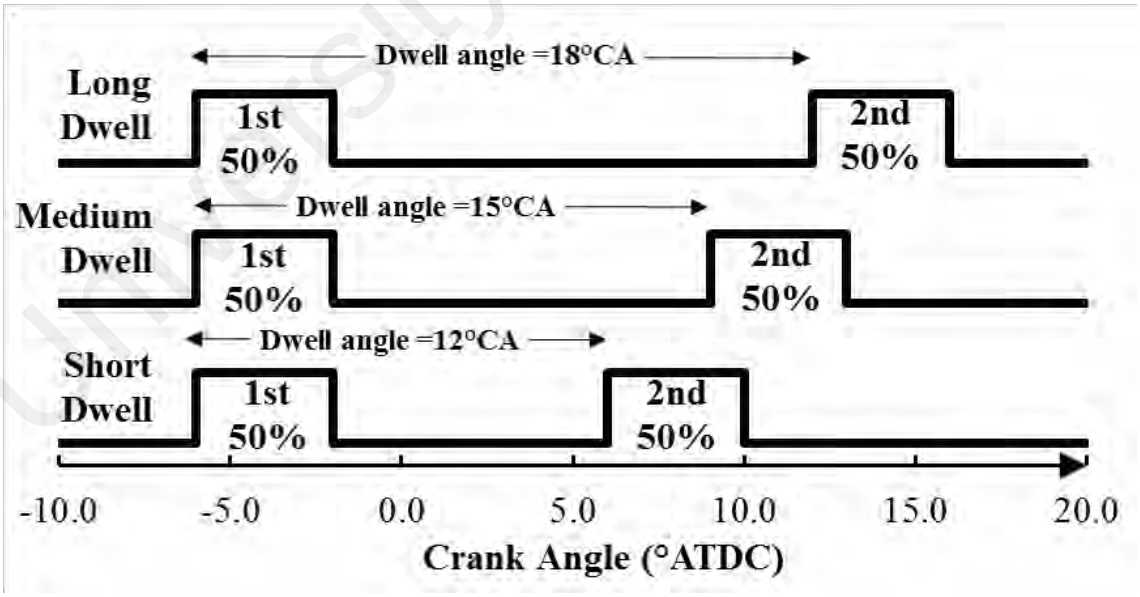

Figure 3.5: Timing chart at three different dwell angle and with first SOI of -6°ATDC for third test series

In the fourth test series, the engine torque is held constant at 60 Nm and speed with 2000 rpm, as show in Table 3.4. The effects of biodiesel blended fuels on engine out-

responses, like performance characteristics, combustion and tail-pipe emissions under different first injection SOI timing (-12° ATDC to 2° ATDC) conditions and two-stage fuel injection were studied. Two-stage injection approach can be applied by splitting the single injection event as in conventional diesel engine into two succeeding injection events for each engine combustion cycle with a fixed dwell timing of 15°CA between the succeeding injections. The benefits of this injection strategy is it able to decrease the combustion flame temperature and allow ample fuel and air mixing so that charge homogeneity can be improved. Figure 3.6 describes the timing chart for various kind of two-stage fuel injection strategies investigated in this test series. Clearly, the investigated approaches changing in the splitting schematization of fuel injection at various mass ratio of first injection to second injection of 25:75, 50:50 and 75:25.

According to Table 3.5, test cases examined in this research are designed by manipulating types of fuel, first injection SOI timings and first injection to second injection mass ratios. Different fuel types contain different biodiesel composition and this will greatly affect the exhaust emission. On the other hand, change in SOI timings cause the start of combustion to happen at different position with corresponding condition and the ignition delay to be lengthened or shortened. Fuel injection mass ratios affect the combustion characteristics and engine performance. Hence, the study of simultaneous effects of these three parameters has to be done to optimize the engine performance. A test case consists of combination of three levels, where each level originates from corresponding variable parameter. All possible combinations will be investigated in this experiment. First, combination of baseline diesel and mass ratio of 25:75 is fixed in studying the effect of variation in SOI timings. Then, mass ratio is changed and the steps are repeated. When all mass ratios and SOI timings have been tested using baseline diesel, the entire procedures are carried out using COB20 and COB50 biodiesel. The overall test details including all test series are tabulated in Table 3.7.

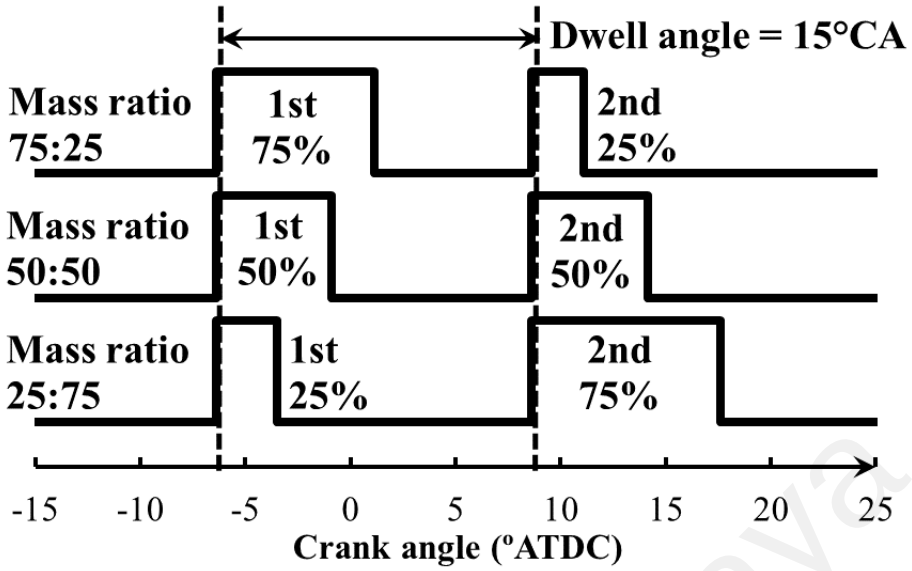

Figure 3.6: Timing chart for fourth test series with various test cases with three different injection mass ratios at SOI= -6ºATDC

Table 3.4: Engine operating condition for fourth test series

Fixed parameter	Value
Engine angular velocity	2000 rpm
Torque	60 Nm
Fuel injection strategy	Two-stage
Dwell angles (°CA)	15

Table 3.5: Test cases for fourth test series

Variable parameter	Level
Types of fuel	Diesel, COB20, and COB50
First injection SOI timings (°ATDC)	-12, -10, -8, -6, -4, -2, 0, 2
Mass ratio (first: second)	25:75, 50:50 and 75:25

Table 3.6: Engine test details

No.	Type of test	Fuel type	Load	Speed (rpm)	Fuel injection parameters	Measurement
1	Effect of different biodiesels and its blends	i. Diesel ii. COB10 - 50 iii. CIB10 - 50 iv. MOB10 - 50	100% of load (wide open throttle)	i. 1500 ii. 2000 iii. 2500 iv. 3000 v. 3500 vi. 4000	All fuel injection parameters (i.e. injection timing, injection duration, rail pressure, with/ without pilot fuel etc.) are fully controlled by the stock ECU and no modification is done to the test engine	i. Torque, Brake power, BSFC, BSEC, BTE ii. CO, NOx, Smoke iii. Combustion pressure, heat release rate iv. PM (engine operate under 16 speed-load condition for 16 mins)
2	Effect of injection timing and split injection strategies	ii. Diesel ii. COB20 iii. COB50	Constant torque of 60 Nm	2000	i. Single, double and triple injection strategies with identical injection pulses. ii. First SOI timing variation from -12° ATDC to 2° ATDC iii. Dwell timing = 1.3 ms iv. Rail pressure = 600 bar	i. BSFC, BTE ii. NOx, Smoke iii. Peak mean gas temperature, peak heat release rate iv. Combustion pressure, heat release rate
3	Effect of two-stage injection dwell angle and injection timing variation	i. Diesel ii. COB20 iii. COB50	Constant torque of 60 Nm	2000	i. Two-stage injection strategies with identical injection pulses. ii. Injection mass ratio (first: second) = 50:50 iii. First SOI timing variation from -12° ATDC to 2° ATDC iv. Dwell angle = 12°CA, 15°CA, and 18°CA v. Rail pressure = 600 bar	i. BSFC, BTE ii. NOx, Smoke iii. Peak mean gas temperature, peak heat release rate iv. Combustion pressure, heat release rate
4	Effect of two-stage injection fuel quantity and injection timing variation	i. Diesel ii. COB20 iii. COB50	Constant torque of 60 Nm	2000	i. Two-stage injection strategies. ii. Injection mass ratio (first: second) = 25:75, 50:50, and 75:25. iii. First SOI timing variation from -12° ATDC to 2° ATDC iv. Dwell angle = 15°CA v. Rail pressure = 600 bar	i. BSFC, BTE ii. NOx, Smoke iii. Peak mean gas temperature, peak heat release rate iv. Combustion pressure, heat release rate

A commercial diesel fuel is used as baseline fuel for comparison purposes in each test scheme. The engine has no starting difficulty and it functioned adequately over the whole test when biodiesel blends were used to operate the engine at room temperature. The tests were carried out when the steady-state conditions were reached. Water coolant and engine oil are both kept at optimum temperature of 85°C and 90°C, respectively, and exhaust gas is warmed sufficiently. Every test case is repeated for two times to obtain average value in order to improve the accuracy in the study. Repeatability is as high as 95% for every case tested.

3.7 Engine test system and setup

The experimental investigation is carried out using thirteen (13) fuel samples including baseline diesel, B10, B20, B30 and B50 of coconut oil (COB), *calophyllum inophyllum* (CIB), *moringa oleifera* (MOB) biodiesel blends. The blend compositions of all fuel samples are given in Table 3.7.

Table 3.7: Blend fuel composition (% volume)

No.	Fuel type	Diesel proportion (%)	Biodiesel proportion (%)
1	Diesel	100	0
2	COB10	90	10
3	COB20	80	20
4	COB30	70	30
5	COB50	50	50
6	CIB10	90	10
7	CIB20	80	20
8	CIB30	70	30
9	CIB50	50	50
10	MOB10	90	10
11	MOB20	80	20
12	MOB30	70	30
13	MOB50	50	50

The experimental work is carried out with a four cylinder, high-pressure common-rail turbocharged diesel engine. A 150 kW eddy current engine dynamometer were used to maintain the variation of speeds and loads. The intake airflow is measured with a Bosch air mass sensor. In addition, a Kobold DOM-A05 HR11H00 positive displacement gear wheel flow meter with measuring range of 0.5- 36 L/hr, which interfaced with a Kobold ZOD-Z3KS2F300 flow rate counter is employed to measure the fuel consumption of the engine. The calibration is performed by Kobold Messring GmbH and the calibrated flowmeter "K" factor is 2,790 pulses per litre. Temperature values of ambient air, exhaust gas, lubricant oil and cooling water were measured by K-type thermocouples. The specifications of the test engine are given in Table 3.8.

Table 3.8: Specifications of the test engine

Engine type	Diesel, four-stroke, turbocharged, DI engine
Fuel injection system	High-pressure common-rail (up to 140 MPa)
Number of cylinder	4
Number of valve per cylinder	2
Bore	76.0 mm
Stroke	80.5 mm
Connecting rod length	135 mm
Displacement	1461 cm^3
Compression ratio	18.25 : 1
Maximum power	48 kW @ 4000 rpm
Maximum torque	160 Nm @ 2000 rpm
Turbocharger	Yes

Pressure developed in cylinder during combustion is monitored by using Kistler 6058A piezoelectric sensor. The pressure sensor is mounted on engine by using glow plug adapter while charge amplifier, DAQ-Charge-B is utilized to amplify the signal from pressure sensor. Based on the pressure data obtained, the corresponding HRR and temperature values could be calculated using law of thermodynamics. The incremental crank encoder is also used so that at every interval of 0.125°CA, the in-cylinder pressure reading can be taken. The engine is started and run steadily for a certain amount of time, before the taking of pressure readings began. The pressure data of 100 consecutive cycles is taken and the average pressure of each data point is obtained. The signals produced by the encoder and pressure sensor were feed into a high-speed data acquisition system. Other lower speed data acquisition system and engine control module (ECM) were in-house built by utilizing Arduino microcontrollers. Figure 3.7 shows the test rig of the engine and schematic diagram of the experiment setup is shown in Figure 3.8.

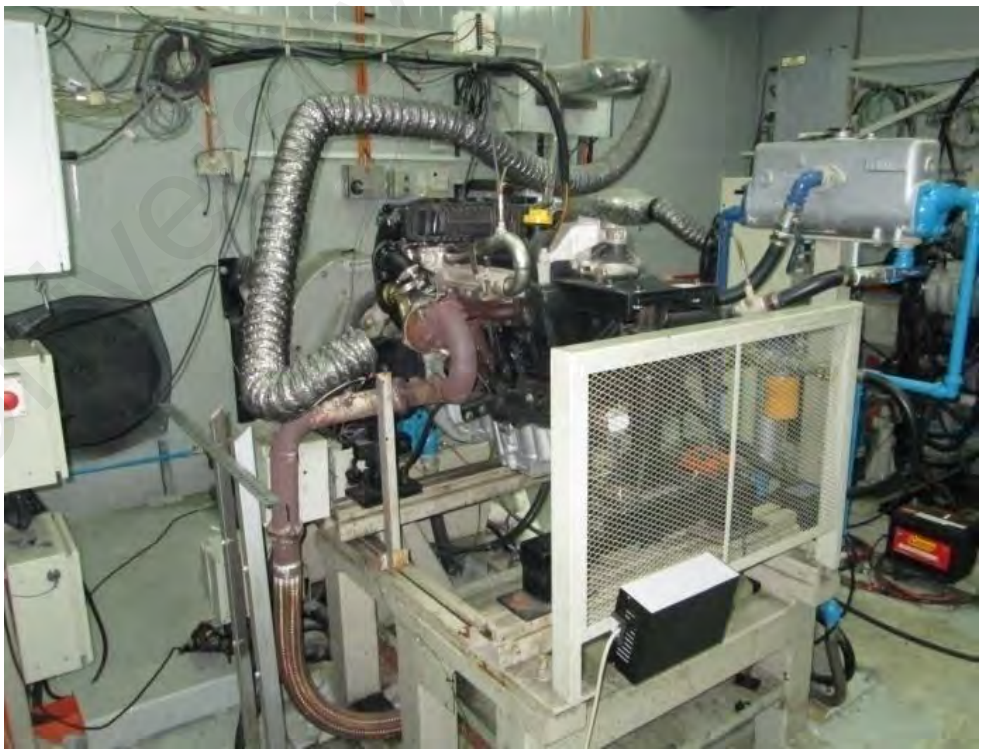

Figure 3.7: Engine test bed

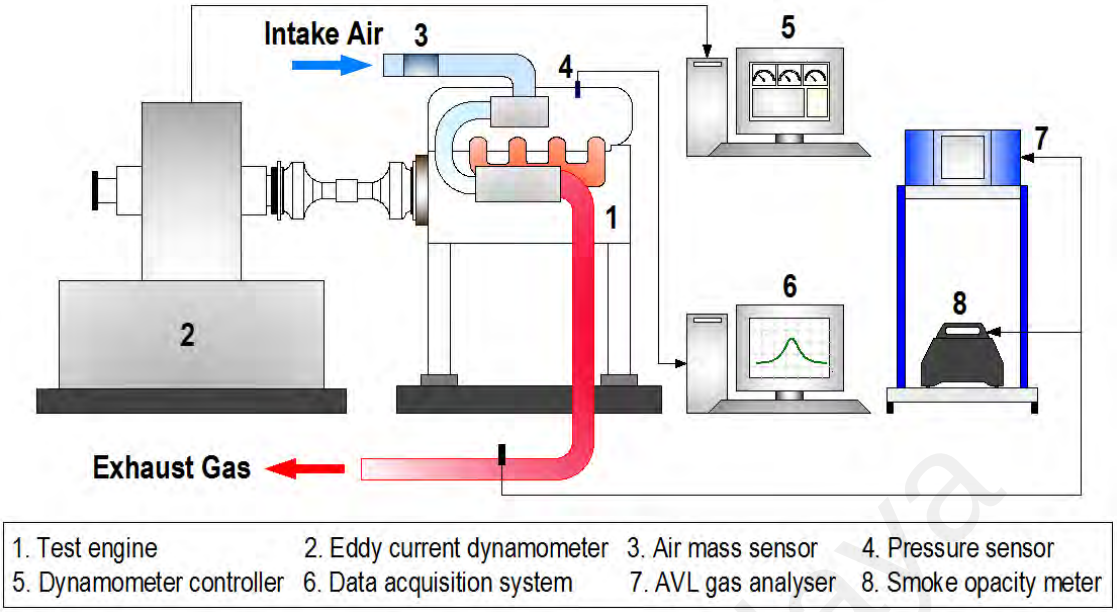

Figure 3.8: Schematic diagram of the experiment setup

The variable of the engine ECU (stock) is recorded through an on-board diagnostic (OBD) connection. The following parameters are consistently recorded (with 4 Hz of sampling rate) throughout the engine testing: the engine speed, accelerator pedal position (load demand), intake air pressure (boost pressure), intake air temperature, fuel rail pressure and engine coolant temperature. To determine the timing for both pilot and main injections, the injector voltage supply is tapped and channeled to a high speed data acquisition system. Besides, other data were also recorded with additional sensors by means of REO-dCA program and for the following measurements: engine speed, engine torque, fuel volume flow rate, exhaust gas temperature, cooling water temperature for inlet and outlet of heat exchanger for engine coolant and engine oil. For emission characterization, the exhaust emissions and smoke opacity were measured with an AVL DICOM 4000 5-gas analyzer and an AVL DiSmoke 4000 portable smoke opacity meter, respectively. All emissions were measured during steady-state engine operation. The measurement range and resolution of both of the instruments are provided in Table 3.9.

Table 3.9: Measuring components, ranges and resolution of the AVL DICOM 4000 gas analyzer and DiSmoke 4000 smoke analyzer

Equipment	Measurement principle	Component	Measurement range	Resolution
Gas analyzer	Non-dispersive infrared	Carbon monoxide (CO)	0-10% Vol.	0.01% Vol.
	Electrochemical	Nitrogen oxides (NO_x)	0-5,000 ppm	1 ppm
	Calculation	Excess air ratio (λ)	0-9,999	0.001
Smoke opacimeter	Photodiode detector	Opacity (%)	0-100%	0.10%

All related microcontroller boards were connected to the central computer via a serial USB for data acquisition. The data acquisition system is responsible for collecting signal, rectifying, filtering and converting the signal to the data to be read. The user can monitor, control and analyse the data using a LabVIEW based GUI program. All data could be logged simultaneously by clicking the record button and at the rate of 5 Hz.

3.8 PM sample collection

In the present study, although the engine PM emissions were not measured based on a legislated procedure with diluted exhaust gas, it is interesting to observe the results of simple tests with undiluted exhaust gas, and subsequent analyzing the collected PM samples in term of mass, elemental composition and surface morphology. To establish of undiluted exhaust PM sampling, a portion of raw exhaust gas is sampled in the centre of exhaust pipe in order to avoid capturing wall deposits. This portion of gas is drawn through a sampling system and the flow is controlled with a rotameter as shown in Figure 3.9. This require the design and installation of exhaust gas sampling system. In particular, this involved the installation of cooling coil, solenoid valves, filter holder, fittings, rotameter (2-25 L/min; Dwyer lnstruments, lnc.), sampling pump and electronic control system. Exhaust gas cooling is required to protect the sampling system from high temperature and is achieved by using a custom made circular stainless steel cooling coil, with ambient air as the cooling medium. Cooling coil is connected straight to the engine exhaust stream. Quartz filter is one of the most important experimental items for this

research. The characteristics of quartz filter being used in this research is in Table 3.10. A 47 mm PALL, 2500 QAT-UP Tissuquartz PM filters are used for PM collection. Quartz filter is a high purify microfibers for collecting diesel particulates and trace level environmental pollutants. It is superior purify for collection of organic carbon and has low metal background with free binder. It can withstand temperature up to 1000 °C and high flow rate. It is specified in NIOSH Method 5040 for elemental carbon for diesel particulates. All quartz filters were baked in the furnace (Nabertherm B180 furnace) at 900 °C for 2.5 hours and weighed before and after being loading with PM (Rojas et al., 2011; Tsai, et al., 2010). The weighing procedure is performed twice to obtain an average weight with a Scaltec SBA 31 analytical micro balance with sensitive to ±0.0001g. The weight of the filter is recorded for the calculation of PM mass. The quartz filters were conditioned and dried for 24 hours in desiccator before sampling. The blue silica gel in the space below the platform is used as the desiccant, as shown in Figure 3.10. By doing this method, which ensured precise measurements of mass of particulates (Agarwal, et al., 2011; Rojas, et al., 2011; Tsai, et al., 2010). Next, a 47 mm in-line aluminum filter holder is used to hold the quartz filter for PM sampling. For each test, the filter holder is fully disassembled and flushed on a regular basis with cleaning detergent to remove any organic materials. Subsequently, the aforementioned of preconditioned filter is then carefully transferred with tweezers into the filter holder and internally supported by a stainless steel support screen. After the installation, the filter holder is then placed in between the solenoid valve A and the 3-ways fitting, as illustrated in Figure 3.9. From the diagram, it can be seen that two solenoid valves are employed for directing the gas samples. The solenoid valve A and B are located upstream and downstream of the filter holder, respectively, to control the flow of gas sample. At steady engine operation and during sampling process, the solenoid valve A and B are turned ON and OFF, respectively, to divert gas sample passes through the filter assembly, then through

rotameter, and finally through the sampling pump. In the case of non-sampling condition (i.e. during transient engine conditions), the solenoid valve A and B are turned OFF and ON, respectively, to bypass gas sample from passes through the filter assembly. The switching configuration of both of the valves is indicated in

Table 3.11. Before the testing, the rotameter is adjusted and calibrated with BIOS DEFENDER Model 510H air calibrator to ensure a consistent flow rate of 15 L/min is achieved throughout the testing. This flow rate is chosen such that at the end of each test, the quantity of the PM sample is sufficient for analysis. For each testing having a different blend fuel, engine is flushed before the next testing. This ensured that no residue or fuel from previous testing in the fuel line. Hence, accurate results for each testing is ensured. For the sampling of exhaust PM, another sequence of engine test cycle which composed of 16 different steady-state modes at various loads and speed conditions is proposed and as shown in Table 3.12. The selected operation points cover a wide range of the engine operation map (cover all four quadrants of the speed-load regime) and the specific test sequence is programmed in the test bed dynamometer controller. The hold duration for each test point is programmed for 60 s to ensure stabilization on a repeatability of experiments and the transition delay between two successive test points is set to 10 s. This has resulted in a total of 16 minutes of steady engine operating duration for each fuels blend to ensure that a minimum of 0.0013g of particulates can be accumulated and collected (Lapuerta, et al., 2008c). For different fuel blends for each testing, engine is flushed before the next testing with different blend fuel. After testing, quartz filters were unloaded from the filter holder and conditioned for 24 hours in desiccator and weighed. Next, the filter holder is cleaned with cleaning detergent after each testing for accurate results. The PMs' mass are calculated by the difference between quartz filter mass after sampling which is already being conditioned in desiccator and quartz filter mass before sampling which also is being conditioned in desiccator. These values were the PMs' mass

that being exerted from the diesel engine exhaust. The morphology and size of PM of each fuel blend were obtained with a scanning electron microscope (SEM). Furthermore, the morphology SEM images of each sample's surface is investigated. Besides, the element composition of the sample is analyzed by Energy-dispersive X-ray Spectroscopy (EDX) at 3000x magnification level. Figure 3.11 shows the flow chart for PM sampling used in the present study.

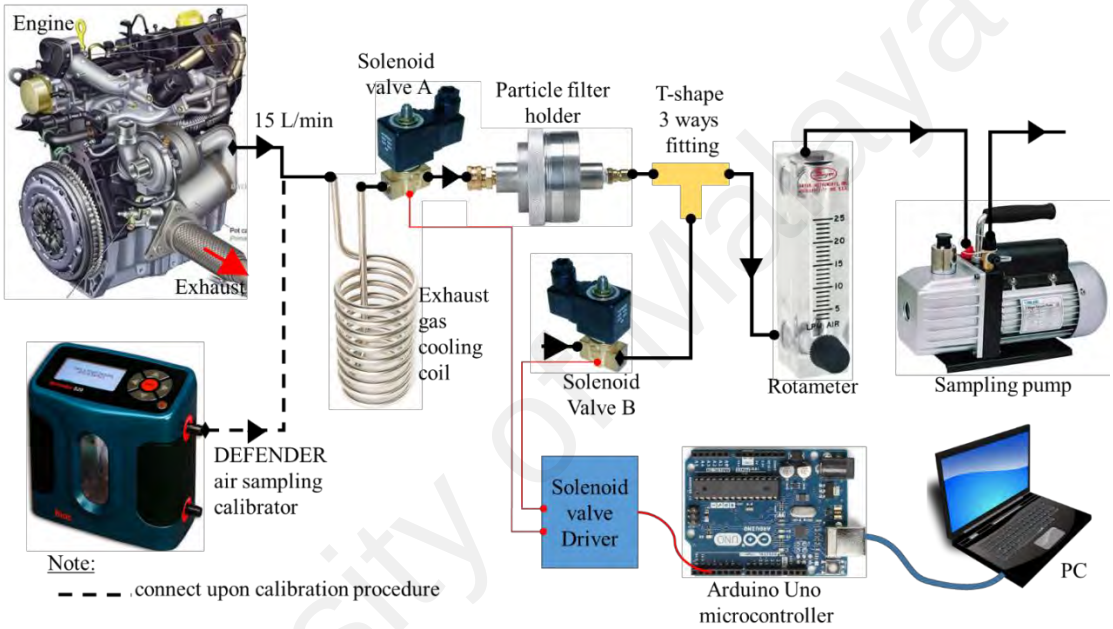

Figure 3.9: Exhaust particulate sampling flow diagram

Table 3.10: Specifications of the quartz filter for exhaust particulate sampling

Brand	PALL
Quartz type	Tissuquartz
Thickness	432 µm
Maximum temperature	1000 °C

Figure 3.10: Quartz filters in desiccator

Table 3.11: Switching configuration of solenoid valve A and B

State	Solenoid valve		Result
	A	B	
1	ON	ON	Non-sampling
2	ON	OFF	Sampling
3	OFF	ON	Non-sampling
4	OFF	OFF	Non-sampling

Table 3.12: Sequence of test modes for the comparison of fuels

Mode	Engine Speed (rpm)	Load (%)	Torque (Nm)	Duration (sec)
1	3850	100	Maximum*	60
2	3850	75	75	60
3	3850	50	50	60
4	3850	25	25	60
5	3100	100	Maximum*	60
6	3100	75	90	60
7	3100	50	60	60
8	3100	25	30	60
9	2350	100	Maximum*	60
10	2350	75	120	60
11	2350	50	80	60
12	2350	25	40	60
13	1600	100	Maximum*	60
14	1600	75	105	60
15	1600	50	70	60
16	1600	25	35	60

Note: * maximum torque value depend on fuel type

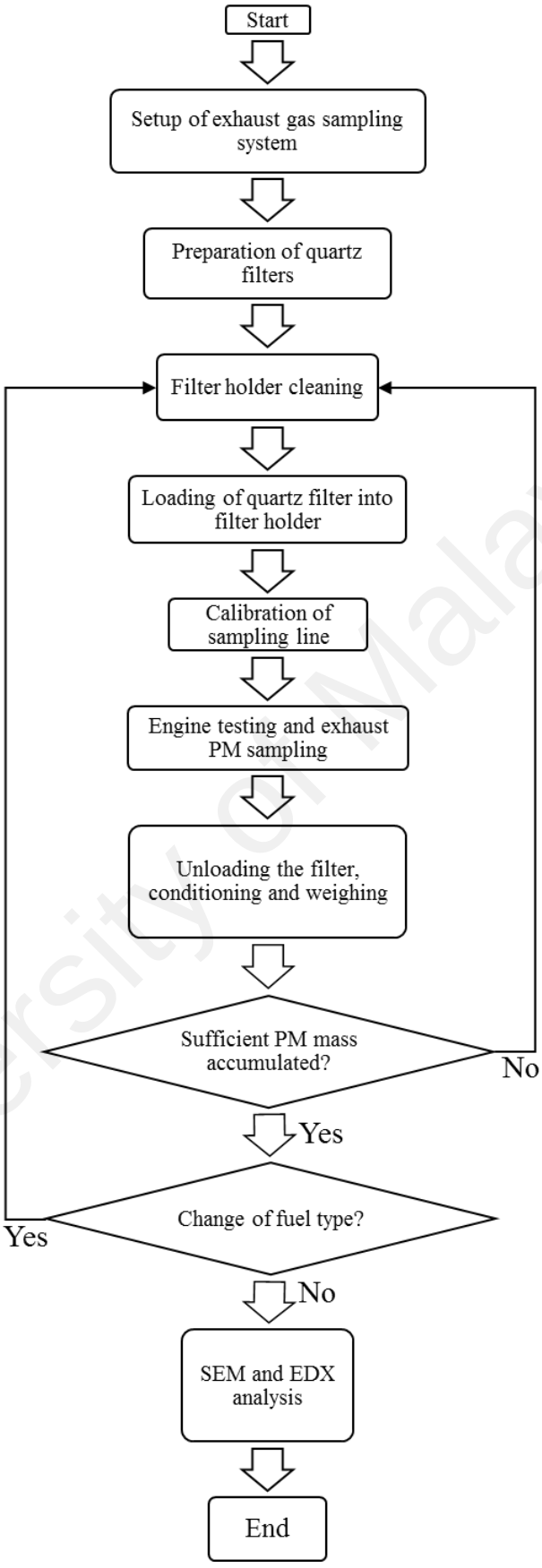

Figure 3.11: Flow chart for PM sampling

3.9 Engine control module (ECM)

A commercially available Arduino microcontroller is used as the fuel injection engine control module (ECM) for the engine. Three interrupt service routines in the microcontroller were used to collect the signals from incremental encoder and engine camshaft and the schematic diagram can be seen in Figure 3.12. Generally, two microcontroller are needed for the control of injection timing and the other one for the control of injection pulse-width. Furthermore, programming coding is wrote by using the C programming language. The codes were uploaded to microcontroller through serial communication with personal computer. By using LabVIEW to create the graphic user interface (GUI) program in order to control and investigate the engine parameters containing engine speed, start of injection (SOI) timing, number of injections (single, double and triple injection), closed-loop engine speed control mode selection and opening pulse-width (PW). The LabVIEW graphic user interface tab for fuel injection parameter is shown in Figure 3.13. A dedicated engine speed controller coding is used to regulate the amount of diesel injected in order to keep engine rpm to within ±10 rpm from the set point. This engine speed controller coding consist of a fine-tuned proportional-integral (PI) control loop. By establish this approach, the speed controller could banish a large amount of minor steady-state error and disturbance spanning the whole engine operating range. Besides, programmable peak and hold pulse-width-modulation (PWM) is incorporated in engine controller to vary the current supplied to solenoid injectors for common-rail direct injection to operate efficiently. With these specifically designed control unit, all engine parameters could be flexibly and fully controlled.

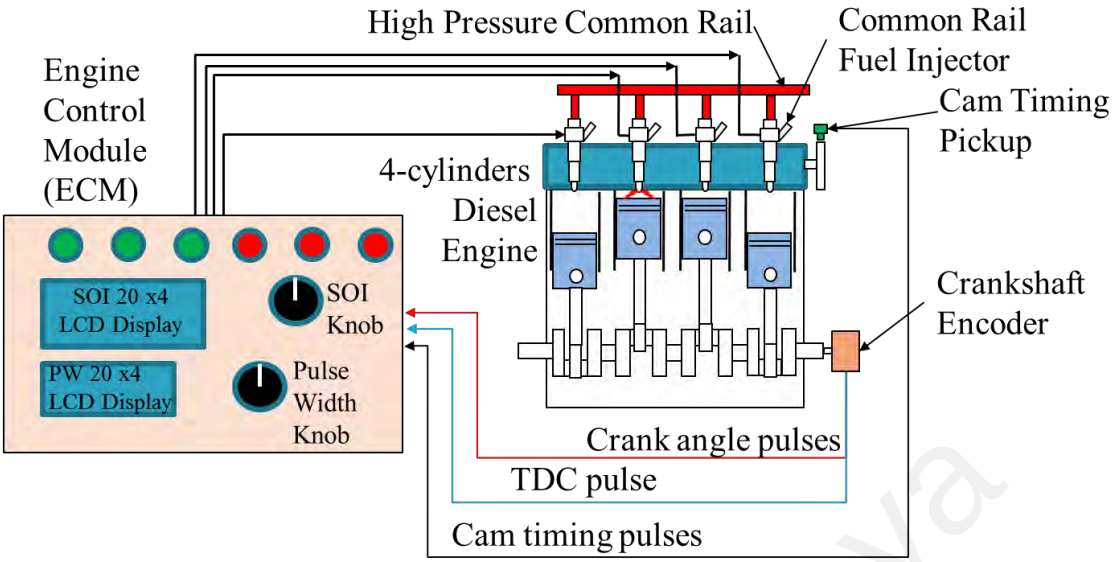

Figure 3.12: Schematic diagram of the custom-made ECM setup

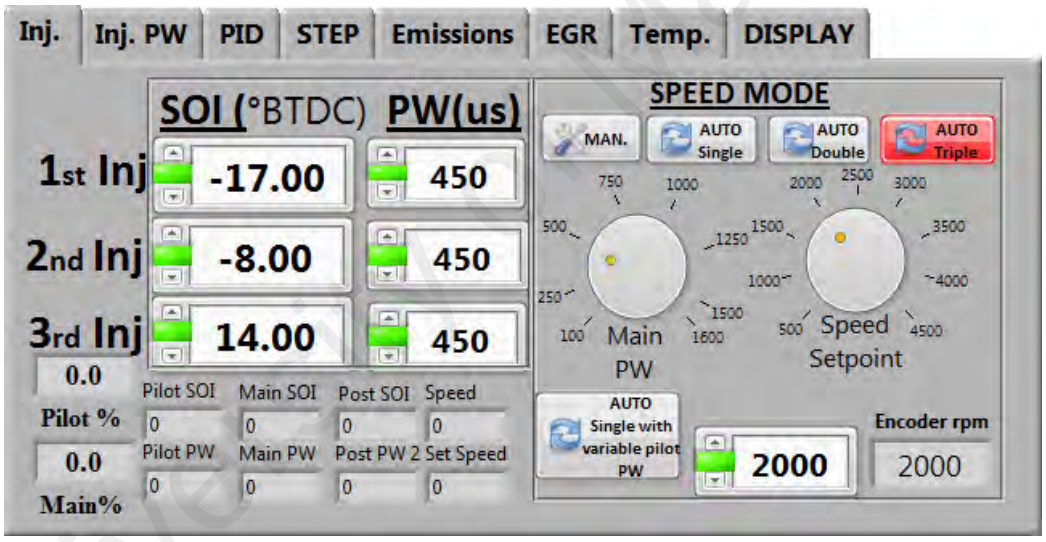

Figure 3.13: LabVIEW graphic user interface tab for fuel injection parameter

3.10 Calculation methods

3.10.1 Engine performance

The engine performance in this work is evaluated based on BSFC, BSEC, brake power and BTE. Basically, BSFC is a measure of the fuel efficiency of an engine that burns fuel and produces shaft power. Another more scientifically rational parameter to compare the performance of fuels with different calorific values is the BSEC. Mathematically, the BSEC is the product of the BSFC and calorific value of fuel. It measures the input energy

required to develop a unit output power. The lower the value, the better the efficiency of energy consumption is. Besides, the power developed by the engine at the output shaft is measured by applying the brake with eddy current dynamometer and is therefore called brake power. Furthermore, the efficiency of conversion of the heat energy produced by the actual combustion of the fuel into the power output of the engine is commonly expressed as BTE. The related equations for BSFC, BSEC, brake power and BTE are determined and calculated according to the following equations:

$$\text{BSFC(g/kWh)} = \frac{\text{Fuel consumption } (g/h)}{\text{Brake Power (kW)}} \tag{3.1}$$

$$\text{BSEC(MJ/kWh)} = \frac{\text{Calorific value (MJ/kg)} \times \text{Fuel Consumption (g/h)}}{1000 \times \text{Brake Power (kW)}} \tag{3.2}$$

$$\text{Brake power (kW)} = \frac{2 \times \pi \times \text{Engine speed (rpm)} \times \text{Torque(Nm)}}{60000} \tag{3.3}$$

$$\text{BTE (\%)} = \frac{\text{Brake power (kW)} \times 360}{\text{Calorific value } (\frac{\text{MJ}}{\text{kg}})) \times Fuel\ consumption(\frac{L}{h}) \times Density(\frac{kg}{L})} \tag{3.4}$$

3.10.2 HRR analysis

Analysis of HRR provides valuable insights into the rate of heat release during the combustion process. The results can facilitate assessment of the rate of combustion and combustion-related problems. In the present study, the calculation of HRR is based on the cylinder pressure and volume measurements. The HRR formula, as given in Equation (3.5), is derived from the first law of thermodynamics. For simplification purposes,

leakage and heat transfer to the wall are assumed to be negligible and were excluded during the derivation of this equation.

$$\frac{dQ}{d\theta} = \frac{\gamma}{\gamma - 1} P \frac{dV}{d\theta} + \frac{1}{\gamma - 1} V \frac{dP}{d\theta} \tag{3.5}$$

where $\frac{dQ}{d\theta}$ is the HRR per crank angle, θ is the crank angle, P is the pressure, V is the cylinder volume, and γ is the specific ratio which is taken to be 1.37.

Another worthy observation that can be further analyzed from the HRR diagram is the variations in ID (ignition delay). When the piston is close to TDC, the fuel vaporization effect causes a negative heat release and this event is termed ID. Mathematically, ID is defined as the crank angle interval measured from start of injection (SOI) timing to start of combustion (SOC) timing which is typically determined from the fuel injector signal and HRR data, respectively. For instance, the sample of calculation for ID can graphically be found from Figure 3.14.

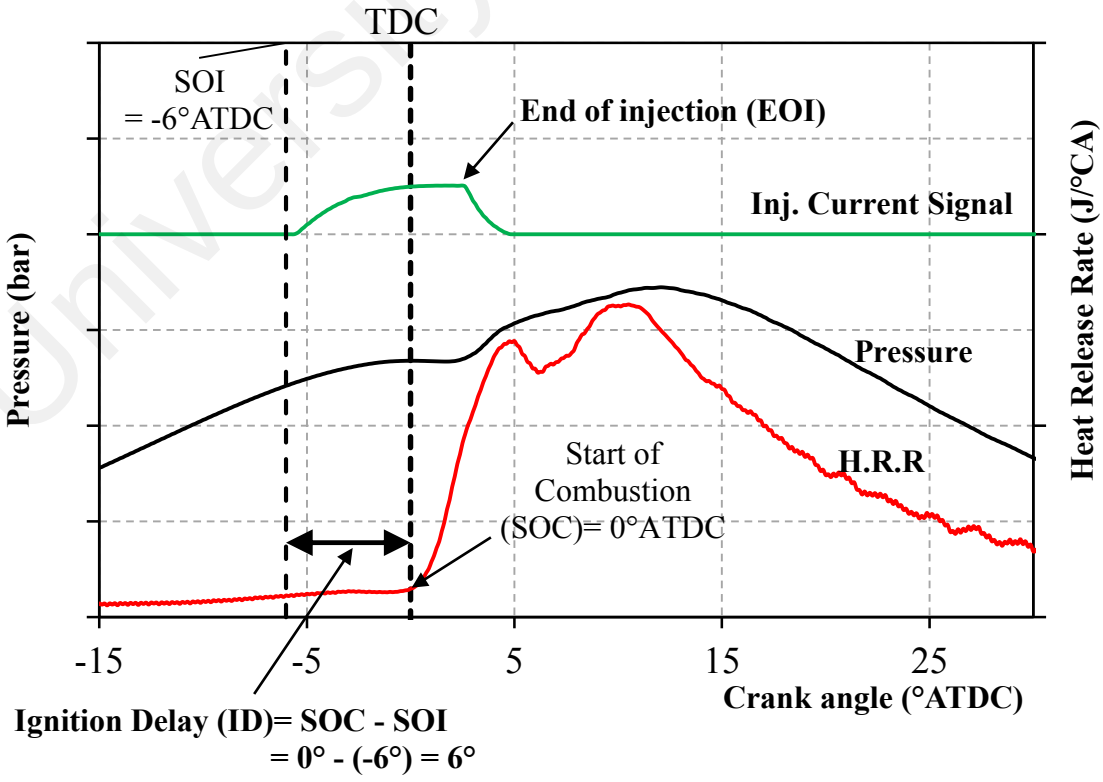

Figure 3.14: Sample of calculation for ignition delay (ID)

3.10.3 Statistical and equipment uncertainty analysis

In any experiment, errors and uncertainties can arise from instrument selection, condition, calibration, environment, observation, reading and test procedure. The measurement range, accuracy and percentage uncertainties which associated with the instruments used in this experiment are listed in Table 3.13. Uncertainty analysis is necessary to verify the accuracy of the experiments. Percentage uncertainties of various parameters such as brake power, BSFC, BSEC, carbon monoxide (CO) and nitrogen oxide (NOx) were determined using the percentage uncertainties of various instruments employed in the experiment. To compute the overall percentage uncertainty due to the combined effect of the uncertainties of various variables, the principle of propagation of errors is considered and can be estimated as ±3%. The overall experimental uncertainty is computed as follows:

Overall experimental uncertainty = Square root of [(uncertainty of fuel flow rate)^2 + (uncertainty of brake power)^2 + (uncertainty of BSFC)^2 + (uncertainty of BSEC)^2 + (uncertainty of CO)^2 + (uncertainty of NOx)^2 + (uncertainty of smoke)^2 + (uncertainty of pressure sensor)^2 + (uncertainty of crank angle encoder)^2] = Square root of [$(0.5)^2 + (0.3)^2 + (1.5)^2 + (1.5)^2 + (1)^2 + (1.3)^2 + (1)^2 + (0.5)^2 + (0.03)^2$] = 3%

Table 3.13: List of measurement accuracy and percentage uncertainties

Measurement	Measurement range	Accuracy	Measurement techniques	% Uncertainty
Load	±600 Nm	±0.1 Nm	Strain gauge type load cell	±0.25
Speed	0-10,000 rpm	±1 rpm	Magnetic pick up type	±0.1
Time	-	±0.1s	-	±0.2
Fuel flow measurement	0.5-36 L/hr	±0.04 L/hr	Positive displacement gear wheel flow meter	±0.5
Air flow measurement	0.25-7.83 kg/min	±0.07 kg/min	Hot-wire air-mass meter	±2
CO	0-10% by vol.	±0.01%	Non-dispersive infrared	±1
NOx	0-5,000 ppm	±1ppm	Electrochemical	±1.3
Smoke	0-100%	±0.1%	Photodiode detector	±1
EGT sensor	0-1200°C	±0.3°C	Type K thermocouple	±0.15
Pressure sensor	0-25,000 kPa	±10kPa	Piezoelectric crystal type	±0.5
Crank angle encoder	0-12,000 rpm	±0.125°	Incremental optical encoder	±0.03
Computed				
Brake power	-	±0.03 kW	-	±0.3
BSFC	-	±5 g/kWhr	-	±1.5
BSEC	-	±0.2 MJ/kWhr	-	±1.5

CHAPTER 4: RESULTS AND DISCUSSION

4.1 Introduction

In this chapter, the results for all research objectives are presented and discussed. In the first section, the physicochemical and composition of crude coconut, *calophyllum inophyllum* and *moringa oleifera* are comprehensively shown and discussed. This is followed by the result and discussion of physicochemical properties of biodiesel-diesel blends. Generally, biodiesel can be used in a diesel engine either in its neat form or blended with petroleum diesel. Lower-level blends of up to 50% are considered in this study, mainly because they represent a good balance in terms of engine performance, emissions, production cost, cold-weather performance, and materials compatibility. In fact, lower level blends generally do not require major engine modifications. In the second section of this chapter, the results of engine performance, gaseous emissions, particulate matter (PM) and combustion for engine fueled with coconut, *calophyllum inophyllum* and *moringa oleifera* biodiesel blends are presented and analyzed. This is followed with the parametric studies relating with start of injection timing variation and multiple injection schemes using COB20 and COB50 blends and the results are benchmarked with petroleum diesel fuel as baseline. At the last section of this chapter, the impact of two-stage injection dwell angle and mass ratio on engine performance, emissions and combustion characteristics using coconut biodiesel blends are presented and discussed. Note that only COB20 and COB50 were selected for injection parameters studies. This is mainly due to the fact that it is easily available in Malaysia and the use of this feedstock for biodiesel production is the most cost-effective and will pave the way for large-scale production of biodiesel.

4.2 Characterization of crude oil

In this research study, physicochemical properties are measured using the equipment and methods mentioned in section 3.5. The physicochemical properties of crude coconut, *calophyllum inophyllum*, *moringa oleifera* oil and diesel are presented in Table 4.1.

Table 4.1: Physicochemical properties of crude coconut, *calophyllum inophyllum*, *moringa oleifera* oil and diesel

Properties	**Units**	**Coconut Oil**	***Calophyllum Inophyllum* Oil**	***Moringa Oleifera* Oil**	**Diesel**
Kinematic viscosity at 40°C	mm^2/s	42.10	53.45	32.69	3.63
Density at 40°C	kg/m^3	909.0	922.2	905.5	834.4
Flash point	°C	220	218	269	71.5
Cloud point	°C	9	-2	-7	3
Pour	°C	5	-3	-7	0
Calorific value	MJ/kg	37.90	40.10	39.90	45.21
Acid value	mgKOH/g oil	6.0	37.8	1.6	-

It is evident from the Table 4.1 that all crude oil samples used in the present study exhibited higher viscosity compared to diesel fuel. If these fuels to be used in diesel engine, the phenomenon of higher viscosity will reduce the ability of the fuel to evaporate and mix with the air; consequently this mitigates the combustion efficiency and affects various engine parameters. For solving these issues, the typical strategies is to blend the crude oil with diesel fuel or by using the well-known chemical reaction of transesterification process to convert the crude oil to biodiesel. As a result, the viscosity will be tremendously reduced and can be used in CI engines.

From Table 4.1, it can be seen that the *calophyllum inophyllum* oil showed the highest kinematic viscosity of 53.45 mm^2/s and density of 922.2 kg/m^3 at 40°C. Besides, *moringa oleifera* oil exhibited lowest kinematic viscosity (32.69 mm^2/s) and density (905.5 kg/m^3) at 40°C compared to crude coconut and *calophyllum inophyllum* oil. In addition, it can be seen that the calorific value of crude oil is generally lower than that of diesel because of its higher fuel-borne oxygen content (Ramadhas, et al., 2005). This is evidently showed in Table 4.1 with the calorific value of all types of oil are lower than diesel fuel of 45.21

MJ/kg. The results indicated that coconut, *calophyllum inophyllum* and *moringa oleifera* oil exhibited 16.1, 11.3 and 11.8% lower calorific value as compared to diesel fuel. In term of flash point property, the results showed that all crude oils are characterized with higher flash points (>150°C), which indicate that these oils are very safe for handling, transportation and storage. The results revealed that flash points of coconut, *calophyllum inophyllum* and *moringa oleifera* oil are 220, 218 and 269°C respectively. Besides, the acid value results also indicated that, except for *moringa oleifera* oil (1.6 g KOH/g), both of the coconut (6.0 g KOH/g) and *calophyllum inophyllum* (37.8 g KOH/g) exhibited very high amount of acid value. Due to the higher acid value of these crude oils, a two-step (acid-base catalyst) chemical reaction process (i.e. esterification and transesterification) are required for both of the coconut and *calophyllum inophyllum* oil, while *moringa oleifera* oil only need single process of transesterification for conversion of oil to biodiesel.

4.3 Properties of produced biodiesel

The quality of biodiesel depends upon several factors, such as quality and composition of feedstock, production process, handling and storage process. In the present study, the well-known chemical reaction of transesterification is adopted for conversion of oil to biodiesel. The final product of methyl ester's fuel properties is studied and compared with the standards. As tabulated in Table 4.2 is the key physicochemical properties of the converted neat COB (coconut oil), CIB (*calophyllum inophyllum*) and MOB (*moringa oleifera*) in comparison with ASTM standard. The key properties of the petroleum diesel are also listed in this table.

Technically, the fuel density is proportional to the bulk modulus (compressibility of fuel). High bulk modulus shows that the fluid is relatively incompressible. For less compressible fuel, pressure builds more quickly and thus require less time and as a result

injection occurs earlier into the combustion chamber in the compression cycle. Therefore, higher density and bulk modulus of fuel will lead to earlier injection timing. The earlier injection timing can lead to a longer premixed burning phrase and produces higher cylinder temperature or more NO_X emission (Pandey et al., 2012). In the present study, the measurement of fuel density showed that the densities of produced biodiesels are higher than that of diesel fuel as shown in Table 4.2.

Viscosity is considered as one of the most important properties for biodiesel. It is known that the low viscous fuel are easier to vaporize and mix with air. Most of the unburned hydrocarbon deposits found in combustion chamber walls and exhaust pipe are mainly attributed due to partially rich mixture and large fuel droplet sizes which is basically caused by high viscosity (Kannan et al., 2009). From Table 4.2, it can be seen that the viscosity of produced biodiesels are higher than that of diesel fuel. Among all the fuel properties, calorific value has been identified as one of the most important parameter because it influences the combustion temperature in CI engine. As shown in Table 4.2, it can be seen that compared to diesel fuel, the produced biodiesels exhibit slightly lower calorific value, which is associated to its lower mass energy values and higher oxygen content.

Flash point is inversely related to fuel volatility (Hoekman et al., 2012). The minimum temperature at which fuel gives off enough vapor to produce an inflammable mixture is known as flash point. From Table 4.2, it is clearly seen that the produced biodiesels have much higher flash point than diesel fuel. Higher value of flash point indicates that biodiesels are safe in terms of storage, fuel handling and transportation.

Overall, it can be observed that the physicochemical properties of the produced biodiesels are measured and benchmarked against the biodiesel standards based on ASTM D6751. It appears that all of the physicochemical properties of biodiesels are able

to meet the ASTM and biodiesel standard. Subsequently, the flash point is greater than that of petroleum diesel and is appropriated to operate as fuel for transportation. However, the calorific value is lower than that of fossil diesel.

Table 4.2: Physicochemical properties of produced biodiesel compared to diesel

Properties	**Units**	**Standards**	**Limit (ASTM D6751)**	**COB**	**CIB**	**MOB**	**Diesel**
Kinematic viscosity at 40 °C	mm^2/s	ASTM D445	1.9-6.0	4.10	5.07	4.03	3.63
Density at 40°C	kg/m^3	ASTM D1298	870-890	867.0	869.4	866.1	834.3
Flash point	°C	ASTM D93	130 min	182.5	140.0	189.0	71.5
Cloud point	°C	ASTM D2500	-3 to 12	4	1	0	3
Pour point	°C	ASTM D97	-15 to 16	3	1	-1	0
CFPP	°C	ASTM D6371	19	7	6	-2	5
Cetane number	-	ATM D6890	47 min	56.7	55.8	54.3	52.4
Calorific value	MJ/kg	ASTM D240	-	38.70	39.60	39.90	45.21
Acid value	mg KOH/g	ASTM D664	0.5 max	0.05	0.37	0.24	-
Oxidation stability at 110º C (hours)	h	EN ISO 14112	3 min	7.0	6.3	6.5	>100.0
Conradson carbon residue (100% sample)	m/m	ASTM D4530	0.05 max	0.021	0.03	0.042	0.125
Carbon	%wt	ASTM D5291	-	73.2	75.4	76.7	86.1
Hydrogen	%wt		-	12.5	12.7	12.5	13.8
Nitrogen	%wt		-	< 0.1	< 0.1	< 0.1	< 0.1
Oxygen	%wt		-	14.3	11.9	10.8	0.1
Carbon to hydrogen ratio	-	-	-	5.86	5.94	6.14	6.24

4.4 Fatty acid composition of biodiesels

Biodiesel derived from different sources are not identical in term of fatty acid composition. Fatty acid composition affects upon fuel properties such as density, cetane number, calorific value, oxidation stability and low temperature properties. The physicochemical properties of the biodiesel fuel are determined by the composition of fatty acid, fatty acid chain length and number of double bonds present in the molecules. Fatty acid without double bond is known as saturated fatty acid, while fatty acid containing double bond is called unsaturated fatty acid. The results of fatty acid composition of COB, CIB and MOB biodiesels are shown in Table 4.3. It is seen that, saturated fatty acid of COB, CIB and MOB biodiesel is 90.02%, 33.01% and 19.10% respectively. It can be seen that COB contained a higher level composition of saturated (90.02%) and unsaturated (9.98%) fatty acids. Ironically, the MOB contains a saturation-unsaturation ratio of 19.10:80.90, in which the level of unsaturated fatty acids is about four time higher than that of saturated fatty acids. Besides, it is found that CIB contained a moderate level composition of saturated (33.01%) and unsaturated (66.89%) fatty acids.

4.5 Characterization of biodiesel-diesel blends

For engine testing, each of the produced biodiesels is blended with diesel fuel in different proportions. The blend compositions of all fuel samples are given in Table 4.4. The main physicochemical properties of biodiesel blends such as kinematic viscosity, density and calorific value are measured and tabulated in the same table. From the results, it can be seen that blending of biodiesel with diesel results in improvement in kinematic viscosity, density and calorific value. The result also shows that the kinematic viscosity and density of all the fuel blends increased when the concentration of the biodiesel increased. CIB biodiesel blends show the highest kinematic viscosity and density, while MOB biodiesel blends show the lowest kinematic viscosity and density. All biodiesel blends are found met the ASTM D6751 standard for biodiesels kinematic viscosity range

(< 6.00 mm^2/s). In contrary, the calorific value decreased when the blending ratio of biodiesel increased. The results show that all biodiesel blends have lower calorific value compared to diesel fuel. In fact, for the corresponding blend ratio, it is found that MOB biodiesel blends show the highest calorific value compared to other type of biodiesel.

Table 4.3: Fatty acid composition of COB, CIB and MOB biodiesel

Property	Systematic name	COB	CIB	MOB
Carbon chain length distribution (wt.%)				
Saturated fatty acid				
C4:0 (Butyric)	Butanoic	0.6	0.45	0.5
C6:0 (Caproic)	Hexanoic	0.3	0	0
C8:0 (Caprylic)	Octanoic	6.19	0	0
C10:0 (Capric)	Decanoic	5.46	0	0.28
C11:0 (Undecylic)	Undecanoic	0	0	0
C12:0 (Lauric)	Dodecanoic	44.58	0.17	0.72
C14:0 (Myristic)	Tetradecanoic	17.98	0	0.45
C15: 0 (Pentadecylic)	Pentadecanoic	11.09	15.02	12.26
C16:0 (Palmitic)	Hexadecanoic	0.6	0.45	0.5
C18:0 (Stearic)	Octadecanoic	3.22	16.92	4.39
Unsaturated fatty acid				
C16:1n7 (Palmitoleic)	(9Z)-Hexadec-9-enoic acid	0	0.24	0
C18:1n9c (Oleic)	(9Z)-Octadec-9-enoic acid	8.37	39.15	26.99
C18:2n6c (Linoleic)	(9Z,12Z)-9,12-Octadecadienoic acid	2.21	26.35	47.19
C18:3n6 (γ-linoleic)	all-cis-6,9,12-octadecatrienoic id	0	0.89	0.86
C18:3n3 (α-linolenic)	(9Z,12Z,15Z)-9,12,15-Octadecatrienoic	0	0	5.95
C20:3n6 (Dihomo-γ-linolenic)	cis,cis,cis-8,11,14-Eicosatrienoic	0	0.26	0.42
Fatty acid saturation /unsaturation ratio (wt.%/ wt.%)		90.02/ 9.98	33.01/ 66.99	19.10/ 80.90

Table 4.4: Blend fuel compositions (% volume) and the main fuel properties of biodiesel blends

Fuel	Diesel proportion (% vol.)	Biodiesel proportion (% vol.)	Fuel Properties		
			Kinematic viscosity at 40 °C, mm^2/s	Density at 40°C, kg/m^3	Calorific value, MJ/kg
Diesel	100	0	2.99	834.3	45.21
COB10	90	10	3.28	834.9	44.67
COB20	80	20	3.35	838.1	43.91
COB30	70	30	3.43	841.4	43.22
COB50	50	50	3.62	848.3	41.70
CIB10	90	10	3.87	838.4	44.80
CIB20	80	20	3.94	841.8	44.21
CIB30	70	30	4.01	845.2	43.60
CIB50	50	50	4.25	851.7	42.38
MOB10	90	10	3.31	834.8	44.93
MOB20	80	20	3.39	838.2	44.30
MOB30	70	30	3.48	841.6	43.69
MOB50	50	50	3.69	848.5	42.67

4.6 Effect of biodiesel blends on engine out-response

In this study, the effect of COB, CIB and MOB biodiesel diesel blends on a medium-duty multi-cylinder diesel engine is investigated and discussed in this section. The findings of the key studies investigated in this section included of engine performance, gaseous emissions, exhaust PM characterization and combustion analysis, which will greatly facilitate scientists and policymaker involved in biodiesel research to grasp quick information on the engine-out responses with CIB and MOB biodiesel as potential non-edible biodiesel sources and compare with those of edible source of COB biodiesel.

4.6.1 Engine performance analysis of COB, CIB and MOB biodiesel blends

In order to analyze and compare the engine parameters such as torque, brake power, BSFC, BSEC and BTE when fueled with COB, CIB and MOB biodiesel diesel blends, the test engine is operated at full load condition with six levels of engine speeds.

4.6.1.1 Engine torque

The common-rail diesel engine is operated at full load condition with six levels of engine speeds from 1500 to 4000 rpm with 500 rpm step. Figure 4.1 shows the variations in engine torque compared to the baseline diesel for different biodiesel blends under full load conditions. The general trend indicated that the maximum engine torque is happened at engine speed of 2000 rpm for all types of fuel and biodiesel blends. With biodiesel in the blend, the general trend shows that the engine torque of biodiesel blends is consistently lower than that of baseline diesel across all tested engine speeds. This decrement is expected and well aligned with other researcher (Liaquat et al., 2013). This can be explained with the combined effect of lower calorific value and higher viscosity compared to diesel. Essentially, fuel with higher viscosity may worsen in injection efficiency and atomization characteristics, and adversely affect fuel combustion leading to lower engine torque. Meanwhile, calorific value is a measure of the amount of energy produced by the complete combustion of fuel. Lower calorific value of fuel implies lower amount of heat released by the fuel in engine, hence, resulted in lower engine torque. Besides, the engine torque values are also reduced with higher biodiesel concentration in the blend. A direct comparison of engine torque between all the tested fuels at 2000 rpm is shown in Figure 4.2. The result revealed that with the increase in the biodiesel blending ratio, the changing in engine torque is more noticeable and larger. Among the tested biodiesel blends, COB blends produced higher engine torque compared to MOB and CIB blends due to its relatively lower kinematic viscosity and higher calorific value. The plot showing the relationship between engine torque and calorific value and kinematic viscosity for all fuels can be seen in Figure 4.3 and Figure 4.4, respectively. A maximum engine torque recorded for diesel, COB10, MOB10 and CIB10 are 148.00 Nm, 147.66 Nm, 147.08 Nm, and 146.22 Nm respectively at 2000 rpm.

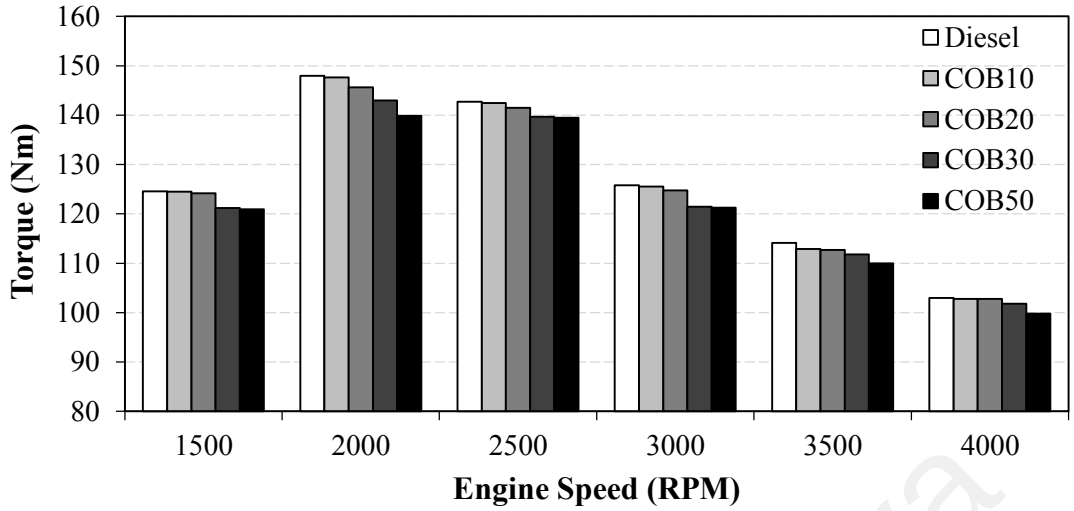

(a)

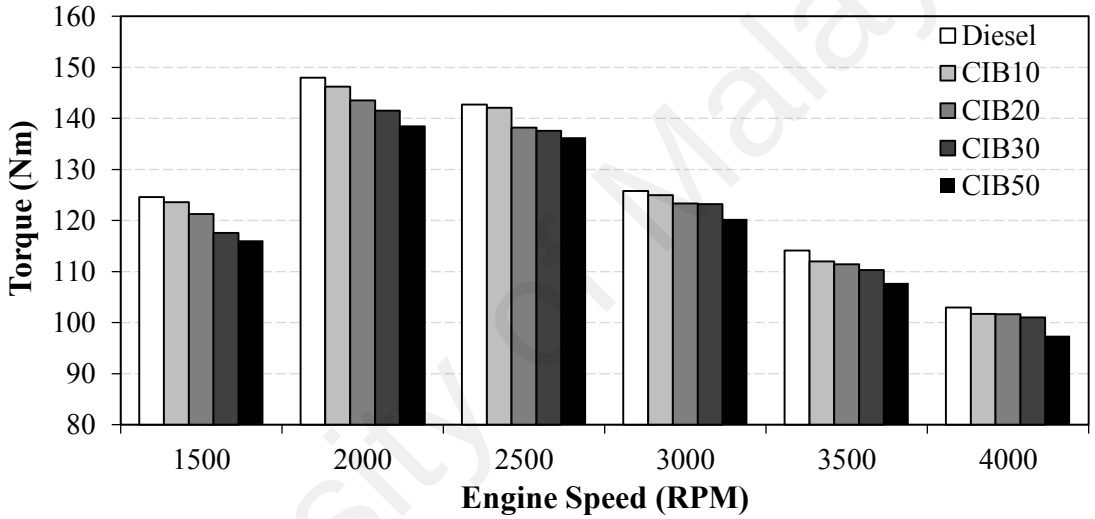

(b)

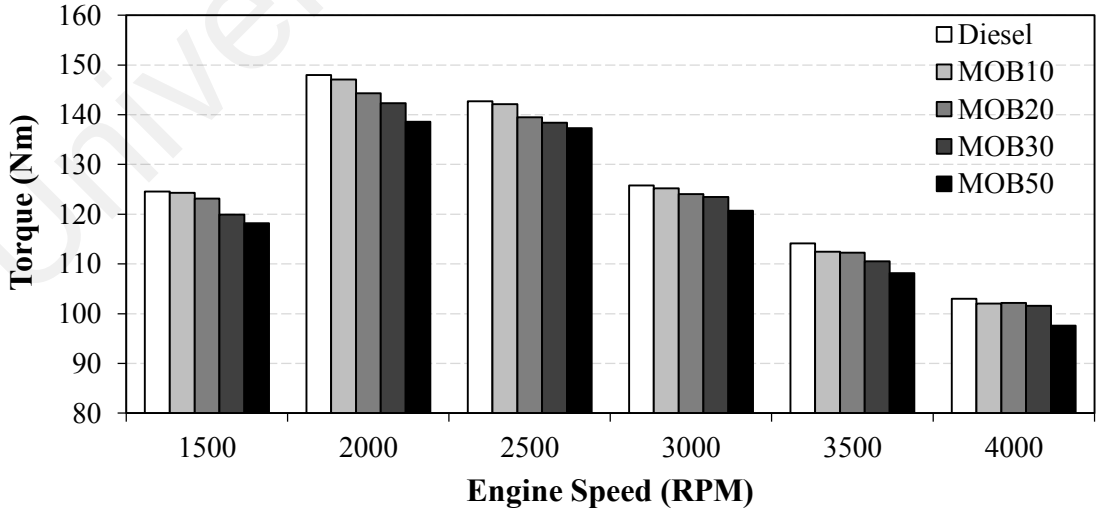

(c)

Figure 4.1: Torque versus engine speed for (a) COB (b) CIB and (c) MOB biodiesel blends compared with baseline diesel

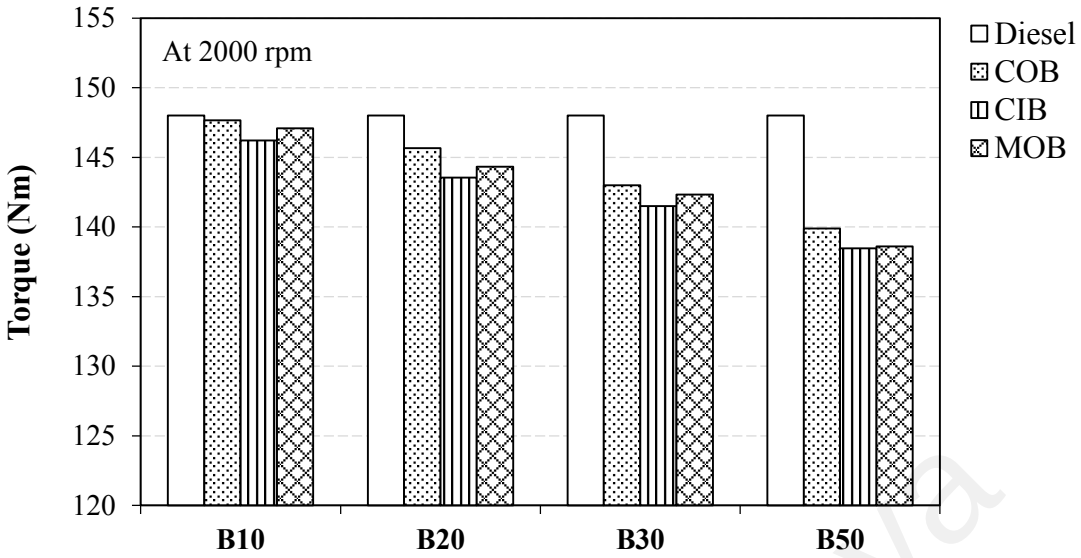

Figure 4.2: Comparison of engine torque at 2000 rpm for all fuels

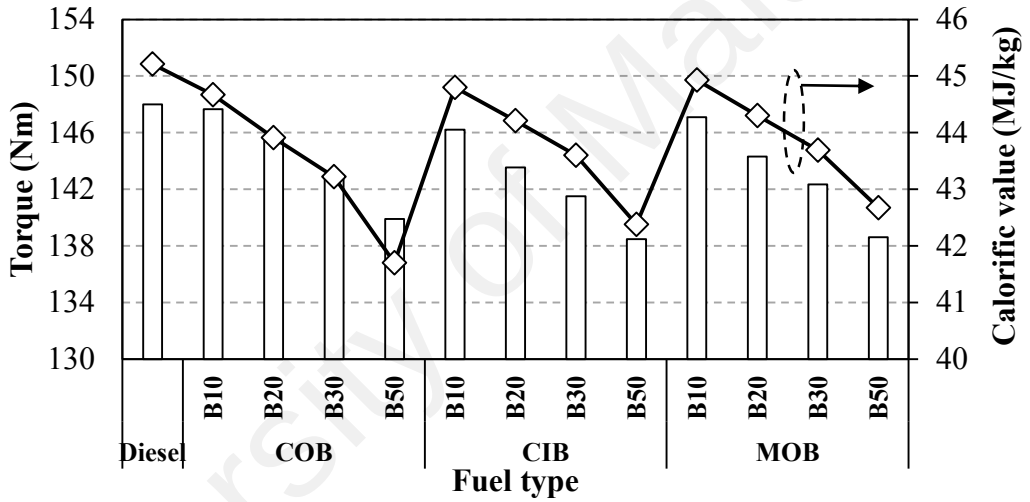

Figure 4.3: Relationship between engine torque at 2000 rpm and calorific value for all fuels

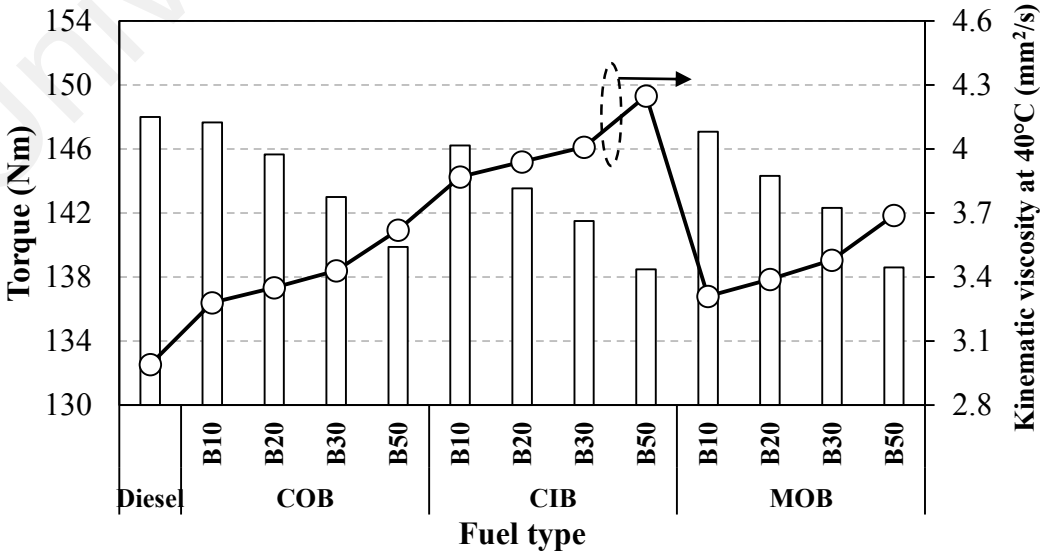

Figure 4.4: Relationship between engine torque at 2000 rpm and kinematic viscosity for all fuels

4.6.1.2 Brake power

The engine power for various biodiesel blend fuels and diesel at full load conditions is indicated in Figure 4.5. As can be observed, maximum brake power of 31 kW is generated with baseline diesel fuel at 2000 rpm. Besides, it is found that the brake power of biodiesel blends is lower than diesel fuel across all engine speeds, in which the observation is also reported by most of the researchers (Liaquat, et al., 2013; Mofijur et al., 2014; Monirul et al., 2016; Zareh et al., 2017). This phenomenon can be associated with the greater viscosity and low calorific value of biodiesel blends, thus aggravates the fuel evaporation process. Consequently, this reduces the combustion efficiency and lower the brake power for engine running with biodiesel-diesel blend fuels. Also, it is observed that COB biodiesel blends produced higher brake power compared to MOB and CIB biodiesel blends. The maximum brake power of COB10, MOB10 and CIB10 is 30.92 kW, 30.80 kW and 30.62 kW, respectively at 2000 rpm as shown in Figure 4.6. The higher kinematic viscosity, higher density and lower calorific value of CIB biodiesel caused poorer mixture formation and lower brake power.

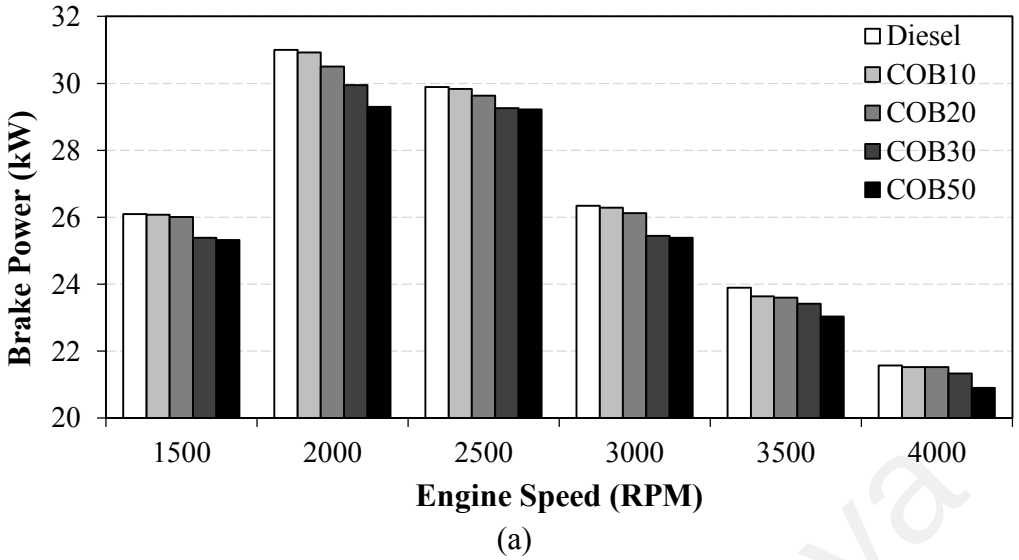

(a)

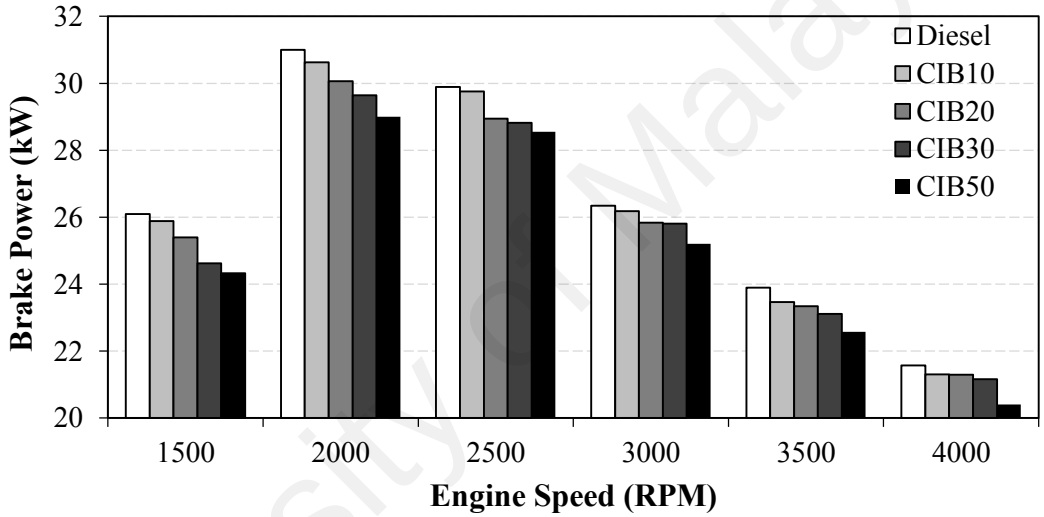

(b)

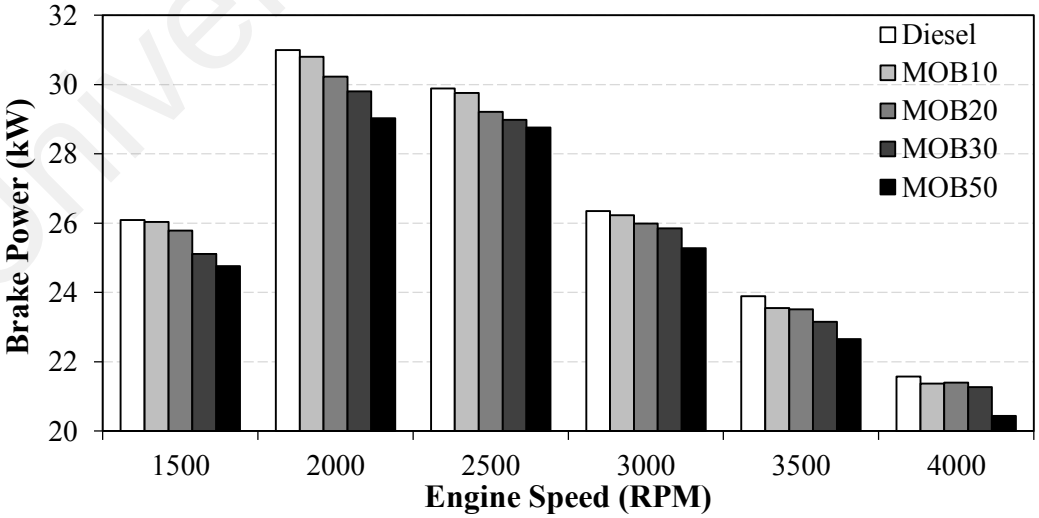

(c)

Figure 4.5: Brake power versus engine speed for (a) COB (b) CIB and (c) MOB biodiesel blends compared with diesel

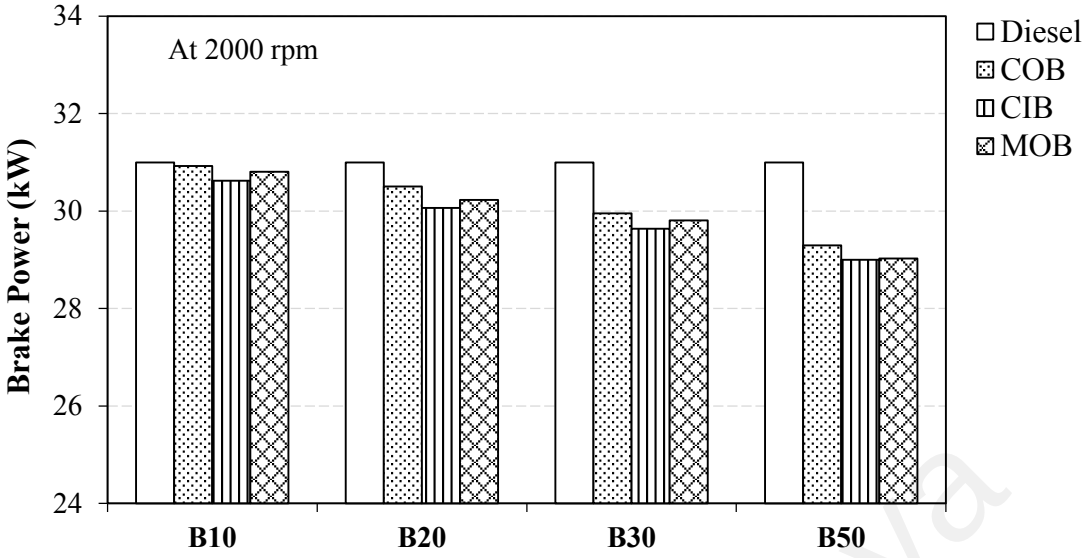

Figure 4.6: Comparison of brake power at 2000 rpm for all fuels

4.6.1.3 Brake specific fuel consumption (BSFC)

Figure 4.7 reveals the variation of BSFC at different engine speeds for diesel, COB, CIB and MOB blend fuels. The results indicated that the BSFC of all biodiesel blends is consistently larger than that of baseline diesel across all engine speeds and this phenomenon is well aligned with many researchers (Ashok et al., 2017; Liaquat, et al., 2013; Rizwanul Fattah et al., 2014; Zareh, et al., 2017). Particularly, a very similar observation is noticed by Sayin and Gumus (Sayin & Gumus, 2011), H.G. How et al. (How, et al., 2014), M.A. Kalam et al. (Kalam et al., 2016) and Hwai Chyuan Ong et al. (Ong et al., 2014) that higher biodiesel blend will translate to the increment in BSFC. This can be associated with the combination effects of lower calorific value, higher density and greater kinematic viscosity of biodiesel blends, which are the main culprits behind this issue. Essentially, fuel with greater viscosity may worsen in injection efficiency and spray atomization, and adversely affect fuel combustion and engine power. To compensate this effect, more quatity of fuel needs to be injected to attain the same engine power, thus has resulted in higher BSFC (as according to Equation 3.1). Similary, lower heating value of the biodiesel blends implies lower amount of heat released by the fuel in engine, hence, resulted in lower engine power and higher BSFC, as

aforementioned. Besides, since diesel engine fuel is delivered on a volume basis, thus the higher density of biodiesel blends caused higher fuel mass injection (i.e. Density (ρ) = mass (m) / volume (V)), thus has resulted in higher BSFC (as according to Equation 3.1). Furthermore, a direct comparison of BSFC between all the tested fuels at 2000 rpm is presented in Figure 4.8. The maximum BSFC is recorded for diesel, COB50, MOB50, and CIB50 with the BSFC value of 231.6 g/kWh, 234.1 g/kWh, 239.5 g/kWh, and 240.8 g/kWh, respectively at 2000 rpm. This can be associated to the lower brake power, lower calorific value and highest kinematic value of all B50 fuels compared to other lower blend fuels.

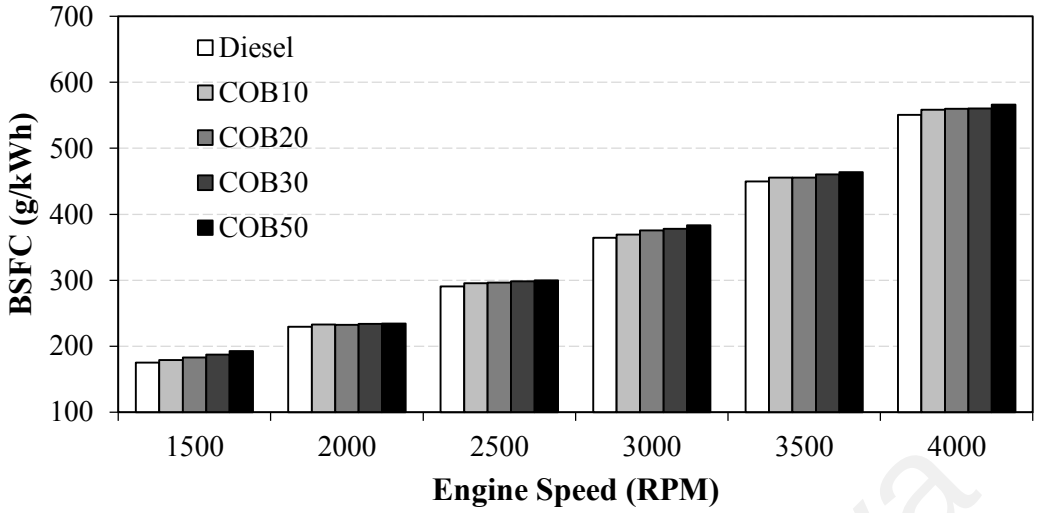

(a)

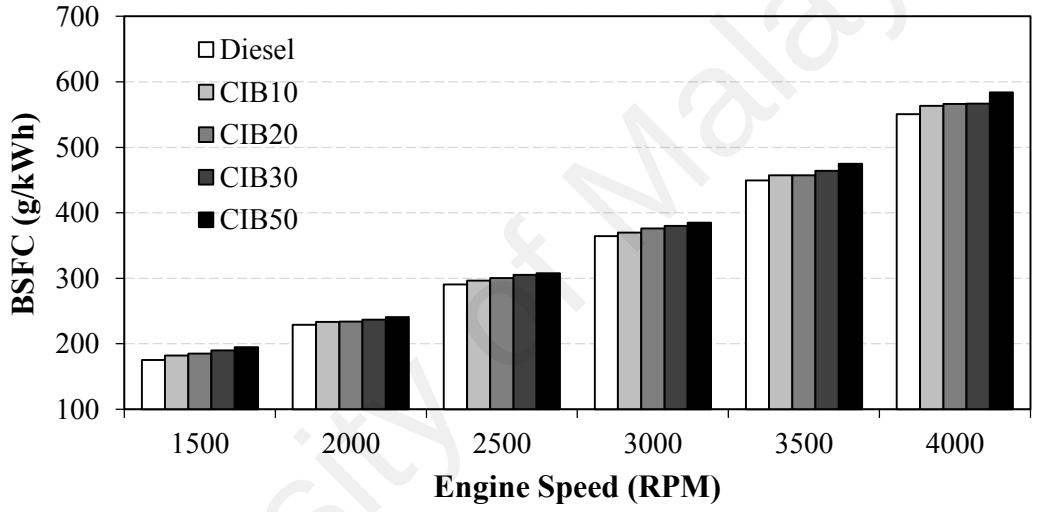

(b)

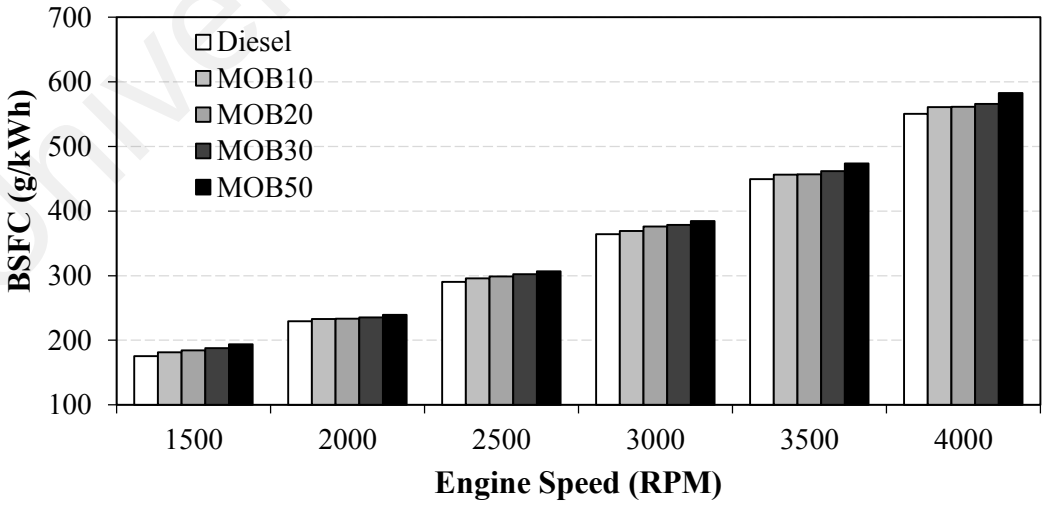

(c)

Figure 4.7: BSFC versus engine speed for (a) COB (b) CIB and (c) MOB biodiesel blends compared with diesel

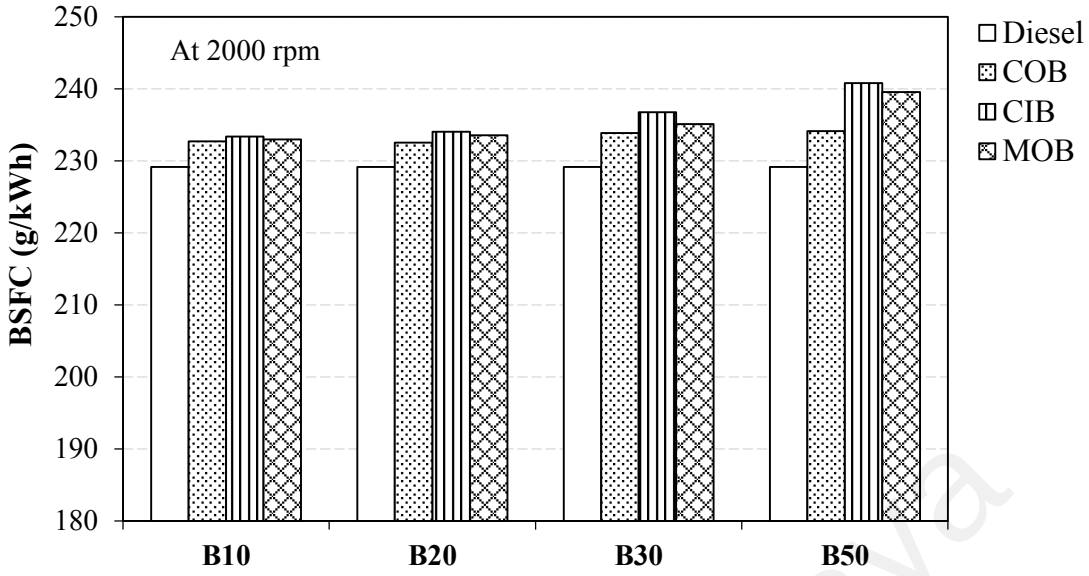

Figure 4.8: Comparison of BSFC at 2000 rpm for all fuels

4.6.1.4 Brake specific energy consumption (BSEC)

The BSEC for all the tested fuels at various engine speeds as shown in Figure 4.9. BSEC is a more acceptable parameter which typically used to show the relative effectiveness of energy consumption for fuels with different energy contents (i.e. calorific value). The lower the BSEC value, the better the utilization of fuel energy to produce useful work. Based on the results, it is generally noticed that biodiesel blends have constantly produce lower BSEC compared to baseline diesel for all engine speeds, except for 1500 rpm. However, the variation is not prominent, especially for lower engine speed of below 2000 rpm. The lower BSEC of biodiesel blends implied that the energy utilization is actually much better than that of diesel across the entire engine speeds. The fuel-bound oxygen content which available in biodiesel blends had led to a more complete combustion. Besides, the variation of BSEC for all fuels at 2000 rpm is shown in Figure 4.10. It can be observed that the BSEC for COB20, CIB20 and MOB20 are 10.37 MJ/kWh, 10.34 MJ/kWh, and 10.35 MJ/kWh respectively, compared to diesel fuel (10.47 MJ/kWh) at 2000 rpm. In addition, the result also shows that with the increases in biodiesel concentration in the blend, the variation in BSEC is more prominent.

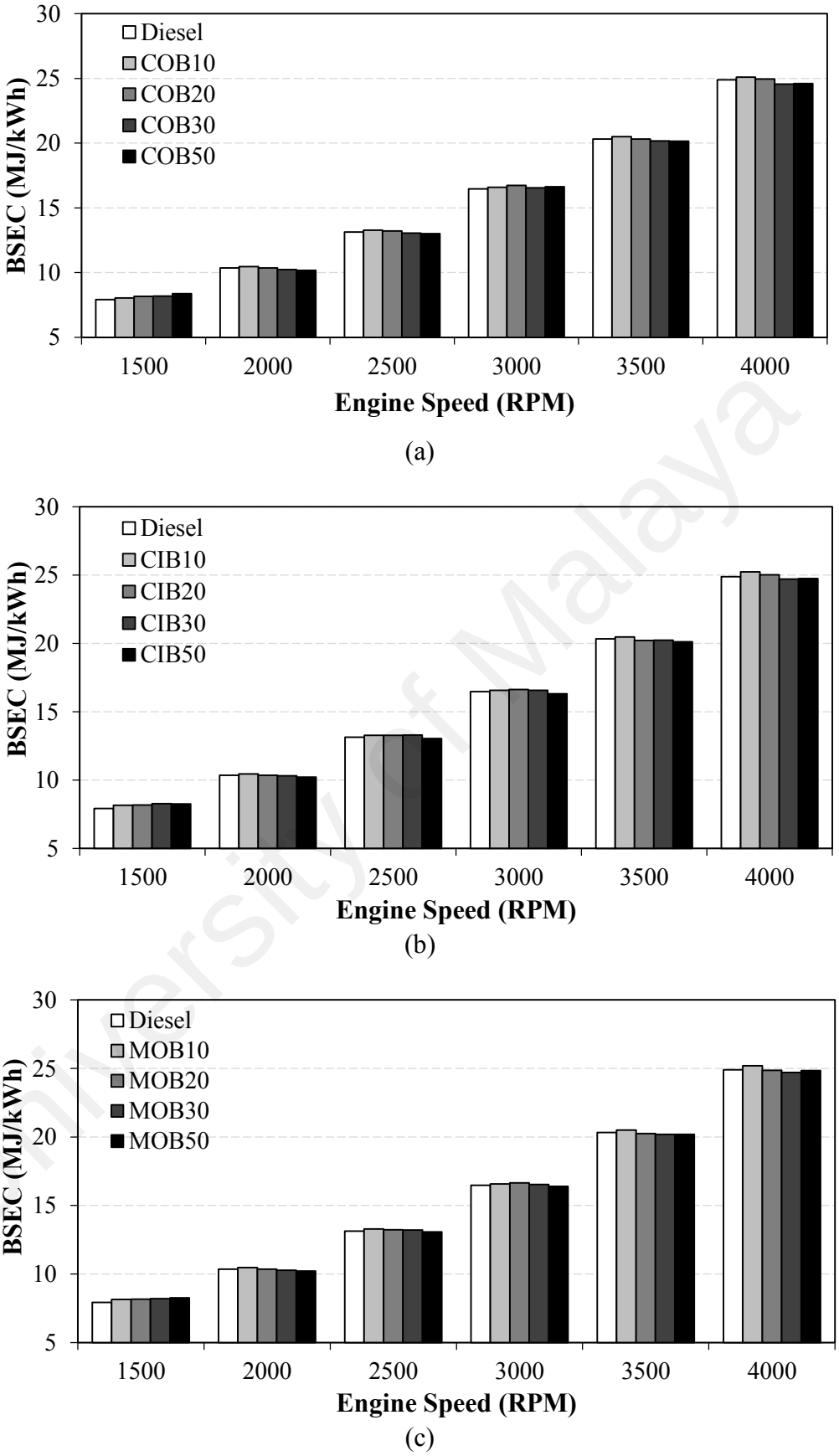

Figure 4.9: BSEC versus engine speed for (a) COB (b) CIB and (c) MOB biodiesel blends compared with diesel

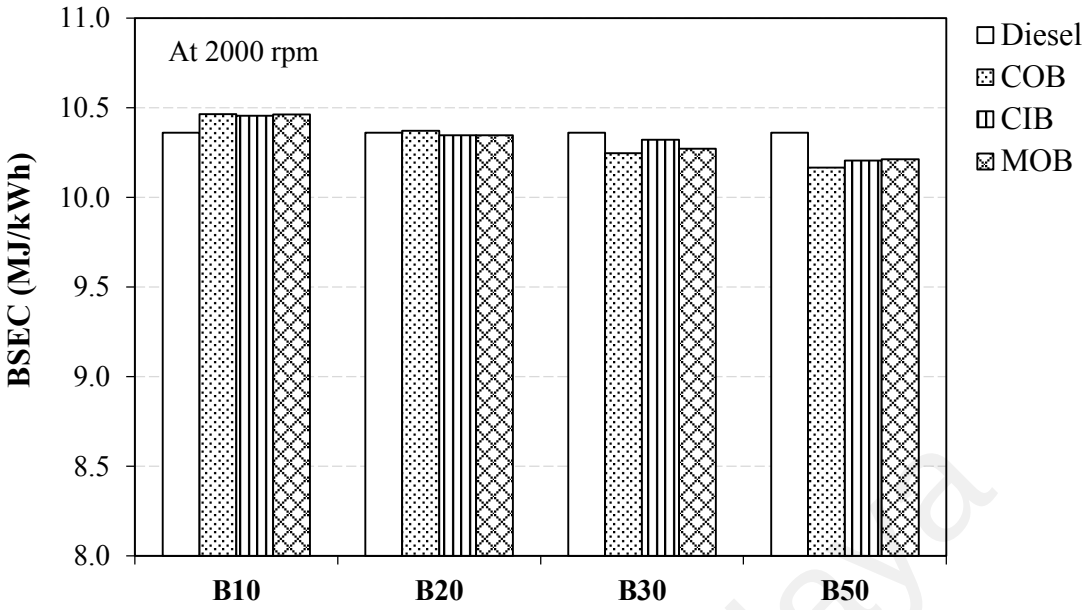

Figure 4.10: Comparison of BSEC at 2000 rpm and full load conditions for all fuels

4.6.1.5 Brake thermal efficiency (BTE)

In general, the BTE for biodiesel blend fuels is lower compared to those of baseline diesel under all speed conditions as shown in Figure 4.11. The lower BTE across all engine speeds for engine operation with biodiesel blends can be explained with the aforementioned phenomenon of increased in BSFC. However, the increment effect of BTE of B50 for all type of biodiesel at 2000 rpm can be related with the better utilization of fuel energy to produce useful work, as explained in the aforementioned observation of BSEC result. The increased availability of fuel bound oxygen content in the biodiesel fuels, which improve the efficiency of combustion and causes larger BTE when compared with baseline diesel. A direct comparison of BTE between all the tested fuels at 2000 rpm is presented in Figure 4.12. The BTE for diesel, COB20, CIB20 and MOB20 are 34.39 %, 34.71 %, 34.79 % and 34.80%, respectively at 2000 rpm.

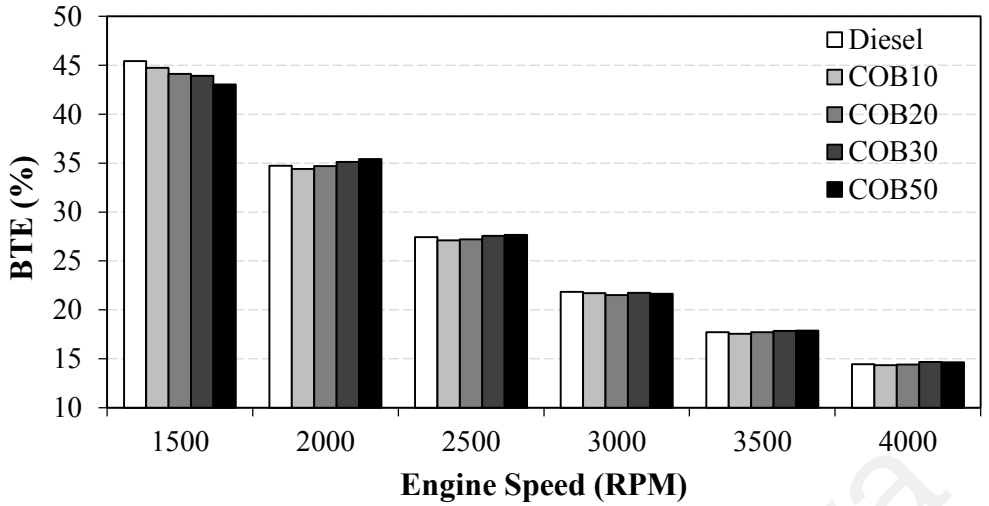

(a)

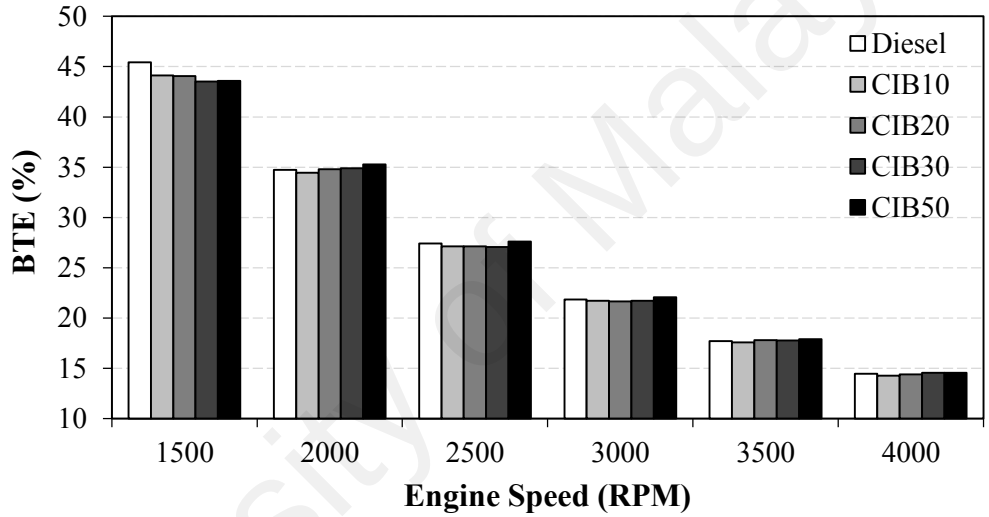

(b)

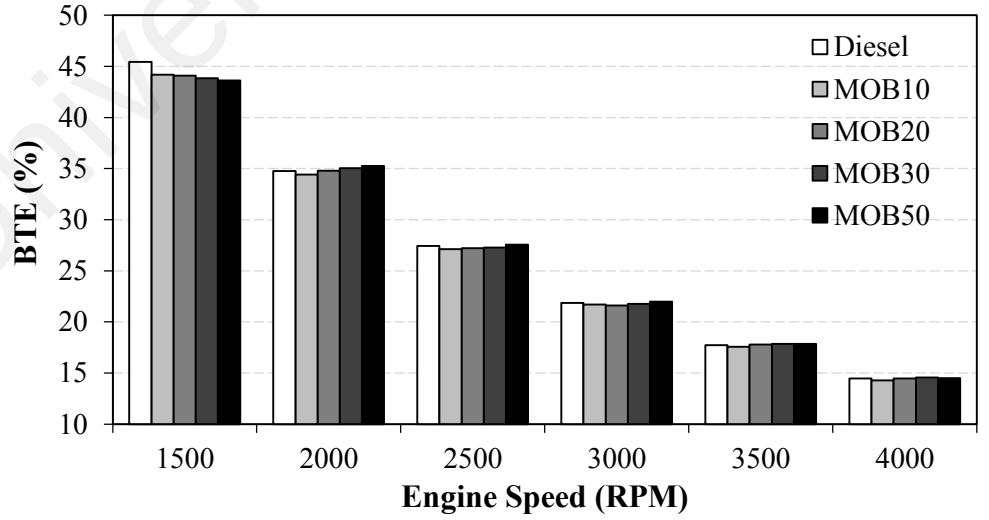

(c)

Figure 4.11: BTE versus engine speed for (a) COB (b) CIB and (c) MOB biodiesel blends compared with diesel

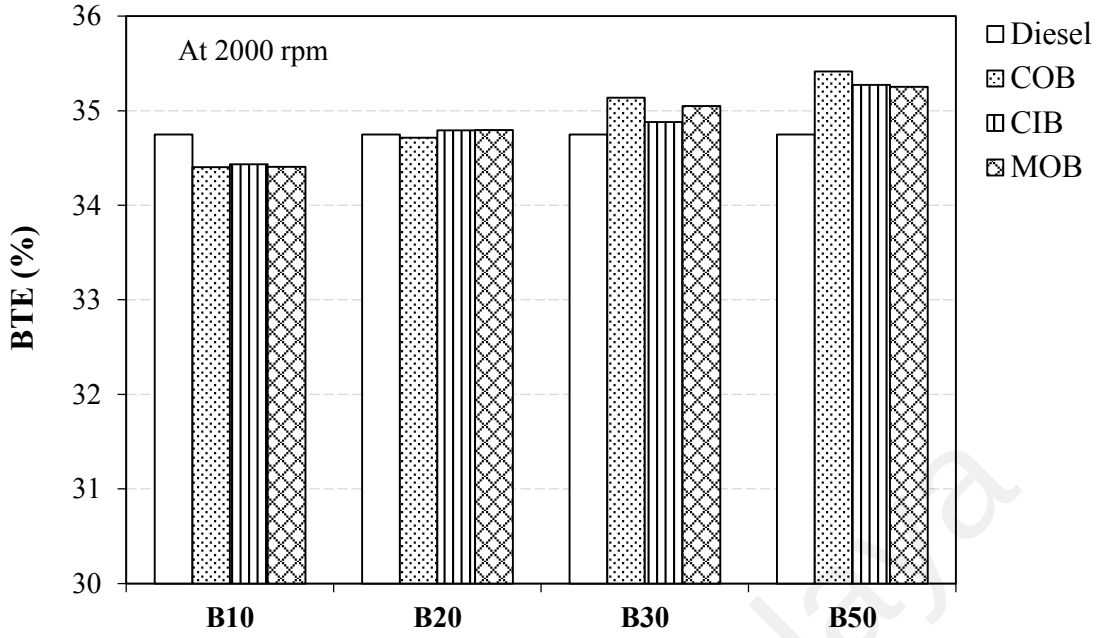

Figure 4.12: Comparison of BTE at 2000 rpm for all fuels

4.6.2 Exhaust emissions study

In order to analyze the parameters such as CO, NOx and smoke opacity emissions with different speed conditions, the emission characteristics performance of diesel, COB, CIB and MOB biodiesel diesel blends are carried out. In addition, the engine exhaust PM that being released from the diesel engine exhaust using various biodiesel fuel blend which governs the surface morphology, size and weight, and chemical components are also presented and discussed.

4.6.2.1 Carbon monoxide (CO)

Carbon monoxide (CO) from exhaust tailpipe is mainly associated with the incomplete combustion of the fuels. This gas is highly dangerous and toxic because it prevent the ability of blood to transfer oxygen to our body tissue and results in fatal poisoning. Figure 4.13 shows the variation in CO emissions of the engine under various engine speed for all biodiesel blends and diesel fuel. Generally, the result suggested that higher biodiesel blend ratio will lower the emissions of CO. In fact, this observation is well aligned with most of the literature (Han et al., 2008; How et al., 2012; Karavalakis

et al., 2011a; Kinoshita et al., 2006; Özener, et al., 2014). This phenomenon can be related to the oxygen enrichment in biodiesel fuel and consequently allow for cleaner combustion to occur during the combustion process (Carraretto et al., 2004; Sayin & Gumus, 2011). Another noteworthy observation is that the CO emission levels at 1500 rpm is significantly high compared to other engine speeds for all fuels. This can be related to the introduction of early pilot injection fuel by the stock ECU for this type of engine, thus has resulted in fuel impingement to the cylinder wall. Interestingly, as compare to baseline diesel, the use of COB50, CIB50 and MOB50 fuels have successfully reduced the CO emissions by almost 71%, 61% and 64% respectively, compared to diesel fuel at 1500 rpm. This again reaffirmed that the advantages of biodiesel with high fuel borne oxygen content in CO emissions reduction. Besides, a direct comparison of CO emissions between all the tested fuels at a specific engine speed of 2000 rpm can be seen in Figure 4.14. From the results, it can be seen that the effect of COB fuel blends on CO emissions suppression is more prominent as compared to CIB and MOB fuels across all biodiesel blend ratio.

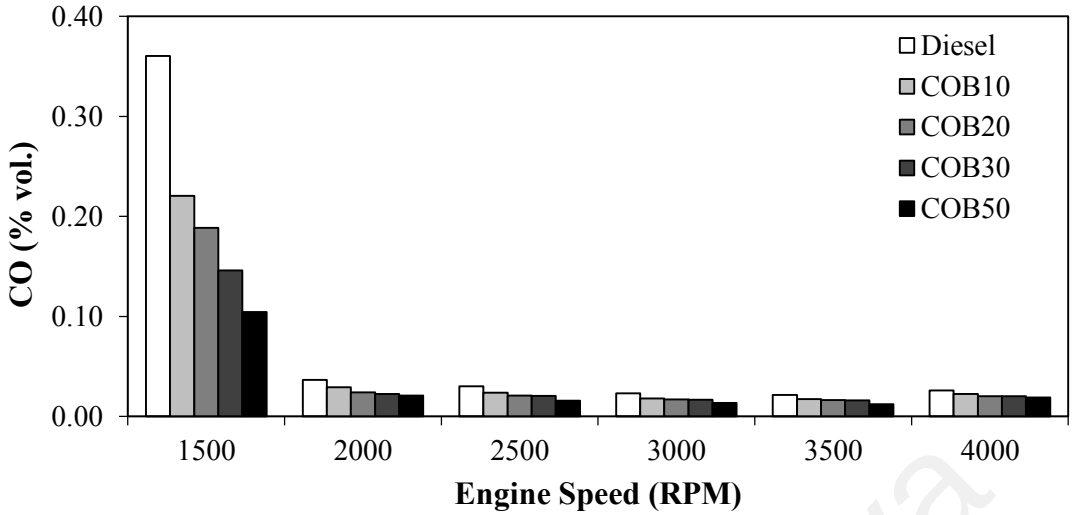

(a)

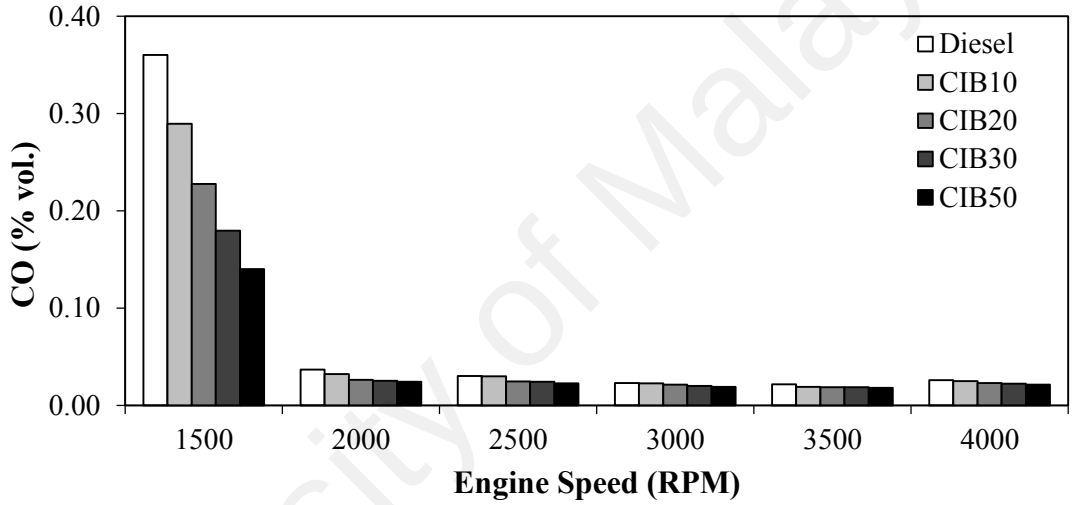

(b)

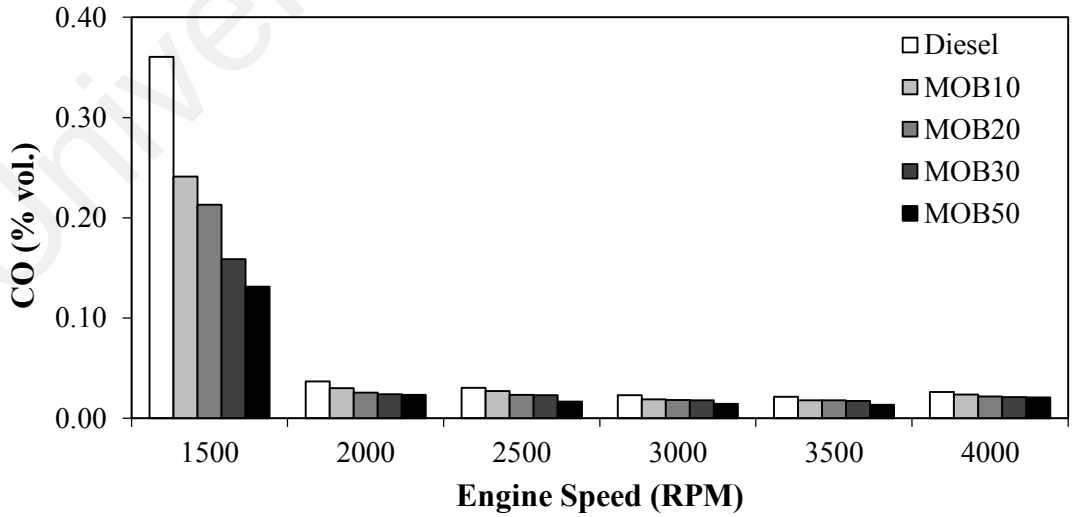

(c)

Figure 4.13: CO emissions versus engine speed for (a) COB (b) CIB and (c) MOB biodiesel blends compared with diesel

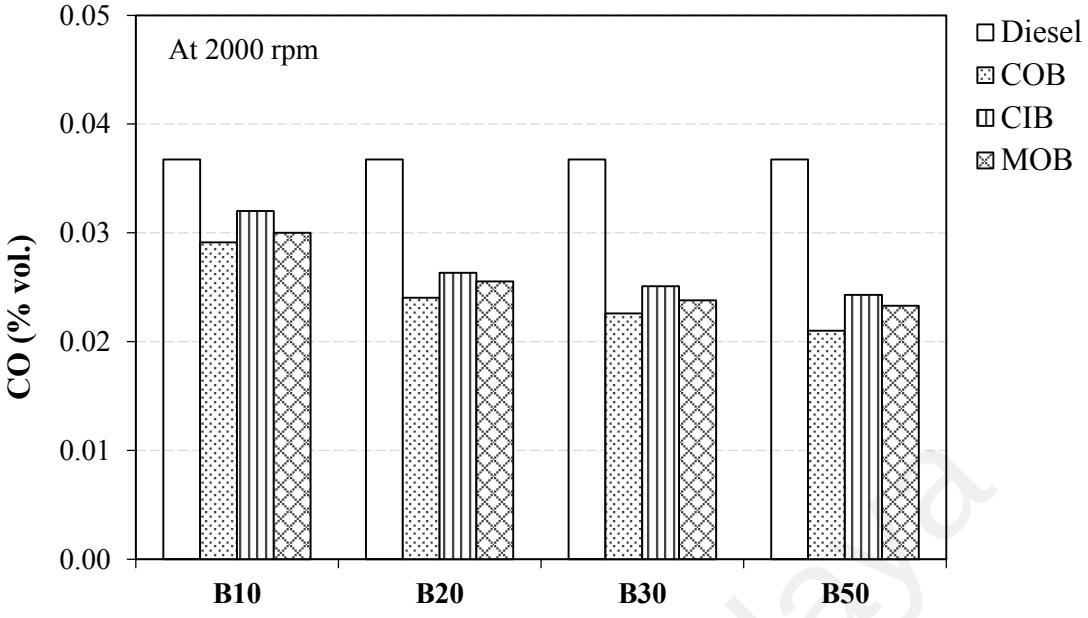

Figure 4.14: Comparison of CO at 2000 rpm for all fuels

4.6.2.2 Nitrogen oxide (NOx)

NOx is a harmful and undesirable emission product which produced while fuel combustion occurs, especially at high temperatures of combustion. In the exhaust emissions, nitric oxide (NO) is the main NOx emissions, come with a little quantity of nitrogen dioxide (NO_2). The formation of NOx dependence on engine operating conditions, fuel type and fuel properties (Szybist, et al., 2007). Figure 4.15 shows that the emissions of NOx for all biodiesel blends are consistently higher than baseline diesel fuel across all engine speeds. This phenomenon can be related with the intrinsic oxygen content (approximately 10.8 – 14.3% by weight) in the biodiesel as presented at Table 4.2. The findings are agreed with the results of NOx as reported in the literature (Agarwal, 2007; Devan & Mahalakshmi, 2009; Kumar & Sharma, 2016; Rashed et al., 2016a). This oxygenated fuel may provide additional oxygen for the formation of NOx. Besides, the Figure 4.16 shows a direct comparison of NOx emissions between baseline diesel, COB, CIB, and MOB biodiesel blends at a specific engine speed of 2000 rpm. In general, the results indicated that MOB biodiesel blends produced higher NOx emissions than COB and CIB fuels across all biodiesel blend ratios. In fact, the NOx emissions is found to

progressively increase with higher MOB content in blend. This phenomenon is predominantly due to the use of biodiesel fuels with greater degrees of unsaturation of fatty acid compositions, as it is evidently seen in Table 4.3. Consequently, the higher quantity of double bonds molecule in its fatty acid composition has led to the disposition of free radicals that stimulates the effect of NOx formation via both the prompt and thermal processes (Palash et al., 2013a).

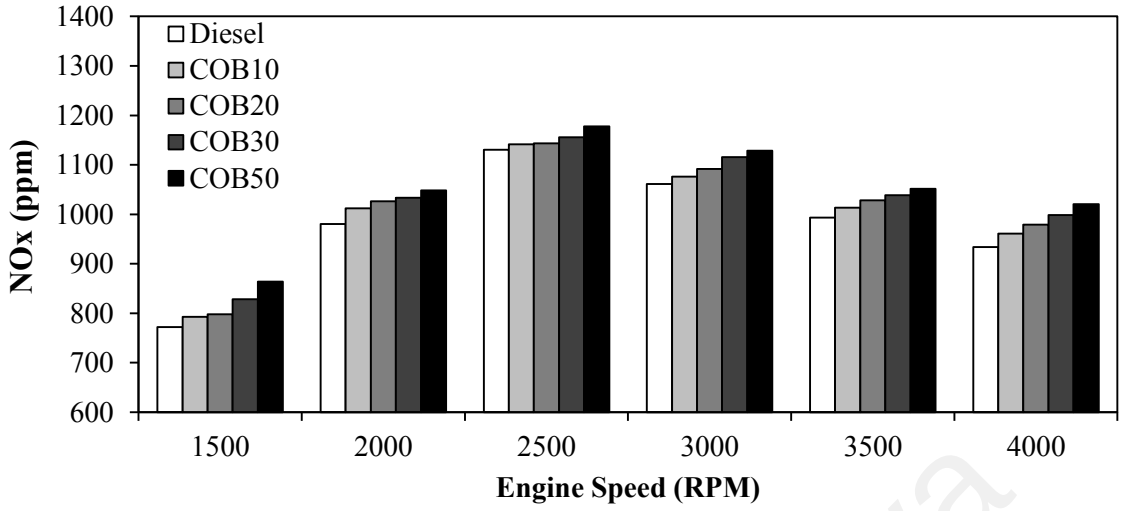

(a)

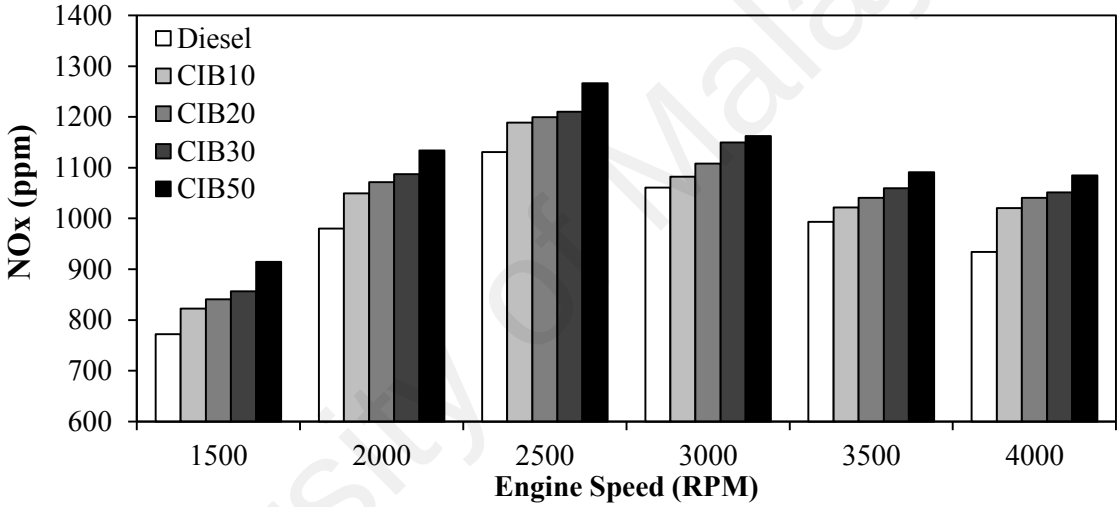

(b)

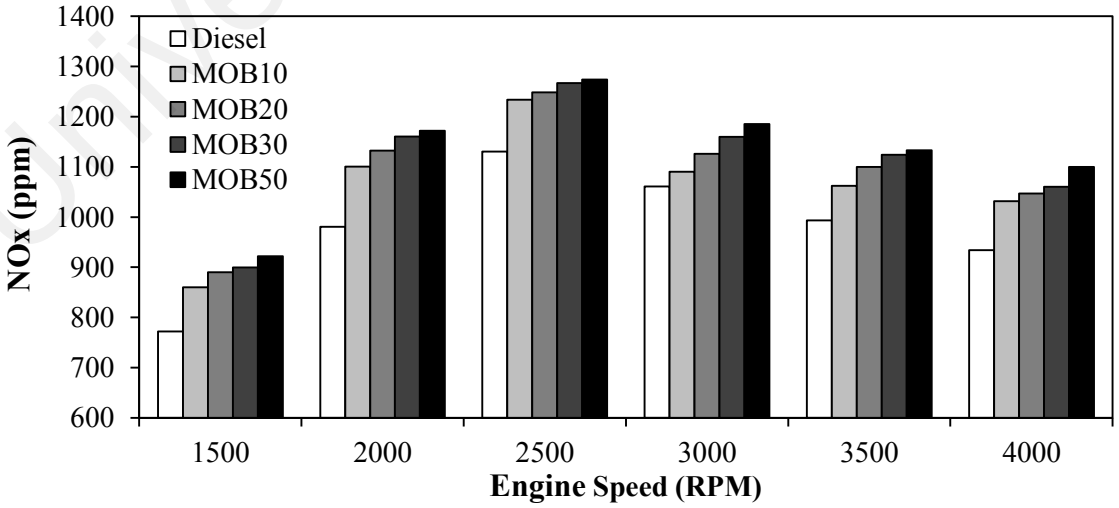

(c)

Figure 4.15: NO_x emissions versus engine speed for (a) COB (b) CIB and (c) MOB biodiesel blends compared with diesel

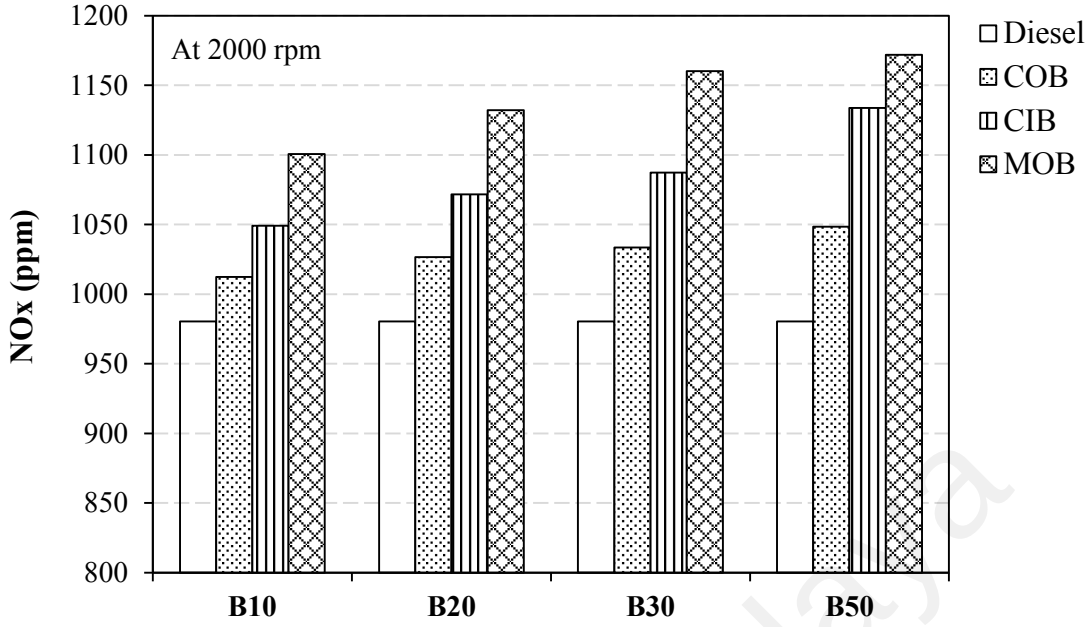

Figure 4.16: Comparison of NO_x emissions at 2000 rpm for all fuels

4.6.2.3 Smoke opacity

Smoke is produced due to the partial reaction of the carbon content in liquid fuel and incomplete combustion of hydrocarbon fuel (Lin & Li, 2009). Figure 4.17 shows the emission of smoke opacity for COB, CIB and MOB biodiesel blends. By relating the effect of biodiesel contents to the smoke opacity, it is noticed that generally the increment in biodiesel concentration caused the decreases in smoke opacity. This decrement effects is mostly because of the lower carbon content and oxygen enrichment in biodiesel as shown in Table 4.2, which result in cleaner combustion and diminish the formation of smoke (Gumus, et al., 2012; Kinoshita, et al., 2006; Rashed et al., 2016b; Suryawanshi, 2006b). Interestingly, the results also indicated that the highest reduction of 62%, 57.9%, and 59.5% is achieved with COB50, CIB50 and MOB50 biodiesel blend, respectively, when compare with diesel fuel at 4000 rpm. Besides, a direct comparison of smoke opacity levels between all the tested fuels at a specific engine speed of 2000 rpm can be seen in Figure 4.18. The results indicated that the COB biodiesel blends showed the highest smoke opacity reduction by 40.2%, follow by MOB (36.5%) and CIB (28.3%), when compare to diesel fuel at 2000 rpm.

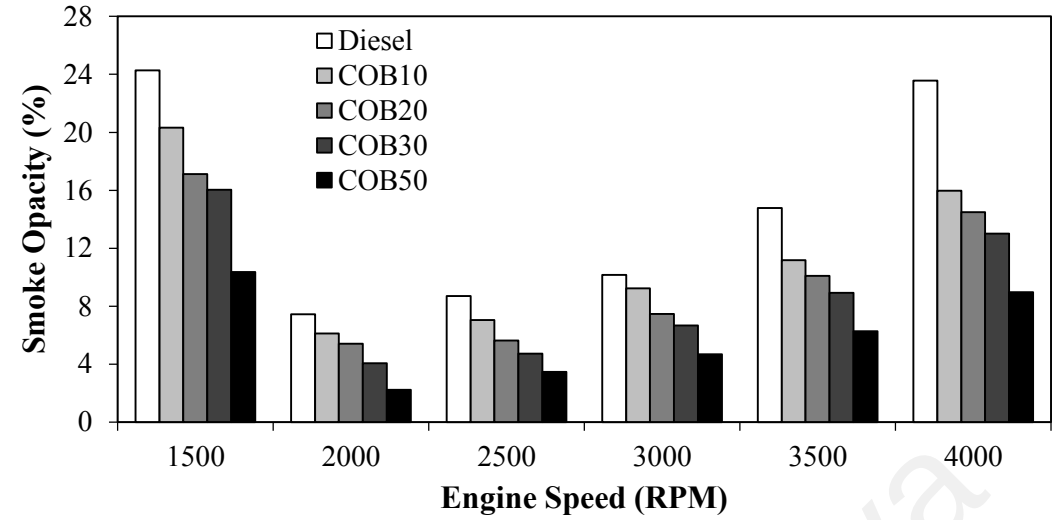

(a)

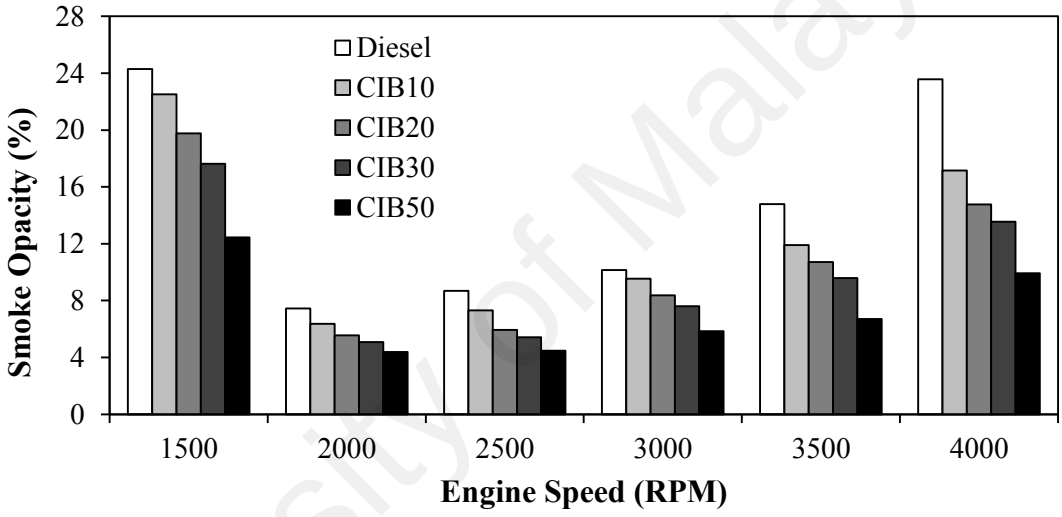

(b)

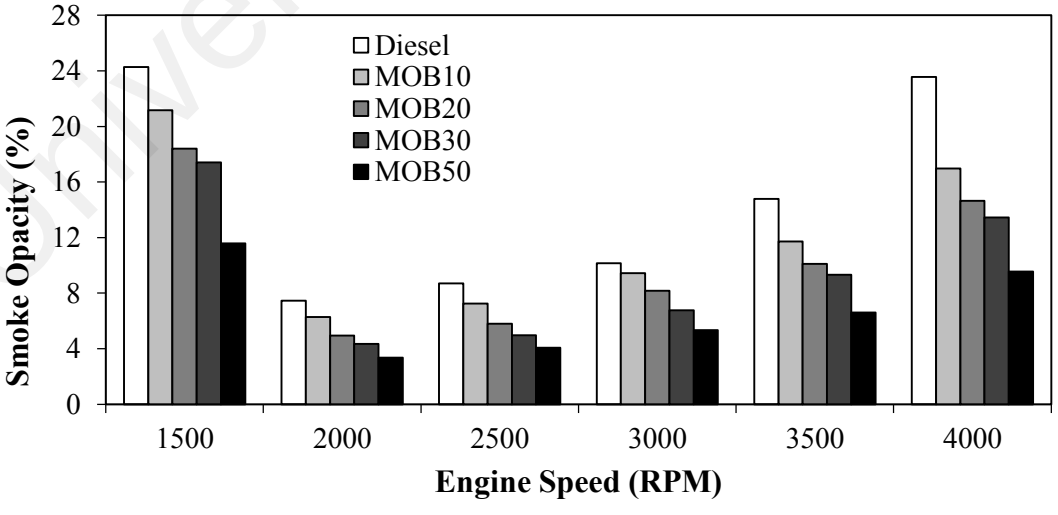

(c)

Figure 4.17: Smoke opacity versus engine speed for (a) COB (b) CIB and (c) MOB biodiesel blends compared with diesel

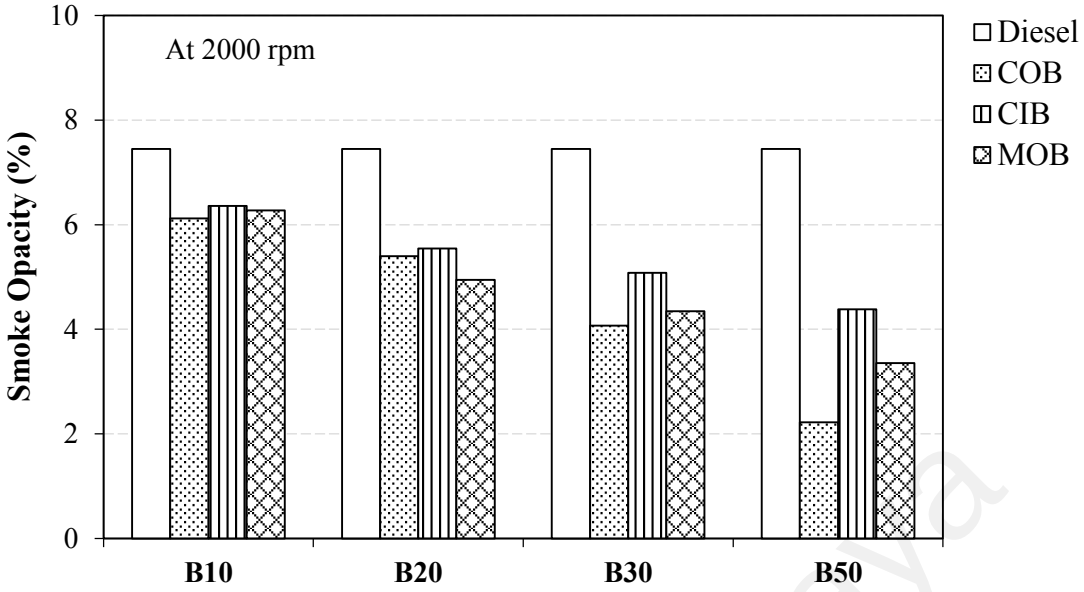

Figure 4.18: Comparison of smoke opacity at 2000 rpm for all fuels

4.6.2.4 PM characterization

For PM analysis, the particulate emitted from the engine tail pipe is collected through quartz filters (47 mm) by using sampling pump at constant flow rate. This particulate emission test is operated at 16 different modes at various speeds and load conditions as shown in Table 3.12 on Chapter 3. This has resulted in a total of 16 minutes of steady engine operating duration for each fuels blend to ensure that a minimum of 0.0013g of PM mass can be accumulated and collected (Lapuerta, et al., 2008c). For each fuel blend, the mass of PM which accumulated on the quartz filter is characterized and compared. Besides, the exhaust particulate morphology and the element composition of the sample are analyzed and discussed in the section below.

(a) PM mass

Figure 4.19 shows the exhaust particulate mass in the engine exhaust from various fuel blends tested in this study, with engine operated at 16 different modes at various speeds and load conditions. It can be seen that all of the biodiesel blends emitted lower levels of PM than the reference fossil diesel, and it is suggested that this is attributable to the presence of oxygen within the test fuel molecules (Table 4.2). This enhances the

pyrolytic reactions of fuel during the combustion process, thus reduced the exhaust PM mass (Tinsdale et al., 2010). By relating the influence of biodiesel concentrations to the PM mass, it is generally found that as the biodiesel concentration increases, the PM mass will reduce, irrespective of the type of biodiesel used. The reduction of PM mass emitted is mostly because of the lower C/O ratio of biodiesel fuel, which cause cleaner combustion and enhance the rate of soot oxidation. Another possible explanation is the impurities level of biodiesel fuels is substantially lower than that of fossil diesel, thus lower the tendency of carbon deposition and decrease the PM mass levels (Ng, et al., 2011). Notably, this phenomenon is to be expected with the lower level of conradson carbon residue value for all biodiesel fuels as compared to baseline diesel, as shown in Table 4.2. For these reasons, the use of COB showed considerable reduce in PM levels as it has the lowest conradson carbon residue value as compared to CIB and MOB. For instance, it is observed that COB50 achieved the highest reduction in PM mass of 38.5% followed by 37.1% for CIB50 and MOB50, as compared to baseline diesel.

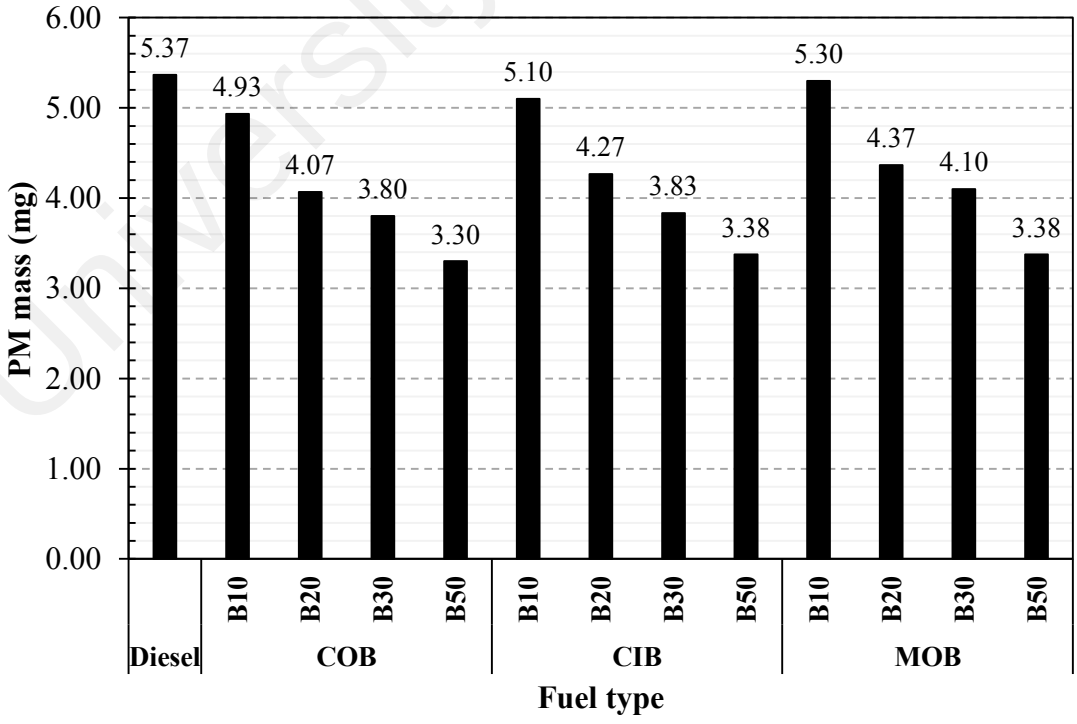

Figure 4.19: PM mass for all fuels under 16 modes speed-load test

(b) Chemical elements of PM

Figure 4.20 presents the element composition of PM for all fuel blends with EDX analysis. Generally, the EDX analysis showed that the collected PM for all tested fuels consists of three main elements such as carbon (C), oxygen (O) and silicon (Si) contents. For carbon (C) element, fossil diesel shows 81.5% which is the maximum among all the tested fuels. By relating the effect of biodiesel contents to the element composition of PM, it is generally found that the carbon element decreased with the increment of biodiesel concentration for all type of biodiesel. Besides, the results also indicated that the combined elements of oxygen and silicon contents of PM for all biodiesel blends were higher than that of diesel fuel. Particularly, B50 of COB, CIB and MOB showed the highest oxygen elements of 22.7%, 19.4%, and 25.6%, respectively, as compared to diesel fuel (15.3%). This can be explained with the higher oxygen content in biodiesel fuel blends, which promoted for more complete combustion and emitted less carbon particles. Lastly, for silicon (Si) element, the percentage of chemical element for PM for all biodiesel fuel blends are generally higher than that of fossil diesel. The precursors of silicon (Si) may be an inorganic component in the biomass. During the combustion process, these inorganic components can be converted into aerosols and coming out in the form of particulates (Ashraful et al., 2015).

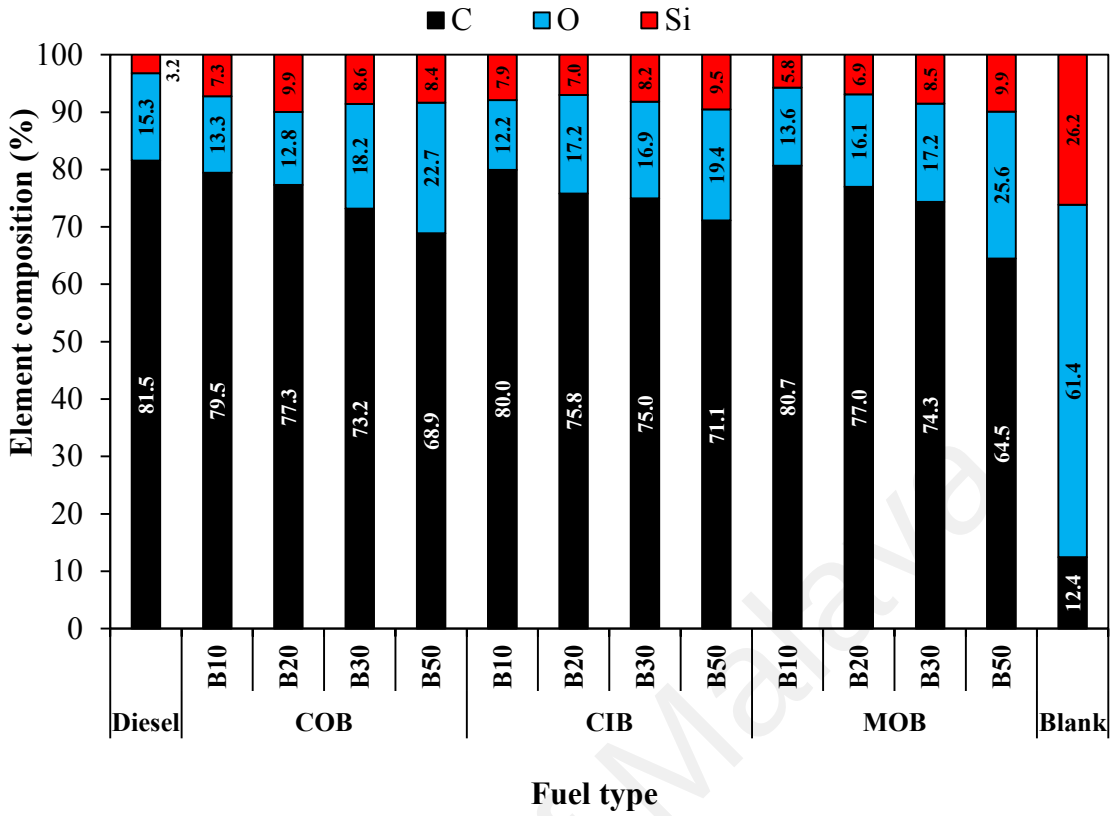

Figure 4.20: Element composition of PM for all tested fuels under 16 modes speed-load test

(c) Surface morphology of PM

The collected exhaust PM sample on quartz filters for all fuels are presented in half of its total size as shown in Figure 4.21. Noted that all filters are exposed for the same sampling duration of 16 minutes through filter holder assembly connected to PM sampling train. Generally, the blackening of the quartz filter paper primarily depends on the soot concentration in the exhaust gas. As can be seen, the degree of blackening of the quartz filters in the case of biodiesel blended fuels is less apparent as compared to baseline diesel. In fact, the blackening degree decreased with the increment of biodiesel concentration for all type of biodiesel. The oxygen content of the biodiesel may contribute to improved fuel oxidation even in locally rich fuel combustion zones, thus resulting in the reduction of exhaust soot concentration and lower blackening of the filter (Tziourtzioumis & Stamatelos, 2014). In addition, the morphology of particulate agglomerates on the filters is captured by using SEM and the images as shown in Figure

4.22. All the PMs were scanned under magnification level of 500x. It can be seen that the concentration of diesel particulate emission accumulated more particles as compared to those of biodiesel blends. From the SEM images, it is showed that more PM is trapped deep in the quartz filter for baseline diesel fuel. For all type of biodiesel, the particle agglomeration decreases sharply with higher biodiesel contents and B50 shows the lowest agglomeration than B30, B20, B10 and baseline diesel. For the same biodiesel concentration, all type of biodiesel shows comparable particle agglomeration. Besides, baseline diesel exhaust particulate shows larger size granular structure whereas biodiesel blends reveal least size granular structure. As for all type of B50 fuels, the PMs are smaller and more confined compared to baseline diesel, B10, B20 and B30. Furthermore, the PMs morphology shows that it has spherical shape with the primary particles arranged in a chain-like structure. PMs should have a typical morphology which is the spherical shape with the primary arranged in a chain like structure whereby it can led to measure the particulate matters' size from the micrographs (Salamanca, et al., 2012b). Hence, the results that being gathered for this research are aligned with previous studies.

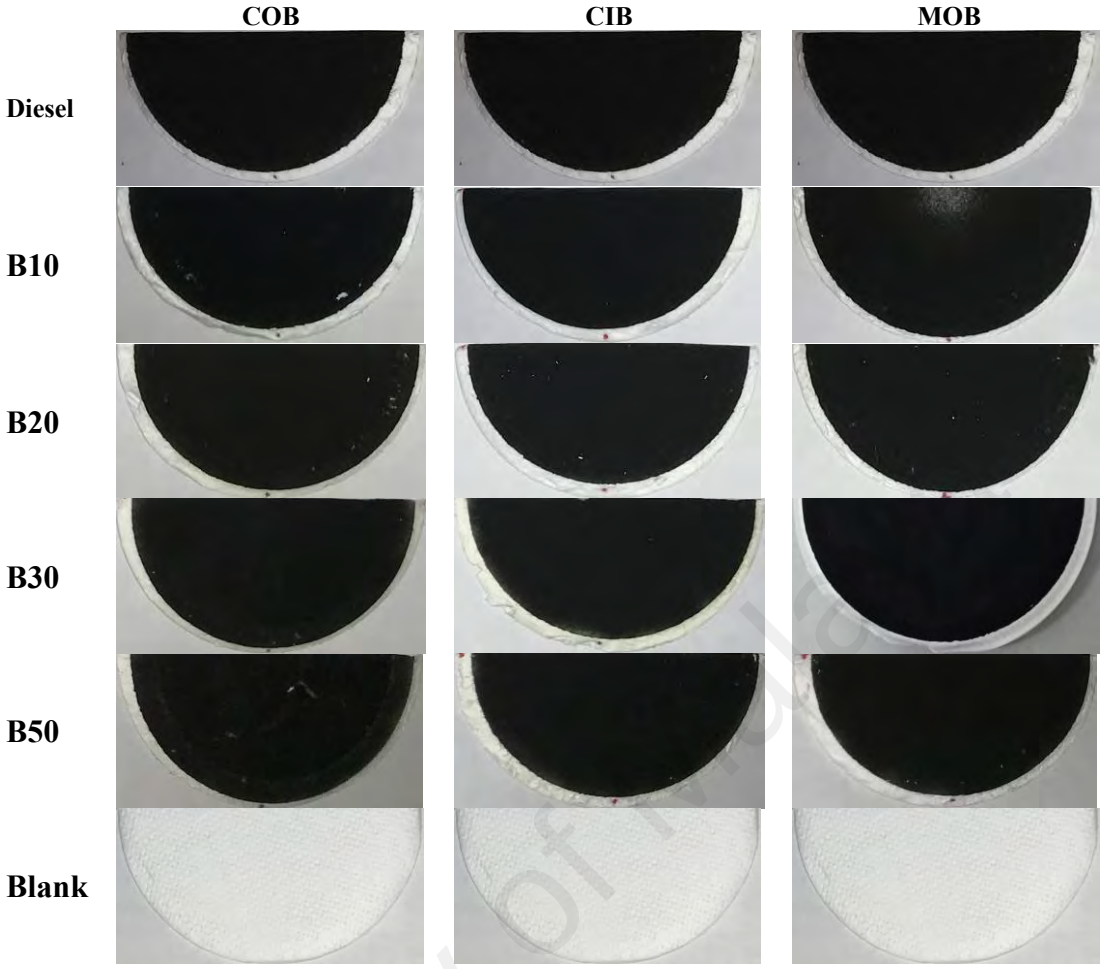

Figure 4.21: Comparison of PM samples collected on the quartz filter for all fuels under 16 modes speed-load test

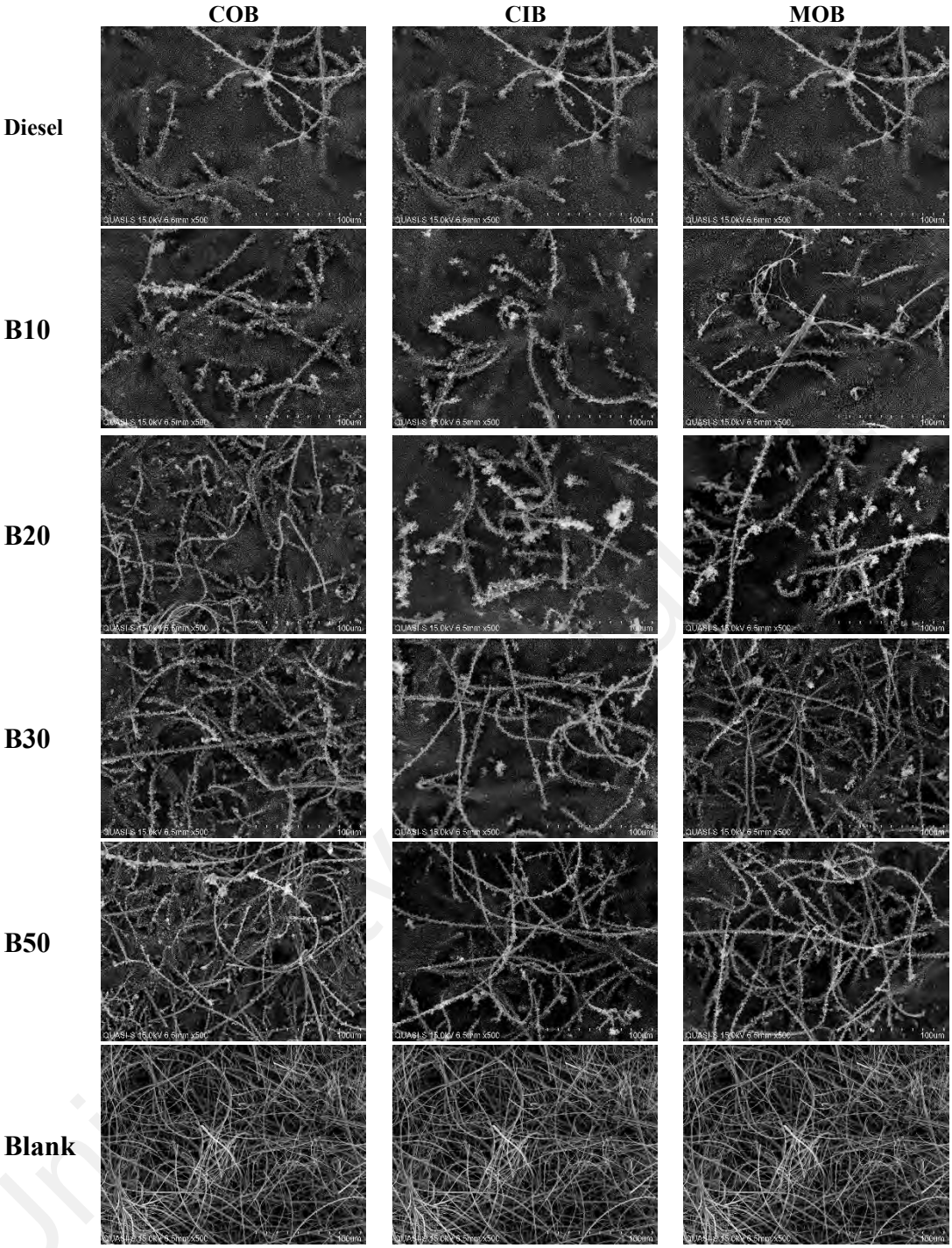

Figure 4.22: SEM images (at 500x) of all particulate samples for all fuels under 16 modes speed-load test

4.6.3 Combustion characteristics

4.6.3.1 Cylinder combustion pressure

Figure 4.23 to Figure 4.25 shows the comparison in between in-cylinder combustion pressure for all each type of fuels at different engine speeds. More specifically, sub-figure of a, b and c represents the variation of cylinder combustion pressure at 2000 rpm, 3000 rpm and 4000 rpm, respectively. Generally, with higher concentration of biodiesel in the blends, the cylinder peak pressure is reduced across all engine speeds. This similar phenomenon was also discovered by Ashok et al. (Ashok, et al., 2017). At engine speed of 2000 rpm, there are slight decreases in peak cylinder pressure for all biodiesel blend fuels when compare with baseline diesel. The lowest peak cylinder pressure is found to be 108 bar at 14.125 °ATDC with COB50, while the highest peak cylinder pressure is 110.92 bar at 14 °ATDC with COB10. When engine speed reached 3000 rpm, the lowest peak cylinder pressure is set up as 109.4 bar at 10.75 °ATDC with COB50 and the maximum peak cylinder pressure is recorded as 111.2 bar at 11.125 °ATDC with baseline diesel. With further increment of engine speed to 4000 rpm, it can be found that the lowest peak cylinder pressure is 113.2 bar at 7.125 °ATDC with COB50 and the baseline diesel shows the highest peak cylinder pressure of 117.5 bar at 7 °ATDC. Similarly, for CIB fuel blends, there are little decreases in peak cylinder pressure across all blended fuels when compare with baseline diesel at engine speed of 2000 rpm. Particularly, the recorded lowest peak cylinder pressure is 108.5 bar at 14 °ATDC with CIB50, while the highest peak cylinder pressure is found to be 110.17 bar at 13.875 °ATDC with CIB20. With higher speed of 3000 rpm, the lowest peak cylinder pressure is set up as 111.3 bar at 10.625 °ATDC with CIB50 and the maximum peak cylinder pressure is 111.9 bar at 10.625 °ATDC with CIB30. At 4000 rpm, the lowest peak cylinder pressure is found to be 115.9 bar at 6.875 °ATDC with CIB50 and the highest peak cylinder pressure which is 117.5 bar at 7 °ATDC with baseline diesel. For MOB fuel blends, there are some

decreases in peak cylinder pressure for all biodiesel blend fuels when compare with baseline diesel for engine speed of 2000 rpm. The lowest peak cylinder pressure is 107.8 bar at 14.125 °ATDC with MOB50, while the maximum peak cylinder pressure is at 110.733 bar at 13.75 °ATDC with baseline diesel. When engine speed reached 3000 rpm, the MOB50 produced the lowest peak cylinder pressure of 110.6 bar at 10.75 °ATDC while MOB 30 achieved the maximum peak cylinder pressure of 111.7 bar at 10.75 °ATDC. With the highest engine speed of 4000 rpm, the lowest peak cylinder pressure is found to be 115 bar at 7.25 °ATDC with MOB50 and the highest peak cylinder pressure which is 117.5 bar at 7 °ATDC with baseline diesel. In general, with higher concentration of biodiesel in the blend, the peak cylinder pressure is reduced for all type of biodiesel as shown in Figure 4.26. This is predominantly due to the relatively lower calorific value of biodiesel when compare with baseline diesel and the decreasing effect of calorific value with higher biodiesel concentration blends.

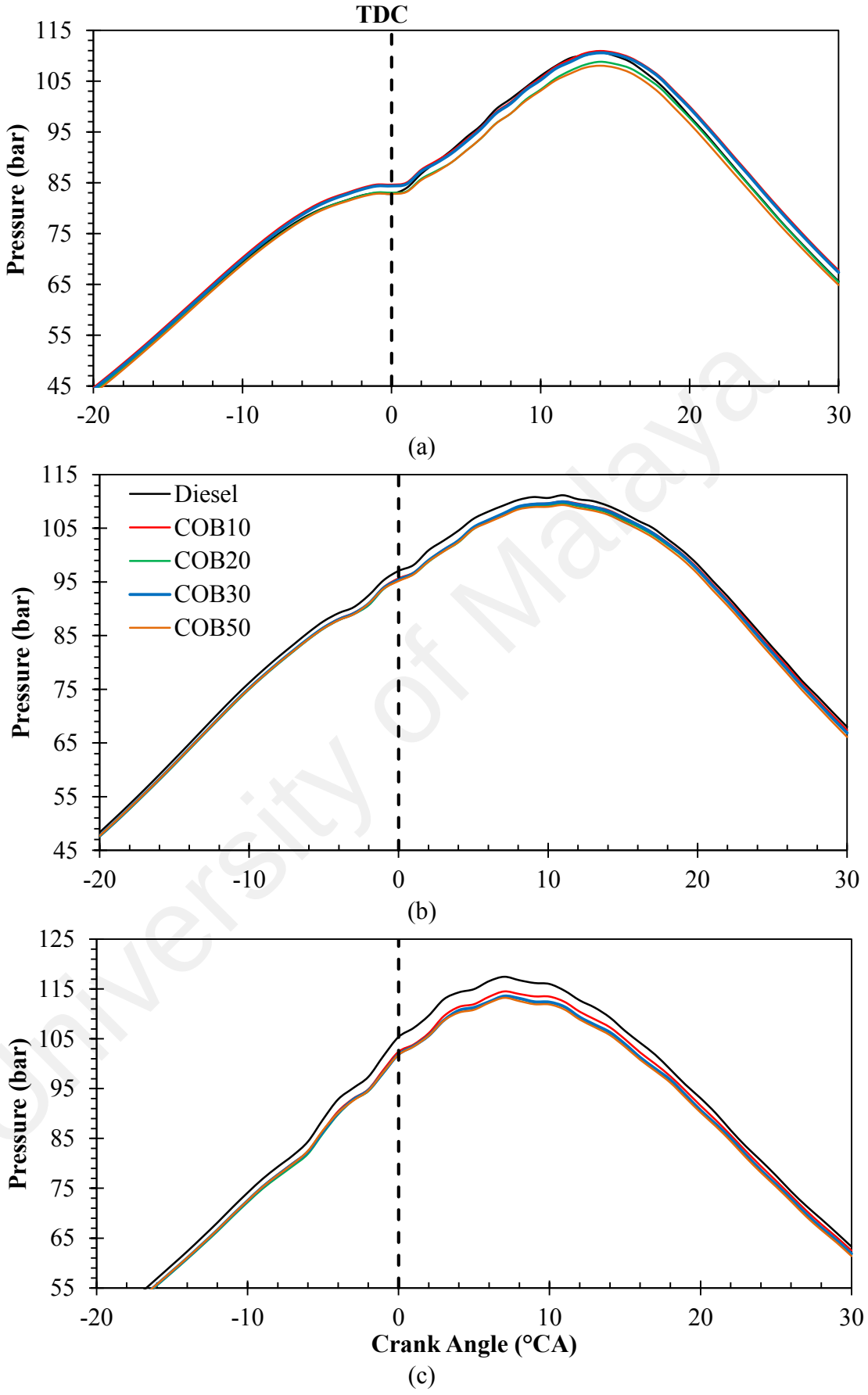

Figure 4.23: Cylinder pressure versus crank angle degree for various COB blends and diesel fuel at (a) 2000 rpm, (b) 3000 rpm and (c) 4000 rpm

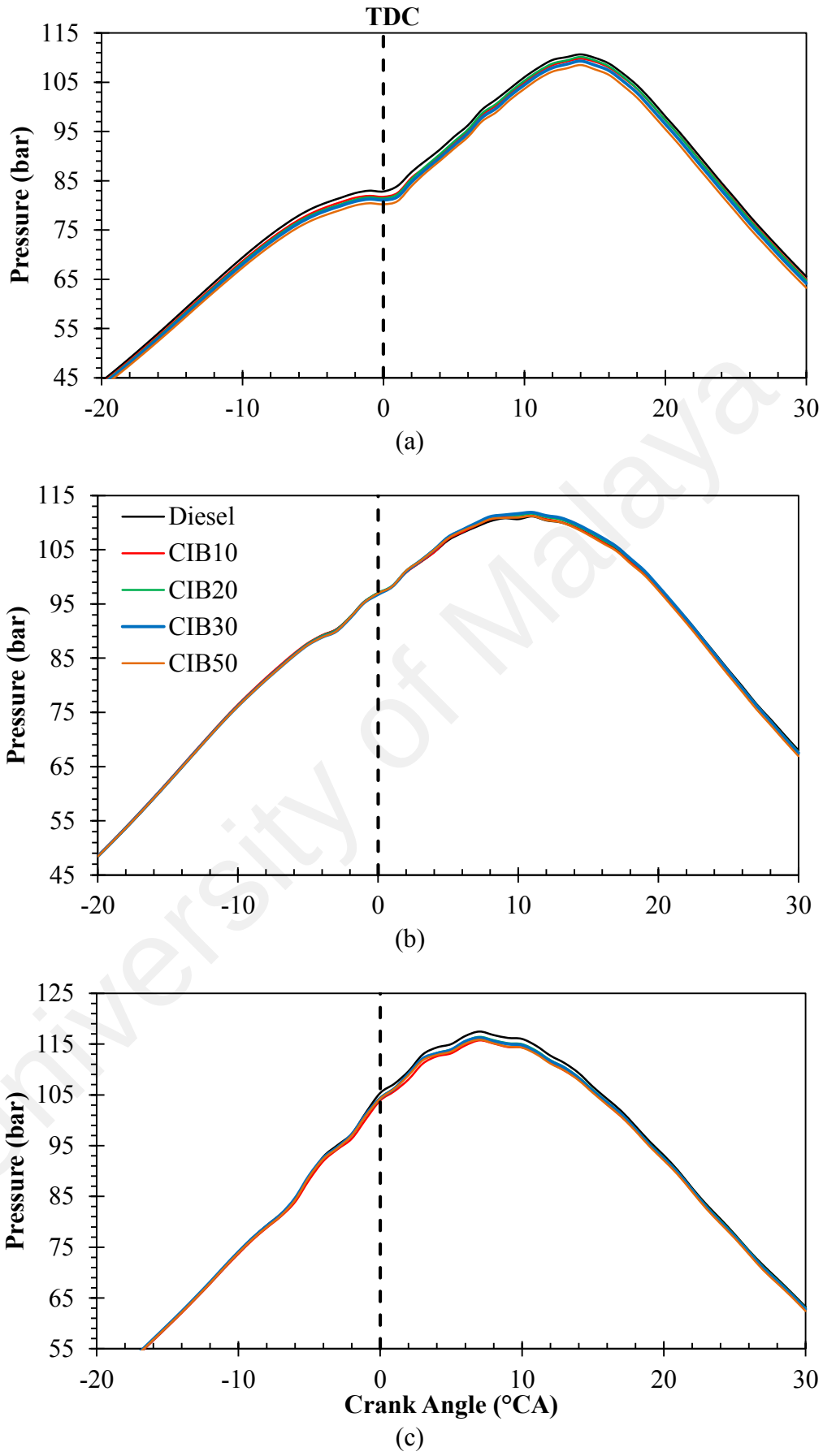

Figure 4.24: Cylinder pressure versus crank angle degree for various CIB blends and diesel fuel at (a) 2000 rpm, (b) 3000 rpm and (c) 4000 rpm

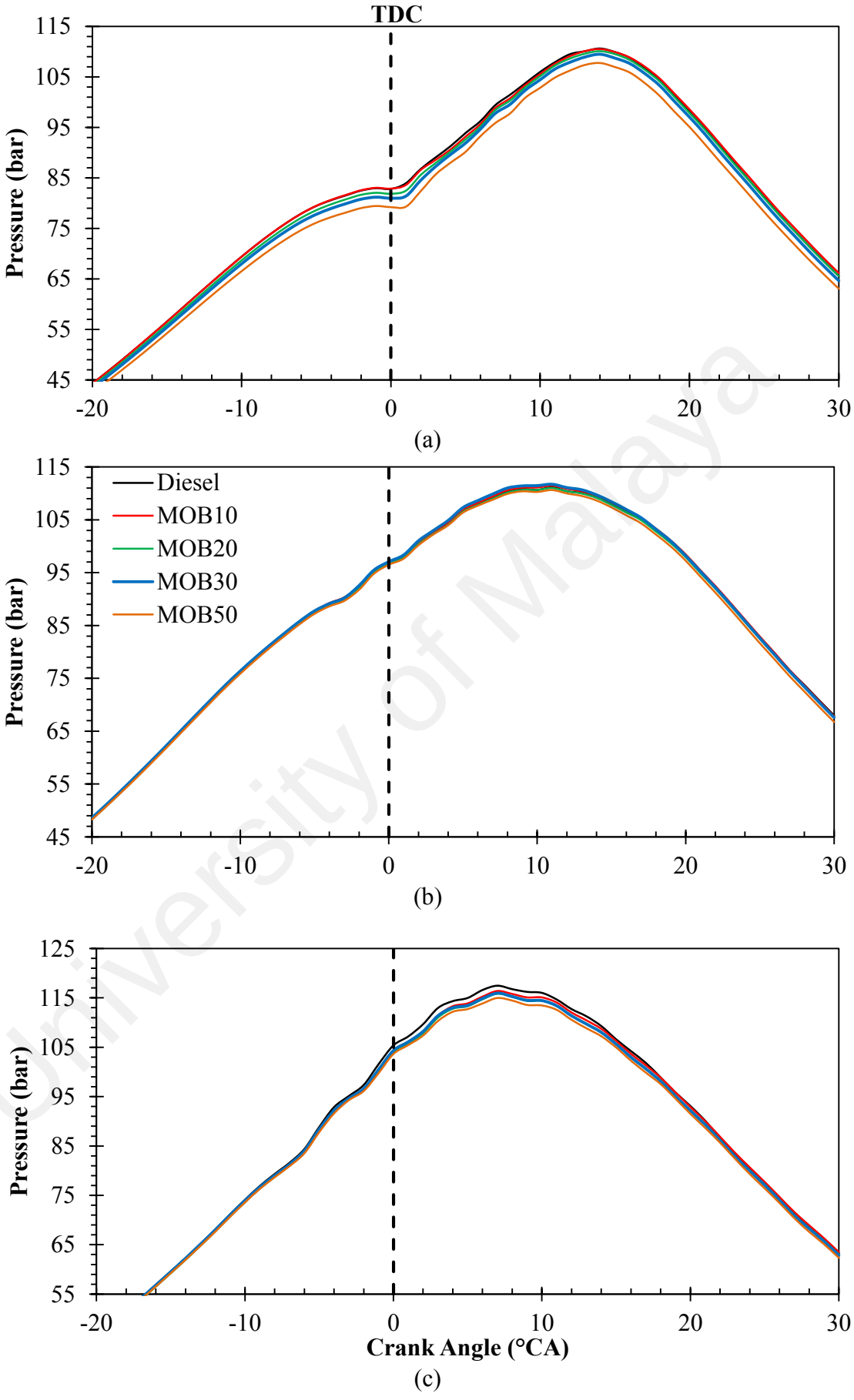

Figure 4.25: Cylinder pressure versus crank angle degree for various MOB blends and diesel fuel at (a) 2000 rpm, (b) 3000 rpm and (c) 4000 rpm

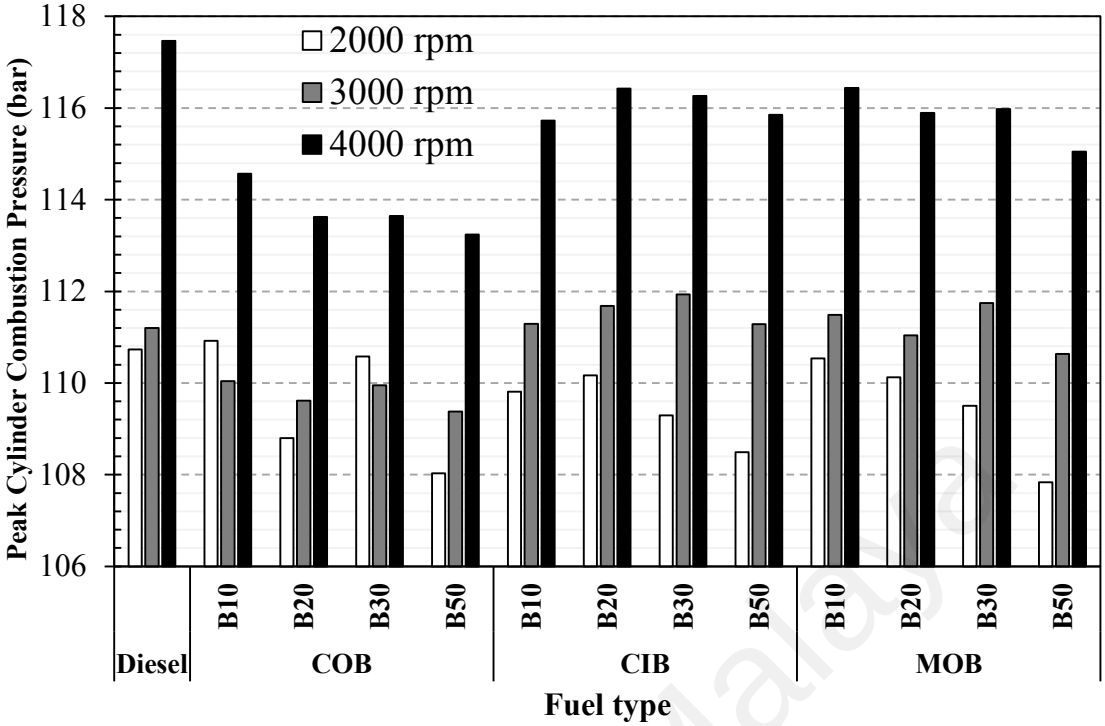

Figure 4.26: Peak cylinder pressure for various type of biodiesel-diesel blend fuels at different engine speeds

4.6.3.2 Heat release rate (HRR)

Figure 4.27 to Figure 4.29 shows the HRR results for all fuels under different engine speeds. Generally, it can be observed that the PHRR of baseline diesel that occurred during the premixed combustion phase is consistently higher than that of biodiesel blends across all engine speeds. Kinoshita et al. (Kinoshita, et al., 2006) and Ashok et al. (Ashok, et al., 2017) also reported the similar observation. In fact, a marginally decreases in the PHRR can be noticed with higher biodiesel fractions in the blend as shown in Figure 4.30. This is in very good agreement with the research works of (Kalam, et al., 2016). This phenomenon can be associated to the aforementioned effects of relatively lower calorific value of biodiesel blended fuels when compare with diesel. Another explanation is that it may be due to relatively larger viscosity of biodiesel blended fuels, which cause slow vaporization of biodiesel and subsequent reduction of heat release during premixed combustion phase.

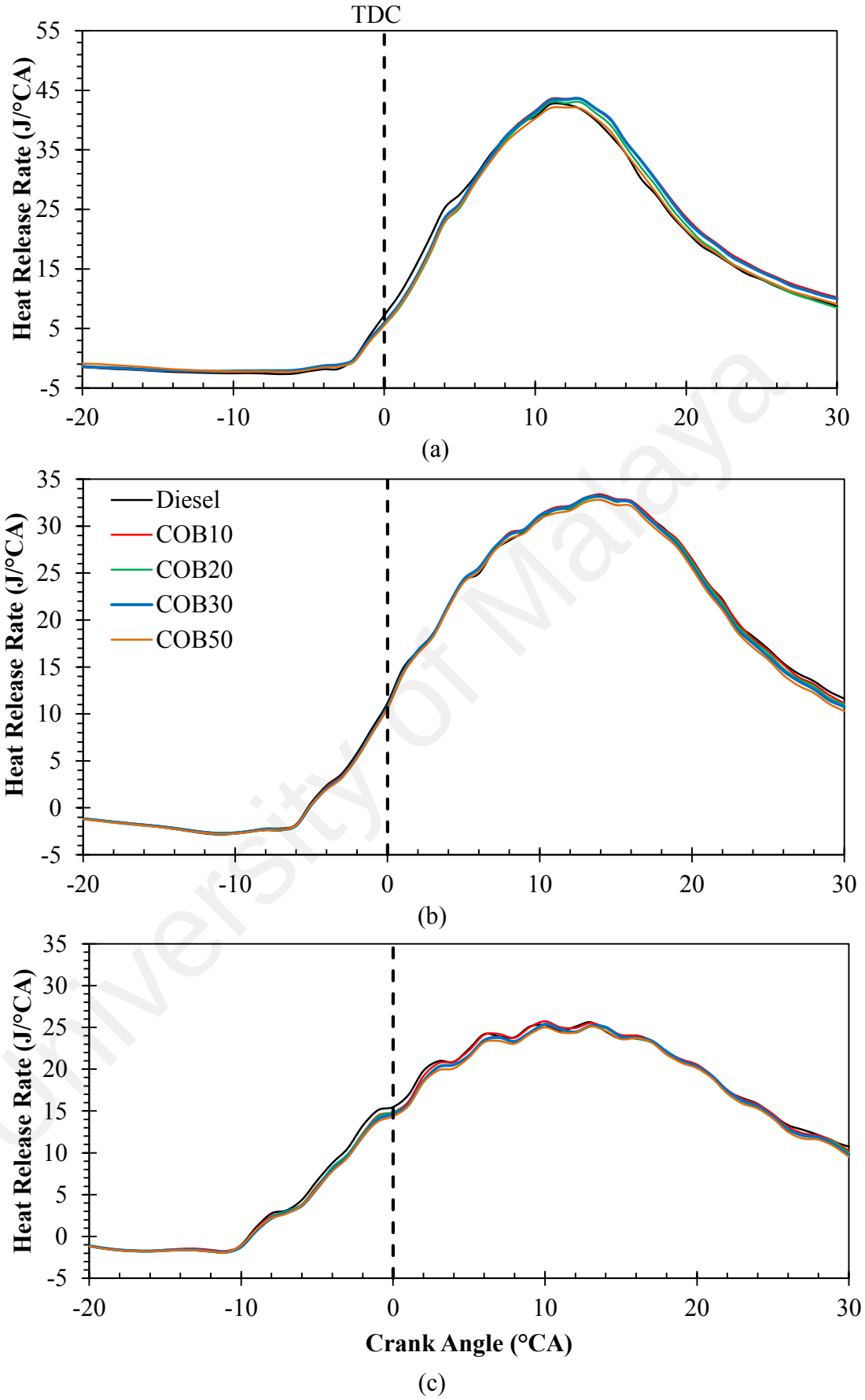

Figure 4.27: HRR versus crank angle degree for various COB blends and diesel fuel at (a) 2000 rpm, (b) 3000 rpm and (c) 4000 rpm

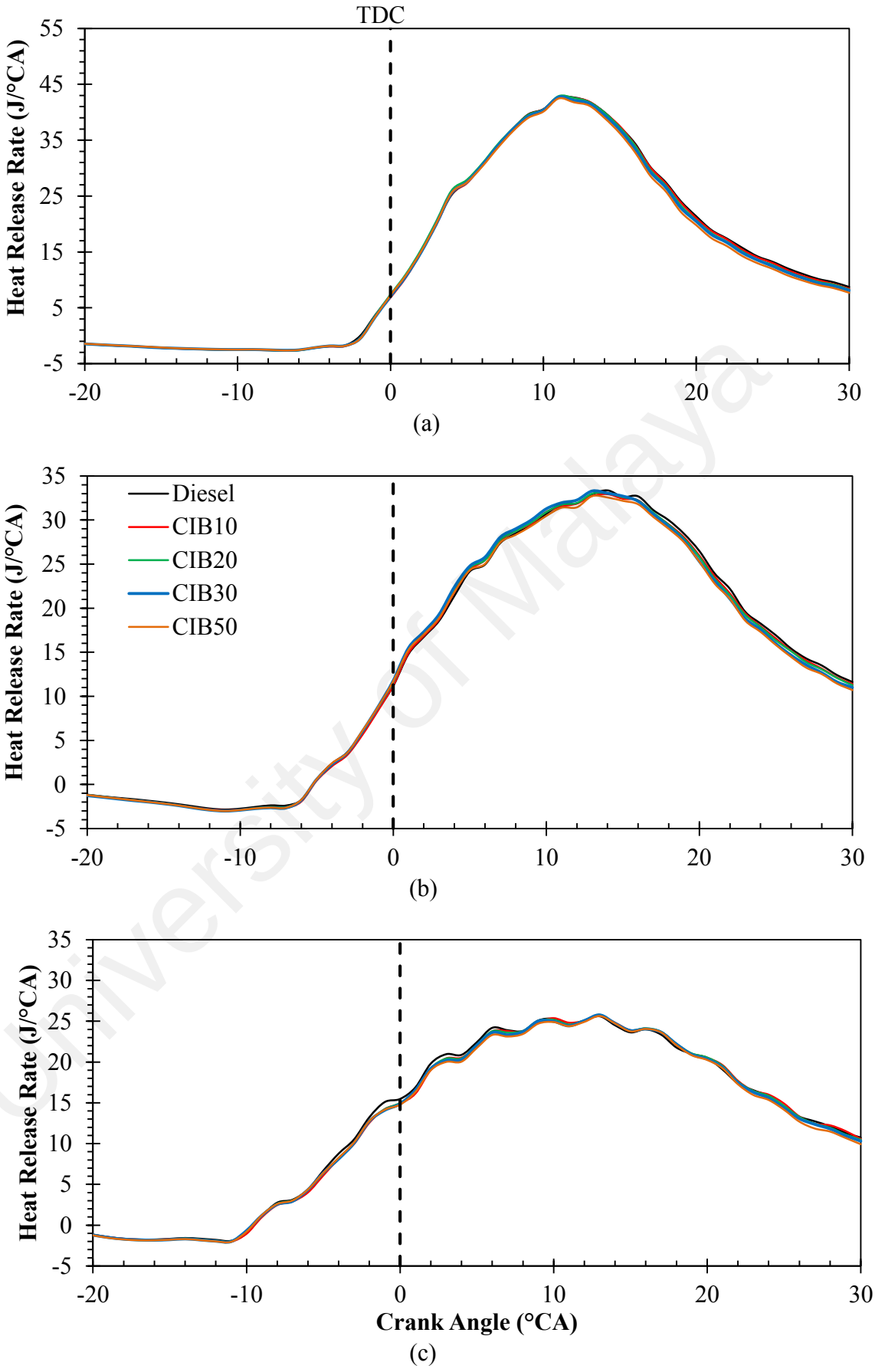

Figure 4.28: HRR versus crank angle degree for various CIB blends and diesel fuel at (a) 2000 rpm, (b) 3000 rpm and (c) 4000 rpm

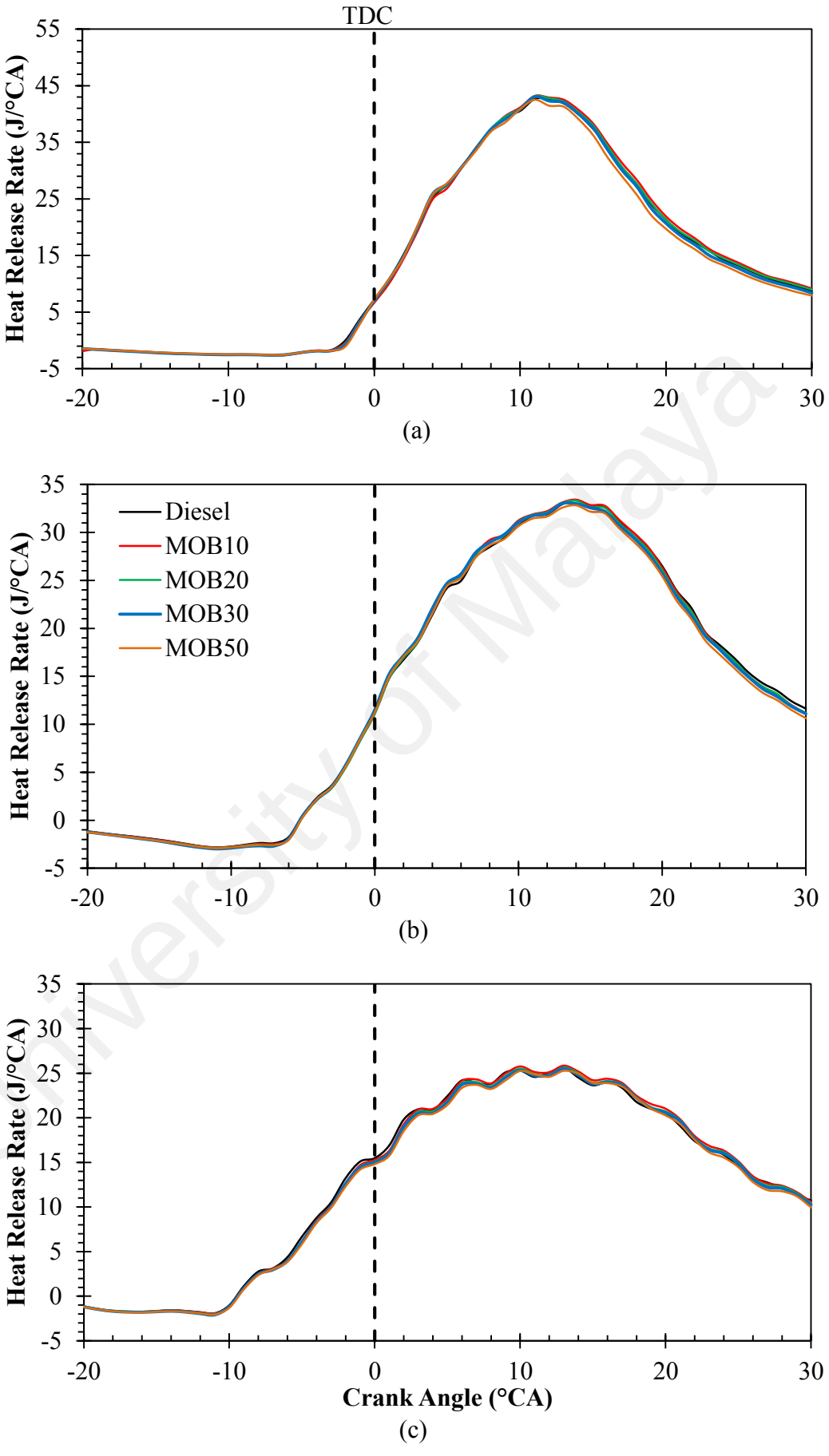

Figure 4.29: HRR versus crank angle degree for various MOB blends and diesel fuel at (a) 2000 rpm, (b) 3000 rpm and (c) 4000 rpm

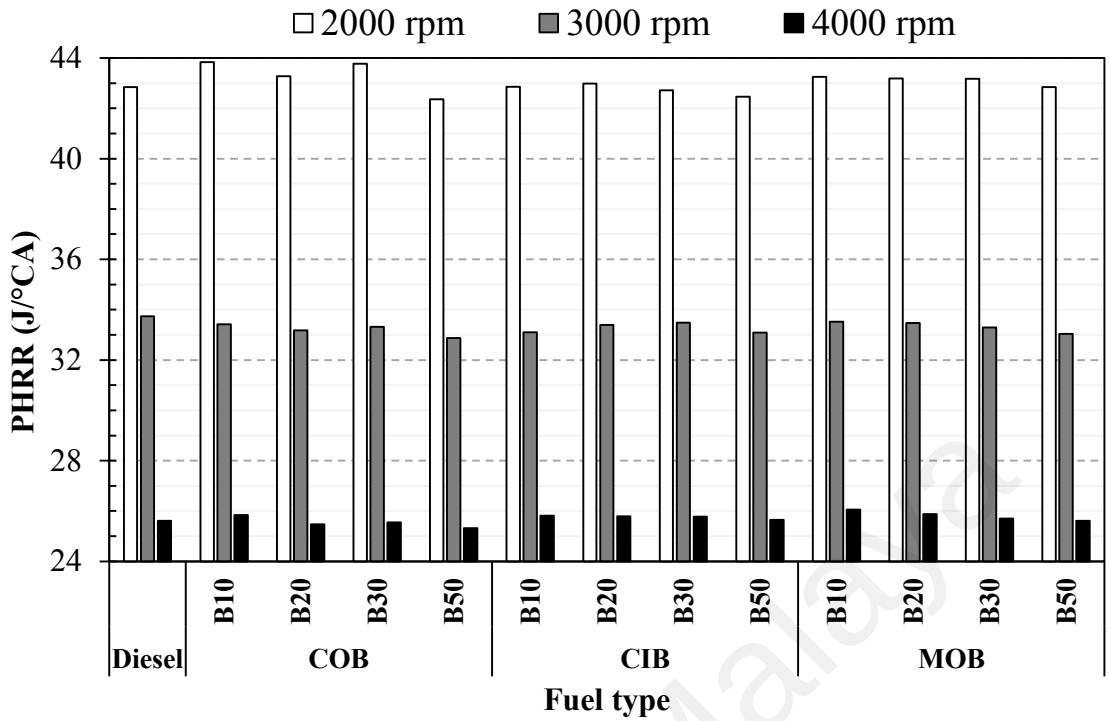

Figure 4.30: PHRR for various type of biodiesel-diesel blend fuels at different engine speeds

4.6.4 Summary

In this test series, the effects of adding of edible (COB) and non-edible (CIB and MOB) biodiesel into fossil diesel fuel on engine performance, exhaust gas emissions, and combustion were investigated in a turbocharged, high-pressure common-rail diesel engine under six different speed operations and full load conditions. The key physicochemical properties of pure biodiesel, biodiesel-diesel blends and diesel are characterized, analysed and benchmarked with ASTM standard. The test fuels used were a conventional diesel fuel and four different fuel blends (B10, B20, B30, and B50) for each type of biodiesel fuels. The results showed that all biodiesel fuels and its blends have physicochemical properties relatively close to those of petroleum diesel. The experimental results also suggested that there are some penalties in engine brake power, BSFC, and NOx with the presence of biodiesel fuel in the blend. Moreover, improvement in BTE and exhaust emissions are observed in using biodiesel fuel blends across all engine speeds. The emission improvement is characterized by lower CO and reduced

smoke emissions. Also, for the comparisons on torque, brake power, BSFC, BSEC, and CO among using COB, CIB, and MOB biodiesel blends, the results showed that the differences were mainly caused by the fuel viscosity related to the spray atomization. Peak combustion pressure and peak HRR were also reduced for biodiesel blends. In term of PM analysis, the results showed that all biodiesel blends emitted lower levels of PM than the reference fossil diesel. Overall, the results indicated that both of the non-edible biodiesels of CIB and MOB can be used satisfactorily in the modern high-pressure common-rail diesel engine and achieved comparable results as those of edible biodiesel source of COB.

4.7 Effect of injection timing and split injection strategies on engine out-response

In this study, the effects of biodiesel blends, fuel injection timing and split injection schemes on the engine performance, emissions and combustion characteristics were investigated. Parametric studies relating with start of injection timing variation and multiple injection schemes using COB20 and COB50 blends were performed and benchmarked with petroleum diesel fuel as baseline.

4.7.1 SOI variation and split injection strategies on engine performance

Effects of biodiesel blends, injection timing variation and split injection scheme on BTE and BSFC were discussed in this section. Figure 4.31 delineates the changes in BTE with various SOI timings and split injection schemes of the engine fuelled with COB20, COB50 and baseline diesel. It is found that the BTE for baseline diesel is constantly higher than that of COB20 and COB50 at every SOI timing. Literally, peak BTE of baseline diesel, COB20 and COB50 are observed to be 33.5%, 32.6% and 32.1% respectively at SOI timing equals -12°ATDC and with single injection scheme. Besides, the outcomes also show that difference in SOI timing profoundly affects BTE. Advanced SOI timings causes increment in BTE for all fuel type tested. The improvement is

attributable to the longer ignition delay (physical delay) which in turn brings about a better mixing. This results in more efficient combustion and a greater BTE. Another explanation can be made where at advanced injection timing, the engine attains peak combustion pressure near to TDC. Hence, greater effective pressure can be produced to generate useful work (Bari et al., 2004). Nonetheless, for the corresponding SOI timing, there is a perpetual decline of BTE by an average of 5.2% and 13.1% for the case of double and triple injection, respectively, in comparison to the BTE of single injection operation using baseline diesel. It may be due to the combustion process occurs over a longer period for double and triple split injection. Thus, the heat losses through the cylinder wall is increases due to longer combustion duration, and consequently less useful mechanical work is generated. Another explanation is that the power output is reduced because a greater quantity of fuel is combusted when the cylinder expansion occurs. Subsequently, the cylinder pressure increases only when volume of cylinder is expanding quickly. Therefore, a smaller effective pressure will be produced. Another observation is that when single injection scheme is implemented at SOI of -12ºATDC, it is found that BTE decreases with increasing of biodiesel blend. This trend is discovered for other SOI and split injection scheme, which is in accordance with other researches (Gnanasekaran et al., 2016; Yehliu, et al., 2010). The lower BTE can be due to the fact that diesel engine used in the present study is not purposely designed for the use of biodiesel. Besides, with the addition of biodiesel fuel in the blend, the oxygen content is richer than that of conventional diesel. This causes biodiesel blended fuels to have a lower calorific value in comparison to baseline diesel properties as shown in Table 4.4. Another important engine performance characteristic is the BSFC. According to the results, BSFC values obtained when COB20 and COB50 biodiesel blended fuels are used are consistently larger than that of baseline diesel at all SOI timing and injection schemes. The greater BSFC value of both COB20 and COB50 indicates that more fuel is needed to generate the same power

amount. This expectation is made due to the low heating value of COB20 and COB50 than that of petroleum diesel as shown in Table 4.4, which is about 2.9% and 7.8%, respectively less than heating value of petroleum diesel fuel. Moreover, it is discovered that the changes in injection timing has caused impact on the magnitude of the BSFC. Reduction in BSFC can be achieved by advancing the SOI timing from 2°ATDC when different types of diesel are used. When SOI is implemented earlier, there is continuous improvement in combustion effectiveness and quality. This explains the decrement in BSFC. As BSFC decreases under fixed value of brake power output, less amount of fuel is being injected to enable a more efficient combustion process to occur. This occurs particularly when earlier SOI timing is set. In addition, it can be noticed that for the respective SOI timing, the BSFC is increased with the increasing in number of split injections for all fuels. These results are consistent with other researchers (Chen, 2000; Pierpont et al., 1995). By diving the main fuel injection into two and three parts reduced the peak combustion pressure, thus lower the amount of fuel injected when TDC is reached. This causes reduction in work done. Another possible explanation is that it may be due to the longer combustion duration, thus increased the heat loss when higher number of split injections is being used. As a result, BSFC has to be increased to supply more energy.

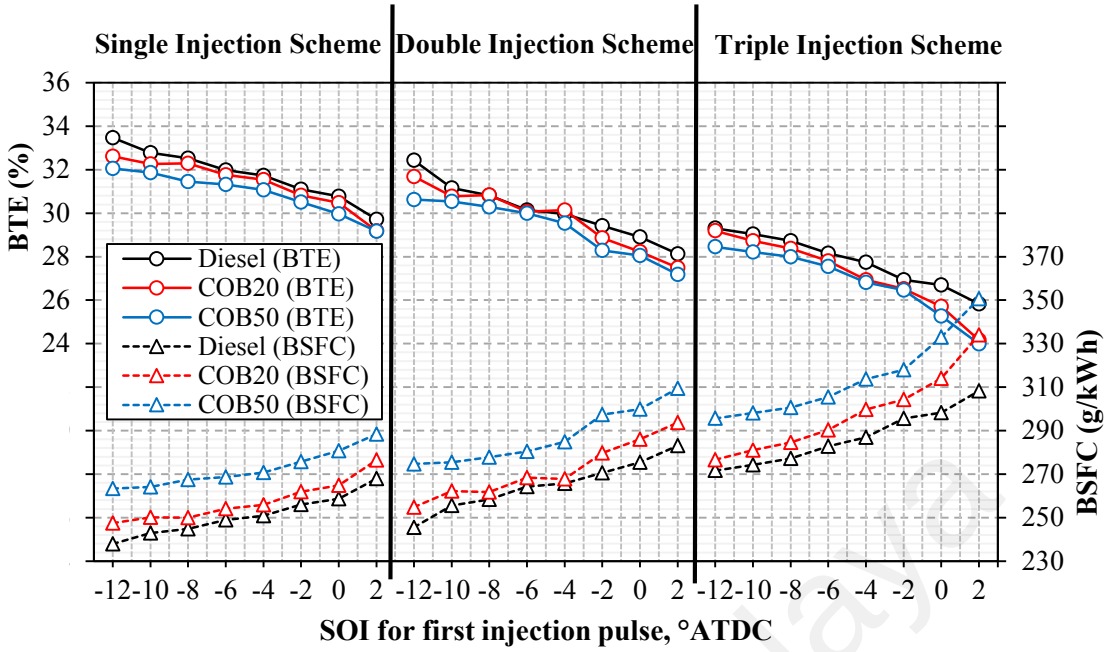

Figure 4.31: BTE and BSFC for various fuels, start of injection timings and split injection schemes

4.7.2 SOI variation and split injection strategies on exhaust emissions

Effects of biodiesel blends, injection timing and split injection scheme on NOx and smoke emissions amount were discussed in this section. The trend of NOx emissions when various test fuels are used at different SOI timings as well as split injection schemes is displayed in Figure 4.32. It is found that advanced SOI timing causes an increase in NOx emission amount for all fuel types and multiple injection scheme. Increasing trend is observed in NOx emissions when SOI timing is advanced. This condition suggests that the ignition and combustion of mixture occur earlier and result in early formation of peak pressure around TDC. This causes the combustion to happen at a higher temperature and promotes the thermal or Zeldovich NOx formation mechanism. The results also imply that both COB20 and COB50 biodiesel blends tend to diminish NOx emissions over all SOI timings and split injection strategies. This is due to the rather greater cetane number and smaller calorific value of the COB20 and COB50 in comparison with baseline diesel. The factors subsequently reduce the heat release rate during the premix combustion phase and lower the peak combustion temperature. The discovery can be explained by comparing the in-cylinder mean gas temperature results depicted in Figure 4.35. Besides,

a considerably lower NOx emission level under 100 ppm can be attained by applying late SOI timing for COB20 and COB50 fuel operations and with triple injection scheme. With injection performed lately, the retardation of combustion phasing will happen progressively in the expansion stroke and moves away from TDC. This effect causes a decrease in combustion gas temperature and reducing NOx formation. Meanwhile, dividing the main injection into two and three parts lowered the NOx emissions. This can be attributed to the improvements made in the injection process of modulating the injection rate for multiple injection strategy, thus splitting the heat release process into separate portions and reduced in peak rate of heat release. This shows that split injection is effective in reducing NOx emissions. The smoke formed due to the unfinished combustion of the hydrocarbon in the fuel and partial oxidation of the carbon content in the fuel. The amount of smoke emissions of each test fuel at different SOI timings and injection schemes is delineated in Figure 4.32. Overall, it is discovered that drop in level of smoke emission occurs when COB20 and COB50 are employed at every SOI timing. Less smoke is emitted than when diesel fuel is utilized at each SOI timing, mainly due to richer fuel-borne oxygen, less carbon content, and the absence or lesser quantity of aromatics hydrocarbon in biodiesel blends. The results also indicate that with advanced SOI timings, the smoke emissions were reduced when double injection strategy is carried out, and somewhat remained unchanged during operation of single injection strategy. This is because when SOI timing is advanced, gas temperature developed will be higher, in which fuel and oxygen reaction will be improved. As a result, both injection schemes will yield lower emission level of smoke. The second possible reason is the presence of enough time for the fuel to vaporize and form mixture with air, thus allowing effective mixing and complete combustion. However, the triple injection scheme operation shows slightly higher smoke emission with earlier SOI timings. It may be due to the decrease in the in-cylinder combustion temperature (as shown in Figure 4.35) that prevent high burn

rates, which leads to incomplete combustion with increased smoke emissions. This implies that multiple injections are able to jeopardize smoke emissions level when the optimization of injection timing is not implemented well. By operating the engine with COB50 fuel, smoke emission can be diminished without affecting the reduction effect in NOx emissions amount. The results show that a similar smoke emission level (i.e. below 6% for diesel operation with single injection scheme) can be obtained when the COB50 is used along with the strategies of retarded SOI timing and triple injection scheme. Therefore, simultaneous decrease in NOx and smoke emission level from the baseline levels of pure diesel is achievable with the usage of COB50 biodiesel blended fuel in conjunction with the application of retarded SOI timing and triple injection scheme in a diesel engine.

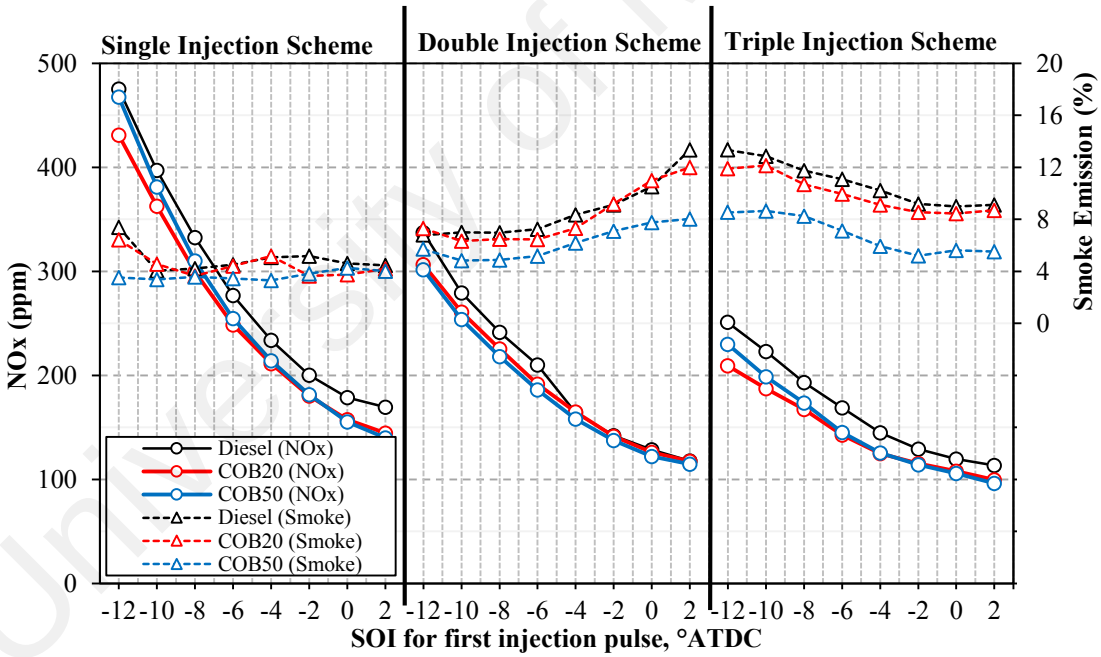

Figure 4.32: NOx and smoke emission for various fuels, SOI timings and injection strategies

4.7.3 SOI variation and split injection strategies on combustion process

To investigate the influence of injection scheme and types of fuel on combustion characteristics, 100 consecutive cycles of cylinder combustion pressure were logged and processed. The average values were calculated and compared. Figure 4.33 depicts the

graphs of injector current profile, combustion pressure and HRR of the engine, utilizing baseline diesel at SOI of -6°ATDC (nominal timing) and with various injection strategies. From the injector current profile, it can be seen that the fuel injection event is formed by two and three identical injection pulses for double and triple injection schemes, respectively. Besides, the engine operated with multiple injection schemes had significant impact on the combustion process. The crank angle position of peak pressure is advanced towards the compression stroke with greater number of injection schemes. Also, the location of start of combustion (SOC) timing for double and triple injection scheme occurred 0.5°CA and 1°CA respectively, more advanced than that of single injection scheme. Additionally, in double injection test case, peak pressure undergoes a minor decline in the range of 1.7 bar. However, triple injection strategy has resulted in a slight increases in the range of 1 bar is discovered for peak pressure. Two and three notable HRR peaks can be noticed for double and triple injection strategies, respectively. Besides, it can be seen that the occurring position for the first peak of HRR curve, when double and triple injection strategies are conducted, is shifted earlier by 0.5° CA and 1° CA respectively, in comparison with single injection strategy. The main cause for the first HRR peak timing to occur early is the advanced occurrence in SOC timing and subsequently leads to the earlier HRR rise. Besides, the two diffusion burns resulting from the subsequent fuel pulses occur at about the same time after start of injection for both timings (ignition delay_2 is approximately same with ignition delay_3) but lower intensities are evidently seen. The second and third fuel pulse ignite almost immediately soon after the SOI_2 and SOI_3 since they are directly injected into the main combustion zones.

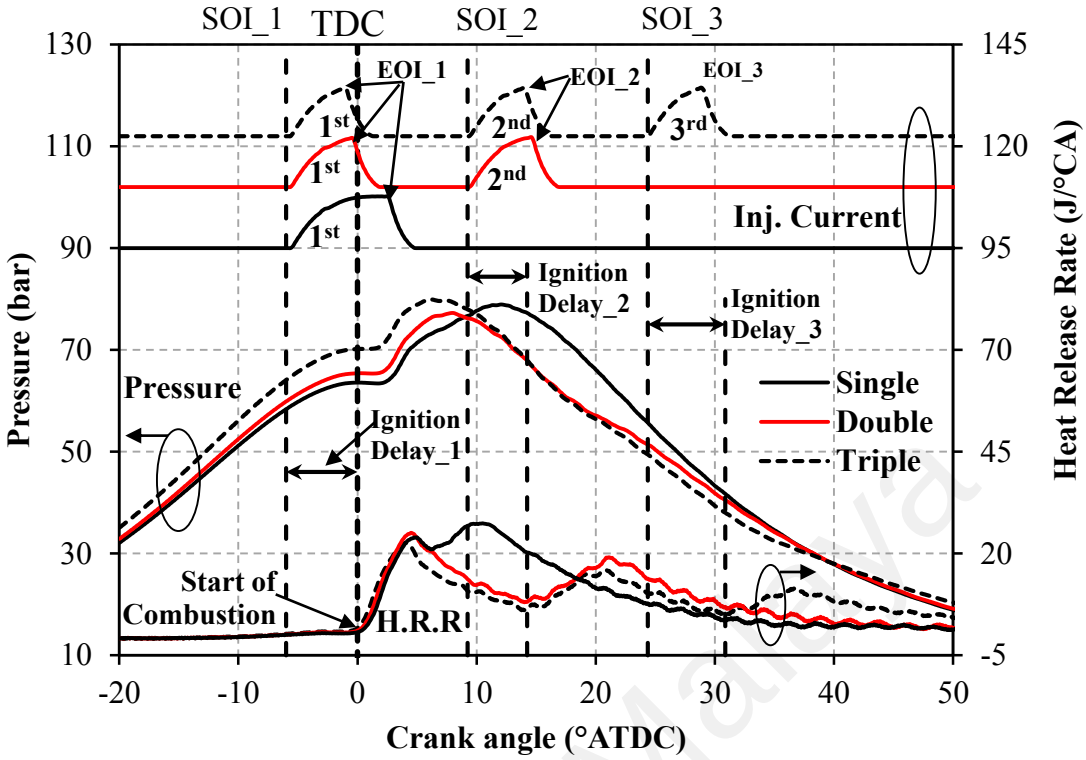

Figure 4.33: In-cylinder combustion pressure, HRR and injector current patterns for baseline diesel with various injection strategy at SOI of -6°ATDC

Figure 4.34 indicates the plot of combustion pressure and HRR variations as a function of crank angle at various SOI timings, single injection strategy and with all types of fuel tested. Overall, the pressure peak of combustion constantly rises and advances towards the location of TDC with earlier SOI timing for all fuels. Greater effective work can be generated via the larger pressure and this helps in enhancing BTE and reducing BSFC. Besides, the HRR plots also exhibit a resembling patterns as that of combustion pressure in which first peak of HRR associated with the premixed combustion phase is advanced towards compression stroke with earlier SOI timing when different fuels are utilized. With SOI timing advancement toward the TDC point in cylinder expansion stroke, the peak HRR correspond to the premixed combustion phase became initially reduce and kept unchanged. With the increasing of biodiesel in the fuel blend, the HRR pattern is almost the same as that of conventional diesel, however it can be noticed that larger fraction of fuel is consumed during the mixing controlled combustion phase. This

can be shown by the wider plateau after the first peak of HRR. In fact, this phenomenon can be observed clearly in the late SOI condition of 2°ATDC, in comparison with earlier SOI timing. The reason is that biodiesel has a greater cetane number than that of baseline diesel. This causes ignition delay to be shortened, thereby producing a lower peak of HRR. In general, it is discovered that COB20 and COB50 combustion release 1.4 J/°CA and 4.3 J/°CA, respectively lower in HRR peak compared to baseline diesel over the entire range of SOI timings.

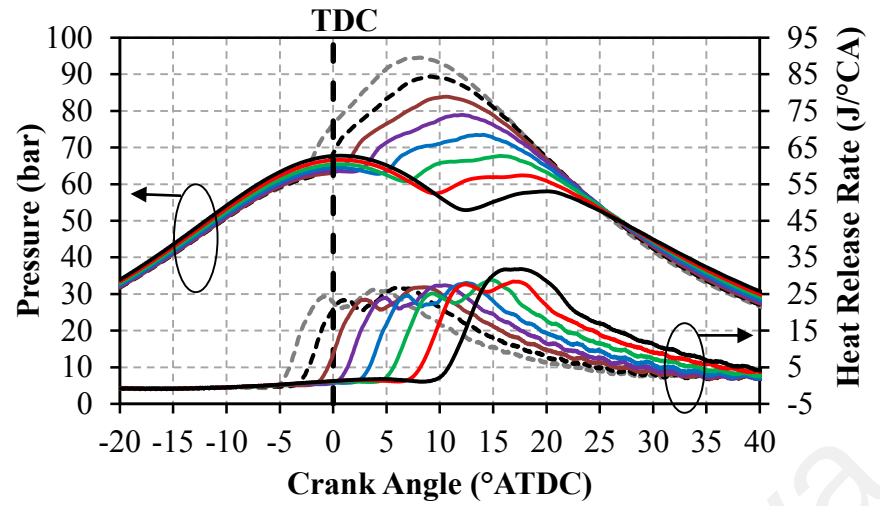

(a) Diesel

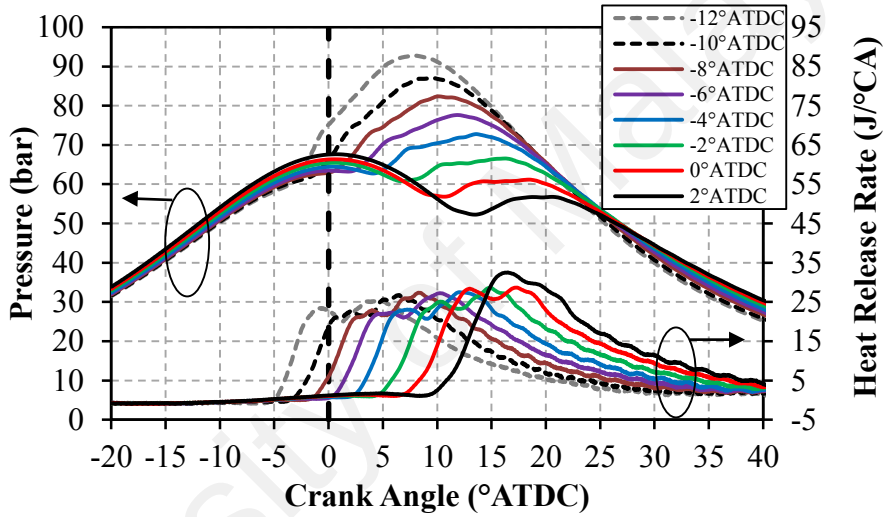

(b) COB20

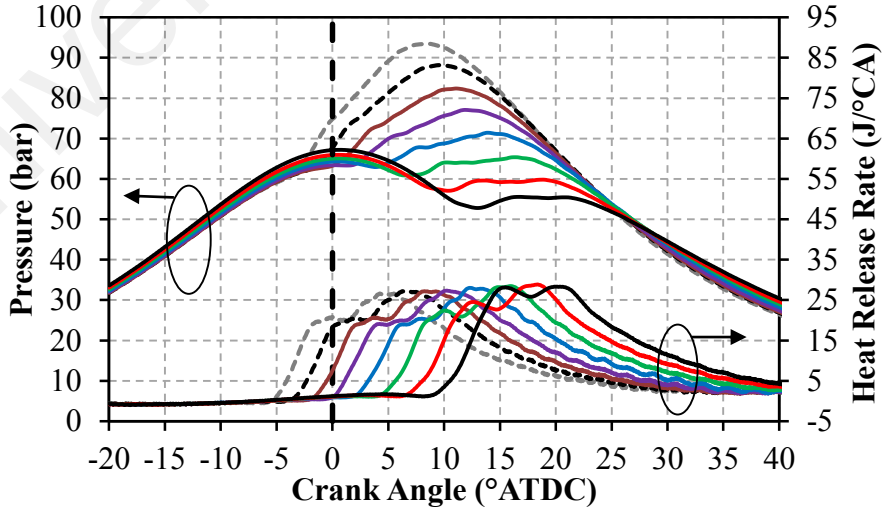

(c) COB50

Figure 4.34: In-cylinder combustion pressure and HRR plots for (a) baseline diesel, (b) COB20, (c) COB50 at different SOI timings and single injection strategy

Effects of biodiesel blends, injection timing and split injection scheme on peak mean gas temperature (PMGT) and PHRR were discussed in the following section. Figure 4.35 shows the changes in PMGT with various SOI timings and split injection strategies of the engine operated with COB20, COB50 and baseline fuel. The PMGT of COB20 and COB50 are always found lower than that of baseline diesel over the entire range of SOI timings. Indeed, the results show that the highest PMGT of baseline diesel, COB20 and COB50 are 1964K (at SOI = -12°ATDC), 1922K (at SOI = 2°ATDC) and 1955K (at SOI = -12°ATDC) respectively and with single injection scheme. Besides, it is observed that SOI timing variation profoundly influences the magnitude of PMGT. For single injection scheme, when SOI timing is set earlier, the PMGT will increase for all fuel type tested. The incremental effect is due to the higher peak combustion pressure, which results in a higher PMGT. However, for the corresponding SOI timing, there is a continuous reduction of the PMGT by an average of 5.1% and 9.3% for the case of double and triple injection, respectively, as compared to those of baseline diesel single injection operation. Another observation is that when triple injection scheme is implemented at SOI of -12ºATDC, it is found that PMGT decreases with biodiesel blended fuels. Another important combustion characteristic is the magnitude of PHRR. According to Figure 4.35, it can be seen that COB20 and COB50 are consistently exhibit lower PHRR compared to baseline diesel for all SOI timings and injection schemes, except for the single injection operation. This is because biodiesel has a greater cetane number in comparison with baseline diesel, as shown in Table 4.2. Consequently, biodiesel has a shorter ignition delay and a smaller peak of HRR, as aforementioned. Also, it can be seen that for a specific SOI timing, the PHRR is decreased with the increasing in number of split injections for all fuels. By diving the main fuel injection into two and three parts may reduced the quantity of fuel combusted in the premixed burn stage, thus lower PHRR.

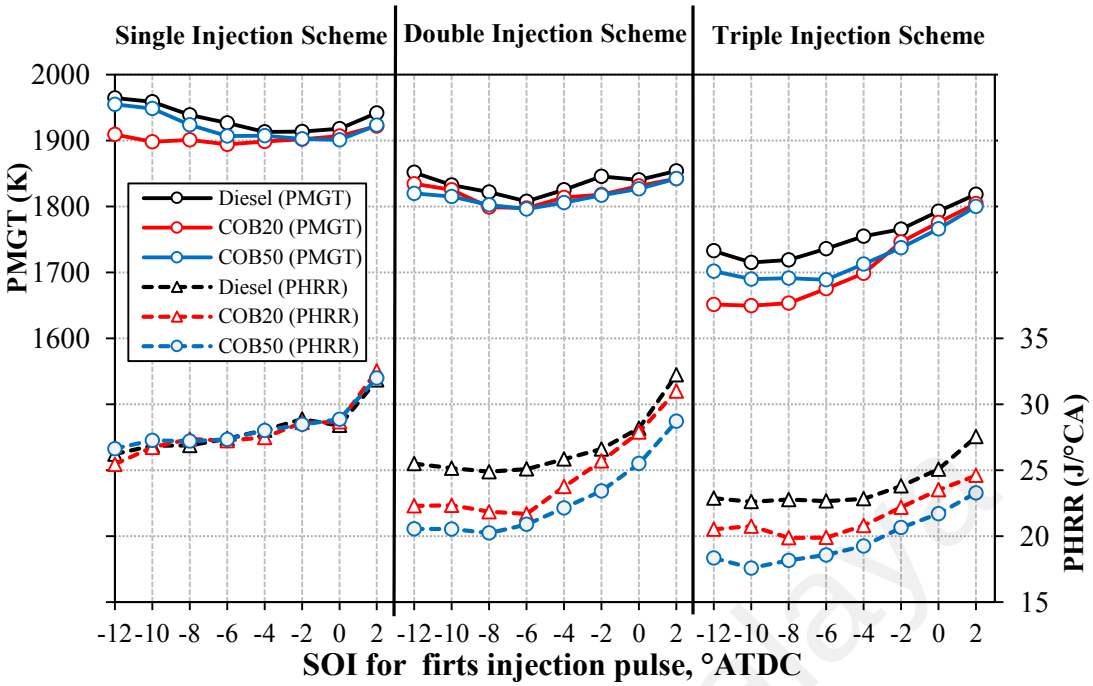

Figure 4.35: PMGT and PHRR for various fuels, SOI timings and injection strategies

Multiple injections approach, comprises pilot and post injections are commonly used to mitigate PM/ smoke, controlling amount of NOx, managing engine combustion noise and to handling exhaust pipe after treatment equipment in diesel engine. Combustion pressure and HRR data of (a) single, (b) double, (c) triple injection at different SOI timings using baseline diesel as fuel can be obtained from Figure 4.36. The beneficial effect of double and triple split injections were discussed in this section by directly comparing different injection strategies with the corresponding SOI timing. This allows one to point out the differences in the combustion events that are responsible for results observed in NOx and smoke emissions. First, the double injection at later SOI of 2° ATDC is compared to the single injection with similar injection timing in order to further analyze the benefits of one injection interruption. The HRR data shows that the two combustion events start deviating once the first fuel pulse of the double injection has been terminated after a premixed burn of about the same intensity, as can be clearly seen in Figure 4.33. For double injection, as larger amount of the injected fuel has already been consumed in the premixed flame. Thus, the following combustion process during the

injection dwell (i.e. the duration between the SOI_1 and SOI_2 as depicted in Figure 4.33) is characterized by a fuel-air mixture that burns at very high temperatures. Consequently, the second fuel injection in double injection burns as a diffusion flame only. The fuel mixes with the hot gases remaining in the combustion chamber and ignites after a very short ignition delay. Besides, the double injection has a lower peak mean gas temperature that keeps the NOx production on a lower level, as shown in Figure 4.35. The subsequent fuel injection causes another, slightly lower HRR and flame temperature rise, which lasts for about 20° CA in the combustion cycle and ensured lower NOx production. Further optimization of split injections in terms of NOx and smoke emissions can be accomplished by using additional injection pulses, which is called triple injection. The experimental observation made by Pierpont found that the optimized triple injection, as the most sophisticated, but also most complicated injection strategy, can lower emissions beyond the capability of double injections (Bakenhus & Reitz, 1999; Pierpont, et al., 1995). The direct comparison of double and triple injection with the same injection timing as shown in Figure 4.33, reveals that the two combustion events resulting from these strategies differ only in the second half. This combustion phase is most responsible for overall smoke emissions. The fuel combustion of the third injected fuel during piston expansion cooling stroke can be used to ensure a proper oxidation of the fuel-air mixture. This positive effect of the soot oxidation during the last stage of the combustion process can be noticed with the lower smoke emission level compared to the double injection, as is reflected in Figure 4.32 with the late SOI timing of 2° ATDC. Another interesting observation is that because of the similarity of the second and third fuel injection event, it is no surprise that the second and third peak HRR are almost identical for triple injection case (see Figure 4.36c).

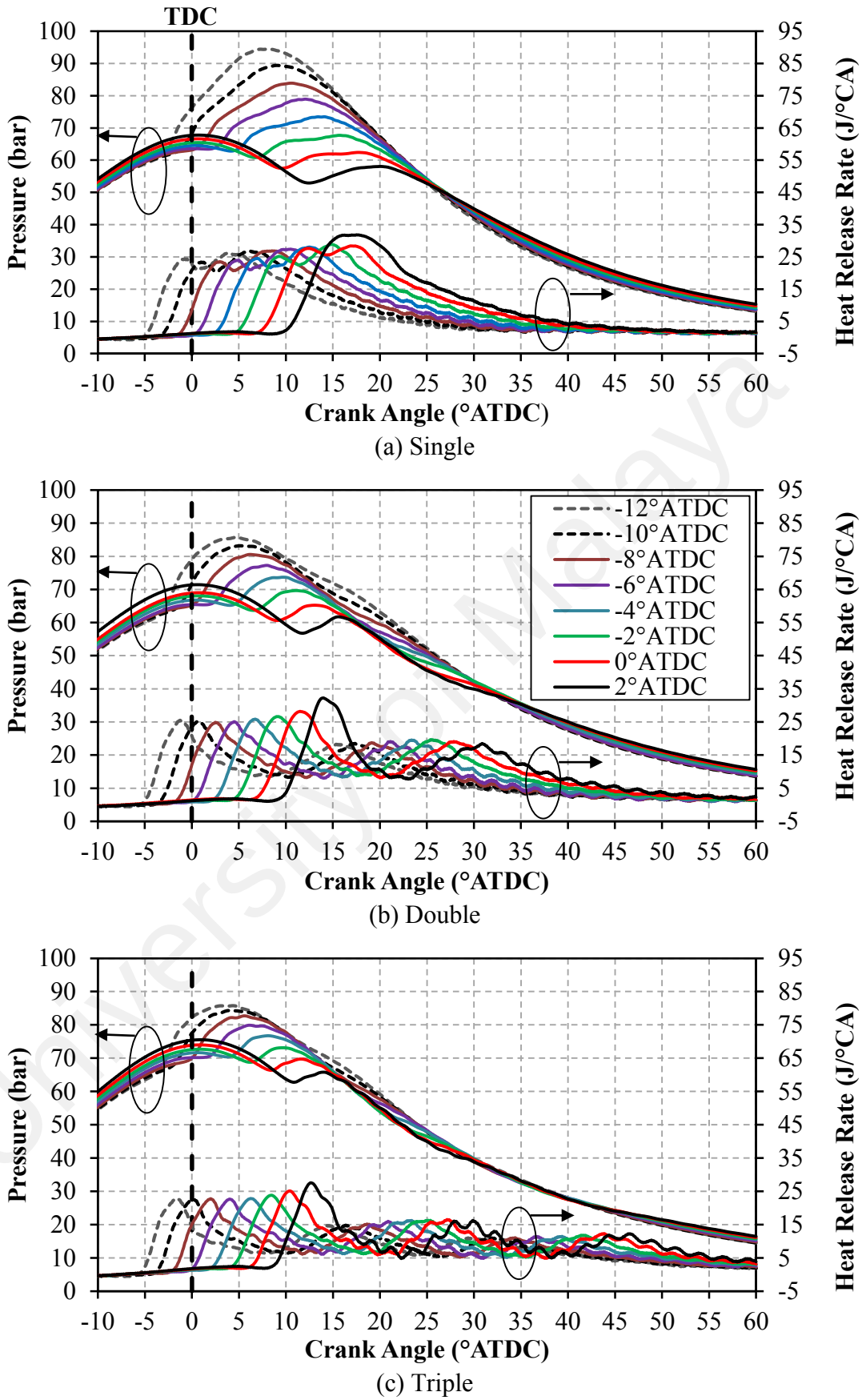

Figure 4.36: Combustion pressure and HRR curves for (a) single, (b) double, (c) triple injection at various SOI timings and with baseline diesel.

4.7.4 Summary

In this test series, the engine performance, combustion, and exhaust gas emissions characteristics of baseline diesel, COB20 and COB50 fuels have been empirically tested in a medium-duty common-rail DI diesel engine. By holding the engine speed at 2000 rpm and at 60 Nm load as experimental condition, investigation of the effect of SOI timing and multiple injection strategies had been successfully carried out. Below are the main conclusions which are inferred from the present work.

i. The diesel engine emissions, performance and combustion characteristics are affected by SOI timing and split injection scheme significantly for all types of fuel tested.
ii. A considerably lower level of NOx, which is below 100 ppm, can be attained by retarded SOI timing for COB20 and COB50 fuel operations and with triple injection scheme.
iii. Simultaneous NOx and smoke emission decrement from the baseline levels of petroleum diesel fuel can be achieved by utilizing COB50 in conjunction with implementation of retarded SOI timing and employment of triple injection scheme in a diesel engine.
iv. Multiple split injections is a practical strategies to simultaneously decrease NOx and smoke emissions when the SOI timing is fine-tuned and is an ideal alternative to operate with biodiesel fuel.

4.8 Effect of two-stage injection dwell angle on engine out-response

In this test series, the effect of percentage of biodiesel blends and injection strategies such as variation in SOI timing and dwell angle on diesel engine performance are investigated. The tests were performed at constant speed of 2000 rpm and 60 Nm of torque operation with COB20 and COB50.

4.8.1 Two-stage injection dwell angle variation on engine performance

The data obtained has been plotted in graph form. The performance and emission characteristics of diesel engine when the percentage of biodiesel blend, SOI and dwell angle change were analyzed based on the graphs plotted. In this section, the effects of the stated engine parameters on BTE and BSFC is examined. Figure 4.37 shows the BTE and BSFC of diesel engine when the parameters as shown are varied. It can be seen that BTE of biodiesel blend fuels is always lower than baseline diesel across all SOI timings and dwell angles. By focussing on test case with SOI timing of -6°ATDC and dwell angle equals to 12°CA, comparison can be made where the BTE values are 30.6%, 30.5% and 30.4% for petroleum diesel, COB20 and COB50 blends respectively. Moreover, the results suggest SOI timing is one of the key factors which affect BTE. When SOI timing is advanced, the BTE of all type of fuel improves. This is also discovered for other dwell angle operations. This is because when the SOI is advanced, the ignition delay of the first injection will increase, causing more homogeneous mixture to form. This leads to a more complete combustion. Besides, according to Figure 4.40, the PHRR occurs nearest to TDC at the most advanced SOI. This will produce higher effective pressure to perform greater useful work (Bari, et al., 2004). Nevertheless, for the corresponding SOI timing, slight fall of BTE level occurs with a value of 0.1% and 1.6% for the case of dwell angles of 15°CA and 18°CA, respectively, in comparison with that of baseline diesel at 12°CA dwell angle. Peak pressure decreases when dwell angle is increased where the useful work done on the piston will drop (Liu & Song, 2016; Park, et al., 2004). Besides, heat loss

will increase with longer combustion process for dwell angles of 15°CA and 18°CA. The energy which is converted into useful mechanical work will be less. Another possible explanation is that at retarded crank angle, cylinder expansion cooling effect will take place. The volume of cylinder will increase quickly where the increment rate of pressure will be lower. Effective pressure which is lower will be achieved and this produce a lower power output (Hampson & Reitz, 1998). On the other hand, by zeroing in on test case with SOI of -6ºATDC and dwell angle of 12°CA, it can be seen that increasing percentage of biodiesel blend will reduce the BTE level. This phenomenon is observed in test case with different SOI timings and dwell angles and the trend is also reported by other researchers (Raheman & Ghadge, 2007; Shivakumar, et al., 2011; Yehliu, et al., 2010). One of the reasons is that the properties of biodiesel is different from baseline diesel. Diesel engine used is not specifically tailored to be operated with biodiesel. Furthermore, oxygen content of biodiesel blends is higher than that of pure diesel. This will affect biodiesel blends in such a way that the fuel's calorific value will be lower compared to that of pure diesel as indicated in Table 4.4. Lower part of Figure 4.37 depicts the variation of BSFC with changing engine parameters. When COB20 or COB50 biodiesel blends is used to run in diesel engine, the BSFC value obtained is invariably larger than that of petroleum diesel across all SOI timings and dwell angles. This phenomenon is aligned with Dhar and Agarwal (Dhar & Agarwal, 2015), Raheman and Ghadge (Raheman & Ghadge, 2007), Sayin and Gumus (Sayin & Gumus, 2011) and Ganapathy et al. (Ganapathy, et al., 2011). When higher BSFC is observed, more fuel is necessary to maintain the same power output. This is not surprising in view of the lower calorific value of COB20 and COB50 biodiesel blends in comparison with that of baseline diesel, which is approximately 2.9% and 7.8%, respectively lower, as shown in Table 4.4. In addition, changes in injection timing can influence the BSFC profoundly. Advancing SOI timing from crank angle of 2ºATDC to -12ºATDC had caused the reduction in BSFC when

different fuels are tested. This is in accordance with results obtained by Badami et al. (Badami et al., 2002). According to Chen (Chen, 2000), by performing the first injection earlier, it is possible to reduce BSFC. The occurrence may be explained by the fact that at the moment SOI is carried out earlier, there is constant refinement in the effectiveness and quality of combustion. With the same magnitude of brake power output, the decreasing effect of BSFC implies that less fuel is supplied to enable a more effective combustion process to occur. Besides, for most of the SOI timings, the BSFC elevates with the larger dwell angles for all type of fuels. These outcomes are congruous with other researchers' observations (Badami, et al., 2002; Chen, 2000; d'Ambrosio & Ferrari, 2015; Qi, et al., 2011). At retarded SOI timing of second injection due to large dwell angle, turbulence effect will be low. The less enhance mixing of air and fuel will result in incomplete combustion where energy produced will be lower. Besides, at retarded crank angle, expansion cooling effect will take place and this will result in lower rate of combustion. Another reasonable explanation is that it is because of the longer combustion period which increased the amount of heat loss when dwell angle is increased. As a consequence, BSFC has to be greater to generate more useful work.

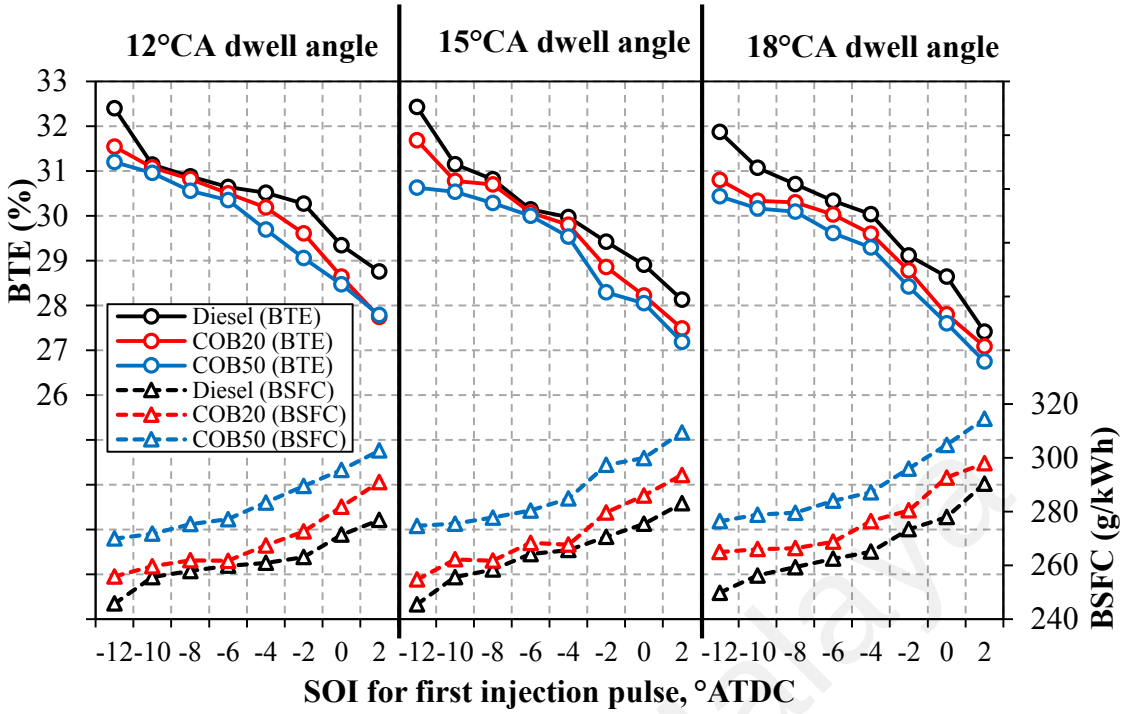

Figure 4.37: BTE and BSFC data for different types of fuel, SOI timings and dwell angles

4.8.2 Two-stage injection dwell angle variation on exhaust emissions

Impacts of percentage of biodiesel blends, SOI timing and dwell angle on NOx and smoke emissions are analyzed in this section. The NOx amount released when different test fuels are utilized at varying SOI timings and dwell angles is delineated in Figure 4.38. The graph shows that advancing SOI timing will give rise in NOx level for all test fuels and dwell angles. Research of Dhar and Agarwal (Dhar & Agarwal, 2015) also showed that NO_x level increases with advancing injection timing. The increasing pattern in NOx indicates that with SOI implemented earlier, the mixture of air and fuel can be ignited and burnt in advance, therefore causing early formation of pressure peak near TDC. This brings about a greater combustion temperature and aids in thermal or Zeldovich NOx formation. Moreover, according to Liu and Song (Liu & Song, 2016), when late second injection is carried out due to retarded SOI, the cylinder volume expansion and heat transfer will reduce the temperature, causing NO_x emission amount to decrease. The outcome also points out that both of the COB20 and COB50 biodiesel blends show a

tendency to reduce the NOx released across every SOI timing and dwell angle. Besides, the COB20 and COB50 biodiesel blends have a lower calorific value and greater cetane number in comparison with that of baseline diesel. As a consequence, lower HRR and PMGT will be developed during premix combustion stage. This finding can be explained by observing the PMGT data tabulated in Figure 4.40. Moreover, a considerably low level of NOx near 110 ppm is achievable via late SOI timing for fuel operations conducted using COB20 or COB50 biodiesel blends with dwell angle 18°CA. The increase in dwell angle causes slight decrease in NO_x emission for all fuels and SOI cases. The observation is compatible with the research results of B. Yang et al. (Yang et al., 2002), Liu and Song (Liu & Song, 2016), Dhar and Agarwal (Dhar & Agarwal, 2015), Chen (Chen, 2000) and Qi et al. (Qi, et al., 2011). With retarded injection, the combustion phase will occur late in the expansion stroke from TDC point. This phenomenon results in decreased temperature of combustion and less NOx formation. Besides, the concentration of oxygen is lower at retarded crank angle. Less oxygen atoms will be available to react with nitrogen atoms to form NO_x molecules. In addition, according to Pontoppidan et al. (Pontoppidan et al., 2002), the rise of temperature occurs with respect to single injection containing both first and second injection, which is higher, if the first injection is kept close to the second injection. However, if the second injection is performed further from first injection, the total duration for the whole process to occur will increase. The injected mass fraction during each injection will be reduced, leading to a leaner mixture burnt at a lower temperature. As a result, NO_x emission amount will decrease. According to Bianchi et al. (Bianchi et al., 2001), when dwell angle between two injections is reduced, the mass of fuel burnt at high temperature will increase, causing the NO_x emission amount to increase. Besides, smoke formation happens due to ineffective combustion of hydrocarbon and partial reaction of carbon content in diesel. The smoke amount released for test cases with different fuels at various SOI timings and dwell angles is displayed in

Figure 4.38. Overall, it can be observed that amount of smoke emitted is lower when COB20 or COB50 biodiesel blend is employed at different SOI timings. Zhang et al. (Zhang et al., 2013) and Shivakumar et al. (Shivakumar, et al., 2011) discovered that the amount of soot which leads to smoke of biodiesel is less than baseline diesel. According to Jeon and Park (Jeon & Park, 2015), even though soot particles are formed at high production rate when biodiesel is burnt, the soot is eliminated by the active oxidation process. Lower smoke level of combustion of biodiesel is attributable to the more oxygen and less carbon content and the non-existing or low quantity of aromatic compound in biodiesel (Canakci et al., 2006; Lapuerta et al., 2008a). Moreover, when SOI is retarded, the smoke emission amount is generally increases for all types of fuel across all dwell angles. This result is compatible with findings of Shivakumar et al. (Shivakumar, et al., 2011), Ganapathy et al. (Ganapathy, et al., 2011), Saravanan et al. (Saravanan et al., 2014) and Hashizume et al. (Hashizume et al., 1998). Advanced SOI timing will increase in-cylinder temperatures. This enhances the chemical reaction between fuel and oxygen, subsequently giving rise to less smoke emitted. A second possible reason is the fact that sufficient time will be available for the evaporation and mixing of fuel with air to happen, resulting in more effective mixing and combustion. In addition, when SOI of first injection is retarded, the injection is performed nearer to TDC where the piston wall is closer to the injector. The fuel injected can easily be impinged on the piston wall, causing the quenching of fuel by wall to occur (Pontoppidan, et al., 2002). This reduces the temperature of fuel and cause incomplete combustion. When SOI is advanced earlier than -2°ATDC onwards, the smoke emission amount exhibits a decreasing trend for most of the SOI and types of diesel when dwell angle is increased. The observation is in accordance with Park et al. (Park, et al., 2004), Hashizume et al. (Hashizume, et al., 1998) and Cung et al. (Cung, et al., 2015) research. When the dwell angle between two injections is small, the ignition delay for second injection will be short. The diesel injected

during second injection does not have enough time to mix with the air. Besides, the diesel will be injected directly at the flame produced via first injection. The combustion during first injection will be lack of oxygen because the diesel from second injection will entrain the burnt gas of first injection. This causes low HRR and temperature, resulting in large amount of smoke released. When injection strategies employing COB50 biodiesel blend and 18°CA dwell angle are conducted, smoke emission amount can be decreased while ensuring a reduction in NOx at the same time. The results indicate that retardation of SOI to achieve a low NO_x emission of 110 ppm can be achieved with smoke emission level still remains below 6%. Hence, simultaneous NOx and smoke amount decrement compared to that of petroleum diesel is viable with the application of COB50 biodiesel blend and implementation of retarded SOI timing and larger dwell angle of 18°CA in the test engine.

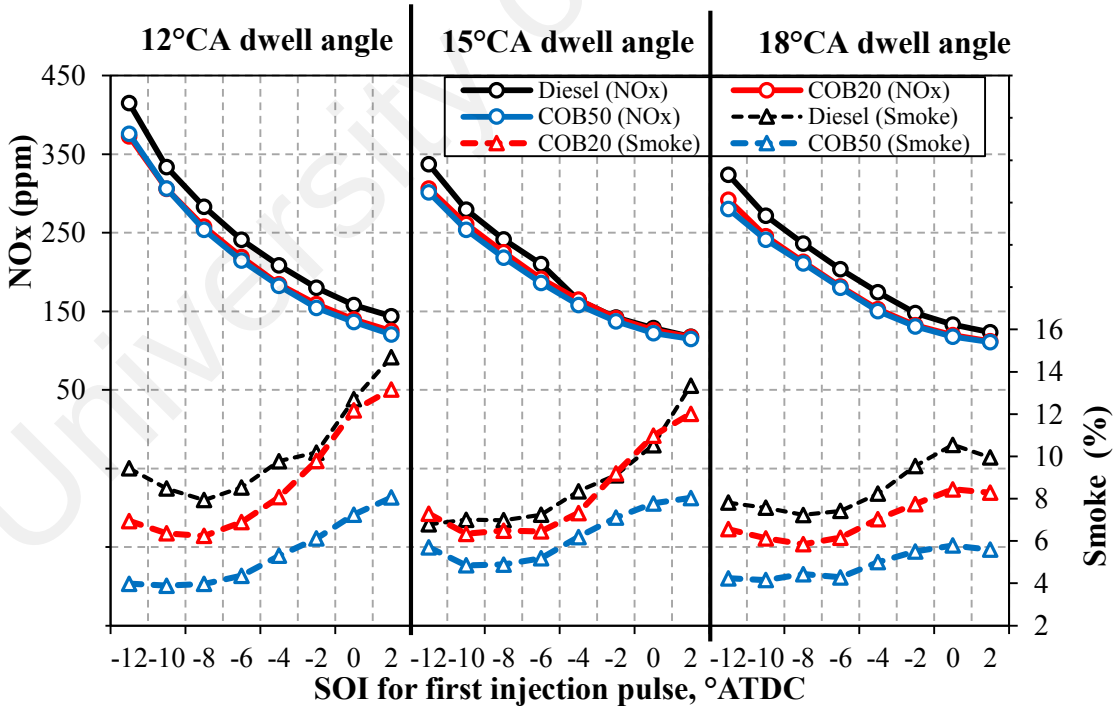

Figure 4.38: NOx and smoke emission for different types of fuel, SOI timings and dwell angles

4.8.3 Two-stage injection dwell angle variation on combustion process

Using pressure sensor, pressure developed in cylinder can be obtained and recorded for 100 successive cycles. The average value of pressure is calculated for each crank angle. Subsequently HRR can be evaluated from pressure data. Figure 4.39 depicts the combustion pressure curve, HRR curve and profile of injector current of test engine run using petroleum diesel at -6ºATDC SOI timing with varying dwell angles. It is clearly shown by the Figure 4.39 that each test case investigated involves two similar injection pulses. Due to longer combustion period, heat loss when longer dwell angle is applied is more and greater amount of fuel is injected to compensate the energy loss. This results in longer injection current and injector activation timing. It can be observed that difference in dwell angles affects the combustion characteristics. The pressure peak increases with increasing dwell angles. After the peak pressure occurs, the rate of decrease in pressure is higher with longer dwell angle, where the pressure when dwell angle is set as 12°CA is the highest after 15°ATDC. The SOC of all test cases conducted happen at the same crank angle. One of the factors which influence SOC timing is the quantity of fuel injected. If a large amount of fuel is introduced, a longer air fuel mixing time will be required and this will cause a retarded SOC timing. Since the amount of fuel injected are similar for every test case implemented, the SOC will occur at the same crank angle. Two noteworthy HRR peaks can be noticed for every dwell angle. First peaks of HRR of different test cases are formed at almost the same crank angle due to the equal amount of fuel injected at the same SOI timing. However, the second peaks of HRR were located at different crank angles when different dwell angles were applied. The shorter the dwell angles, the more advanced the second peak of HRR is. Ignition delay_1 is longer than ignition delay_2 when the dwell angle is set as 12ºCA and 15ºCA. This is due to the high cylinder temperature when second injection is performed. The injection of fuel towards main combustion zone which forms during the first injection causes the fuel to be burnt

immediately. Comparing ignition delay_2 of test cases with different dwell angle, it is observed that the greater the dwell angle, the longer the ignition delay_2. This is attributable to the lower cylinder temperature achieved after a greater dwell angle has passed. Larger heat loss and expansion cooling effect have taken place where low temperature will result in longer time required to heat up the fuel.

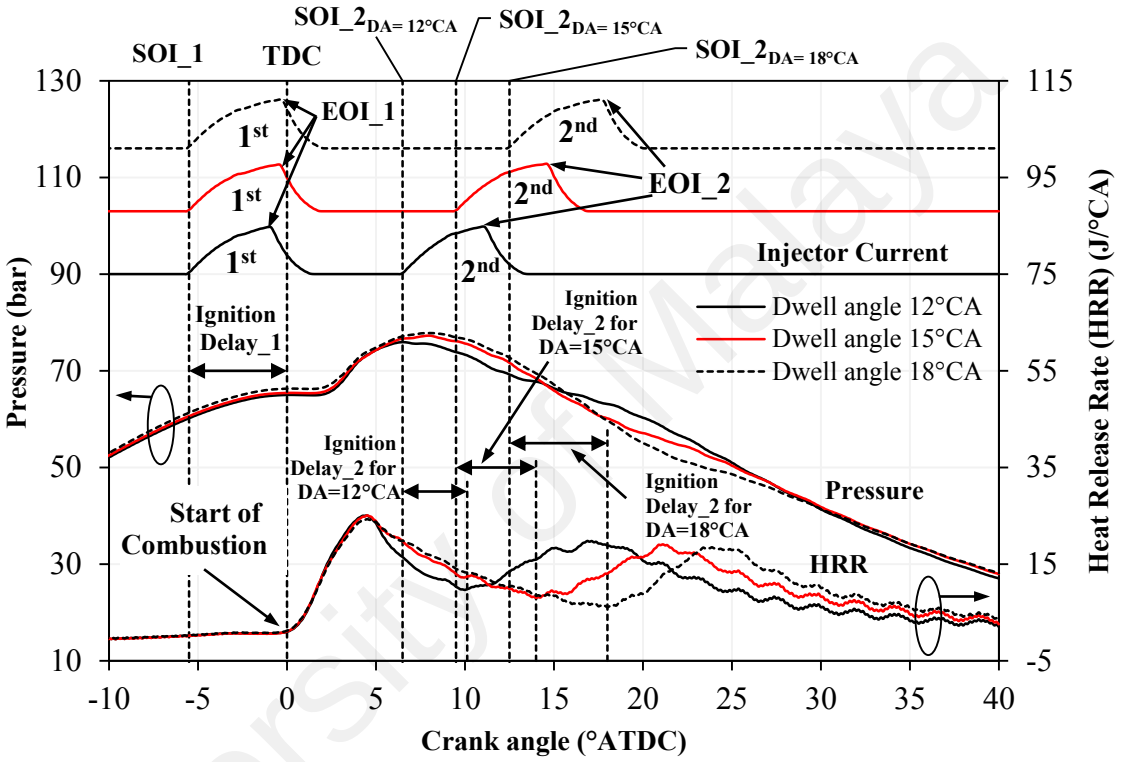

Figure 4.39: Combustion pressure, HRR and injector current data for test case employing baseline diesel with different dwell timings at -6°ATDC SOI.

Influences of percentage of biodiesel blend, SOI timing and dwell timing on PMGT and PHRR are examined in section below. Figure 4.40 shows the changes in PMGT with various SOI timings and dwell timings of test engine fuelled with baseline diesel, COB20 and COB50 biodiesel blends. There is no consistent trend observed with increasing percentage of biodiesel blends. However, the variation in SOI timings does give rise to considerably constant pattern. For every type of fuel and injection dwell angle tested, it is discovered that initially PMGT decreases with retarding SOI timing until a minimum PMGT value is reached around SOI timing of -6ºATDC. Then, with SOI performed later,

PMGT will rise. The initial decrement in PMGT value can be attributable to the lower peak pressure developed nearer to TDC when SOI timing is retarded based on Figure 4.41. Due to the low peak pressure, PMGT achieved will be lower. With retarding SOI timing from -12ºATDC to -6ºATDC, the peak pressure will occur at late crank angle and decrease on account of the cylinder expansion, causing a decrease in temperature. The elevation of PMGT with retarding SOI timing when SOI is perform late at the range of -6ºATDC to 2ºATDC can be explained by observing BSFC trend from Figure 4.37 and HRR curve from Figure 4.41. With late SOI timing, combustion will occur at crank angle when the volume of cylinder is large and rate of expansion is rapid. In order to develop pressure which is ample to produce enough effective work done to maintain equal power output, temperature achieved in cylinder has to be high. Combustion of larger amount of fuel is evident by observing Figure 4.37 where BSFC increases with retarding SOI timing. This will lead to a higher HRR peak as delineated in Figure 4.41, which subsequently result in higher PMGT. On the other hand, it can be seen that when dwell angle is fixed as 18ºCA, the PMGT values attained for most of the test cases associated are lower than their counterparts when dwell angle is 12ºCA or 15ºCA. This may indicate that longer dwell timing will cause a decrease in PMGT developed. The same observation is reported by Hashizume et al. (Hashizume, et al., 1998). When dwell timing is increased, combustion will continue for a longer duration. The fuel burnt per unit time will reduce, where the rate of rising of temperature will be lower. Expansion cooling effect further promotes the decrement in cylinder temperature. As a result, PMGT achieved will be lower. PHRR is also one of the noteworthy variables associated with combustion characteristics. From Figure 4.40, it is delineated that COB20 and COB50 biodiesel blends exhibit PHRR which is constantly less than that of pure diesel when different SOI timings and dwell angles are tested. The trend is observed by Yoon et al. (Yoon et al., 2009), Zhang et al. (Zhang, et al., 2013) and Ganapathy et al. (Ganapathy, et al., 2011) in

their studies. The trend occurs primarily owing to the greater cetane number of biodiesel in comparison with that of petroleum diesel, thus leading to shorter ignition delay and smaller PHRR. When SOI is retarded, PHRR during the premixed combustion phase increases when different types of fuel are used at any dwell angle. This observation is compatible with Park et al. (Park, et al., 2004) and Chen (Chen, 2000) findings where heat release increases when pilot injection is performed nearer to TDC. The combustion phase occurs at a more retarded crank angle which is further away from TDC when injection is performed at a later timing. The pressure produced will be lower due to cylinder volume expansion process. The useful work done on the piston will be lower. To compensate the decrease in work done, BSFC is increased where higher amount of fuel is injected according to Figure 4.37. As a result, the combustion will continue for a longer time where HRR can rise to a higher value before the fuel is burnt out. Also, it can be seen that PHRR increases slightly when dwell angle is increased from dwell angle 12°CA to 15°CA. This trend happens for most of the SOI applied. At dwell angle equal to 12°CA, the interval between two injections is too short (Park, et al., 2004). The second injection will be introduced to the flame produced by the combustion of first injection. The fuel injected during second injection will entrain the burnt gas, reducing the amount of oxygen required for combustion. As a result, PHRR achieved when dwell angle is fixed as 12°CA will be lower. When dwell angle is increased from 15°CA to 18°CA, PHRR decreases slightly at most of the SOI tested. Combustion duration increases with increasing dwell angle. Amount of fuel burnt per unit time will decrease, causing PHRR to drop.

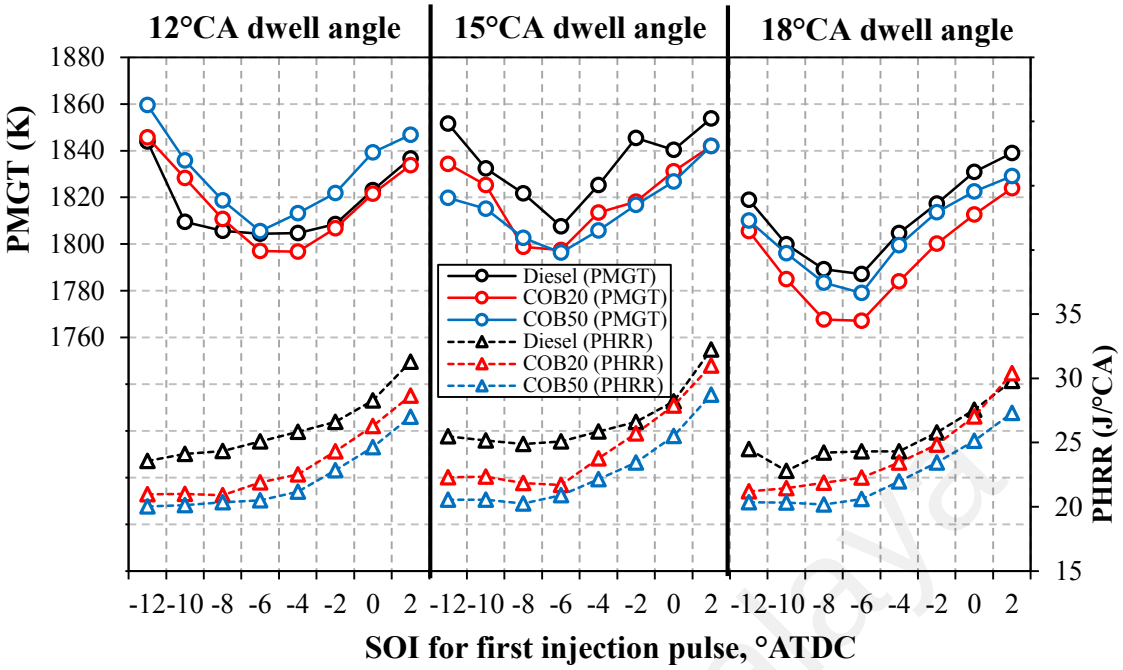

Figure 4.40: PMGT and PHRR for different fuels, SOI timings and dwell angles.

Dwell timing is one of the parameters which can be adjusted to improve the NO_x and smoke emission amount. Figure 4.41 displays the data of combustion pressure and HRR for dwell angles equal to 12°CA, 15°CA and 18°CA at different SOI timings when baseline diesel is utilized. The influences of dwell timing on in-cylinder pressure and HRR will be analyzed here by directly comparing outcomes of corresponding SOI timings under dwell angle subgroups. The comparison enables one to point out the differences in the combustion events that are responsible for results observed in NOx and smoke emissions. The HRR data collected signifies that the two combustion events begin to deviate as the first fuel injection pulse of double injection has been stopped after a premixed combustion of about the similar intensity, which can be evidently observed in Figure 4.39. Combustion process which occurs after the premixed combustion phase during the duration between SOI_1 and SOI_2 features a high initial in-cylinder temperature in virtue of the burning of a huge amount of fuel injected during the first injection. For this reason, the second injection fuel is combusted in form of diffusion flame. Only a very short ignition delay is available for the mixing process of fuel and hot

gases to transpire. The successive fuel injection leads to another lower HRR peak and rise in flame temperature, which happens for approximately 20° CA in combustion cycle. The occurrence enables lower quantity of NOx to be produced. Further optimization of multiple injection scheme in the context of NOx and smoke emissions amount can be achieved by employing a larger dwell angle.

From Figure 4.41, it is observed that peak pressure increases with advancing SOI when baseline diesel is used. This observation is obtained for different dwell angles. Dhar and Agarwal (Dhar & Agarwal, 2015), Ganapathy et al. (Ganapathy, et al., 2011), Jeon and Park (Jeon & Park, 2015) and Wei et al. (Wei, et al., 2017) discovered the same trend in their research. According to heat release rate curve, when SOI is advanced, the start of combustion will happen nearer to TDC. This will produce a higher pressure at TDC and create a larger useful work done. Retarding SOI will cause the combustion to occur at a later timing, where cylinder volume expansion happens. The peak pressure achieved will be lower and the useful work done will be reduced. Besides, when SOI is advanced, a longer ignition delay will be available before the pressure and temperature is high enough to initiate combustion (Mohamed Shameer, et al., 2017). The air fuel mixing time will be longer to enable a more complete combustion to occur and thus leads to a higher temperature and pressure. Advancing SOI will cause the peak pressure and PHRR to occur at an earlier crank angle (Wei, et al., 2017).

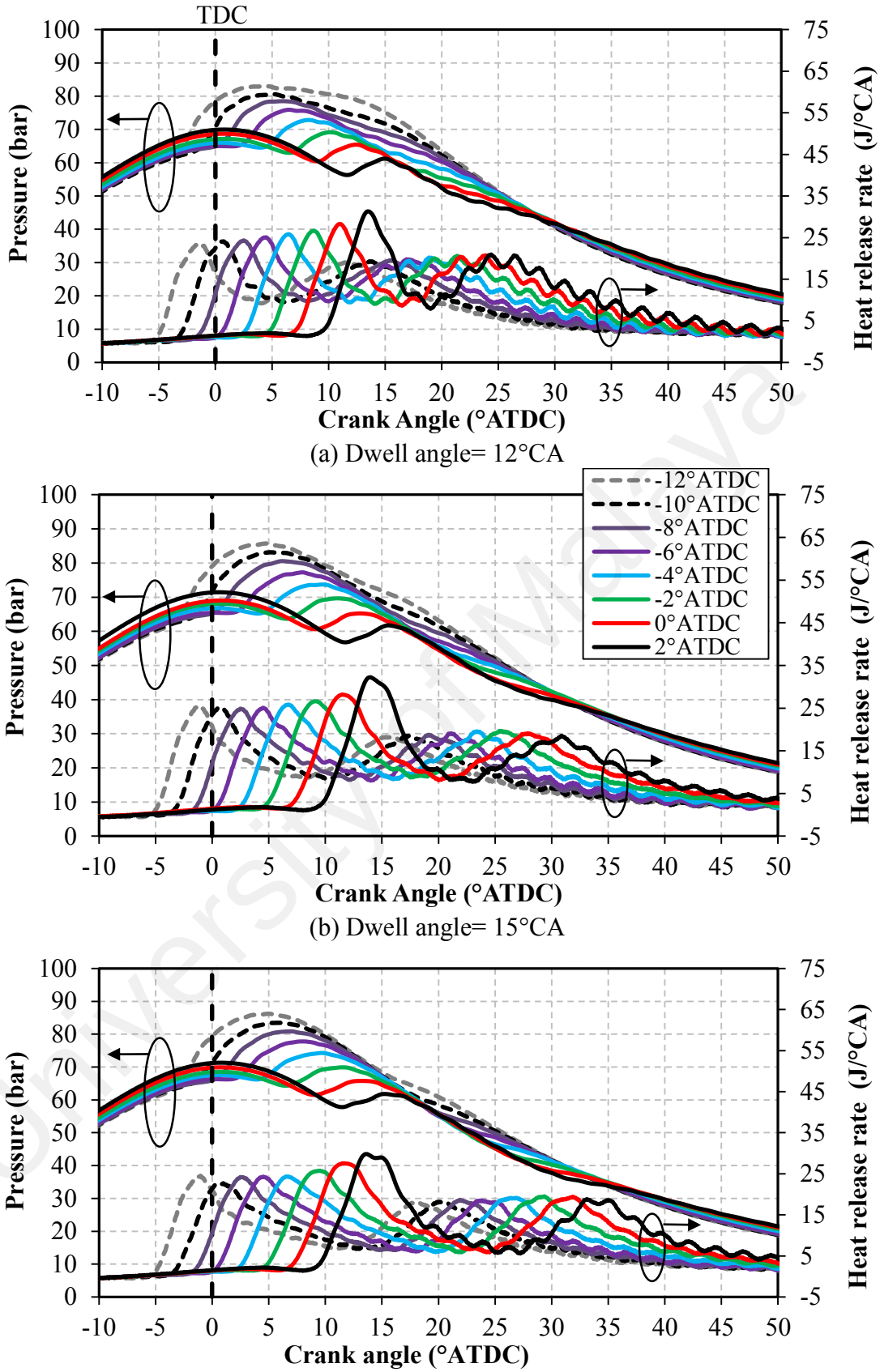

Figure 4.41: In-cylinder combustion pressure and HRR curves for dwell angle of a) 12°CA, b) 15°CA, and c) 18°CA under different SOI timings using baseline diesel.

Referring to Figure 4.42, when dwell angle is set as 12°CA and SOI is fixed as -6°ATDC, the start of combustion is advanced when the percentage of biodiesel blends increases. On dwell angle equal to 15°CA and 18°CA, the same trend is observed. The result is compatible with Zhang et al. (Zhang, et al., 2013), Ganapathy et al. (Ganapathy, et al., 2011) and Yoon et al. (Yoon, et al., 2009) research finding. This is because biodiesel has a higher cetane number, bulk modulus, sound velocity and viscosity (Alam et al., 2004; Lapuerta, et al., 2008a; Monyem et al., 2001; Szybist et al., 2005). Its ignition delay is shorter, causing it to burn earlier. However, PHRR decreases with increasing percentage of biodiesel blends (Yoon, et al., 2009). The ignition delay of biodiesel is shorter, resulting in less air fuel mixing time. The combustion of the biodiesel will be less intense compared to baseline diesel, thus producing a lower PHRR. Besides, the calorific value of biodiesel is less than baseline diesel (Zhang, et al., 2013). With same amount of fuel burnt, the heat released by biodiesel will be less. When PHRR is lower, the heat released will be lower. Thus, the peak pressure developed by burning biodiesel at any dwell angle will be smaller, as shown in Figure 4.42 (Yoon, et al., 2009). It is observed that the start of combustion of second injection is slightly advanced for baseline diesel compared to biodiesel even though the SOI of second injection is fixed at 6°ATDC when dwell angle is 12°CA. This can be due to the higher PHRR achieved during the first injection by using baseline diesel. The gas temperature after the combustion of the first injection of baseline diesel will be higher. This condition reduces the ignition delay of second injection, leading to an advanced start of combustion of baseline diesel.

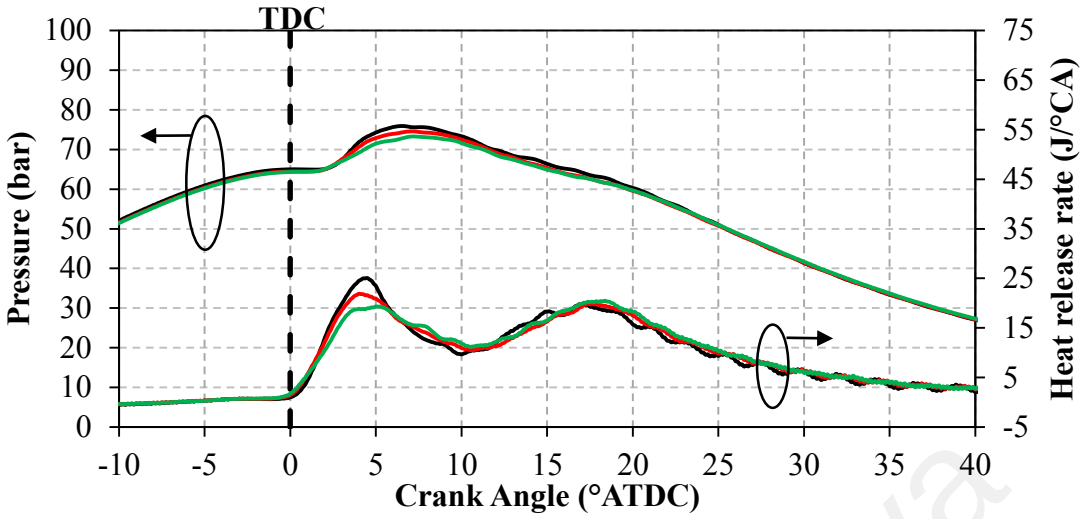

(a) Dwell angle= 12°CA

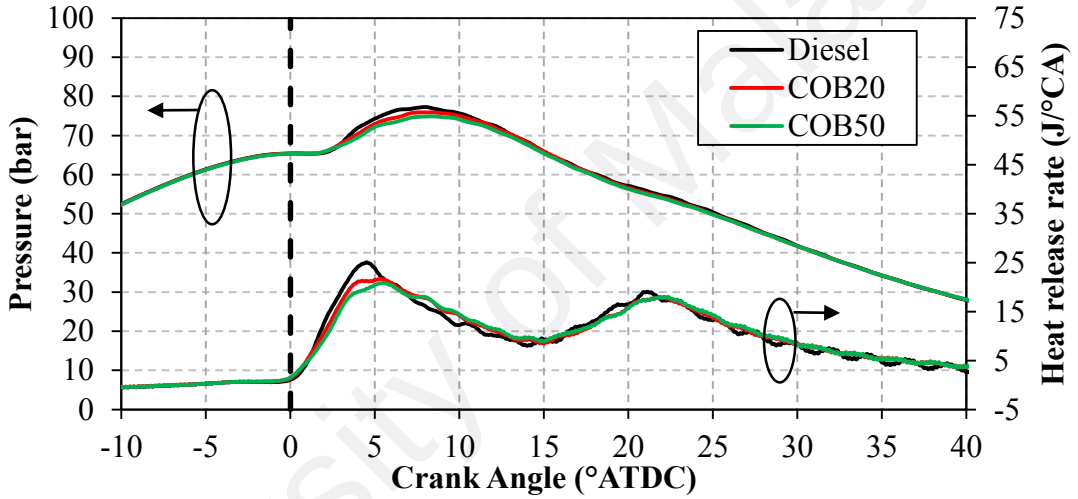

(b) Dwell angle= 15°CA

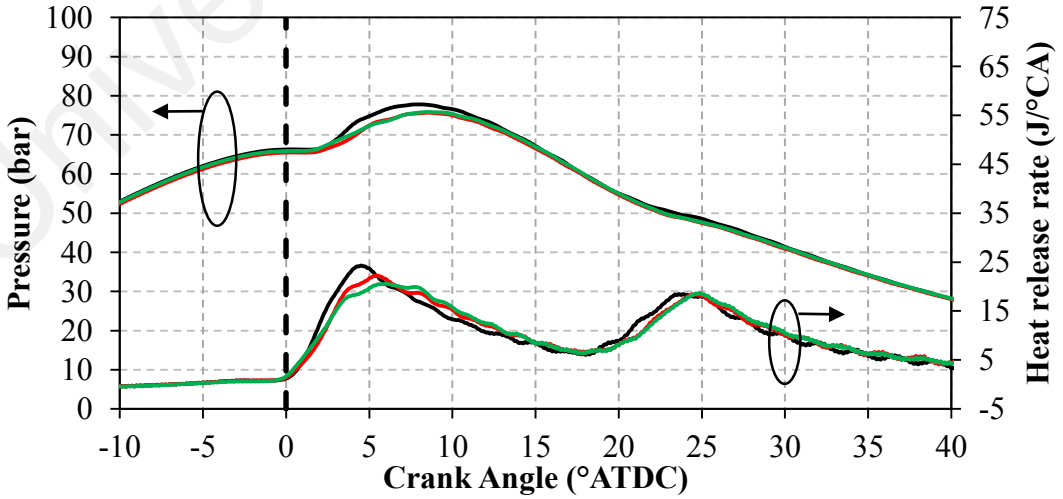

(c) Dwell angle= 18°CA

Figure 4.42: In-cylinder combustion pressure and HRR curves for dwell angle of a) 12°CA, b) 15°CA, and c) 18°CA using different types of fuel at SOI of -6°ATDC.

Referring to Figure 4.43, when baseline diesel is used at SOI equals -6°ATDC, the heat release rate when dwell angle is 12°CA drops at a higher rate after the first PHRR is reached compared to dwell angles 15°CA and 18°CA. This happens to COB20 and COB50 biodiesel as well. When a shorter dwell angle is used, the second injection will be introduced to the flame produced by the combustion of first injection. The gas temperature and the oxygen amount available for combustion will decrease due to the second injection diesel vaporization. As a result, the second injection which is close to the combustion of first injection will interrupt with the combustion and cause the rapid drop in heat release rate (Badami, et al., 2002). The earlier reduction in heat release rate will cause the peak pressure to decrease due to less energy produced near TDC. This explained the lower peak pressure achieved when shorter dwell angle is set. In addition, it is found that PHRR of second injection combustion is higher when dwell angle of 12°CA is applied compared to dwell angle of 15°CA and 18°CA. Smaller dwell angle will shorten the combustion duration, causing the same amount of fuel to be burnt at a shorter time interval, hence increasing HRR of second peak. When dwell angle increases, the second injection will be performed at a retarded timing further away from TDC. Expansion of cylinder volume will cause reduction in pressure and gas temperature, therefore lowering the rate of combustion of second injection diesel. Besides, a longer dwell angle will increase the heat loss during the entire period of combustion process (Dhar & Agarwal, 2015). Moreover, the direct comparison of various dwell angles under SOI timing of -6ºATDC also shows slight difference in the peak pressure and second PHRR. Combustion phasing is one of the factors which responsible for diesel engine smoke emissions. The diesel combustion with longer dwell angle can be performed to enable a longer ignition delay for better air fuel mixing. This enables a sufficient oxidation of air-fuel mixture can happen. The favorable impact of soot oxidation in the last combustion phase can be noticed when smoke emission becomes lower, as what is

displayed in Figure 4.38 when longer dwell angle of 18°CA is applied compared to dwell angle of 15°CA and 12°CA.

4.8.4 Summary

In this test series, the engine parameters such as types of fuel, SOI timing and dwell angle have been investigated. Different combinations of the parameters have been implemented to understand their impacts on the characteristics of combustion. Via this study, the optimum conditions when the pollutant emissions highlighted can be lessened simultaneously have been inferred. Conclusions about the optimized injection strategies are made as follow:

i. Types of fuel and SOI timing affect exhaust emissions, engine performance and combustion characteristics significantly while dwell angle causes a slight variation in the outcome studied.
ii. Increase in percentage of biodiesel blends causes reduction in NOx and smoke emission amount.
iii. Retarded SOI timing improve NOx emission but this occurs in the expense of increasing smoke emission.
iv. By retarding SOI timing in conjunction with long dwell angle, it is possible to reduce NOx emission without causing much increase in smoke emission.

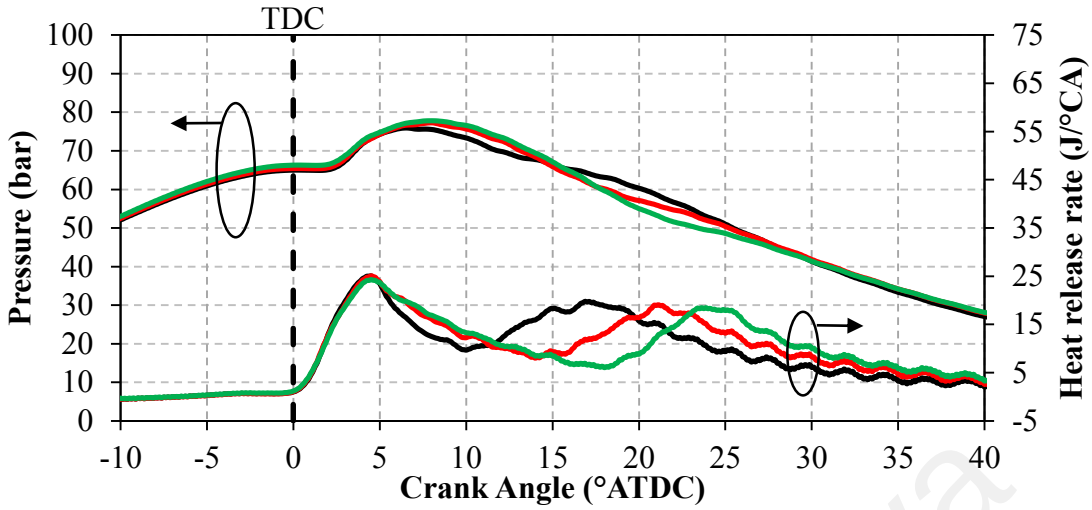

(a) Diesel

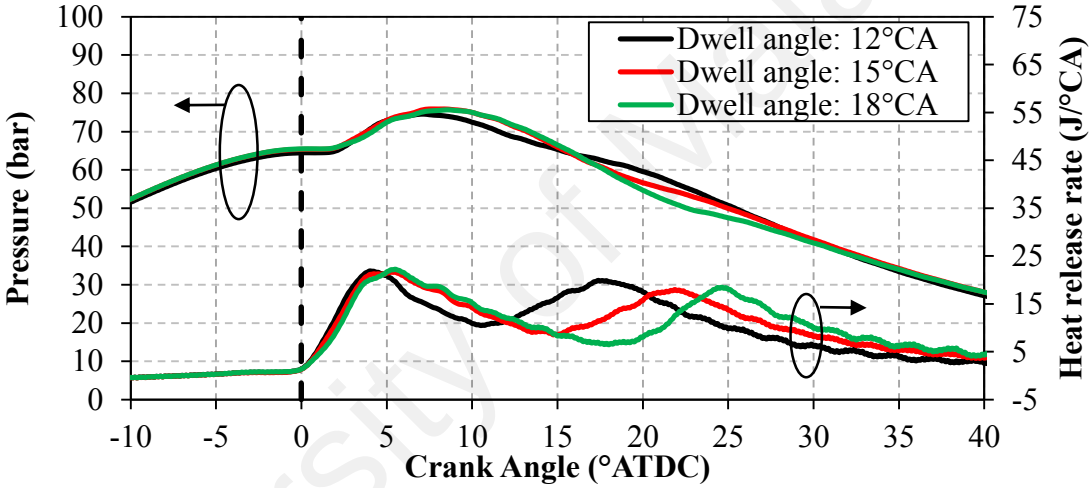

(b) COB20

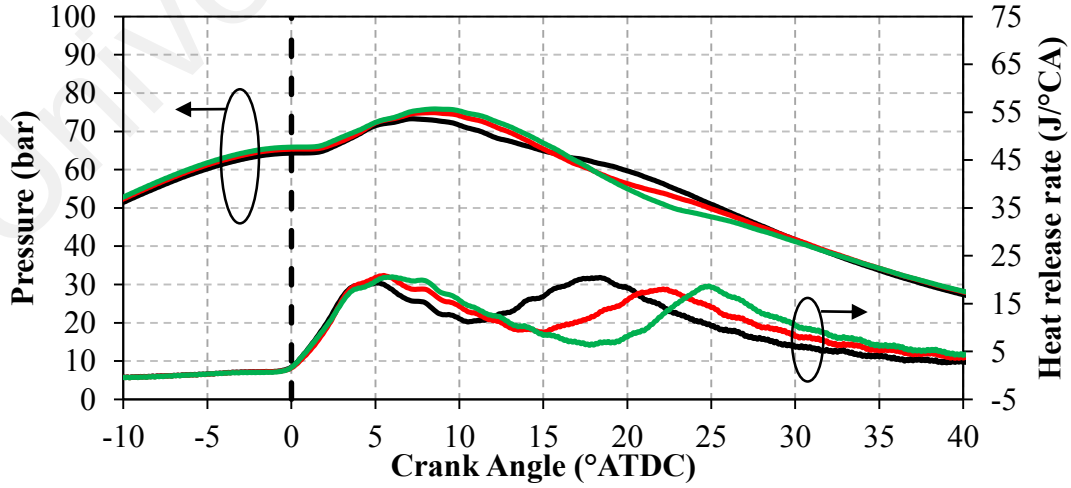

(c) COB50

Figure 4.43: In-cylinder combustion pressure and HRR curves using a) baseline diesel, b) COB20, and c) COB50 with different dwell angles at SOI of -6°ATDC.

4.9 Effect of two-stage injection fuel quantity on engine out-response

In this experiment test series, the effects of biodiesel blends, SOI timing and injection mass ratios on the engine performance, combustion characteristics and exhaust waste emission are investigated. Two-stage injection scheme for fuel of different biodiesel percentage is carried out where first and second injections were implemented with different SOI timings at various mass ratio. The tests were performed at constant speed of 2000 rpm and 60 Nm of torque operation with COB20 and COB50.

4.9.1 Two-stage injection fuel quantity variation on engine performance

Figure 4.44 represents the changes in BSFC and BTE with various kinds of fuel, SOI timings and injection mass ratios. It is observed that introduction of biodiesel into conventional diesel tend to reduce the BTE of the engine. This happens for all SOI timings and injection mass ratios tested. The phenomenon is similar to the observation reported by Chhabra et al. (Chhabra et al., 2017), where an increase in biodiesel blends causes a slight decrease in BTE. The cause of this outcome may be due to the lower calorific value of biodiesel. Biodiesel which contains higher oxygen content will exhibit a decrement in calorific value. Besides, the retardation of SOI timing causes decrease in BTE when different percentage of biodiesel blends are used under various injection mass ratio conditions. When injection mass ratio is set as 25:75, the peak pressure occurs almost exactly at TDC (refer to Figure 4.48). The pressure level is more symmetrical about TDC compared to other injection mass ratio strategies, where the comparably high pressure at compression stroke will cause inefficiency in producing useful work done. When SOI timing is retarded, peak pressure will increase. The rise of pressure will cause the pressure level to become more symmetrical about TDC, causing the BTE to reduce. On the other hand, even though BTE decreases with later SOI timing at injection mass ratio equaling 50:50 and 75:25, the factor of this declination is different. Besides, the pressure curve also reveal that decrement and retardation of peak pressure in expansion stroke will

happen when SOI timing is retarded. Peak pressure which happens later will have its magnitude reduced due to cylinder expansion. As a result the useful work done to the piston of cylinder will be lower. Consequently, BTE will decrease.

According to Figure 4.44, when the engine is operated at first SOI of -6°ATDC by using baseline diesel as fuel, it is observed that BTE increases with increasing mass ratio of first injection. First injection combustion phase is nearer to TDC compared to second injection combustion phase. The increase in mass of first injection will cause the peak pressure of first injection combustion phase to rise more sharply compared to the increase in peak pressure of second injection combustion phase when the mass of second injection is increased (Fang et al., 2012; Park, et al., 2011; Wei, et al., 2017). This phenomenon can be observed with the peak pressure formed due to combustion of first injection diesel increases with increasing mass ratio of first injection (refer to Figure 4.46). The combustion phase of second injection occurs at retarded timing where cool expansion effect takes place. The temperature, HRR and gas pressure are lower, causing the work done produced to be less. Hence, an increase in mass of later injection will cause the BTE to decrease (Mathivanan, et al., 2016). The decreasing trend gradient of BTE with retarding SOI timing becomes less steep when the mass ratio of first injection is increased. This indicates that the sensitivity of BTE towards the change in SOI timing decreases with rise in mass ratio of first injection. When mass ratio of injection is 25:75, the deterioration in BTE is due to the increase in peak pressure in compression stroke. At mass ratio equals 50:50 and 75:25, the reduction in BTE is due to the peak pressure which occurs further away from TDC. It can be seen that the effect of increasing peak pressure occurs at compression stroke is more significant than the effect of retardation of peak pressure, hence the sensitivity of BTE decreases with increasing first injection mass ratio.

According to Figure 4.44, the increase in percentage of biodiesel blend leads to the increase in BSFC across all SOI timing and injection mass ratio. The same result is discovered by Bhusnoor et al. (Bhusnoor et al., 2007) and Ozsezen and Canakci (Ozsezen & Canakci, 2011). The observation can be attributable to the decreasing BTE when biodiesel is utilized. With a lower BTE, more fuel has to be injected to maintain the engine speed at 2000 rpm under a load of 60 Nm, resulting in a higher BSFC. In addition, results shows that the BSFC increases with SOI carried out later, which is compatible with observation of Weall and Collings (Weall & Collings, 2007) and Zhu et al. (Zhu et al., 2003). The changes are again related to the decrease in BTE with retardation of SOI timings as explained before. Besides, it can be observed that the BSFC drops when the mass of first injection increases. This trend happens when engine is operated at different SOI by using different types of diesel. The decrease in amount of fuel needed to produce the same energy when the mass ratio of first injection increases can be associated to the increase in BTE. The peak pressure at TDC increases, causing the useful work done to rise. As a result, less fuel is needed to maintain the same engine rotational speed. It can be observed that the sensitivity of BSFC towards the retardation of SOI timing reduces with the increasing amount of first injection. This is also due to the reason as stated to explain the change in BTE. Rate of decrease in BTE declines with increasing first injection mass ratio. Thus, the rate of increase in fuel consumption will decrease when larger amount of fuel is injected firstly.

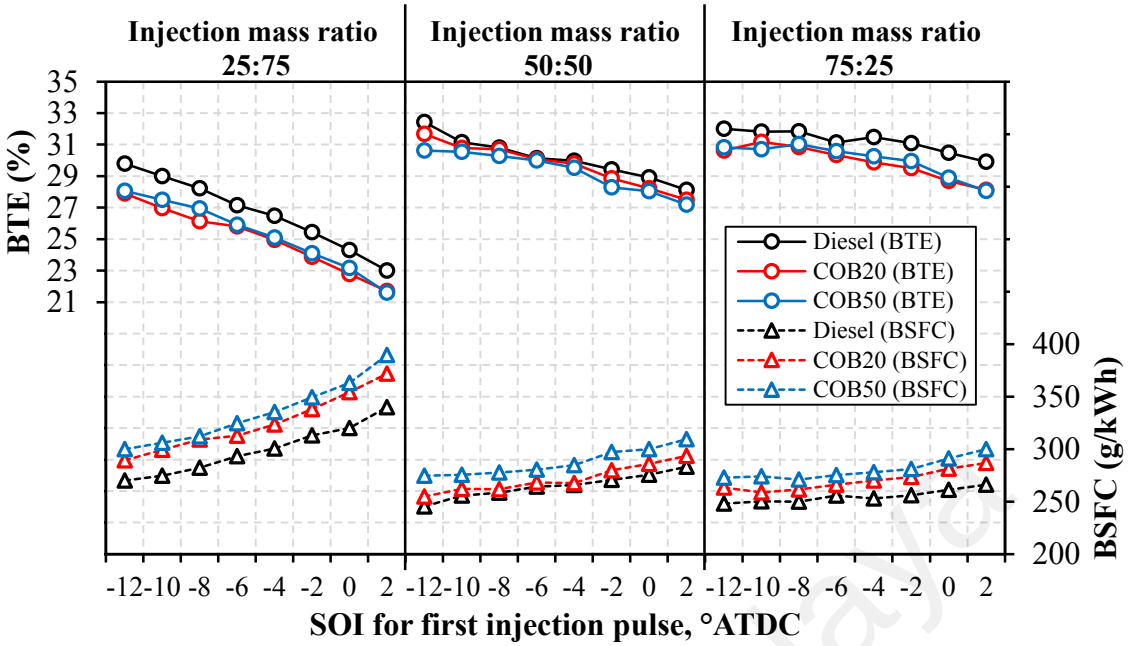

Figure 4.44: BSFC and BTE for different fuels, injection mass ratios and SOI timings

4.9.2 Two-stage injection fuel quantity variation on emissions

Effects of biodiesel blend ratios, first SOI timing and fuel injection mass ratio on NO_x and smoke emissions are examined in the section below. The NO_x amount emitted when different test fuels are used at varying SOI timings and fuel injection mass ratios is delineated in Figure 4.45. The graph indicates that retarding SOI timing will reduce in NO_x level for all test fuels and fuel injection mass ratio. By applying a late SOI timing, the research done by Weall and Collings (Weall & Collings, 2007) also yielded a lower NO_x emission level. The same observation is also reported by Han et al. (Han et al., 1996) and Gomes and Yates (Gomes & Yates, 1998). The decreasing pattern in NOx indicates that with SOI implemented later, the air-fuel mixture will ignite and burn later, therefore causing later formation of pressure peak near TDC. This lower the combustion temperature and avoids forming excessive NOx via thermal or Zeldovich mechanism. Another possible explanation is with retarded SOI, the cylinder volume expansion and heat transfer will reduce the temperature, causing NOx emission amount to decrease. Besides, for the corresponding SOI timing, the NOx result also reveals that both of the

COB20 and COB50 biodiesel blends does not alter much across all SOI timing and injection mass ratio compared to that of baseline diesel. Specifically, when injection mass ratio is fixed as 25:75, the increase in percentage of biodiesel blends does not significantly promote decrement in NO_x emission. In fact, at injection mass ratio equals 50:50 and 75:25, NO_x emission of biodiesel blended fuels is slightly lower than that of baseline diesel across all SOI timings. This may be due to the higher cetane number and lower calorific value of COB20 and COB50 fuel blends compared to that of conventional diesel. These combined effects caused a reduction in combustion temperature and HRR during premix combustion stage (refer to Figure 4.47), thus resulting in lower emission of NO_x. Moreover, a considerably lower level of NOx below 90 ppm is achievable via late SOI timing for fuel operations conducted using COB20 or COB50 biodiesel blends with injection mass ratio of 25:75. Besides, when SOI is fixed at -12°ATDC, it can be seen that NO_x rises sharply with increases first injection mass ratio. This phenomenon can be observed for all types of fuels and is compatible with the research done by Nehmer and Reitz (Nehmer & Reitz, 1994), which showed that higher fuel quantity of first injection could cause increment in NO_x emission. In addition, Wei et al. (Wei, et al., 2017) and Yang et al. (Yang, et al., 2002) also discovered that NO_x emission amount tend to elevate with greater quantity of pilot injection fuel. This occurrence may be explained by the fact that combustion of first injection fuel occurs near TDC where pressure and temperature is considerably high. Hence, the NO_x emission will elevate on this account. Moreover, the increment in first injection mass ratio will also cause more fuel to be combusted earlier in the cylinder and at high temperature environment, thus resulting in longer residence time and generate greater amount of NO_x. Another interesting trend is the strong correlations between NO_x emission and SOI timing variation can be observed with the rising in first injection mass ratio. This suggests that first injection fuel combustion is responsible for the main source of NO_x formation. With a large amount of fuel burnt

during first injection, advanced SOI timing will exaggerate the effect of NO_x formation. Meanwhile, retarded SOI timing will drastically inhibit NO_x production. On the other hand, with reduced first injection fuel fraction, the NO_x emission released during first combustion will be reduced and the effect of SOI timing retardation toward NO_x variation is less pronounced. This shows that two-stage injection with relatively small fraction of first injection fuel will enable stable combustion event and is an effective approach in reducing NOx emissions. Smoke formation can be related to incomplete combustion of hydrocarbon and partial reaction of carbon content in fuel. The smoke results for all test fuels under various SOI timings and injection mass ratios is displayed in Figure 4.45. Overall, it can be observed that amount of smoke emitted is lower when COB20 or COB50 biodiesel blend is employed across all SOI timings and injection mass ratios. This is in accordance with the research observation of Bhusnoor et al. (Bhusnoor, et al., 2007), Weall and Collings (Weall & Collings, 2007) and Mizushima et al. (Mizushima et al., 2013). According to Kawano et al. (Kawano et al., 2008), the PM and soot emission of biodiesel blends will be lower than that of pure diesel, thus producing a lower smoke intensity. By utilizing fuel with higher oxygen content, formation of polycyclic aromatic hydrocarbon (PAH) can be contained. Particle inception and coagulation will happen at a slower pace (Kitamura et al., 2002). Incomplete combustion in the local fuel-rich regions will be less likely to occur compared to that of petroleum diesel. As a result, the smoke emission will be diminished when biodiesel is used. The results also indicate that with advanced SOI timings, the smoke emissions were generally decreased for all injection mass ratio. This is due to when SOI timing is advanced, combustion gas temperature is higher, in which fuel oxidation will be improved. Another possible reason is the ample time for the fuel to vaporize and form mixture with air, thus permitting thorough mixing and complete combustion. Moreover, it can be seen that lowest smoke is emitted when injection mass ratio is 75:25. This is ascribed to the effective oxidation reaction which

occurs during the subsequent second injection fuel combustion after the main, thus able to maintain the smoke level well below 5% for all fuel types. The results exhibit some similarities with Mobasheri and Peng (Mobasheri & Peng, 2012) observation, where the smoke emission decreases with the increasing first main injection mass percentage from 65% to 80%. It is also noteworthy that when COB50 biodiesel blend and 25:75 injection mass ratio are tested, the smoke emission amount can be reduced while ensuring a reduction in NOx at the same instant. The results show that retardation of SOI to achieve a low NOx emission of 82 ppm can be achieved with smoke emission level still remains below 5%. Hence, simultaneous NOx and smoke amount reduction compared to that of fossil diesel is feasible with the application of COB50 biodiesel blend and execution of retarded SOI timing and injection mass ratio of 25:75.

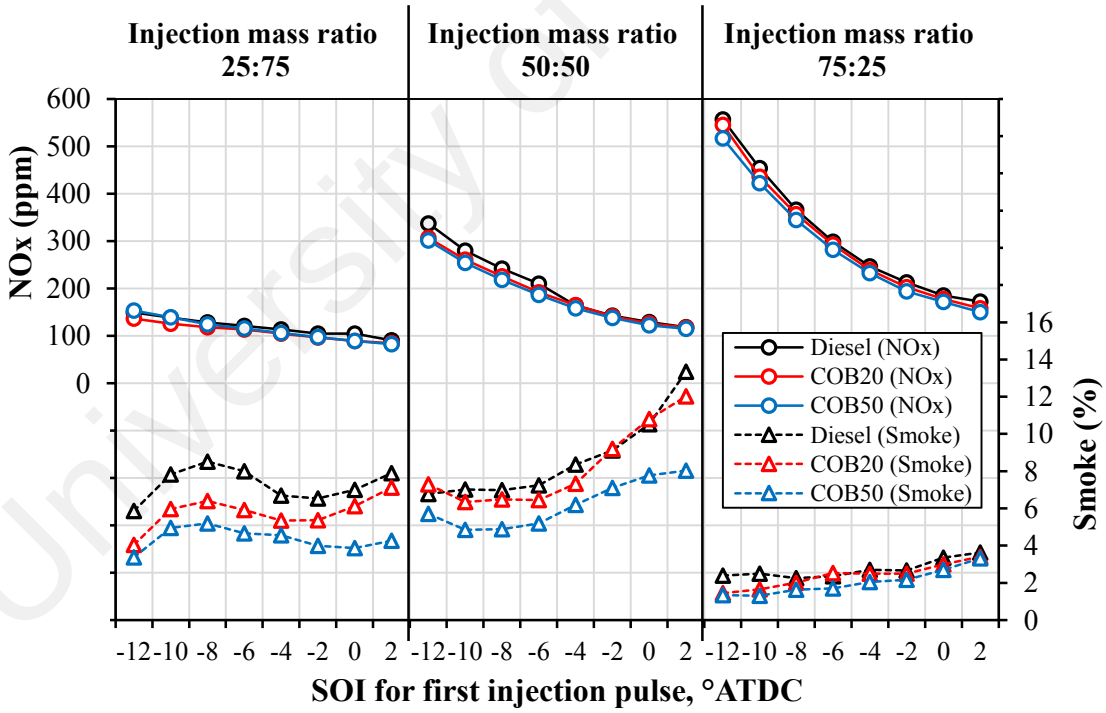

Figure 4.45: NO_x and smoke emissions for different fuels, injection mass ratios and first injection SOI timings.

4.9.3 Two-stage injection fuel quantity variation on combustion process

With the use of piezoelectric pressure sensor, the variation of in-cylinder pressure during combustion event can be precisely measured and recorded for 100 successive

cycles. The average value of pressure is processed for each crank angle. Meanwhile, HRR can be determined from pressure data. Figure 4.46 shows the combustion pressure curve, HRR curve and profile of injector current of test engine using petroleum diesel at SOI timing of -6ºATDC with varying injection mass ratios. Based on injection current profile, it can be seen that every test case investigated involves two consecutive injection pulses. Also, it can be seen that the first and second SOI timing remain constant when injection strategies of different mass ratios are compared. Due to the extended combustion period, heat losses when the approach of 25:75 injection mass ratio is applied is more significant, hence greater quantity of fuel need to be injected to compensate the energy loss. This causes in longer main injection opening timing to enable sufficient quantity of fuel to be injected into the engine. Besides, it can be observed that difference in injection mass ratio affects the combustion characteristics significantly. The pressure peak increases with increasing in mass ratio of first injection. After the peak pressure occurs, the combustion pressure decreasing rate (i.e. slope of the pressure curve) is more rapidly with larger mass ratio of first injection. The SOC of all test cases conducted happened at the difference crank angle. One of the factors which influence SOC timing is the quantity of fuel injected during first injection. If a large amount of fuel is introduced, a longer air fuel mixing time will be required and this will cause a retarded SOC timing. From the results, it can be seen that the occurring crank angle position for the SOC of first injected fuel, when 50:50 and 75:25 injection mass ratios are conducted, is shifted later by 1.375° CA and 1.5° CA respectively, in comparison with injection mass ratio of 25:75. Two noteworthy HRR peaks can be noticed for all injection mass ratios. First peaks of HRR of different test cases are formed at slightly different crank angle (within the range of 2°CA) due to the unequal quantity of fuel injected at the same SOI timing. However, the second peaks of HRR were shifted earlier by 4.75° CA and 16.875° CA for 50:50 and 75:25 injection mass ratio operation respectively, and gets lowered in comparison with the case of 25:75

injection mass ratio. This clearly shows that the decrement in the quantity of second injected fuel will cause an advance in second peaks of HRR timing. The main cause for the second HRR peak timing to occur early is the shorter ignition delay (i.e. ID_2) and subsequently leads to the earlier HRR rise. The parameter of ignition delay in a diesel engine is defined as the time interval between the SOI and the SOC. As can be seen, comparing ID_2 of test cases with different injection mass ratio, it is observed that the greater the fraction of second injected fuel, the longer the ID_2. This is attributable to the extension of air fuel mixing time and fuel vaporization of the fuel. Besides, the pre-injection of a small quantity of fuel as in 25:75 injection mass ratio operation permits stable main combustion as well as allows for extensive combustion phasing retard, which effectively lower the NOx emissions.

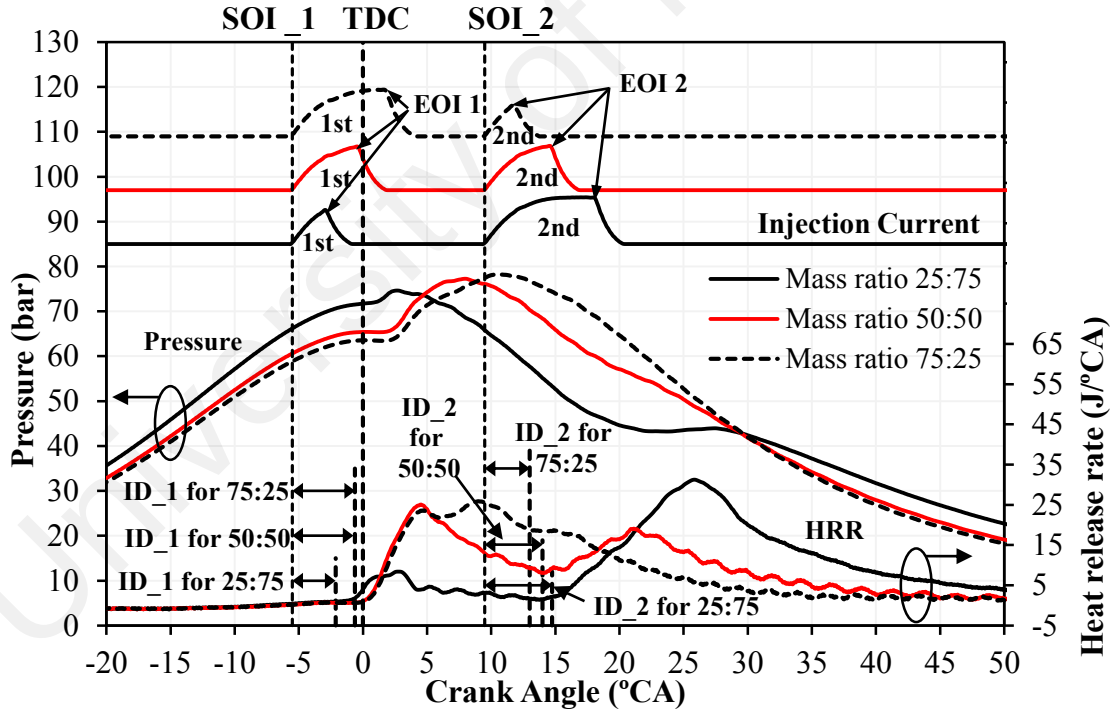

Figure 4.46: Combustion pressure, HRR and injector current profiles for baseline diesel with various injection mass ratios at SOI of -6°ATDC (Note that ID_1 and ID_2 represent ignition delay for first and second injected fuel, respectively)

Figure 4.47 shows the variation of PHRR and PMGT with different types of fuel and injection strategies. Generally, it can be noticed that for most of the SOI timings and injection mass ratios tested, PMGT of baseline diesel is higher than that of COB20 and

COB50. This phenomenon is aligned with Mizushima et al. (Mizushima, et al., 2013). This can be associated with the lower heating value of COB20 and COB50 fuels compared to that of baseline diesel. In addition, temperature developed through adiabatic flame is lower due to the disparity of carbon (C), hydrogen (H) and oxygen (O) ratio in the fuel. The lower hydrogen-carbon (HC) ratio in biodiesel may cause the combustion temperature to be lower. These factors will result in lower PMGT of COB20 and COB50 in comparison with the baseline diesel operation. Besides, different injection mass ratio strategies exhibit different trends of PMGT with the variation of SOI timings. When injection mass ratio of 25:75 is applied, a retarding SOI timing causes an increase in PMGT. This can be associated with the combustion phase of second injected fuel occurs at a more retarded crank angle which is further away from TDC in the expansion stroke when injection is performed at a later timing. The pressure produced will be lower due to cylinder volume expansion process. The useful work done on the piston will be lower. To compensate the decrease in work done, BSFC is increased where higher amount of fuel is injected (refer to Figure 4.44). As a result, the combustion of greater quantity of fuel will lead to a higher cylinder temperature. Besides, with injection mass ratio of 50:50 is applied, it is observed that initially PMGT dropped with retarding SOI timing until a minimum PMGT value is reached near SOI timing of -6ºATDC. Then, with SOI performed later, PMGT will increase. The initial decrement in PMGT can be attributable to the lower peak pressure developed nearer to TDC when SOI timing is retarded. Due to the low peak pressure, PMGT achieved will be lower. With retarding SOI timing from -12ºATDC to -6ºATDC, the peak pressure will occur at late crank angle and decrease on account of the cylinder expansion, causing a decrease in temperature. The elevation of PMGT with retarding SOI timing when SOI is perform late at the range of -6ºATDC to 2ºATDC can be explained by observing BSFC trend and HRR curve. With late SOI timing, combustion will occur at crank angle when the volume of cylinder is large and

rate of expansion is rapid. In order to develop pressure which is ample to produce enough effective work done to maintain equal power output, temperature achieved in cylinder has to be high. Combustion of larger amount of fuel is evident by observing the increasing effect of BSFC with retarding SOI timing. This will lead to a higher HRR peak, which subsequently result in higher PMGT. On the other hand, for the cases with injection mass ratio of 75:25, the PMGT values attained for most of the test cases are higher than their counterparts when injection mass ratio is 50:50. The incremental effect is due to the higher peak combustion pressure, which results in a higher PMGT. Another noteworthy combustion parameter is the PHRR. The significant influence of injection mass ratio on the combustion characteristics is also manifested in the trend of PHRR with change in SOI timings based on Figure 4.47. Injection mass ratio of 25:75 is applied with different types of fuel and various SOI timing. Initially, the PHRR increases with retarding SOI timing. This is attributable to the increasing fuel consumption when SOI is carried out late. More fuel will be combusted where the heat release rate will rise. However, after the SOI of -2ºATDC, PHRR begins to decrease. The decrement trend can be associated with the considerably late second combustion process of overly late second injected fuel (refer to Figure 4.48). When injection mass ratio of 50:50 is employed, PHRR will be located at the first peak of HRR curve. According to Figure 4.47, PHRR seems to rise steadily with SOI is perform at the range of -12ºATDC to 0ºATDC and increases exponentially afterward for all types of fuel. This is because retardation in SOI timing results in injection of larger quantity of first injected fuel as aforementioned. The combustion will yield higher PHRR.

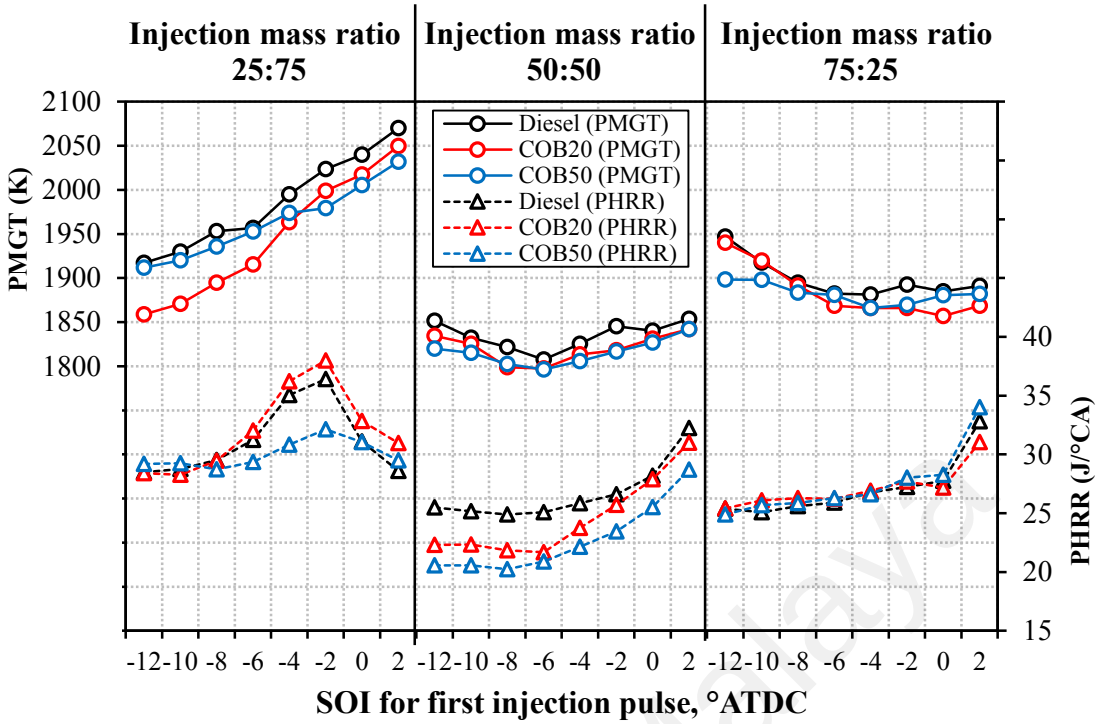

Figure 4.47: PHRR and PMGT for different fuels, injection mass ratios and SOI timings.

In this section, the traits of combustion pressure and HRR curves when different injection mass ratios and SOI timings are tested using baseline diesel will be highlighted and discussed. According to Figure 4.48, with injection mass ratio of 25:75, the peak pressure of every SOI timing occurs near TDC. The peak pressure seems to rise slightly from SOI timing -12ºATDC to 2ºATDC in general. The possible reason which leads to this condition is the late second injection timing, which causes the temperature to remain higher than that of earlier injection timing due to less heat loss within smaller crank angle between TDC and end of combustion. After passing TDC, it can be observed that pressure level drops and remains at a nearly constant value before decreases to a lower level. Crank angle recorded when the pressure level starts to remain constant for advance SOI timing is nearer to TDC and the temporarily fixed pressure level will be higher. The constant trend of pressure level happens by the reason of the second injection diesel combustion which increases the temperature in cylinder and prevents the drop in pressure. On account of the piston location near TDC, the magnitude of pressure when injection strategy with

advanced SOI timing is utilized will be higher. Regarding HRR curve, it is noticed that the combustion of second injected fuel produces a higher HRR peak compared to that of the first stage combustion. The phenomenon occurs by virtue of the larger fuel mass ratio of second injection. It is interesting to discover that the first combustion HRR peak produced, when SOI timing is equal to 0ºATDC or 2ºATDC, is much higher than those of advanced SOI timing cases. Earlier first injections are conducted near to the TDC at compression stroke, where the temperature and pressure elevates sharply with retarding crank angle. The high cylinder temperature will cause the ignition delay to decrease and results in lower HRR. When late injection is performed at SOI timing of 0ºATDC and 2ºATDC, cylinder temperature starts to reduce. The ignition delay will be longer where air fuel mixing can be implemented more completely. The combustion of refined mixture will bring about higher HRR. Focusing on second combustion HRR, it can be noticed that PHRR rises with retarded SOI timing from -12ºATDC to -2ºATDC before it start to decreases at SOI timing 0ºATDC and 2ºATDC. The increasing pattern occurs owing to the elevation of fuel consumption. When SOI timing is set as either 0ºATDC or 2ºATDC, first combustion can be carried out effectively, resulting in a higher cylinder temperature and shorter ignition delay of second combustion. Poor air fuel mixing transpires where the second combustion PHRR will be lower. Besides, due to cylinder volume expansion, the cylinder temperature will decrease sharply at retarded crank angle, further reduce the HRR. When injection mass ratio is set as 50:50 and 75:25, it can be seen that first injection diesel combustion generates peak pressure and PHRR. This is because of the position of piston which is nearer to TDC when first injection diesel combustion happens. Another interesting phenomenon is that with retarding SOI timing, the peak pressure and PHRR will shift and occur at a later timing. With a retarded SOI timing, the pressure peak which is formed due to the combustion of first injection diesel has its magnitude reduced (Gomes & Yates, 1998; Weall & Collings, 2007; Zhu, et al., 2003). Expansion of cylinder volume

and shorter ignition delay may be accountable for this phenomenon. SOI timing which is too advanced on the other hand causes a high peak pressure as the enhanced air fuel mixing enables great amount of fuel to be combusted at the same time (Bhusnoor, et al., 2007). Observing HRR curve, PHRR increases slightly with retarding SOI timing. A considerable rise in PHRR can be noticed when SOI timing is set as either 0ºATDC or 2ºATDC. This can be explained by applying the same reasons as provided in the discussion when injection mass ratio is set as 25:75. Unlike the case with injection mass ratio of 50:50, the HRR curve does not reveal two visible peaks when injection mass ratio of 75:25 is employed. In fact, the HRR curve of first combustion increases to a maximum value smoothly and decreases afterwards. The trend when injection mass ratio of 75:25 is applied can be ascribed to the first injection mass ratio which is too large. Besides, the direct comparison of 50:50 and 75:25 injection mass ratio with the same SOI reveals that the two combustion events resulting from these strategies differ only in the second half (as shown in Figure 4.46). This combustion phase is most responsible for overall smoke emissions. The fuel combustion of the small fraction of second injected fuel during cool piston expansion stroke can be utilized to achieve a better oxidation of the fuel-air mixture. This positive effect of the soot oxidation during the post stage of the combustion process can be noticed with the lower smoke emission level compared to the case with injection mass ratio of 50:50, as is reflected in Figure 4.45.

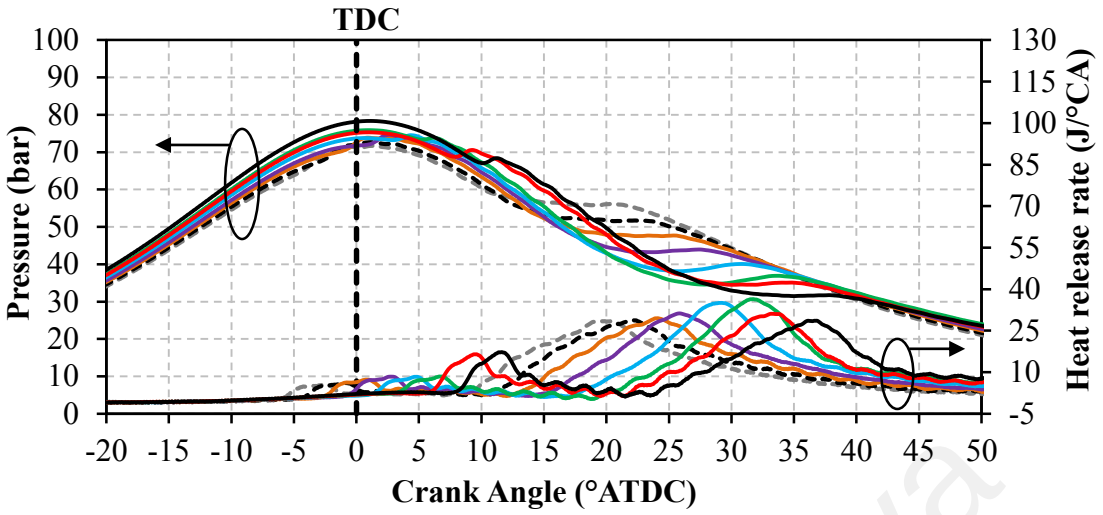

(a) Mass ratio = 25:75

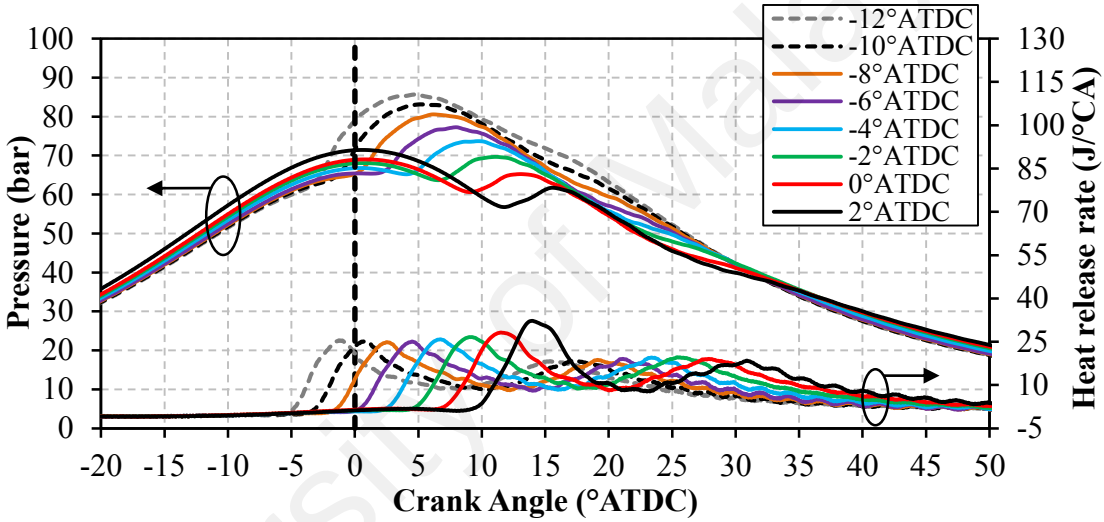

(b) Mass ratio = 50:50

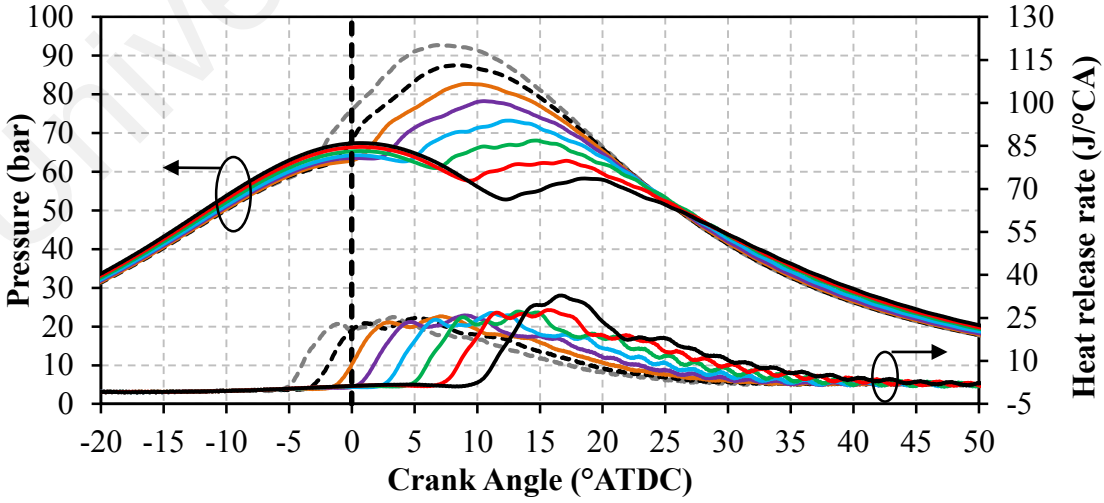

(c) Mass ratio = 75:25

Figure 4.48: HRR and combustion pressure curves for different injection mass ratios at different SOI timings and with baseline diesel.

Figure 4.49 shows the comparison of pressure and HRR results when different types of fuel are used. The comparison is implemented for all cases of injection mass ratio at constant SOI of -6ºATDC. Generally, it can be seen that the peak pressure developed is the highest when baseline diesel is used across all injection mass ratio. The trend is compatible with the study of Bhusnoor et al. (Bhusnoor, et al., 2007). This is because petroleum diesel has a higher calorific value compared to biodiesel. With the same fuel amount, the heat energy released to act on the piston is greater for petroleum diesel in comparison with that of biodiesel. Another possible reason is that biodiesel has poor volatility and high viscosity, causing ineffective atomization to happen during preparation of mixture. On the other hand, there are a few differences observed for HRR curve obtained under different injection mass ratio schemes. It is found that under injection mass ratio of 25:75, the first combustion HRR curves are almost the same magnitude for different fuel types. When 50:50 injection mass ratio is tested, HRR curve for first injected of baseline diesel fuel exhibits the highest peak. This is followed by COB20 and COB50 biodiesel in sequence due to their lower calorific values. The observation is compatible with Mizushima et al. (Mizushima, et al., 2013) results where pilot injection diesel combustion HRR is higher for ultra-low sulfur diesel. Besides, for HRR curve of 75:25 injection mass ratio scheme, the first appeared of peak HRR value at around 4.5°CA reduces with increasing percentage of biodiesel blend. After the first HRR local maximum, HRR curve rises to a higher HRR peak and it increases with increasing percentage of biodiesel blend. Also, the occurrence of peak values for baseline diesel, COB20 and COB50 biodiesel are located almost at the same timing. With a greater quantity of injected fuel, more time is needed for air to mix well with fuel, causing the lower HRR of baseline diesel as compared to that of biodiesel blend fuels. Unlike the COB20 and COB50 biodiesel blends, the oxygen content in the fuel will ensure a more complete combustion, consequently increasing PHRR as compared to that of baseline

diesel. Observing the start of combustion timing, it can be seen that the higher the percentage of biodiesel blends, the more advanced the timing for combustion to begin. Shelke et al. (Shelke et al., 2016), Szybist and Boehman (Szybist & Boehman, 2003) and Bittle et al. (Bittle et al., 2009) also reported the same results when comparing pure diesel with biodiesel blends. The phenomenon is due to the higher cetane number and shorter ignition delay of biodiesel as compared to that of baseline diesel.

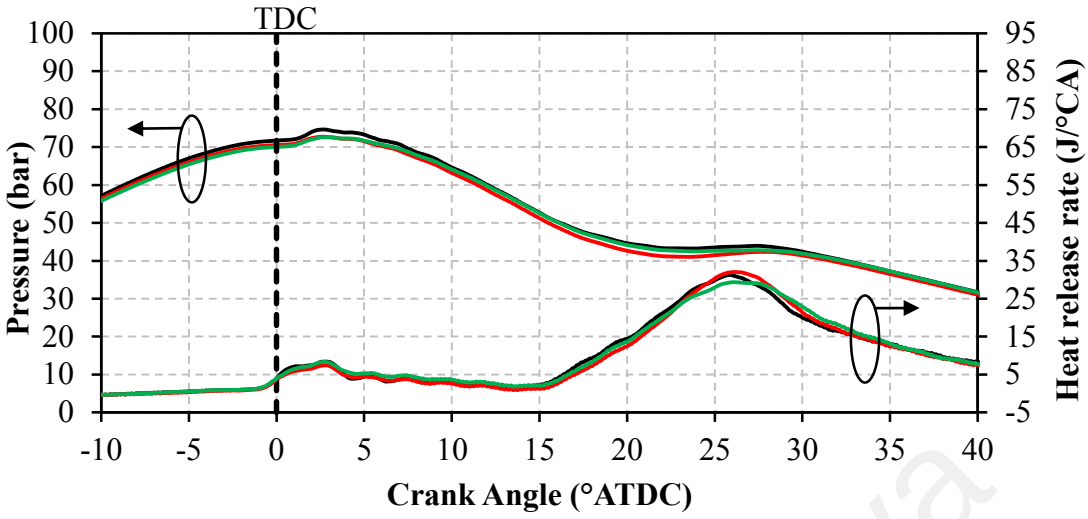

(a) Mass ratio = 25:75

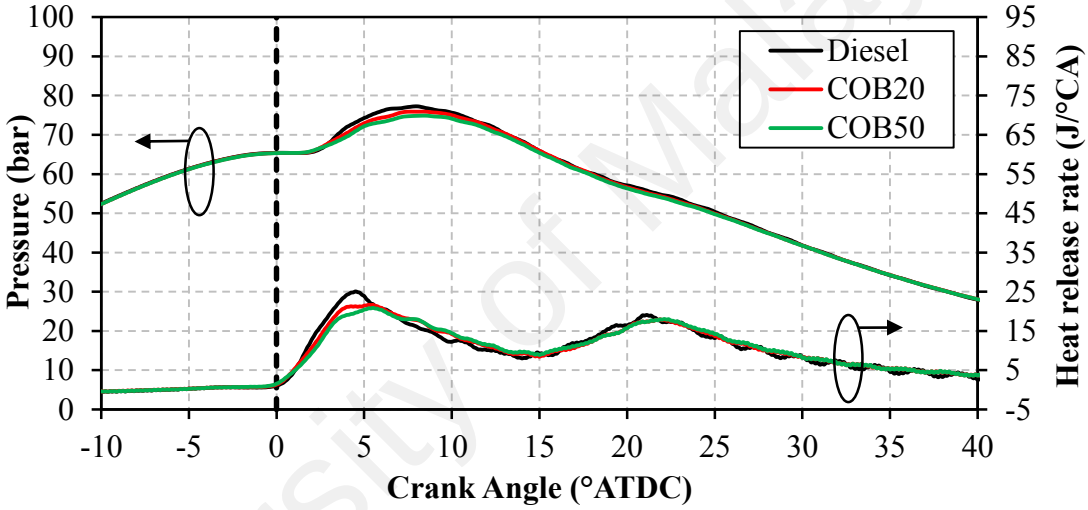

(b) Mass ratio = 50:50

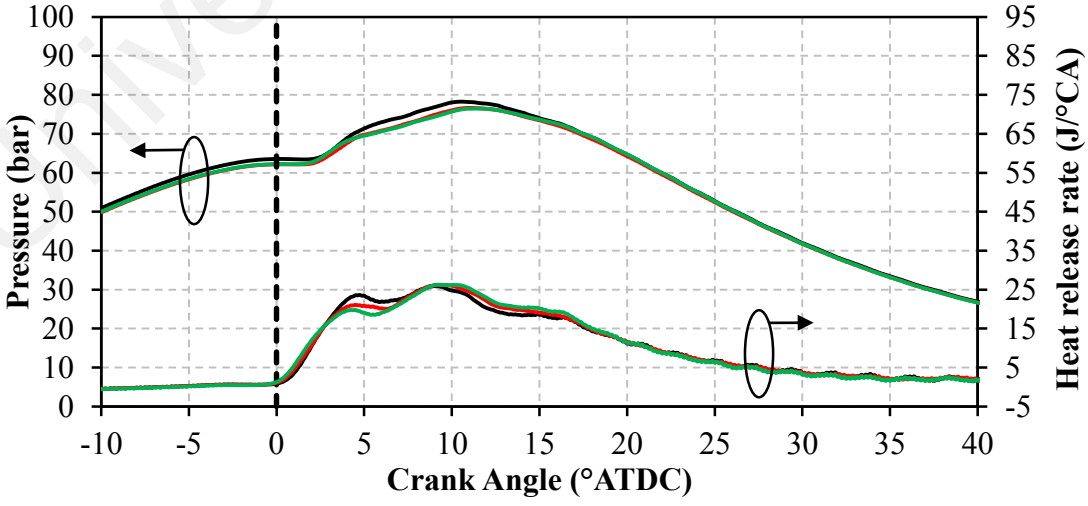

(c) Mass ratio = 75:25

Figure 4.49: HRR and combustion pressure curves for different injection mass ratios using different fuels at -6°ATDC SOI.

4.9.4 Summary

The main objective of this test series is to investigate the engine parameters such as types of fuel, SOI timing and injection mass ratio on engine out-responses. Different combinations of the parameters have been implemented to understand their impacts on the characteristics of combustion. Via this study, the optimum conditions when the pollutant emissions highlighted can be lessened simultaneously have been inferred. Based on the experimental results, the following are the inferences made from this test series:

i. To achieve maximum BTE, injection mass ratio of 75:25 should be conducted at advanced SOI timing using baseline diesel. Minimum BSFC can be yielded by applying the same injection strategies carried out to achieve maximum BTE.
ii. Lowest NOx emission level can be attained by carrying out injections at mass ratio of 25:75 with retarding SOI timing using COB50 biodiesel blend, but with some penalties in BTE.
iii. Smoke emission can be minimized by employing COB50 biodiesel blend and fixing injection mass ratio as 75:25 and with earlier SOI timing.
iv. Simultaneous NOx and smoke amount reduction compared to that of fossil diesel is feasible with the application of COB50 biodiesel blend and execution of retarded SOI timing and injection mass ratio of 25:75.
v. Two-stage fuel injection with different mass ratio is a practical strategies to simultaneously decrease NOx and smoke emissions when the SOI timing is fine-tuned and is an ideal alternative to operate with biodiesel fuel.

CHAPTER 5: CONCLUSIONS AND RECOMMENDATIONS

5.1 Conclusions

This dissertation was dedicated to evaluate the potential of biodiesel production from edible (coconut) and non-edible (*calophyllum inophyllum* and *moringa oleifera*) sources as a potential biodiesel feedstock. Besides, the use of COB blend fuels in engine operating with current and future combustion strategies is also successfully assessed through the present study.

The major conclusions on the basis of experimental results are as follows:

1. Biodiesel blends from different feedstock exhibited promising physicochemical properties as petroleum diesel.

2. (a) There are some penalties in engine brake power, BSFC, and NOx with the presence of biodiesel fuel in the blend. However, improvement in BTE, CO and smoke emissions has been observed in using biodiesel fuel blends across all engine speeds.

   (b) Reduction in peak combustion pressure and HRR has been observed for all biodiesel blends. Besides, COB blends exhibited the lowest CO emission while NOx emission of MOB blends is the lowest.

   (c) All biodiesel blends emitted lower level of PM than the baseline diesel.

   (d) Alternative fuels from COB, CIB and MOB exhibited high potential as substitution to petroleum based fuels in modern high-pressure common-rail diesel engine without modification.

3. (a) The effect of SOI timing variation and split injection scheme showed significant variation in engine emissions, performance and combustion characteristics for all fuels.

   (b) A considerably lower level of NOx, which is below 100 ppm has been reported by retarding SOI timing for COB20 and COB50 fuel operations and with triple injection scheme.

   (c) Simultaneous NOx and smoke emission decrement from the baseline levels of petroleum diesel fuel has been achieved by utilizing COB50 in conjunction with implementation of retarded SOI timing and employment of triple injection scheme in a diesel engine.

   (d) The results showed that multiple split injections is a practical strategies to simultaneously decrease NOx and smoke emissions when the SOI timing is fine-tuned and is an ideal alternative to operate with biodiesel fuel.

4. (a) Retardation of SOI timing along with long dwell angle showed reduction in NOx emission without causing much increase in smoke emission.

   (b) Maximum BTE has been observed with injection mass ratio of 75:25 at advanced SOI timing by using baseline diesel.

   (c) The lowest NOx emission level has been reported with the combination of injections mass ratio of 25:75 and retarded SOI timing using COB50 biodiesel blend, but with some penalties in BTE.

   (d) In addition, minimum smoke emission has been witnessed by employing COB50 biodiesel blend and fixing injection mass ratio as 75:25 and with earlier SOI timing.

(e) Simultaneous NOx and smoke amount reduction compared to that of fossil diesel is feasible with the application of COB50 biodiesel blend and execution of retarded SOI timing and injection mass ratio of 25:75.

5.2 Recommendations for future work

This research work has been carried out to produce biodiesel from multiple feedstocks and to assess their performance in a modern high-pressure common-rail diesel engine. Also, varies state-of-art of injection strategies have been tested with biodiesel-diesel blends in diesel engine. In this regard, the following recommendations for the future work are proposed:

i. A more extensive injection parameters (i.e. injection pressure and multiple injections with 3 pulses or above per combustion cycle) should be studied more deeply and optimized.
ii. Due to limited facility available of exhaust dilution tunnel, it is suggested that PM emissions analysis should be studied and compared under diluted exhaust gas conditions.
iii. More extensive in-cylinder engine flow and combustion modeling analysis using 2 or 3 dimensional Computational Fluid Dynamics (CFD) are necessary to predict the in-cylinder air and fuel mixing and to optimize the combustion process of the engine, especially for multiple injection strategies.

REFERENCES

Ackerman, A. S., Toon, O. B., Stevens, D. E., Heymsfield, A. J., Ramanathan, V., & Welton, E. J. (2000). Reduction of tropical cloudiness by soot. *Science, 288*(5468), 1042-1047.

Adams, C. A., Loeper, P., Krieger, R., Andrie, M. J., & Foster, D. E. (2013). Effects of biodiesel–gasoline blends on gasoline direct-injection compression ignition (GCI) combustion. *Fuel, 111*, 784-790.

Agarwal, A. K. (2007). Biofuels (alcohols and biodiesel) applications as fuels for internal combustion engines. *Progress in Energy and Combustion Science, 33*(3), 233-271.

Agarwal, A. K., Gupta, T., & Kothari, A. (2010). Toxic Potential Evaluation of Particulate Matter Emitted from a Constant Speed Compression Ignition Engine: A Comparison between Straight Vegetable Oil and Mineral Diesel. *Aerosol Science and Technology, 44*(9), 724-733.

Agarwal, A. K., Gupta, T., & Kothari, A. (2011). Particulate emissions from biodiesel vs diesel fuelled compression ignition engine. *Renewable and Sustainable Energy Reviews, 15*(6), 3278-3300.

Ahmad, A. L., Yasin, N. H. M., Derek, C. J. C., & Lim, J. K. (2011). Microalgae as a sustainable energy source for biodiesel production: A review. *Renewable and Sustainable Energy Reviews, 15*(1), 584-593.

Al-Dawody, M. F., & Bhatti, S. K. (2013). Optimization strategies to reduce the biodiesel NOx effect in diesel engine with experimental verification. *Energy Conversion and Management, 68*, 96-104.

Alam, M., Song, J., Acharya, R., Boehman, A., & Miller, K. (2004). *Combustion and Emissions Performance of Low Sulfur, Ultra Low Sulfur and Biodiesel Blends in a DI Diesel Engine*. http://dx.doi.org/10.4271/2004-01-3024

Altıparmak, D., Keskin, A., Koca, A., & Gürü, M. (2007). Alternative fuel properties of tall oil fatty acid methyl ester–diesel fuel blends. *Bioresource Technology, 98*(2), 241-246.

Ashok, B., Nanthagopal, K., & Sakthi Vignesh, D. (2017). Calophyllum inophyllum methyl ester biodiesel blend as an alternate fuel for diesel engine applications. *Alexandria Engineering Journal*.

Ashraful, A. M., Masjuki, H. H., & Kalam, M. A. (2015). Particulate matter, carbon emissions and elemental compositions from a diesel engine exhaust fuelled with diesel–biodiesel blends. *Atmospheric Environment, 120*, 463-474.

Atabani, A. E., Mahlia, T. M. I., Masjuki, H. H., Badruddin, I. A., Yussof, H. W., Chong, W. T., & Lee, K. T. (2013a). A comparative evaluation of physical and chemical properties of biodiesel synthesized from edible and non-edible oils and study on the effect of biodiesel blending. *Energy, 58*, 296-304.

Atabani, A. E., Silitonga, A. S., Badruddin, I. A., Mahlia, T. M. I., Masjuki, H. H., & Mekhilef, S. (2012). A comprehensive review on biodiesel as an alternative energy resource and its characteristics. *Renewable and Sustainable Energy Reviews, 16*(4), 2070-2093.

Atabani, A. E., Silitonga, A. S., Ong, H. C., Mahlia, T. M. I., Masjuki, H. H., Badruddin, I. A., & Fayaz, H. (2013b). Non-edible vegetable oils: A critical evaluation of oil extraction, fatty acid compositions, biodiesel production, characteristics, engine performance and emissions production. *Renewable and Sustainable Energy Reviews, 18*(Supplement C), 211-245.

Atabani, A. E., Silitonga, A. S., Ong, H. C., Mahlia, T. M. I., Masjuki, H. H., Badruddin, I. A., & Fayaz, H. (2013c). Non-edible vegetable oils: A critical evaluation of oil extraction, fatty acid compositions, biodiesel production, characteristics, engine performance and emissions production. *Renewable and Sustainable Energy Reviews, 18*(0), 211-245.

Atadashi, I. M., Aroua, M. K., Abdul Aziz, A. R., & Sulaiman, N. M. N. (2012). Production of biodiesel using high free fatty acid feedstocks. *Renewable and Sustainable Energy Reviews, 16*(5), 3275-3285.

Attfield, M. D., Schleiff, P. L., Lubin, J. H., Blair, A., Stewart, P. A., Vermeulen, R., . . . Silverman, D. T. (2012). The Diesel Exhaust in Miners Study: A Cohort Mortality Study With Emphasis on Lung Cancer. *JNCI: Journal of the National Cancer Institute, 104*(11), 869-883.

Badami, M., Mallamo, F., Millo, F., & Rossi, E. E. (2002). *Influence of Multiple Injection Strategies on Emissions, Combustion Noise and BSFC of a DI Common Rail Diesel Engine*. http://dx.doi.org/10.4271/2002-01-0503

Bakenhus, M., & Reitz, R. D. (1999). *Two-Color Combustion Visualization of Single and Split Injections in a Single-Cylinder Heavy-Duty D.I. Diesel Engine Using an Endoscope-Based Imaging System*. http://dx.doi.org/10.4271/1999-01-1112

Balat, M. (2011). Potential alternatives to edible oils for biodiesel production – A review of current work. *Energy Conversion and Management, 52*(2), 1479-1492.

Balat, M., & Balat, H. (2008). A critical review of bio-diesel as a vehicular fuel. *Energy Conversion and Management, 49*(10), 2727-2741.

Balat, M., & Balat, H. (2010). Progress in biodiesel processing. *Applied Energy, 87*(6), 1815-1835.

Bari, S., Yu, C. W., & Lim, T. H. (2004). Effect of Fuel injection timing with waste cooking oil as a fuel in a direct injection diesel engine. *Proceedings of the Institution of Mechanical Engineers, Part D: Journal of Automobile Engineering, 218*(1), 93-104.

Basinger, M., Reding, T., Rodriguez-Sanchez, F. S., Lackner, K. S., & Modi, V. (2010). Durability testing modified compression ignition engines fueled with straight plant oil. *Energy, 35*(8), 3204-3220.

Bergvall, C., & Westerholm, R. (2009). Determination of highly carcinogenic dibenzopyrene isomers in particulate emissions from two diesel- and two gasoline-fuelled light-duty vehicles. *Atmospheric Environment, 43*(25), 3883-3890.

Bernama. (2016). Implementation of 'Euro 5' emission standards on vehicles will benefit Malaysia, minister says. Retrieved 18th September 2017 http://www.themalaymailonline.com/malaysia/article/implementation-of-euro-5-emission-standards-on-vehicles-will-benefit-malays#IMH6yQRVyDUR7JAh.99

Bhusnoor, S. S., Babu, M. K. G., & Subrahmanyam, J. P. (2007). *Studies on Performance and Exhaust Emissions of a CI Engine Operating on Diesel and Diesel Biodiesel Blends at Different Injection Pressures and Injection Timings*. http://dx.doi.org/10.4271/2007-01-0613

Bianchi, G. M., Pelloni, P., Corcione, F. E., & Luppino, F. (2001). *Numerical Analysis of Passenger Car HSDI Diesel Engines with the 2nd Generation of Common Rail Injection Systems: The Effect of Multiple Injections on Emissions*. http://dx.doi.org/10.4271/2001-01-1068

Bittle, J. A., Knight, B. M., & Jacobs, T. J. (2009). The Impact of Biodiesel on Injection Timing and Pulsewidth in a Common-Rail Medium-Duty Diesel Engine. *SAE Int. J. Engines, 2*(2), 312-325.

Borrás, E., Tortajada-Genaro, L. A., Vázquez, M., & Zielinska, B. (2009). Polycyclic aromatic hydrocarbon exhaust emissions from different reformulated diesel fuels and engine operating conditions. *Atmospheric Environment, 43*(37), 5944-5952.

Bozbas, K. (2008). Biodiesel as an alternative motor fuel: Production and policies in the European Union. *Renewable and Sustainable Energy Reviews, 12*(2), 542-552.

British Petroleum (BP). (2017). BP Energy Outlook 2017 edition Retrieved 24th October, 2017, from https://www.bp.com/content/dam/bp/pdf/energy-economics/energy-outlook-2017/bp-energy-outlook-2017.pdf

Buono, D., Senatore, A., & Prati, M. V. (2012). Particulate filter behaviour of a Diesel engine fueled with biodiesel. *Applied Thermal Engineering, 49*(Supplement C), 147-153.

Busch, S., Zha, K., & Miles, P. C. (2015). Investigations of closely coupled pilot and main injections as a means to reduce combustion noise in a small-bore direct injection Diesel engine. *International Journal of Engine Research, 16*(1), 13-22.

Buyukkaya, E. (2010). Effects of biodiesel on a DI diesel engine performance, emission and combustion characteristics. *Fuel, 89*(10), 3099-3105.

Canakci, M. (2007a). Combustion characteristics of a turbocharged DI compression ignition engine fueled with petroleum diesel fuels and biodiesel. *Bioresource Technology, 98*(6), 1167-1175.

Canakci, M. (2007b). The potential of restaurant waste lipids as biodiesel feedstocks. *Bioresource technology, 98*(1), 183-190.

Canakci, M., Erdil, A., & Arcaklioğlu, E. (2006). Performance and exhaust emissions of a biodiesel engine. *Applied Energy, 83*(6), 594-605.

Cardone, M., Mazzoncini, M., Menini, S., Rocco, V., Senatore, A., Seggiani, M., & Vitolo, S. (2003). Brassica carinata as an alternative oil crop for the production of biodiesel in Italy: agronomic evaluation, fuel production by transesterification and characterization. *Biomass and Bioenergy, 25*(6), 623-636.

Caresana, F. (2011). Impact of biodiesel bulk modulus on injection pressure and injection timing. The effect of residual pressure. *Fuel, 90*(2), 477-485.

Carraretto, C., Macor, A., Mirandola, A., Stoppato, A., & Tonon, S. (2004). Biodiesel as alternative fuel: Experimental analysis and energetic evaluations. *Energy, 29*(12–15), 2195-2211.

Cha, J., Yang, S. Y., Naser, N., Ichim, A. I., & Chung, S. H. (2015). *High Pressure and Split Injection Strategies for Fuel Efficiency and Emissions in DI Diesel Engine*. https://doi.org/10.4271/2015-01-1823

Chang, T.-H., & Su, H.-M. (2010). The substitutive effect of biofuels on fossil fuels in the lower and higher crude oil price periods. *Energy, 35*(7), 2807-2813.

Chauhan, B. S., Kumar, N., & Cho, H. M. (2012). A study on the performance and emission of a diesel engine fueled with Jatropha biodiesel oil and its blends. *Energy, 37*(1), 616-622.

Chen, S. K. (2000). *Simultaneous Reduction of NOx and Particulate Emissions by Using Multiple Injections in a Small Diesel Engine*. http://dx.doi.org/10.4271/2000-01-3084

Chhabra, M., Sharma, A., & Dwivedi, G. (2017). Performance evaluation of diesel engine using rice bran biodiesel. *Egyptian Journal of Petroleum, 26*(2), 511-518.

Chisti, Y. (2007). Biodiesel from microalgae. *Biotechnology Advances, 25*(3), 294-306.

Chuepeng, S., Xu, H., Tsolakis, A., Wyszynski, M., & Price, P. (2011). Particulate Matter size distribution in the exhaust gas of a modern diesel Engine fuelled with a biodiesel blend. *Biomass and Bioenergy, 35*(10), 4280-4289.

Colton, B. (2014). The Outlook for Energy: A View to 2040 - ExxonMobil Retrieved 28th July, 2015, from http://cdn.exxonmobil.com/~/media/global/Reports/Outlook%20For%20Energy/2015/2015-Outlook-for-Energy_print-resolution

Coronado, C. R., de Carvalho Jr, J. A., & Silveira, J. L. (2009). Biodiesel CO2 emissions: A comparison with the main fuels in the Brazilian market. *Fuel Processing Technology, 90*(2), 204-211.

Corrêa, S. M., & Arbilla, G. (2006). Aromatic hydrocarbons emissions in diesel and biodiesel exhaust. *Atmospheric Environment, 40*(35), 6821-6826.

Cung, K., Moiz, A., Johnson, J., Lee, S.-Y., Kweon, C.-B., & Montanaro, A. (2015). Spray–combustion interaction mechanism of multiple-injection under diesel engine conditions. *Proceedings of the Combustion Institute, 35*(3), 3061-3068.

d'Ambrosio, S., & Ferrari, A. (2015). Potential of multiple injection strategies implementing the after shot and optimized with the design of experiments procedure to improve diesel engine emissions and performance. *Applied Energy, 155*, 933-946.

Delphi. (2017). Worldwide emissions standards. Passenger cars and light duty Retrieved 18th September, 2017, from https://www.delphi.com/docs/default-source/worldwide-emissions-standards/delphi-worldwide-emissions-standards-passenger-cars-light-duty-2016-7.pdf

Demirbas, A. (2005). Biodiesel production from vegetable oils via catalytic and non-catalytic supercritical methanol transesterification methods. *Progress in Energy and Combustion Science, 31*(5–6), 466-487.

Demirbas, A. (2007). Importance of biodiesel as transportation fuel. *Energy Policy, 35*(9), 4661-4670.

Demirbas, A. (2009). Progress and recent trends in biodiesel fuels. *Energy Conversion and Management, 50*(1), 14-34.

Demirbas, A. (2010). New Biorenewable Fuels from Vegetable Oils. *Energy Sources, Part A: Recovery, Utilization, and Environmental Effects, 32*(7), 628-636.

Devan, P. K., & Mahalakshmi, N. V. (2009). A study of the performance, emission and combustion characteristics of a compression ignition engine using methyl ester of paradise oil–eucalyptus oil blends. *Applied Energy, 86*(5), 675-680.

Dhar, A., & Agarwal, A. K. (2015). Experimental investigations of the effect of pilot injection on performance, emissions and combustion characteristics of Karanja biodiesel fuelled CRDI engine. *Energy Conversion and Management, 93*, 357-366.

DieselNet. (2017). European Union: emission standards – heavy-duty diesel truck and bus engines. Retrieved November 12 2017 https://www.dieselnet.com/standards/eu/hd.php

El Diwani, G., Attia, N. K., & Hawash, S. I. (2009). Development and evaluation of biodiesel fuel and by-products from jatropha oil. [journal article]. *International Journal of Environmental Science & Technology, 6*(2), 219-224.

Encinar, J., Gonzalez, J., Rodriguez, J., & Tejedor, A. (2002). Biodiesel fuels from vegetable oils: transesterification of Cynara c ardunculus L. oils with ethanol. *Energy & fuels, 16*(2), 443-450.

Fang, Q., Fang, J., Zhuang, J., & Huang, Z. (2012). Influences of pilot injection and exhaust gas recirculation (EGR) on combustion and emissions in a HCCI-DI combustion engine. *Applied Thermal Engineering, 48*, 97-104.

Fang, T., & Lee, C.-f. F. (2009). Bio-diesel effects on combustion processes in an HSDI diesel engine using advanced injection strategies. *Proceedings of the Combustion Institute, 32*(2), 2785-2792.

Fazal, M. A., Haseeb, A. S. M. A., & Masjuki, H. H. (2011). Biodiesel feasibility study: An evaluation of material compatibility; performance; emission and engine durability. *Renewable and Sustainable Energy Reviews, 15*(2), 1314-1324.

Fernanda Pimentel, M., Ribeiro, G. M. G. S., da Cruz, R. S., Stragevitch, L., Pacheco Filho, J. G. A., & Teixeira, L. S. G. (2006). Determination of biodiesel content when blended with mineral diesel fuel using infrared spectroscopy and multivariate calibration. *Microchemical Journal, 82*(2), 201-206.

Ganapathy, T., Gakkhar, R. P., & Murugesan, K. (2011). Influence of injection timing on performance, combustion and emission characteristics of Jatropha biodiesel engine. *Applied Energy, 88*(12), 4376-4386.

Ge, C. J., Kim, S. M., Yoon, K. S., & Choi, J. N. (2015). Effects of Pilot Injection Timing and EGR on Combustion, Performance and Exhaust Emissions in a Common Rail Diesel Engine Fueled with a Canola Oil Biodiesel-Diesel Blend. *Energies, 8*(7).

Gertler, A. W. (2005). Diesel vs. gasoline emissions: Does PM from diesel or gasoline vehicles dominate in the US? *Atmospheric Environment, 39*(13), 2349-2355.

Gnanasekaran, S., Saravanan, N., & Ilangkumaran, M. (2016). Influence of injection timing on performance, emission and combustion characteristics of a DI diesel engine running on fish oil biodiesel. *Energy, 116*, 1218-1229.

Gogoi, T. K., & Baruah, D. C. (2011). The use of Koroch seed oil methyl ester blends as fuel in a diesel engine. *Applied Energy, 88*(8), 2713-2725.

Gomes, P. C. d. F., & Yates, D. A. (1998). *Analysis of the Influence of Injection Timing on Diesel Combustion by the Two-Colour Method*. http://dx.doi.org/10.4271/982890

Graboski, M. S., & McCormick, R. L. (1998). Combustion of fat and vegetable oil derived fuels in diesel engines. *Progress in Energy and Combustion Science, 24*(2), 125-164.

Gumus, M. (2010). A comprehensive experimental investigation of combustion and heat release characteristics of a biodiesel (hazelnut kernel oil methyl ester) fueled direct injection compression ignition engine. *Fuel, 89*(10), 2802-2814.

Gumus, M., Sayin, C., & Canakci, M. (2012). The impact of fuel injection pressure on the exhaust emissions of a direct injection diesel engine fueled with biodiesel–diesel fuel blends. *Fuel, 95*(0), 486-494.

Haik, Y., Selim, M. Y. E., & Abdulrehman, T. (2011). Combustion of algae oil methyl ester in an indirect injection diesel engine. *Energy, 36*(3), 1827-1835.

Hampson, G. J., & Reitz, R. D. (1998). *Two-Color Imaging of In-Cylinder Soot Concentration and Temperature in a Heavy-Duty DI Diesel Engine with*

Comparison to Multidimensional Modeling for Single and Split Injections. http://dx.doi.org/10.4271/980524

Han, D., Duan, Y., Wang, C., Lin, H., Huang, Z., & Wooldridge, M. S. (2016). Experimental study of the two-stage injection process of fatty acid esters on a common rail injection system. *Fuel, 163*(Supplement C), 214-222.

Han, M., Cho, K., Sluder, C. S., & Wagner, R. M. (2008). *Soybean and Coconut Biodiesel Fuel Effects on Combustion Characteristics in a Light-Duty Diesel Engine*. http://dx.doi.org/10.4271/2008-01-2501

Han, Z., Uludogan, A., Hampson, G. J., & Reitz, R. D. (1996). *Mechanism of Soot and NOx Emission Reduction Using Multiple-injection in a Diesel Engine*. http://doi.org/10.4271/960633

Hashizume, T., Miyamoto, T., Hisashi, A., & Tsujimura, K. (1998). *Combustion and Emission Characteristics of Multiple Stage Diesel Combustion*. http://dx.doi.org/10.4271/980505

He, C., Ge, Y., Tan, J., You, K., Han, X., & Wang, J. (2010). Characteristics of polycyclic aromatic hydrocarbons emissions of diesel engine fueled with biodiesel and diesel. *Fuel, 89*(8), 2040-2046.

Herfatmanesh, M. R., Lu, P., Attar, M. A., & Zhao, H. (2013). Experimental investigation into the effects of two-stage injection on fuel injection quantity, combustion and emissions in a high-speed optical common rail diesel engine. *Fuel, 109*, 137-147.

Higgins, T. (2012). Biofuel Outlook. Retrieved from http://www.eia.gov/biofuels/workshop/pdf/terry_higgins.pdf

Hoekman, S. K., Broch, A., Robbins, C., Ceniceros, E., & Natarajan, M. (2012). Review of biodiesel composition, properties, and specifications. *Renewable and Sustainable Energy Reviews, 16*(1), 143-169.

How, H. G., Masjuki, H. H., Kalam, M. A., & Teoh, Y. H. (2014). An investigation of the engine performance, emissions and combustion characteristics of coconut biodiesel in a high-pressure common-rail diesel engine. *Energy, 69*, 749-759.

How, H. G., Teoh, Y. H., Masjuki, H. H., & Kalam, M. A. (2012). Impact of coconut oil blends on particulate-phase PAHs and regulated emissions from a light duty diesel engine. *Energy, 48*(1), 500-509.

Hwang, J., Qi, D., Jung, Y., & Bae, C. (2014). Effect of injection parameters on the combustion and emission characteristics in a common-rail direct injection diesel engine fueled with waste cooking oil biodiesel. *Renewable Energy, 63*(0), 9-17.

International Energy Agency (IEA). (2017). Southeast Asia Energy Outlook 2017 Retrieved 4th June, 2018, from https://www.iea.org/publications/freepublications/publication/WEO2017SpecialReport_SoutheastAsiaEnergyOutlook.pdf

Jain, S., & Sharma, M. P. (2010). Prospects of biodiesel from Jatropha in India: A review. *Renewable and Sustainable Energy Reviews, 14*(2), 763-771.

Jayed, M. H., Masjuki, H. H., Kalam, M. A., Mahlia, T. M. I., Husnawan, M., & Liaquat, A. M. (2011). Prospects of dedicated biodiesel engine vehicles in Malaysia and Indonesia. *Renewable and Sustainable Energy Reviews, 15*(1), 220-235.

Jeon, J., & Park, S. (2015). Effects of pilot injection strategies on the flame temperature and soot distributions in an optical CI engine fueled with biodiesel and conventional diesel. *Applied Energy, 160*, 581-591.

Jeon, J., Park, Y. H., Kwon, S. I., & Park, S. (2016). Effect of Pilot Injection Timings on the Combustion Temperature Distribution in a Single-Cylinder CI Engine Fueled with DME and ULSD. *Oil & Gas Science and Technology–Revue d'IFP Energies nouvelles, 71*(1), 15.

Juneja, H., Ra, Y., & Reitz, R. D. (2004). *Optimization of Injection Rate Shape Using Active Control of Fuel Injection*. http://dx.doi.org/10.4271/2004-01-0530

Kalam, M. A., Rashed, M. M., Imdadul, H. K., & Masjuki, H. H. (2016). Property development of fatty acid methyl ester from waste coconut oil as engine fuel. *Industrial Crops and Products, 87*, 333-339.

Kannan, D., Nabi, M. N., & Hustad, J. E. (2009). Influence of Ethanol Blend Addition on Compression Ignition Engine Performance and Emissions Operated with Diesel and Jatropha Methyl Ester. *SAE Technical Paper* 2009-2001-1808.

Kannan, G. R., Karvembu, R., & Anand, R. (2011). Effect of metal based additive on performance emission and combustion characteristics of diesel engine fuelled with biodiesel. *Applied Energy, 88*(11), 3694-3703.

Karavalakis, G., Bakeas, E., Fontaras, G., & Stournas, S. (2011a). Effect of biodiesel origin on regulated and particle-bound PAH (polycyclic aromatic hydrocarbon) emissions from a Euro 4 passenger car. *Energy, 36*(8), 5328-5337.

Karavalakis, G., Hilari, D., Givalou, L., Karonis, D., & Stournas, S. (2011b). Storage stability and ageing effect of biodiesel blends treated with different antioxidants. *Energy, 36*(1), 369-374.

Kawano, D., Ishii, H., & Goto, Y. (2008). *Effect of Biodiesel Blending on Emission Characteristics of Modern Diesel Engine*. http://dx.doi.org/10.4271/2008-01-2384

Khandal, S. V., Banapurmath, N. R., Gaitonde, V. N., & Hiremath, S. S. (2017). Paradigm shift from mechanical direct injection diesel engines to advanced injection strategies of diesel homogeneous charge compression ignition (HCCI) engines- A comprehensive review. *Renewable and Sustainable Energy Reviews, 70*, 369-384.

Kibazohi, O., & Sangwan, R. S. (2011). Vegetable oil production potential from Jatropha curcas, Croton megalocarpus, Aleurites moluccana, Moringa oleifera and Pachira glabra: Assessment of renewable energy resources for bio-energy production in Africa. *Biomass and Bioenergy, 35*(3), 1352-1356.

Kim, D., & Bae, C. (2017). Application of double-injection strategy on gasoline compression ignition engine under low load condition. *Fuel, 203*(Supplement C), 792-801.

Kinoshita, E., Myo, T., Hamasaki, K., Tajima, H., & Kun, Z. R. (2006). *Diesel Combustion Characteristics of Coconut Oil and Palm Oil Biodiesels*. http://dx.doi.org/10.4271/2006-01-3251

Kitamura, T., Ito, T., Senda, J., & Fujimoto, H. (2002). Mechanism of smokeless diesel combustion with oxygenated fuels based on the dependence of the equivalence ration and temperature on soot particle formation. *International Journal of Engine Research, 3*(4), 223-248.

Koh, M. Y., & Mohd. Ghazi, T. I. (2011). A review of biodiesel production from Jatropha curcas L. oil. *Renewable and Sustainable Energy Reviews, 15*(5), 2240-2251.

Kook, S., & Bae, C. (2004). *Combustion Control Using Two-Stage Diesel Fuel Injection in a Single-Cylinder PCCI Engine*. https://doi.org/10.4271/2004-01-0938

Kumar, K., & Sharma, M. (2016). Performance and emission characteristics of a diesel engine fuelled with biodiesel blends. *International Journal of Renewable Energy Research, 6*(2), 658-662.

Kusdiana, D., & Saka, S. (2001). Kinetics of transesterification in rapeseed oil to biodiesel fuel as treated in supercritical methanol. *Fuel, 80*(5), 693-698.

Lapuerta, M., Armas, O., & Rodríguez-Fernández, J. (2008a). Effect of biodiesel fuels on diesel engine emissions. *Progress in Energy and Combustion Science, 34*(2), 198-223.

Lapuerta, M., Herreros, J. M., Lyons, L. L., García-Contreras, R., & Briceño, Y. (2008b). Effect of the alcohol type used in the production of waste cooking oil biodiesel on diesel performance and emissions. *Fuel, 87*(15), 3161-3169.

Lapuerta, M., Rodríguez-Fernández, J., & Agudelo, J. R. (2008c). Diesel particulate emissions from used cooking oil biodiesel. *Bioresource Technology, 99*(4), 731-740.

Lea-Langton, A., Li, H., & Andrews, G. E. (2008). Comparison of Particulate PAH Emissions for Diesel, Biodiesel and Cooking Oil using a Heavy Duty DI Diesel Engine. *SAE Technical Paper* 2008-2001-1811.

Leung, D. Y. C., Wu, X., & Leung, M. K. H. (2010). A review on biodiesel production using catalyzed transesterification. *Applied Energy, 87*(4), 1083-1095.

Li, N., Hao, M., Phalen, R. F., Hinds, W. C., & Nel, A. E. (2003). Particulate air pollutants and asthma. A paradigm for the role of oxidative stress in PM-induced adverse health effects. *Clin Immunol, 109*(3), 250-265.

Liaquat, A. M., Masjuki, H. H., Kalam, M. A., Fattah, I. M. R., Hazrat, M. A., Varman, M., . . . Shahabuddin, M. (2013). Effect of Coconut Biodiesel Blended Fuels on

Engine Performance and Emission Characteristics. *Procedia Engineering, 56*, 583-590.

Lin, C.-Y., & Li, R.-J. (2009). Engine performance and emission characteristics of marine fish-oil biodiesel produced from the discarded parts of marine fish. *Fuel Processing Technology, 90*(7–8), 883-888.

Lin, L., Cunshan, Z., Vittayapadung, S., Xiangqian, S., & Mingdong, D. (2011a). Opportunities and challenges for biodiesel fuel. *Applied Energy, 88*(4), 1020-1031.

Lin, Y.-C., Hsu, K.-H., & Chen, C.-B. (2011b). Experimental investigation of the performance and emissions of a heavy-duty diesel engine fueled with waste cooking oil biodiesel/ultra-low sulfur diesel blends. *Energy, 36*(1), 241-248.

Lin, Y.-C., Lee, C.-F., & Fang, T. (2008). Characterization of particle size distribution from diesel engines fueled with palm-biodiesel blends and paraffinic fuel blends. *Atmospheric Environment, 42*(6), 1133-1143.

Lin, Y.-C., Lee, W.-J., & Hou, H.-C. (2006). PAH emissions and energy efficiency of palm-biodiesel blends fueled on diesel generator. *Atmospheric Environment, 40*(21), 3930-3940.

Liu, H., Ma, X., Li, B., Chen, L., Wang, Z., & Wang, J. (2017a). Combustion and emission characteristics of a direct injection diesel engine fueled with biodiesel and PODE/biodiesel fuel blends. *Fuel, 209*, 62-68.

Liu, W., & Song, C. (2016). Effect of post injection strategy on regulated exhaust emissions and particulate matter in a HSDI diesel engine. *Fuel, 185*, 1-9.

Liu, Y., Tu, Q., Knothe, G., & Lu, M. (2017b). Direct transesterification of spent coffee grounds for biodiesel production. *Fuel, 199*(Supplement C), 157-161.

Ma, F., & Hanna, M. A. (1999a). Biodiesel production: a review1. *Bioresource Technology, 70*(1), 1-15.

Ma, F., & Hanna, M. A. (1999b). Biodiesel production: a review1Journal Series #12109, Agricultural Research Division, Institute of Agriculture and Natural Resources, University of Nebraska–Lincoln.1. *Bioresource Technology, 70*(1), 1-15.

Macor, A., Avella, F., & Faedo, D. (2011). Effects of 30% v/v biodiesel/diesel fuel blend on regulated and unregulated pollutant emissions from diesel engines. *Applied Energy, 88*(12), 4989-5001.

Mahanta, P., & Shrivastava, A. (2004). Technology development of bio-diesel as an energy alternative. *Department of Mechanical Engineering Indian Institute of Technology*.

Mathivanan, K., Mallikarjuna, J. M., & Ramesh, A. (2016). Influence of multiple fuel injection strategies on performance and combustion characteristics of a diesel fuelled HCCI engine – An experimental investigation. *Experimental Thermal and Fluid Science, 77*, 337-346.

Misra, R. D., & Murthy, M. S. (2010). Straight vegetable oils usage in a compression ignition engine—A review. *Renewable and Sustainable Energy Reviews, 14*(9), 3005-3013.

Mittelbach, M. (1996). Diesel fuel derived from vegetable oils, VI: Specifications and quality control of biodiesel. *Bioresource Technology, 56*(1), 7-11.

Mizushima, N., Kawano, D., Ishii, H., Iwasa, K., Arai, H., & Ishii, D. (2013). *A Study on the Improvement of NOx Emission Performance in a Diesel Engine Fuelled with Biodiesel*. http://dx.doi.org/10.4271/2013-01-2677

Mobasheri, R., & Peng, Z. (2012). *Investigation of Pilot and Multiple Injection Parameters on Mixture Formation and Combustion Characteristics in a Heavy Duty DI-Diesel Engine*. http://dx.doi.org/10.4271/2012-01-0142

Mofijur, M., Masjuki, H. H., Kalam, M. A., Ashrafur Rahman, S. M., & Mahmudul, H. M. (2015). Energy scenario and biofuel policies and targets in ASEAN countries. *Renewable and Sustainable Energy Reviews, 46*, 51-61.

Mofijur, M., Masjuki, H. H., Kalam, M. A., Atabani, A. E., Fattah, I. M. R., & Mobarak, H. M. (2014). Comparative evaluation of performance and emission characteristics of Moringa oleifera and Palm oil based biodiesel in a diesel engine. *Industrial Crops and Products, 53*, 78-84.

Mohamed Shameer, P., Ramesh, K., Sakthivel, R., & Purnachandran, R. (2017). Effects of fuel injection parameters on emission characteristics of diesel engines operating on various biodiesel: A review. *Renewable and Sustainable Energy Reviews, 67*, 1267-1281.

Mohan, B., Yang, W., & Chou, S. k. (2013). Fuel injection strategies for performance improvement and emissions reduction in compression ignition engines—A review. *Renewable and Sustainable Energy Reviews, 28*, 664-676.

Monirul, I. M., Masjuki, H. H., Kalam, M. A., Mosarof, M. H., Zulkifli, N. W. M., Teoh, Y. H., & How, H. G. (2016). Assessment of performance, emission and combustion characteristics of palm, jatropha and Calophyllum inophyllum biodiesel blends. *Fuel, 181*, 985-995.

Montgomery, D. T., & Reitz, R. D. (1996). *Six-Mode Cycle Evaluation of the Effect of EGR and Multiple Injections on Particulate and NOx Emissions from a D.I. Diesel Engine*. http://dx.doi.org/10.4271/960316

Monyem, A., Gerpen, J. H. V., & Canakci, M. (2001). The Effect of Timing and Oxidation on Emissions from Biodiesel-Fueled Engines. *44*(1).

Mueller, C. J., Boehman, A. L., & Martin, G. C. (2009). An Experimental Investigation of the Origin of Increased NOx Emissions When Fueling a Heavy-Duty Compression-Ignition Engine with Soy Biodiesel. *SAE Technical Paper* 2009-2001-1792.

Murillo, S., Míguez, J. L., Porteiro, J., Granada, E., & Morán, J. C. (2007). Performance and exhaust emissions in the use of biodiesel in outboard diesel engines. *Fuel, 86*(12–13), 1765-1771.

Murugesan, A., Umarani, C., Chinnusamy, T. R., Krishnan, M., Subramanian, R., & Neduzchezhain, N. (2009a). Production and analysis of bio-diesel from non-edible oils—A review. *Renewable and Sustainable Energy Reviews, 13*(4), 825-834.

Murugesan, A., Umarani, C., Subramanian, R., & Nedunchezhian, N. (2009b). Bio-diesel as an alternative fuel for diesel engines—A review. *Renewable and Sustainable Energy Reviews, 13*(3), 653-662.

Nabi, M. N., Rahman, M. M., & Akhter, M. S. (2009). Biodiesel from cotton seed oil and its effect on engine performance and exhaust emissions. *Applied Thermal Engineering, 29*(11–12), 2265-2270.

Nehmer, D. A., & Reitz, R. D. (1994). *Measurement of the Effect of Injection Rate and Split Injections on Diesel Engine Soot and NOx Emissions*. http://dx.doi.org/10.4271/940668

Ng, J.-H., Ng, H. K., & Gan, S. (2011). Engine-out characterisation using speed–load mapping and reduced test cycle for a light-duty diesel engine fuelled with biodiesel blends. *Fuel, 90*(8), 2700-2709.

Nik Rosli, A., Rizalman, M., Miroslaw, L. W., Anthanasios, T., & Hongming, X. (2013). Effects of pilot injection timing and EGR on a modern V6 common rail direct injection diesel engine. *IOP Conference Series: Materials Science and Engineering, 50*(1), 012008.

No, S.-Y. (2011). Inedible vegetable oils and their derivatives for alternative diesel fuels in CI engines: A review. *Renewable and Sustainable Energy Reviews, 15*(1), 131-149.

OECD. (2011). OECD Environmental Outlook to 2050 Retrieved 29th July, 2015, from http://www.oecd.org/env/cc/49082173.pdf

Ong, H. C., Mahlia, T. M. I., Masjuki, H. H., & Norhasyima, R. S. (2011). Comparison of palm oil, Jatropha curcas and Calophyllum inophyllum for biodiesel: A review. *Renewable and Sustainable Energy Reviews, 15*(8), 3501-3515.

Ong, H. C., Masjuki, H. H., Mahlia, T. M. I., Silitonga, A. S., Chong, W. T., & Leong, K. Y. (2014). Optimization of biodiesel production and engine performance from high free fatty acid Calophyllum inophyllum oil in CI diesel engine. *Energy Conversion and Management, 81*, 30-40.

Ouenou-Gamo, S., Ouladsine, M., & Rachid, A. (1998). Measurement and prediction of diesel engine exhaust emissions. *ISA Transactions, 37*(3), 135-140.

Owen, N. A., Inderwildi, O. R., & King, D. A. (2010). The status of conventional world oil reserves—Hype or cause for concern? *Energy Policy, 38*(8), 4743-4749.

Ozawa, Y., Soma, Y., Shoji, H., Iijima, A., & Yoshida, K. (2011). The Application of Coconut Oil Methyl Ester for Diesel Engine. *International Journal of Automotive Engineering, 2*, 95-100.

Özener, O., Yüksek, L., Ergenç, A. T., & Özkan, M. (2014). Effects of soybean biodiesel on a DI diesel engine performance, emission and combustion characteristics. *Fuel, 115*(0), 875-883.

Ozsezen, A. N., & Canakci, M. (2011). Determination of performance and combustion characteristics of a diesel engine fueled with canola and waste palm oil methyl esters. *Energy Conversion and Management, 52*(1), 108-116.

Pal, A., Verma, A., Kachhwaha, S. S., & Maji, S. (2010). Biodiesel production through hydrodynamic cavitation and performance testing. *Renewable Energy, 35*(3), 619-624.

Palash, S. M., Kalam, M. A., Masjuki, H. H., Masum, B. M., Rizwanul Fattah, I. M., & Mofijur, M. (2013a). Impacts of biodiesel combustion on NOx emissions and their reduction approaches. *Renewable and Sustainable Energy Reviews, 23*(0), 473-490.

Palash, S. M., Masjuki, H. H., Kalam, M. A., Masum, B. M., Sanjid, A., & Abedin, M. J. (2013b). State of the art of NOx mitigation technologies and their effect on the performance and emission characteristics of biodiesel-fueled Compression Ignition engines. *Energy Conversion and Management, 76*, 400-420.

Pandey, R. K., Rehman, A., & Sarviya, R. M. (2012). Impact of alternative fuel properties on fuel spray behavior and atomization. *Renewable and Sustainable Energy Reviews, 16*(3), 1762-1778.

Park, C., Kook, S., & Bae, C. (2004). *Effects of Multiple Injections in a HSDI Diesel Engine Equipped with Common Rail Injection System*. http://dx.doi.org/10.4271/2004-01-0127

Park, S. H., Kim, H. J., & Lee, C. S. (2016). Effect of multiple injection strategies on combustion and emission characteristics in a diesel engine. *Energy & Fuels, 30*(2), 810-818.

Park, S. H., Yoon, S. H., & Lee, C. S. (2011). Effects of multiple-injection strategies on overall spray behavior, combustion, and emissions reduction characteristics of biodiesel fuel. *Applied Energy, 88*(1), 88-98.

Park, W., Ra, Y., Kurtz, E., Willems, W., & Reitz, R. D. (2015). *Use of Multiple Injection Strategies to Reduce Emission and Noise in Low Temperature Diesel Combustion*. https://doi.org/10.4271/2015-01-0831

Paultan.org. (2017). Singapore switches to Euro 6 emissions standard – more than a dozen car models set to leave the market. Retrieved 18th September 2017 https://paultan.org/2017/09/01/singapore-switches-to-euro-6-emissions-standard-more-than-a-dozen-car-models-set-to-leave-the-market/

Pierpont, D. A., Montgomery, D. T., & Reitz, R. D. (1995). *Reducing Particulate and NOx Using Multiple Injections and EGR in a D.I. Diesel*. http://dx.doi.org/10.4271/950217

Pontoppidan, M., Ausiello, F., Bella, G., & Demaio, A. (2002). *Study of the Impact of Variations in the Diesel-Nozzle Geometry Parameters on the Layout of Multiple Injection Strategy*. http://dx.doi.org/10.4271/2002-01-0217

Prasad, C. V., Krishna, M. M., Reddy, C. P., & Mohan, K. R. (2000). Performance evaluation of non-edible vegetable oils as substitute fuels in low heat rejection diesel engines. *Proceedings of the Institution of Mechanical Engineers, Part D: Journal of Automobile Engineering, 214*(2), 181-187.

Puhan, S., Saravanan, N., Nagarajan, G., & Vedaraman, N. (2010). Effect of biodiesel unsaturated fatty acid on combustion characteristics of a DI compression ignition engine. *Biomass and Bioenergy, 34*(8), 1079-1088.

Puzun, A., Wanchen, S., Guoliang, L., Manzhi, T., Chunjie, L., & Shibao, C. (2011). Characteristics of Particle Size Distributions About Emissions in A Common-rail Diesel Engine with Biodiesel Blends. *Procedia Environmental Sciences, 11*(Part C), 1371-1378.

Qi, D., Leick, M., Liu, Y., & Lee, C.-f. F. (2011). Effect of EGR and injection timing on combustion and emission characteristics of split injection strategy DI-diesel engine fueled with biodiesel. *Fuel, 90*(5), 1884-1891.

Raheman, H., & Ghadge, S. V. (2007). Performance of compression ignition engine with mahua (Madhuca indica) biodiesel. *Fuel, 86*(16), 2568-2573.

Rahman, S. M. A., Masjuki, H. H., Kalam, M. A., Abedin, M. J., Sanjid, A., & Sajjad, H. (2013). Production of palm and Calophyllum inophyllum based biodiesel and investigation of blend performance and exhaust emission in an unmodified diesel engine at high idling conditions. *Energy Conversion and Management, 76*, 362-367.

Ramadhas, A. S., Jayaraj, S., & Muraleedharan, C. (2004). Use of vegetable oils as I.C. engine fuels—A review. *Renewable Energy, 29*(5), 727-742.

Ramadhas, A. S., Jayaraj, S., & Muraleedharan, C. (2005). Biodiesel production from high FFA rubber seed oil. *Fuel, 84*(4), 335-340.

Rashed, M. M., Kalam, M. A., Masjuki, H. H., Mofijur, M., Rasul, M. G., & Zulkifli, N. W. M. (2016a). Performance and emission characteristics of a diesel engine fueled with palm, jatropha, and moringa oil methyl ester. *Industrial Crops and Products, 79*, 70-76.

Rashed, M. M., Masjuki, H. H., Kalam, M. A., Alabdulkarem, A., Rahman, M. M., Imdadul, H. K., & Rashedul, H. K. (2016b). Study of the oxidation stability and exhaust emission analysis of Moringa olifera biodiesel in a multi-cylinder diesel engine with aromatic amine antioxidants. *Renewable Energy, 94*, 294-303.

Rashid, U., Anwar, F., Moser, B. R., & Knothe, G. (2008). Moringa oleifera oil: A possible source of biodiesel. *Bioresource Technology, 99*(17), 8175-8179.

Ravindra, K., Sokhi, R., & Van Grieken, R. (2008). Atmospheric polycyclic aromatic hydrocarbons: Source attribution, emission factors and regulation. *Atmospheric Environment, 42*(13), 2895-2921.

Rizwanul Fattah, I. M., Masjuki, H. H., Kalam, M. A., Wakil, M. A., Ashraful, A. M., & Shahir, S. A. (2014). Experimental investigation of performance and regulated emissions of a diesel engine with Calophyllum inophyllum biodiesel blends accompanied by oxidation inhibitors. *Energy Conversion and Management, 83*, 232-240.

Roh, H. G., Lee, D., & Lee, C. S. (2015). Impact of DME-biodiesel, diesel-biodiesel and diesel fuels on the combustion and emission reduction characteristics of a CI engine according to pilot and single injection strategies. *Journal of the Energy Institute, 88*(4), 376-385.

Rohani, B., & Bae, C. (2017). Effect of exhaust gas recirculation (EGR) and multiple injections on diesel soot nano-structure and reactivity. *Applied Thermal Engineering, 116*, 160-169.

Rojas, N. Y., Milquez, H. A., & Sarmiento, H. (2011). Characterizing priority polycyclic aromatic hydrocarbons (PAH) in particulate matter from diesel and palm oil-based biodiesel B15 combustion. *Atmospheric Environment, 45*(34), 6158-6162.

Sahoo, P. K., & Das, L. M. (2009). Process optimization for biodiesel production from Jatropha, Karanja and Polanga oils. *Fuel, 88*(9), 1588-1594.

Sahoo, P. K., Das, L. M., Babu, M. K. G., & Naik, S. N. (2007). Biodiesel development from high acid value polanga seed oil and performance evaluation in a CI engine. *Fuel, 86*(3), 448-454.

Salamanca, M., Mondragón, F., Agudelo, J. R., Benjumea, P., & Santamaría, A. (2012a). Variations in the chemical composition and morphology of soot induced by the unsaturation degree of biodiesel and a biodiesel blend. *Combustion and Flame, 159*(3), 1100-1108.

Salamanca, M., Mondragón, F., Agudelo, J. R., & Santamaría, A. (2012b). Influence of palm oil biodiesel on the chemical and morphological characteristics of particulate matter emitted by a diesel engine. *Atmospheric Environment, 62*(Supplement C), 220-227.

Saravanan, N., Nagarajan, G., & Puhan, S. (2010). Experimental investigation on a DI diesel engine fuelled with Madhuca Indica ester and diesel blend. *Biomass and Bioenergy, 34*(6), 838-843.

Saravanan, S., Nagarajan, G., Lakshmi Narayana Rao, G., & Sampath, S. (2014). Theoretical and experimental investigation on effect of injection timing on NOx emission of biodiesel blend. *Energy, 66*, 216-221.

Sayin, C., & Gumus, M. (2011). Impact of compression ratio and injection parameters on the performance and emissions of a DI diesel engine fueled with biodiesel-blended diesel fuel. *Applied Thermal Engineering, 31*(16), 3182-3188.

Sayin, C., Gumus, M., & Canakci, M. (2012). Effect of fuel injection pressure on the injection, combustion and performance characteristics of a DI diesel engine fueled with canola oil methyl esters-diesel fuel blends. *Biomass and Bioenergy, 46*, 435-446.

Sequera, A. J., Parthasarathy, R. N., & Gollahalli, S. R. (2011). Effects of Fuel Injection Timing in the Combustion of Biofuels in a Diesel Engine at Partial Loads. *Journal of Energy Resources Technology, 133*(2), 022203-022203.

Shahid, E. M., & Jamal, Y. (2008). A review of biodiesel as vehicular fuel. *Renewable and Sustainable Energy Reviews, 12*(9), 2484-2494.

Sharma, V., Ramawat, K. G., & Choudhary, B. L. (2012). Biodiesel Production for Sustainable Agriculture. In E. Lichtfouse (Ed.), *Sustainable Agriculture Reviews: Volume 11* (pp. 133-160). Dordrecht: Springer Netherlands.

Sharma, Y., & Singh, B. (2008). Development of biodiesel from karanja, a tree found in rural India. *Fuel, 87*(8-9), 1740-1742.

Sharma, Y. C., & Singh, B. (2009). Development of biodiesel: Current scenario. *Renewable and Sustainable Energy Reviews, 13*(6–7), 1646-1651.

Sharma, Y. C., Singh, B., & Upadhyay, S. N. (2008). Advancements in development and characterization of biodiesel: A review. *Fuel, 87*(12), 2355-2373.

Sharon, H., Karuppasamy, K., Soban Kumar, D. R., & Sundaresan, A. (2012). A test on DI diesel engine fueled with methyl esters of used palm oil. *Renewable Energy, 47*(0), 160-166.

Shelke, P. S., Sakhare, N. M., & Lahane, S. (2016). Investigation of Combustion Characteristics of a Cottonseed Biodiesel Fuelled Diesel Engine. *Procedia Technology, 25*, 1049-1055.

Shivakumar, Srinivasa Pai, P., & Shrinivasa Rao, B. R. (2011). Artificial Neural Network based prediction of performance and emission characteristics of a variable compression ratio CI engine using WCO as a biodiesel at different injection timings. *Applied Energy, 88*(7), 2344-2354.

Sidibé, S. S., Blin, J., Vaitilingom, G., & Azoumah, Y. (2010). Use of crude filtered vegetable oil as a fuel in diesel engines state of the art: Literature review. *Renewable and Sustainable Energy Reviews, 14*(9), 2748-2759.

Silitonga, A. S., Masjuki, H. H., Mahlia, T. M. I., Ong, H. C., Chong, W. T., & Boosroh, M. H. (2013). Overview properties of biodiesel diesel blends from edible and non-edible feedstock. *Renewable and Sustainable Energy Reviews, 22*(0), 346-360.

Singh, S. P., & Singh, D. (2010). Biodiesel production through the use of different sources and characterization of oils and their esters as the substitute of diesel: A review. *Renewable and Sustainable Energy Reviews, 14*(1), 200-216.

Srivastava, A., & Prasad, R. (2000). Triglycerides-based diesel fuels. *Renewable and Sustainable Energy Reviews, 4*(2), 111-133.

Srivastava, P. K., & Verma, M. (2008). Methyl ester of karanja oil as an alternative renewable source energy. *Fuel, 87*(8), 1673-1677.

Stone, E., Schauer, J., Quraishi, T. A., & Mahmood, A. (2010). Chemical characterization and source apportionment of fine and coarse particulate matter in Lahore, Pakistan. *Atmospheric Environment, 44*(8), 1062-1070.

Su, W., Lin, T., & Pei, Y. (2003). *A Compound Technology for HCCI Combustion in a DI Diesel Engine Based on the Multi-Pulse Injection and the BUMP Combustion Chamber*. http://dx.doi.org/10.4271/2003-01-0741

Suh, H. K. (2011). Investigations of multiple injection strategies for the improvement of combustion and exhaust emissions characteristics in a low compression ratio (CR) engine. *Applied Energy, 88*(12), 5013-5019.

Suryawanshi, J. G. (2006a). Performance and Emission Characteristics of CI Engine Fueled by Coconut Oil Methyl Ester. *SAE Technical Paper* 2006-2032-0077.

Suryawanshi, J. G. (2006b). *Performance and Emission Characteristics of CI Engine Fueled by Coconut Oil Methyl Ester*. http://dx.doi.org/10.4271/2006-32-0077

Suryawanshi, J. G., & Deshpande, N. V. (2005). Effect of Injection Timing Retard on Emissions and Performance of a Pongamia Oil Methyl Ester Fuelled CI Engine. *SAE Technical Paper* 2005-2001-3677.

Szybist, J. P., & Boehman, A. L. (2003). *Behavior of a Diesel Injection System with Biodiesel Fuel*. http://dx.doi.org/10.4271/2003-01-1039

Szybist, J. P., Boehman, A. L., Taylor, J. D., & McCormick, R. L. (2005). Evaluation of formulation strategies to eliminate the biodiesel NOx effect. *Fuel Processing Technology, 86*(10), 1109-1126.

Szybist, J. P., Song, J., Alam, M., & Boehman, A. L. (2007). Biodiesel combustion, emissions and emission control. *Fuel Processing Technology, 88*(7), 679-691.

Tan, P.-q., Hu, Z.-y., Lou, D.-m., & Li, Z.-j. (2012). Exhaust emissions from a light-duty diesel engine with Jatropha biodiesel fuel. *Energy, 39*(1), 356-362.

Tinsdale, M., Price, P., & Chen, R. (2010). The Impact of Biodiesel on Particle Number, Size and Mass Emissions from a Euro4 Diesel Vehicle. *SAE International Journal of Engines, 3*(1), 597-608.

Torregrosa, A. J., Broatch, A., García, A., & Mónico, L. F. (2013). Sensitivity of combustion noise and NOx and soot emissions to pilot injection in PCCI Diesel engines. *Applied Energy, 104*, 149-157.

Tsai, J.-H., Chen, S.-J., Huang, K.-L., Lin, Y.-C., Lee, W.-J., Lin, C.-C., & Lin, W.-Y. (2010). PM, carbon, and PAH emissions from a diesel generator fuelled with soy-biodiesel blends. *Journal of Hazardous Materials, 179*(1–3), 237-243.

Tziourtzioumis, D. N., & Stamatelos, A. M. (2014). Effects of B20 on the Operation of a Single-Cylinder Engine Equipped with a SiC Diesel Particulate Filter. *Journal of Energy Engineering, 140*(3), A4014009.

UNEP. (2013). Status of fuel quality and vehicle emission standards in asia-pacific. Retrieved July 01 2015 http://www.unep.org/transport/pcfv/PDF/Maps_Matrices/AP/matrix/AsiaPacific_Fuels_Vehicles_Aug2013.pdf

USEPA. (2002). Health assessment document for diesel engine exhaust. National center for environmental assessment, office of transportation and air quality.

Usta, N. (2005). An experimental study on performance and exhaust emissions of a diesel engine fuelled with tobacco seed oil methyl ester. *Energy Conversion and Management, 46*(15–16), 2373-2386.

Veljković, V., Lakićević, S., Stamenković, O., Todorović, Z., & Lazić, M. (2006). Biodiesel production from tobacco (Nicotiana tabacum L.) seed oil with a high content of free fatty acids. *Fuel, 85*(17-18), 2671-2675.

Verma, P., & Sharma, M. P. (2016). Review of process parameters for biodiesel production from different feedstocks. *Renewable and Sustainable Energy Reviews, 62*(Supplement C), 1063-1071.

Weall, A., & Collings, N. (2007). *Highly Homogeneous Compression Ignition in a Direct Injection Diesel Engine Fuelled with Diesel and Biodiesel*. http://dx.doi.org/10.4271/2007-01-2020

Wei, H., Yao, C., Pan, W., Han, G., Dou, Z., Wu, T., . . . Shi, J. (2017). Experimental investigations of the effects of pilot injection on combustion and gaseous emission characteristics of diesel/methanol dual fuel engine. *Fuel, 188*, 427-441.

Wu, F., Wang, J., Chen, W., & Shuai, S. (2009). A study on emission performance of a diesel engine fueled with five typical methyl ester biodiesels. *Atmospheric Environment, 43*(7), 1481-1485.

Wu, X. F., & Chen, G. Q. (2017). Global primary energy use associated with production, consumption and international trade. *Energy Policy, 111*, 85-94.

Yang, B., Mellor, A. M., & Chen, S. K. (2002). *Multiple Injections with EGR Effects on NOx Emissions for DI Diesel Engines Analyzed Using an Engineering Model*. http://dx.doi.org/10.4271/2002-01-2774

Yang, H.-H., Lo, M.-Y., Chi-Wei Lan, J., Wang, J.-S., & Hsieh, D. P. H. (2007). Characteristics of trans,trans-2,4-decadienal and polycyclic aromatic hydrocarbons in exhaust of diesel engine fueled with biodiesel. *Atmospheric Environment, 41*(16), 3373-3380.

Ye, P., & Boehman, A. L. (2012a). An investigation of the impact of injection strategy and biodiesel on engine NOx and particulate matter emissions with a common-rail turbocharged DI diesel engine. *Fuel, 97*, 476-488.

Ye, P., & Boehman, A. L. (2012b). An investigation of the impact of injection strategy and biodiesel on engine NOx and particulate matter emissions with a common-rail turbocharged DI diesel engine. *Fuel, 97*(Supplement C), 476-488.

Yehliu, K., Boehman, A. L., & Armas, O. (2010). Emissions from different alternative diesel fuels operating with single and split fuel injection. *Fuel, 89*(2), 423-437.

Yoon, S. H., Suh, H. K., & Lee, C. S. (2009). Effect of Spray and EGR Rate on the Combustion and Emission Characteristics of Biodiesel Fuel in a Compression Ignition Engine. *Energy & Fuels, 23*(3), 1486-1493.

Zareh, P., Zare, A. A., & Ghobadian, B. (2017). Comparative assessment of performance and emission characteristics of castor, coconut and waste cooking based biodiesel as fuel in a diesel engine. *Energy*.

Zhang, J., Jing, W., Roberts, W. L., & Fang, T. (2013). Soot temperature and KL factor for biodiesel and diesel spray combustion in a constant volume combustion chamber. *Applied Energy, 107*, 52-65.

Zhang, J. J., McCreanor, J. E., Cullinan, P., Chung, K. F., Ohman-Strickland, P., Han, I. K., . . . Nieuwenhuijsen, M. J. (2009). Health effects of real-world exposure to diesel exhaust in persons with asthma. *Res Rep Health Eff Inst*(138), 5-109; discussion 111-123.

Zhang, Y., & Boehman, A. L. (2007). Impact of Biodiesel on NOx Emissions in a Common Rail Direct Injection Diesel Engine. *Energy & Fuels, 21*(4), 2003-2012.

Zhou, A., & Thomson, E. (2009). The development of biofuels in Asia. *Applied Energy, 86, Supplement 1*(0), S11-S20.

Zhu, L., Cheung, C. S., Zhang, W. G., & Huang, Z. (2011). Effect of charge dilution on gaseous and particulate emissions from a diesel engine fueled with biodiesel and biodiesel blended with methanol and ethanol. *Applied Thermal Engineering, 31*(14), 2271-2278.

Zhu, Y., Zhao, H., & Ladommatos, N. (2003). *Computational Study of the Effects of Injection Timing, EGR and Swirl Ratio on a HSDI Multi-Injection Diesel Engine Emission and Performance*. http://dx.doi.org/10.4271/2003-01-0346

List of Publications and Papers Presented

ISI Indexed Journals:

How, H. G., Masjuki, H. H., Kalam, M. A., Teoh, Y. H., & Chuah, H. G. (2018). Effect of Calophyllum Inophyllum biodiesel-diesel blends on combustion, performance, exhaust particulate matter and gaseous emissions in a multi-cylinder diesel engine. Fuel, 227, 154-164. **(ISI Q1)**

How, H. G., Masjuki, H. H., Kalam, M. A., & Teoh, Y. H. (2018). Influence of injection timing and split injection strategies on performance, emissions, and combustion characteristics of diesel engine fueled with biodiesel blended fuels. Fuel, 213, 106-114. **(ISI Q1)**

How, H. G., Masjuki, H. H., Kalam, M. A., & Teoh, Y. H. (2014). An investigation of the engine performance, emissions and combustion characteristics of coconut biodiesel in a high-pressure common-rail diesel engine. Energy, 69(0), 749-759. **(ISI Q1)**

How, H. G., Teoh, Y. H., Masjuki, H. H., & Kalam, M. A. (2012). Impact of coconut oil blends on particulate-phase PAHs and regulated emissions from a light duty diesel engine. Energy, 48(1), 500-509. **(ISI Q1).**

Papers Presented in Conferences:

H.G. How, Y.H. Teoh, H.H. Masjuki, M.A. Kalam. (2017). Effect of Injection Timing on Performance, Emissions, and Combustion Characteristics of Split Injection Strategy Diesel Engine Fueled with Biodiesel Blended Fuels. *The 4th International Conference on Recent Advances in Automotive Engineering & Mobility Research (ReCAR) 2017*, 8th - 10th August 2017, Hotel Bangi-Putrajaya, Bangi, Malaysia.

Y.H. Teoh, **H.G. How**, P.K. Ng, K.S. Jee, H.H. Masjuki, M.A. Kalam. (2016). Application of the TRIZ Approach for NOx Emission Reduction in Diesel Engine. *MyTRIZ Conference 2016*, 25th November 2016, Taylor's University Lakeside campus, Subang Jaya, Selangor, Malaysia.

H.G. How, H.H. Masjuki, M.A. Kalam, Y.H. Teoh. (2015). Evaluation of performance, combustion, regulated and particulate matter emissions of a common-rail DI engine fuelled with Moringa oleifera biodiesel. *The 3rd International Conference on Recent Advances in Automotive Engineering & Mobility Research (ReCAR) 2015*, 1st - 3th December 2015, Holiday Inn Melaka, Malaysia.

How, H. G., Masjuki, H. H., Kalam, M. A., & Teoh, Y. H. (2014). Engine Performance, Emission and Combustion Characteristics of a Common-Rail Diesel Engine Fuelled with Bioethanol as a Fuel Additive in Coconut Oil Biodiesel Blends. The 6th International Conference on Applied Energy (ICAE), Taipei, Taiwan, 30th May -2nd Jun 2014.

How, H. G., Masjuki, H. H., Kalam, M. A., & Teoh, Y. H. (201)3. Effect of Ethanol-Coconut Oil Methyl Ester on the Performance, Emission and Combustion Characteristics of a High-Pressure Common-Rail DI Engine. The 2nd International Conference on Recent Advances in Automotive Engineering & Mobility Research (ReCAR2013), Furama Hotel, Bukit Bintang, Kuala Lumpur, 16th – 18th December 2013.

How, H. G., Masjuki, H. H., Kalam, M. A., Teoh, Y. H & Abdullah, M. A. (2013). Effect of Injection Timing on Performance, Emission and Combustion Characteristics of a Common-Rail Diesel Engine Fuelled with Coconut Oil Methyl Ester. The Proceeding of International Conference on SAE/KSAE 2013 International Powertrains, Fuels & Lubricants Meeting, Seoul, Korea, 21st – 23rd October 2013.